


2012

## Synthesis and Characterization of Red and Near-Infrared BODIPY-based fluorophores for various Biological Applications

Timsy Kaur Uppal

*Louisiana State University and Agricultural and Mechanical College*

Follow this and additional works at: [https://digitalcommons.lsu.edu/gradschool\\_dissertations](https://digitalcommons.lsu.edu/gradschool_dissertations)

 Part of the [Chemistry Commons](#)

---

### Recommended Citation

Uppal, Timsy Kaur, "Synthesis and Characterization of Red and Near-Infrared BODIPY-based fluorophores for various Biological Applications" (2012). *LSU Doctoral Dissertations*. 631.  
[https://digitalcommons.lsu.edu/gradschool\\_dissertations/631](https://digitalcommons.lsu.edu/gradschool_dissertations/631)

This Dissertation is brought to you for free and open access by the Graduate School at LSU Digital Commons. It has been accepted for inclusion in LSU Doctoral Dissertations by an authorized graduate school editor of LSU Digital Commons. For more information, please contact [gradetd@lsu.edu](mailto:gradetd@lsu.edu).

SYNTHESIS AND CHARACTERIZATION OF RED AND NEAR-INFRARED  
BODIPY-BASED FLUOROPHORES FOR VARIOUS BIOLOGICAL APPLICATIONS

A Dissertation

Submitted to the Graduate Faculty of the  
Louisiana State University and  
Agricultural and Mechanical College  
in partial fulfillment of the  
requirements for the degree of  
Doctor of Philosophy

in

The Department of Chemistry

by  
Timsy K. Uppal  
B.S., Miranda House, India, 2003  
M.S., University of Delhi, India, 2005  
August 2012

## **DEDICATION**

Dedicated to my inspiring parents, **Dr. Balbir S. Uppal** and **Kulwant K. Uppal** and my lovely sister **Iru Uppal**, whose unconditional love, continued support and expert counseling, always imbued my life with a joie de vivre and allowed me to fulfill my academic milestones.

## ACKNOWLEDGEMENTS

Numerous fellows have lent their support in innumerable ways from the point when the doctoral level research was merely a thought bubble in my mind to the final dissertation-writing process. It is a great pleasure to thank all those people who made this brain-wrenching task possible.

First and foremost, I would like to express my heartfelt thanks to The Almighty for giving me this miraculous opportunity to travel to the United States and be a part of LSU Graduate School. I could not have been nurtured in a better place. Had he not bestowed his grace and kindness, neither had I found myself at LSU nor had the courage to struggle through this strenuous process. So thank you so much Father God, for adding this beautiful chapter to my life.

It is difficult to overstate my gratitude to my esteemed doctoral mentor, Prof. M. Graça H. Vicente, who cordially accepted me into her research group and trusted in my intellectual capacity. I could not have explored the nadir or reached the zenith and everything in between in my doctoral route, without her valuable guidance, influential inspiration and unwavering faith in my abilities. Her gamut of knowledge, infectious enthusiasm, certitude, earnest endeavors, superb writing skills and diligent work has always helped me broaden my horizon to the amazing world of chemistry. She struck a perfect balance between giving me the liberty to follow my heart whilst reining in my imagination sporadically and averting me from taking wrong turns. *Merci Beaucoup Graça!* You are an epitome of a great, dedicated Professor and I am incredibly proud of having worked under your guidance. Thank you so very much for dedicating voluntary hours in proof-reading innumerable versions of this dissertation and help polish a rudimentary piece into something worthy.

I would like to express my sincere, heartfelt appreciation to Prof. Kevin M. Smith, “The Porphyrin Man”, as the world and I know him. I have always admired him for his perfection,

greatness of mind, dignity of soul, nuts-and-bolts solutions, meticulous and insightful feedbacks on numerous predicaments encountered on my doctoral route. I thank him for serving on my doctoral committee and for always being willing to meet me whenever I barged into his office, unexpectedly.

Heartiest thank you to my doctoral committee members: Dr. Carol M. Taylor and Dr. Jayne Garno, for agreeing to serve on my advisory committee and for influencing my intellectual development when I was just an early bird at LSU. I would also like to thank Dr. Kevin R. Macaluso from the Faculty of Veterinary Medical Sciences for taking time out from his busy schedule to serve as my external invigilator.

I am deeply grateful to the entire Department of Chemistry at LSU, all the faculty members and staff especially Dr. Frank R. Fronczek (expert Ph.D. crystallographer) for sharing his crystallographic expertise, Dr. Xiaoke Hu (cell biologist) for *in vitro* cellular investigations, Dr. Azeem Hasan (Mass Spectrometry Facility Director) for the analytical support and finally Dr. W. Dale Treleaven and Dr. Thomas Weldegheorghis (experienced NMR spectroscopists) for all their help with the NMR predictions. Thank you for being extremely helpful, I assure you all will always have a special place in snug corner of my heart.

I must also acknowledge my collaborators, Dr. Petia Bobadova-Parvanova Assistant Professor in Chemistry, Rockhurst University and Stephanie Maschek, Chemistry major, Rockhurst University, for sharing their computational chemistry expertise while carrying out computational calculations on some of the Benzo-appended BODIPYs listed in Chapter 2.

I am indebted to my many wonderful colleagues or should I say, talented group of scientists in Vicente's Research group: Dr. Alecia M. McCall, Dr. Krystal R. Fontenot, Javoris V. Hollingsworth, R. G. Waruna Jinadasa, Moses I. Ihachi, Benson G. Ongarora, Haijun Wang,

Jamie Hayes, Qianli Meng, Tyrslai Williams, Ning Zhao, Elizabeth Okoth and those in Taylor's Research group: Dr. Benson Edagwa, Douglas Wong and Chamini Karunaratne, who generously shared their meticulous research and insights that supported and expanded my own work, making this bitter-sweet journey, more enlightening, entertaining and a richer experience altogether. And a heartfelt "Thank you" goes out to fellow doctoral colleague and a very dear friend, N. V. S. Dinesh Bhupathiraju for his friendship, breadth of scientific experience, insightful suggestions and technical assistance that provided the impetus for much of the work presented here.

Speaking of friendships, I am forever grateful to my close friends (the backbone holding me together), Dr. Aneesha Virani, Tarun Khanna, Saroj Yadav and Prathvind Bejgum. Thank you for your friendship (which will span lifetime), stimulating advice, constructive criticism and positive outlook that played a pivotal role in shaping my life during these past five years. All the days, late nights and the frustrations when I thought I would never get to this page, you guys were always there to encourage me and believe in my vision. Thank you so much for laughing with me, caring for me, welcoming me into your home and for the great hospitality. Infact, the phrase "Thank you" can never capture the gratitude I want to express.

On a personal front, a million words would be too short to say how grateful I am to my wonderful parents and my adorable sister for their out-pouring love and affection, for supporting me through my trials and tribulations, for bearing the pain of separation as I pursued my dreams, for pulling through admirably with my prolonged renunciation of daughter-responsibilities and for allowing me the space to be myself. Thank you from the bottom of my heart for being my first and best teachers, my role models, excellent cheer leaders and the constant sounding boards while encouraging me towards excellence. You all are the reason I did this and the reason I thrive to be better.

It's been an incredible journey and I am so grateful to all of the amazing people that have helped me along the way. Of course, despite all the assistance provided by each and everybody mentioned above, the numerous flaws that remain in this dissertation are attributable to my sheer negligence.

## TABLE OF CONTENTS

DEDICATION.....	ii
ACKNOWLEDGEMENTS.....	iii
GLOSSARY OF ABBREVIATIONS.....	ix
ABSTRACT.....	xii
CHAPTER 1: INTRODUCTION.....	1
1.1 Structure of BODIPY® dyes.....	1
1.2 Synthetic Methodologies.....	5
1.3 Derivatization of the BODIPY framework.....	11
1.4 Biological applications of the BODIPY dyes.....	18
1.5 Research Outlook.....	30
1.6 References.....	32
CHAPTER 2: SYNTHESIS, COMPUTATIONAL STUDIES AND BIOLOGICAL EVALUATION OF NOVEL SYMMETRICAL AND UNSYMMETRICAL BENZO- APPENDED BODIPYs.....	43
2.1 Introduction.....	43
2.2 Results and Discussion.....	47
2.3 Conclusion.....	90
2.4 Experimental.....	91
2.5 References.....	112
CHAPTER 3: SYNTHESIS AND CHARACTERIZATION OF NOVEL STYRYL- AND LYSYL-BODIPY CONJUGATES FOR BIOLABELING APPLICATIONS.....	116
3.1 Introduction.....	116
3.2 Results and Discussion.....	119
3.3 Conclusion.....	162
3.4 Experimental.....	162
3.5 References.....	173
CHAPTER 4: SYNTHESIS AND APPLICATION OF NOVEL BODIPY-PEG AND BODIPY- CARBOHYDRATE CONJUGATES AS POWERFUL TOOLS FOR BIOIMAGING.....	177
4.1 Introduction.....	177
4.2 Our Approach.....	179
4.3 Results and Discussion.....	183
4.4 Conclusion.....	210
4.5 Experimental.....	211
4.6 References.....	221



APPENDIX.....	227
A. Characterization data for compounds in Chapter 2.....	227
B. Characterization data for compounds in Chapter 3.....	229
C. Characterization data for compounds in Chapter 4.....	231
D. Letters of Permission.....	234
VITA.....	237

## GLOSSARY OF ABBREVIATIONS

$\delta$	Chemical shift
Ac	Acetyl
Boc	t-butoxycarbonyl
BF <sub>3</sub> .OEt <sub>2</sub>	Borontrifluoride dietherate
Bn	Benzyl
BODIPY	Borondipyrromethene
br	broad
<sup>13</sup> C NMR	Carbon 13 Nuclear Magnetic Resonance
d	doublet
DBU	1,8-Diazabicyclo[5.4.0]-undec-7-ene
DCM	Dichloromethane
DDQ	2,3-Dichloro-5,6-Dicyano-1,4-benzoquinone
DMAP	dimethylaminopyridine
DMSO	Dimethylsulfoxide (CH <sub>3</sub> ) <sub>2</sub> SO
Et	Ethyl
EtOAc	Ethyl acetate

EtOH	Ethyl alcohol
FRET	Forster Resonance Energy Transfer
<sup>1</sup> H-NMR	Proton Nuclear Magnetic Resonance
HPLC	High Performance Liquid Chromatography
h	hour(s)
Hz	Hertz
HRMS-ESI	High Resolution (Mass Spectrometry) Electron Spray Ionization
IR	Infrared
J	Coupling constant
MALDI	Matrix Assisted Laser Desorption Ion Ionization
Me	Methyl
MeOH	Methanol
MHz	Megahertz
min	minute(s)
MS	Mass Spectrometry
m/z	mass to charge ratio
NHS	N-hydroxysuccinimide

NIR	Near-infrared
NMR	Nuclear Magnetic Resonance
PDT	Photodynamic Therapy
PEG	Polyethylene glycol
Ph	Phenyl
PMe	Methyl propionate
ppm	parts per million
q	quartet
RBF	round bottom flask
RT	room temperature
s	singlet
t	triplet
TEA	Triethylamine
TFA	Trifluoroacetic acid
THF	Tetrahydrofuran
TLC	Thin Layer Chromatography
p-TsOH	p-Toluenesulfonic acid

## ABSTRACT

4,4-Difluoro-3a,4a-diaza-s-indacene, better known as BODIPY® dyes, have attracted considerable attention due to their intriguing physicochemical and spectral properties, including high absorption coefficient, fluorescence quantum yield and good photochemical stability. Despite the recent progress achieved in this field, the synthesis of BODIPY derivatives that absorb and emit in the red- and NIR-region of the electromagnetic spectrum and their application to biomolecular targets, represents a long-standing challenge in BODIPY chemistry. This research work is therefore focused on the synthesis and characterization of red and NIR-emissive BODIPY-based fluorophores for various bioanalytical and biomedical applications.

**Chapter 1** of this dissertation represents a concise introduction to the fundamental concepts, synthetic routes, post-synthetic modification strategies and various biological applications of BODIPY dyes, that are further elaborated upon in the following Chapters.

**Chapter 2** describes the synthesis, characterization, computational modeling and cellular investigations of a series of new functionalized mono- and dibenzo-appended BODIPYs that are promising fluorophores for biolabeling applications. These ring expanded and constrained BODIPYs were synthesized via two different routes from a common tetrahydroisindole precursor. This work was done in collaboration with Dr. Petia Bobadova-Parvanova of Rockhurst University.

**Chapter 3** reports on the synthesis and characterization of several styryl- and lysyl-BODIPY conjugates, prepared using Knoevenagel condensation reaction, an attractive strategy for the expeditious synthesis of  $\pi$ -extended BODIPYs in moderate to high yields. The effects of the styryl substituents on their photophysical properties and *in vitro* photodynamic activities are also described.

**Chapter 4** discusses an efficient method towards the preparation of a series of BODIPY-PEG and BODIPY-Carbohydrate conjugates via Cu(I)-mediated azide/alkyne cycloaddition, *i.e.* “click” chemistry. Several NIR-emissive BODIPY conjugates that are potential *in vivo* imaging agents were prepared in good to excellent overall yields. The photophysical studies of novel BODIPY-PEG and BODIPY-Carbohydrate conjugates are described in addition to the preliminary *in vitro* investigations.

## CHAPTER 1: INTRODUCTION

### 1.1: Structure of BODIPY<sup>®</sup> Dyes

Recent developments in many different fields of modern science and medicine, such as molecular biology, material science, analytical and environmental chemistry, drug discovery and tissue diagnostics, have fueled the design of new fluorophores that can be excited to emit within the red or near-infrared (NIR) region of the spectrum.<sup>1</sup> This is in part attributed to the optical sensitivity associated with the “biological window” (700-900 nm) of the optical spectrum including minimal interference from the endogenous chromophores, optimal photon penetration through tissue, reduced light scattering and lower damage to the cells/tissues under observation.<sup>2</sup> Though numerous nonradioactive fluorescent organic dyes, such as fluorescein, rhodamines and cyanines, are available, the difluoro-boraindacene family (4,4-difluoro-4-bora-3a,4a-diaza-s-indacene, abbreviated hereafter as BODIPY, registered trademark of Invitrogen (now Life Technologies Inc., Figure 1.1) has earned increasing interest as being one of the more versatile heterocyclic skeleton fluorophores.<sup>3</sup>

BODIPY dye, often referred to as “Porphyrin’s little sister”,<sup>4</sup> consists of a dipyrromethene ligand complexed with a disubstituted boron atom, generally a BF<sub>2</sub> moiety. The dipyrromethene ligand is formed by joining of two pyrrole units via an interpyrrolic methine bridge. Due to BF<sub>2</sub> complexation, the BODIPY fluorophore can be seen as “constrained” cross-conjugated cyanine-type dye with fixed planarity of the chromophoric  $\pi$ -electron system.<sup>5</sup> The rigidity introduced by the boron complexation, further prevents the cis-trans isomerization and interpyrrolic methine chain-twisting, problems commonly associated with comparatively flexible cyanine dyes.

The single crystal X-ray structure of BODIPY chromophoric core indicates a fused ring based framework with strong  $\pi$ -electron delocalization within the central six-membered and two adjacent five-membered pyrrole rings of the dipyrromethene unit (Figure 1.2).<sup>6</sup> This  $\pi$ -electron delocalization is interrupted between both B-N bonds. Deviation from planarity is found for the unsubstituted BODIPY chromophore that exhibits “saddled geometry” due to the boron atom deviating from the mean indacene plane by a  $4.8^\circ$  angle. The average bond length of  $N_1-C_3$  indicates double bond character, compared with the single-bond character of  $N_1-C_4$ . The molecule displays two slightly different B-F bond distances.<sup>7</sup> The bond angles of  $N_1-B_1-N_2$  and  $F_1-B_1-F_2$  indicate a distorted tetrahedron  $BF_2N_2$  configuration. Although BODIPY resembles a typical monomethine cyanine dye with  $6\pi$  electrons delocalized over 5 atoms, the actual fluorophore is found to be isoelectronic with heptamethine cyanines, with  $12\pi$  electrons equally distributed over 11 atoms.<sup>8</sup>

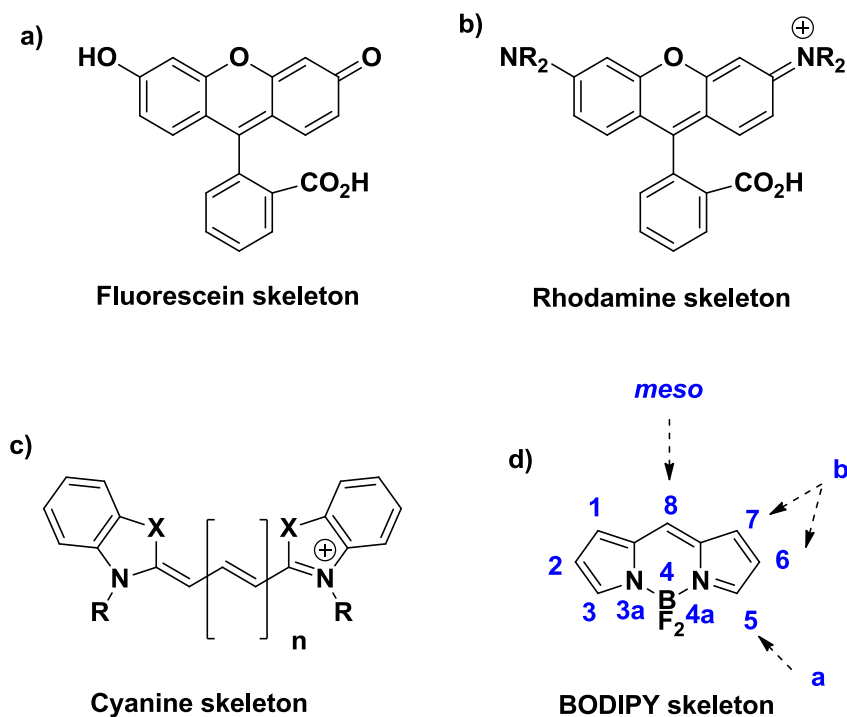


**Figure 1.1:** a)-c) Generic structure of common fluorophores; d) “BODIPY core” and its IUPAC numbering system<sup>5</sup>



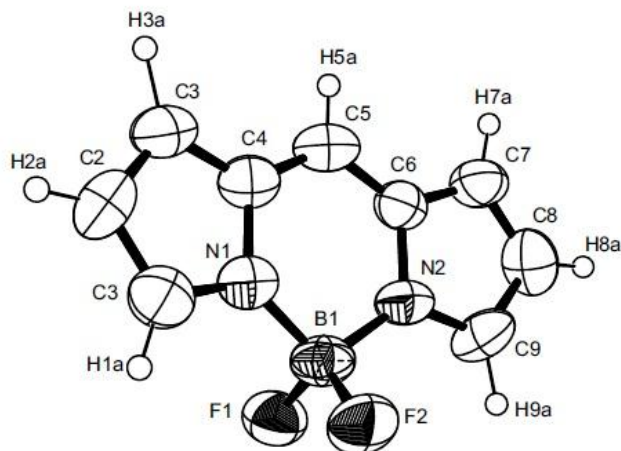


**Figure 1.2:** X-ray crystal structure of unsubstituted BODIPY with atom labels and 50% probability displacement ellipsoids<sup>9</sup>

Each unit cell of BODIPY fluorophore consists of four molecules stacked in a head-to-tail fashion. Such crystal packing arrangement helps to optimize the  $\pi$ - $\pi$  interactions between the hydrophobic BODIPY molecules and variations in the dipole moments caused by the fluorine atoms.<sup>10</sup> Slightly polarized heteroatoms generate various electron-rich and electron-deficient reaction sites at different positions on the internally zwitterionic BODIPY framework. These reaction sites favor both nucleophilic and electrophilic substitution reactions on the BODIPY core, and provide a plethora of new routes for structural modifications on unsubstituted BODIPYs.<sup>11</sup>

The BODIPY and its derivatives are strongly UV-absorbing small molecules with outstanding photophysical characteristics when compared with classical fluorophores, such as fluorescein and tetramethylrhodamines dyes, with fluorescence emissions in the visible region. BODIPY dyes are highly colored, neutral compounds with intense absorption and emission profiles ( $\lambda_{\text{max}}$  between 500-545 nm), high molar absorption coefficients (typically in the region of 40,000 to 80,000  $\text{M}^{-1} \text{cm}^{-1}$ ), high fluorescence quantum yields (normally  $\Phi_{\text{F}} > 0.60$ ),

reasonably long fluorescence lifetimes ( $\tau$  in the nanosecond range) and relatively small Stokes shift (ca.10 nm). In addition, BODIPY dyes have excellent thermal and photostability in both solution and solid states, good solubility in most organic solvents, resistance towards self-aggregation in solution and insensitivity to changes in pH and solvent polarity.<sup>3b, 12</sup>

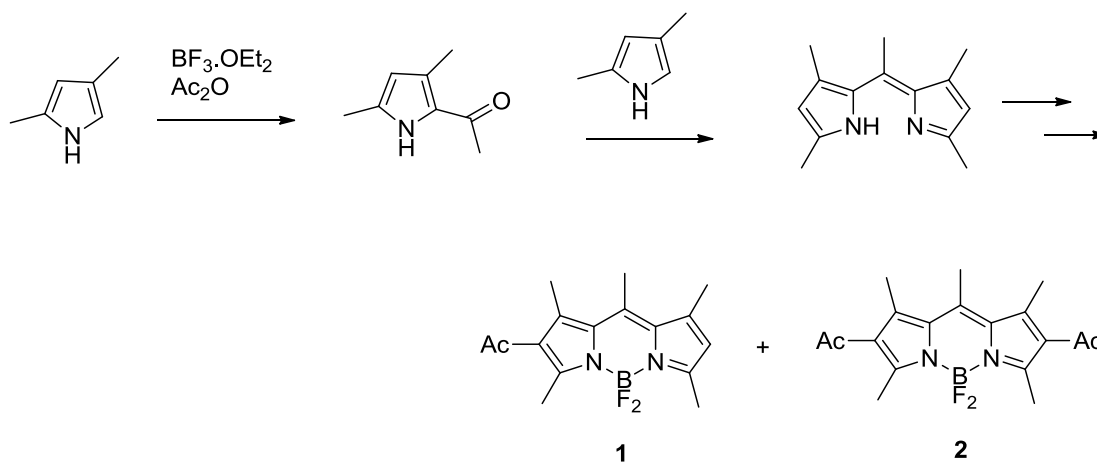
The absorption spectra of a typical BODIPY fluorophore shows a narrow and intense band due to the  $S_0-S_1$  ( $\pi-\pi^*$ ) transition with  $\lambda_{\max}$  between 500-525 nm, a shoulder at high energy centered around  $480 \pm 5$  nm assigned to the 0-1 vibrational transition, and a weak yet broad absorption band around  $375 \pm 5$  nm attributed to the  $S_0-S_2$  ( $\pi-\pi^*$ ) transition.<sup>8, 13</sup> When excited into either the  $S_1$  or  $S_2$  states, a narrow, slightly Stokes-shifted emission band of mirror image shape with  $\lambda_{\max}$  positioned between 530-560 nm is observed from the  $S_1$  state. Phosphorescence is a rare phenomenon in BODIPY-based dyes due to negligible triplet energy state and a slow rate of intersystem crossing (except for one report due to heavy-atom effect of diiodoBODIPY).<sup>14</sup>

The absorption bands of BODIPY dyes can be further shifted to the red or NIR region by facile derivatization of the BODIPY core. The photophysical characteristics of synthetically modified BODIPYs vary with respect to the number, nature, as well as the position of the attached substituents.<sup>15</sup> Additionally, the emission behavior of BODIPY fluorophores are greatly affected by the steric interactions between their components and intramolecular rotations of their chromophoric units.<sup>16</sup>

Ever-growing success of BODIPY dyes has inspired a large amount of research into the design, synthetic modifications and spectroscopic/photophysical characterization of these bright small molecule fluorophores. Many synthetic methodologies and modification techniques discussed hereafter will be used throughout the dissertation.

## 1.2: Synthetic Methodologies

The first synthesis of a green fluorescent BODIPY dye was accidentally achieved in 1968 by Treibs and Kreuzer<sup>17</sup> by reaction of 2,4-dimethylpyrrole with acetic anhydride in the presence of  $\text{BF}_3 \cdot \text{OEt}_2$ . This reaction afforded a mixture of mono- and di-acetylated BODIPY fluorophores, **1** and **2** (Scheme 1.1). It was therefore realized that 2,6-positions on BODIPY chromophore are highly electron deficient i.e. susceptible to electrophilic substitution reactions.



**Scheme 1.1:** Synthesis of mono- and di-acetylated BODIPY fluorophores **1** and **2**

In 1985, Worries and colleagues<sup>18</sup> reported the synthesis of the first water-soluble BODIPY fluorophore for use in angiographic studies. During this period, another group of scientists, Haugland and Kang<sup>19</sup> contributed significantly to the field of fluorescent materials, including BODIPY dyes. Different derivatives of BODIPYs were prepared for lipid and protein systems which eventually made them inventors of nearly 80 United States patents and the largest commercial supplier of BODIPY dyes and its bioconjugates (founder of Molecular Probes, now Life Technologies Inc.). BODIPYs and their bioconjugates are now recognized as fluorescent and photostable substitutes to their predecessors, and are employed mainly for biological labeling applications.<sup>20</sup> However, within the past decade, due to advent of new optoelectronic

and biomedical technologies, there has been a BODIPY renaissance leading to enormous research interest, patents and review articles<sup>3b, 4, 15, 21</sup> illustrating the design of amphiphilic and longer-wavelength absorbing and emitting BODIPY dyes for multifarious applications such as tunable laser dyes,<sup>22</sup> fluorescent labels for biomolecules and cellular imaging,<sup>23, 24</sup> fluorescent switches,<sup>25</sup> photosensitizers,<sup>14, 26</sup> light-emitting devices,<sup>25d, 27</sup> drug delivery agents,<sup>3a, 26c</sup> chemosensors<sup>28 29</sup> and solar cells.<sup>30 31</sup>

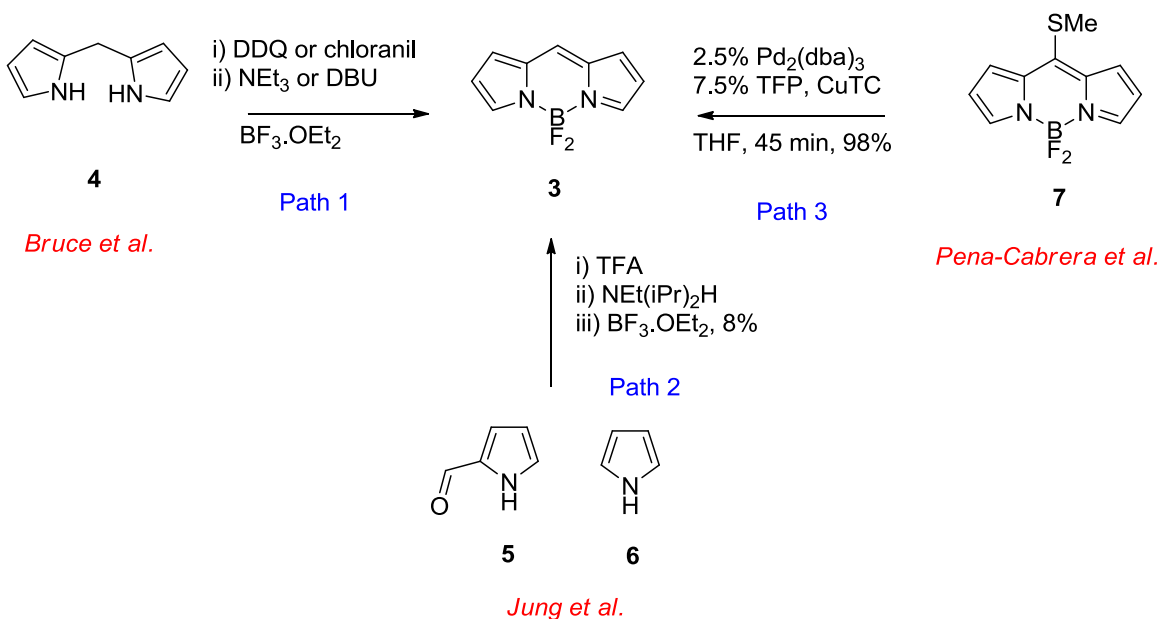
### 1.2.1: Synthesis of the parent BODIPY core

Synthetic approaches to the BODIPY framework are generally based on well-known chemistry of pyrroles and dipyrromethanes, i.e. synthetic precursors for porphyrin and related macrocyclic compounds.<sup>1, 4</sup> Starting from readily available pyrroles, it is relatively easy to produce a variety of dipyrromethene ligands, which after complexation with BF<sub>3</sub> in the presence of a base, generate the required parent BODIPY fluorophore, often in reasonable and reproducible quantities.

While there are a myriad of structurally variant classes of BODIPY dyes mentioned in the literature, the synthesis of the parent unsubstituted BODIPY chromophore remained a challenge until recently<sup>9-11</sup> because of the synthetic limitations related to the highly unstable dipyrromethene precursor.<sup>3b</sup> Three independent research groups reported the synthesis and characterization of the BODIPY core chromophore **3** (Scheme 1.2). In the first report by Bruce and co-workers (Path 1),<sup>9</sup> the unsubstituted BODIPY chromophoric core was synthesized by DDQ oxidation of the dipyrromethane **4** to dipyrromethene. In order to stabilize the highly reactive dipyrromethene core, the DDQ oxidation was carried out at -78°C, under inert conditions, for 1 hour. On reaction completion, the formed dipyrromethene was then reacted *in*

*situ* with DBU and BF<sub>3</sub>.OEt<sub>2</sub> to form targeted compound **3** in 5-10% yield. The structure of the BODIPY was further characterized by <sup>1</sup>H-, <sup>13</sup>C-, <sup>11</sup>B- and <sup>19</sup>F-NMR and X-ray single crystal analysis.

Wild and co-workers,<sup>11</sup> synthesized the desired BODIPY via a classic one-pot asymmetric BODIPY synthesis approach involving acid-catalyzed condensation of pyrrole-2-carbaldehyde **5** and pyrrole **6**, followed by BF<sub>3</sub> complexation in the presence of a base (Path 2). Repeated purification over silica column chromatography afforded the target compound **3** in 8% overall yield. BODIPY **3** exhibits high photostability ( $\tau = 7.2$  ns) but low thermal stability, decomposing at temperatures above 50°C, due to lack of stabilizing substituents. BODIPY **3**, as characterized by UV/Vis and fluorescence spectroscopy, displays a typical green fluorescence with maximum wavelength of absorption and emission at 503 and 512 nm, respectively.



**Scheme 1.2:** Synthesis of the core compound of BODIPY dye **3**

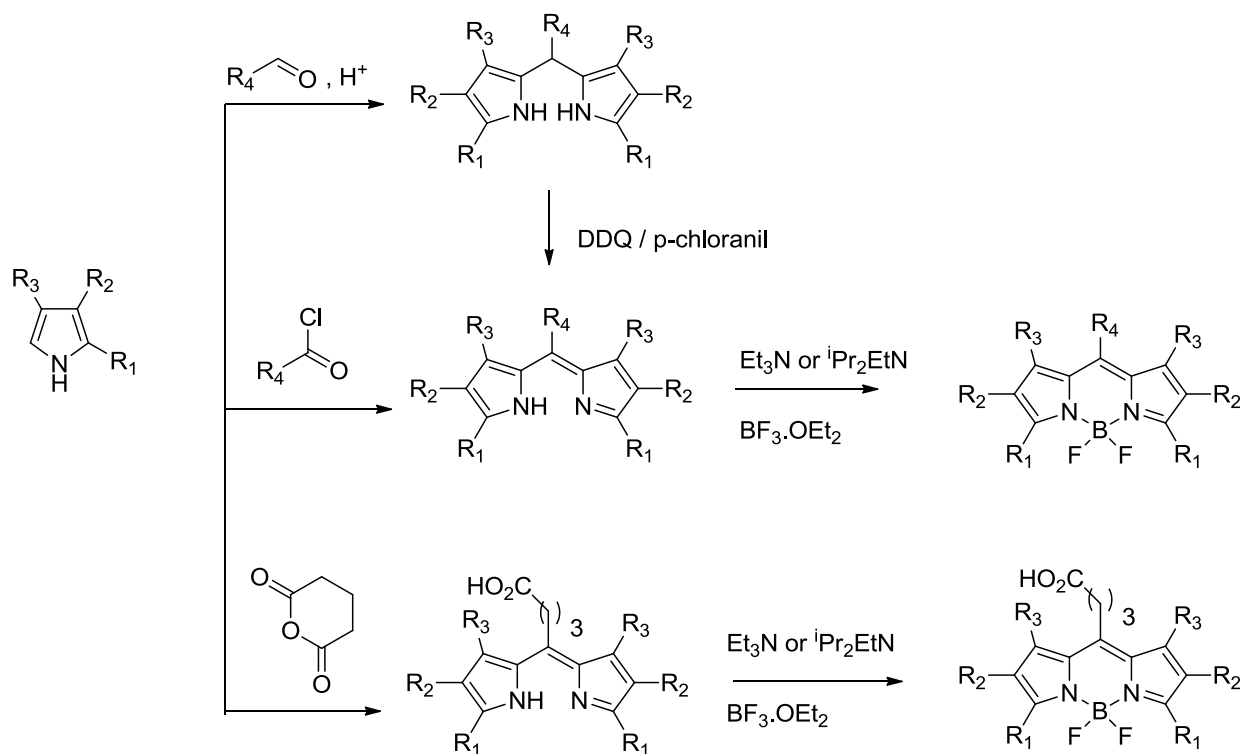
A more efficient route was developed by Pena-Cabrera and co-workers (Path 3),<sup>10</sup> generating the target compound in excellent chemical yield by mild reaction between 8-thiomethyl BODIPY **7**<sup>32</sup> and triethylsilane in the presence of a catalytic amount of palladium and a stoichiometric amount of copper(I) thienyl-2-carboxylate (CuTc) in THF at 55°C for 45 min. BODIPY **3** displays high quantum yields (up to 93%) in nonpolar and polar solvents, including water.

### 1.2.2: Synthesis of symmetric BODIPY dyes

Symmetric BODIPY dyes substituted at the *meso*- or 8-position (Scheme **1.3**) are usually prepared by acid-catalyzed condensation of pyrroles with acid chlorides, anhydrides or aldehydes to generate the dipyrromethene (or dipyrromethanes from aldehydes which are subsequently oxidized). In order to avoid further polymerization, the pyrroles have to be substituted at the C-2 position.<sup>33</sup> The dipyrromethenes are then converted to BODIPY dyes by action of a tertiary base and BF<sub>3</sub>.OEt<sub>2</sub>. Yields for this reaction are generally more than 50% with high purity and reproducibility. BODIPY dyes bearing substituents at the *meso*-position often display enhanced stability with respect to their *meso*-unsubstituted counterparts. A large range of functional groups are compatible with these reaction conditions and these methods are the most popular routes, often referred to as “classical one-pot two/three-step reaction”. The major advantage of the reaction lies in the ability to use the *meso*-substituent as a point of elaboration to build larger architectures, an approach richly explored by many researchers to design BODIPY-based indicators or labels.<sup>34</sup>

Symmetric BODIPY dyes unsubstituted at the *meso*-position are obtained by self-condensation of an appropriate pyrrole carbonyl cation precursor under acidic conditions (for

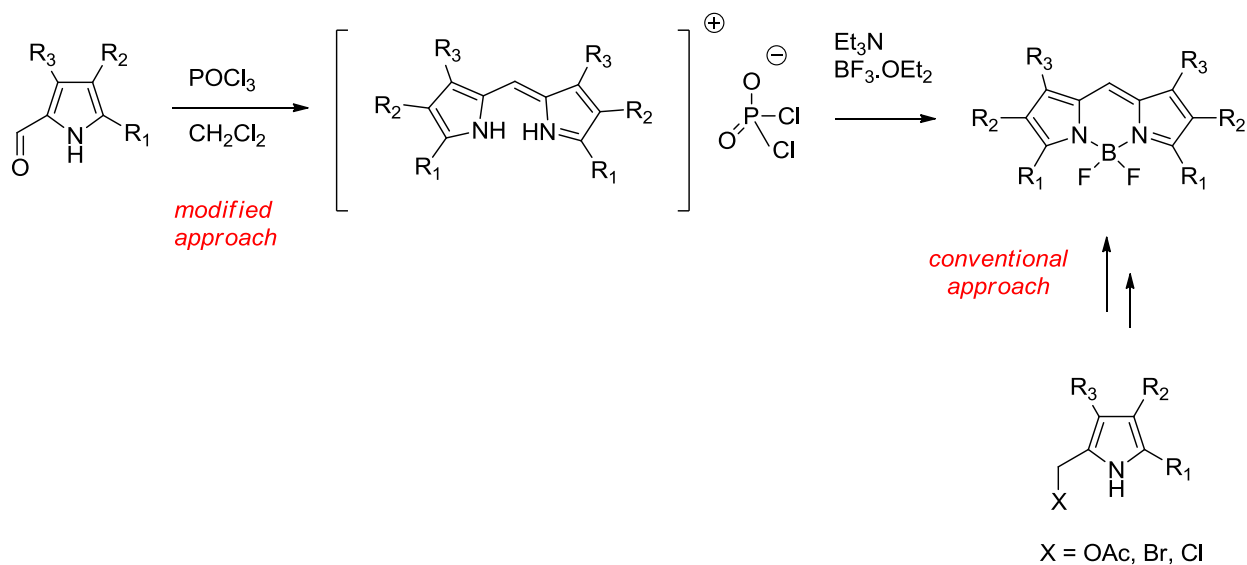
instance, *p*-toluenesulfonic acid, Montmorillonite clay), followed by  $\text{BF}_2$  complexation (conventional approach, Scheme 1.4).<sup>35</sup> The same compound can be prepared *via* self-condensation of pyrrole-2-carbaldehyde in the presence of phosphorus oxychloride, a modified approach recently reported by Wu and Burgess.<sup>36</sup> In the proposed mechanism, phosphorus oxychloride is believed to react with pyrrole-2-carbaldehyde to generate a chlorinated azafulvene, which is then attacked by second pyrrole moiety to form the required dipyrromethenium cation and dichlorophosphate counterion. From this step onwards, the BODIPY is routinely synthesized by trapping the parent dipyrromethene as its  $\text{BF}_2$  complex. The new modified reaction conditions generated products in yields much higher, as compared with the conventional approach.



**Scheme 1.3:** General outline for the synthesis of symmetric BODIPY dyes

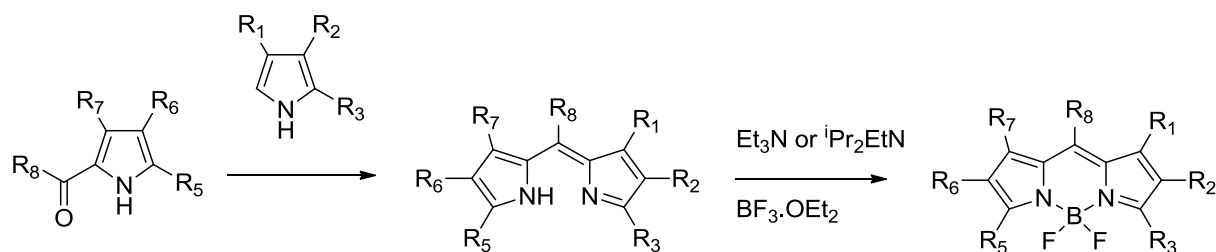
### 1.2.3: Synthesis of asymmetric BODIPY dyes

Asymmetric BODIPY dyes, substituted or unsubstituted at the *meso*-position, are usually obtained by the MacDonald coupling approach, i.e. via acid-catalyzed condensation of a pyrrole-2-carbaldehyde with an  $\alpha$ -free pyrrole.<sup>37</sup> The desired dipyrromethene is generally isolated in its salt form, which on complexation with  $\text{BF}_3 \cdot \text{OEt}_2$  in the presence of a base, usually a tertiary amine, affords the required BODIPY dye (Scheme 1.5). Yields for these reactions are generally very high, but are reduced drastically when an electron-deficient  $\alpha$ -free pyrrole is used. Under such conditions, self-condensation of pyrrole-2-carbaldehyde is the favored reaction and yields the undesired symmetric BODIPY as the major product. The main advantage of this method lies in the possibility to attach different functional moieties on the BODIPY scaffold for further derivatization or bio-conjugation.



**Scheme 1.4:** Syntheses of symmetric *meso*-unsubstituted BODIPYs





**Scheme 1.5:** General outline for the synthesis of asymmetric BODIPY dyes

### 1.3: Derivatization of the BODIPY framework

Typical BODIPY dyes have certain drawbacks, such as relatively low wavelength absorption and emission maxima ( $\lambda_{\text{max}}$  around 500 nm),<sup>38</sup> small Stokes shifts, poor solubility in aqueous media and lack of functional groups for conjugation to biological materials.<sup>39</sup> These drawbacks further limit the full utilization of BODIPY fluorophores for various biomedical and bioanalytical applications. Many of these obstacles can be surmounted via synthetic modifications as the BODIPY chromophore itself is intrinsically electron-rich and can be conveniently derivatized at various positions to analogues that span the entire visible spectrum and beyond. Efforts are underway in various laboratories (Vicente,<sup>40</sup> Ziessel,<sup>3a</sup> Burgess,<sup>25b</sup> Nagano,<sup>14</sup> Rurack and Daub,<sup>41</sup> Akkaya,<sup>42</sup> O'Shea,<sup>43</sup> Carreira,<sup>44</sup> Boens and Dehaen<sup>45</sup>) to investigate new facets of fluorescent BODIPY dyes. A variety of strategies to fine-tune the optoelectronic properties have been achieved by functionalization of the BODIPY scaffold at the 8- (*meso*-), 2,6-, 3,5- positions, the boron center or by rigidification of the BODIPY core.

#### 1.3.1: Functionalization at the *meso*- or 8-position

Functionalization at the C-8 (*meso*) position is relatively easy compared with the substitution at the pyrrolic positions, as it can be achieved by acid-catalyzed condensation of pyrrole with appropriately substituted aryl aldehydes or acyl chlorides.<sup>46</sup> This method continues

to be the most versatile method till date for introduction of various “handles” on the BODIPY core such as ligands,<sup>1, 4, 47</sup> chiral auxiliaries,<sup>48</sup> donor-acceptor groups<sup>49</sup> and water-solubilizing groups<sup>2d, 12b</sup> for applications as chemosensors, pH probes, light-harvesting arrays and biological labels (Figure 1.3, structures 8 to 11). In-depth photophysical studies have been carried out by Boens and co-workers<sup>1, 45, 50</sup> to study the effect of various electron-rich or electron-deficient groups at the C-8 positions. It has been noticed that the spectral characteristics of 8-substituted BODIPYs do not show a marked change due to the orthogonal geometry of the *meso* substituent and the BODIPY fluorophore, which results in poor electronic conjugation between the two moieties. However, the introduction of *ortho*-substituents on the *meso*-phenyl ring, the replacement of phenyl with bulkier aromatic groups or the introduction of 1,7-substituents on the BODIPY skeleton, drastically improve the fluorescence emission efficiency due to restricted intramolecular rotation and steric hindrance between the substituents.<sup>16</sup>

Exchange of C-*meso* for nitrogen atom generates a sub-class of BODIPY dye commonly called “aza-BODIPYs (e.g. 12 and 13).”<sup>25b</sup> Due to structure similarity with phthalocyanines, this subclass of BODIPYs could also be referred to as “Semi-phthalocyanines.” The notable feature of this dye system is its intense absorption and emission bands in the 650-850 range, high molar extinction coefficient, moderate fluorescence quantum yields (0.23-0.36) and insensitivity to the solvent polarity.<sup>51</sup> Further rigidification of the chromophoric core, in turn, improves the stability and spectral properties of the molecule. Though the precursor azadipyrrromethenes were long known, this class of BODIPY has only lately stimulated study. A handful of aza-BODIPYs have been synthesized from substituted-chalcone (O’Shea,<sup>51-52</sup> Akkaya<sup>53</sup> and Burgess<sup>25b</sup>) or from a conformationally restricted pyrrole precursor (Carreira<sup>44</sup>) and investigated as photosensitizers,<sup>54</sup> conformationally restricted NIR imaging probes,<sup>25b, 52, 55</sup> NIR-emitting chemosensors<sup>44</sup> and

fluorescent labels for polymer characterization.<sup>56</sup> These dyes offer a number of advantages in comparison to their carbon analogues, including ease of synthesis and an inherent red-shift in the absorption and emission maxima due to the better stabilization of the HOMO-LUMO energy gap by lone pair on nitrogen at the *meso* position.<sup>4</sup>

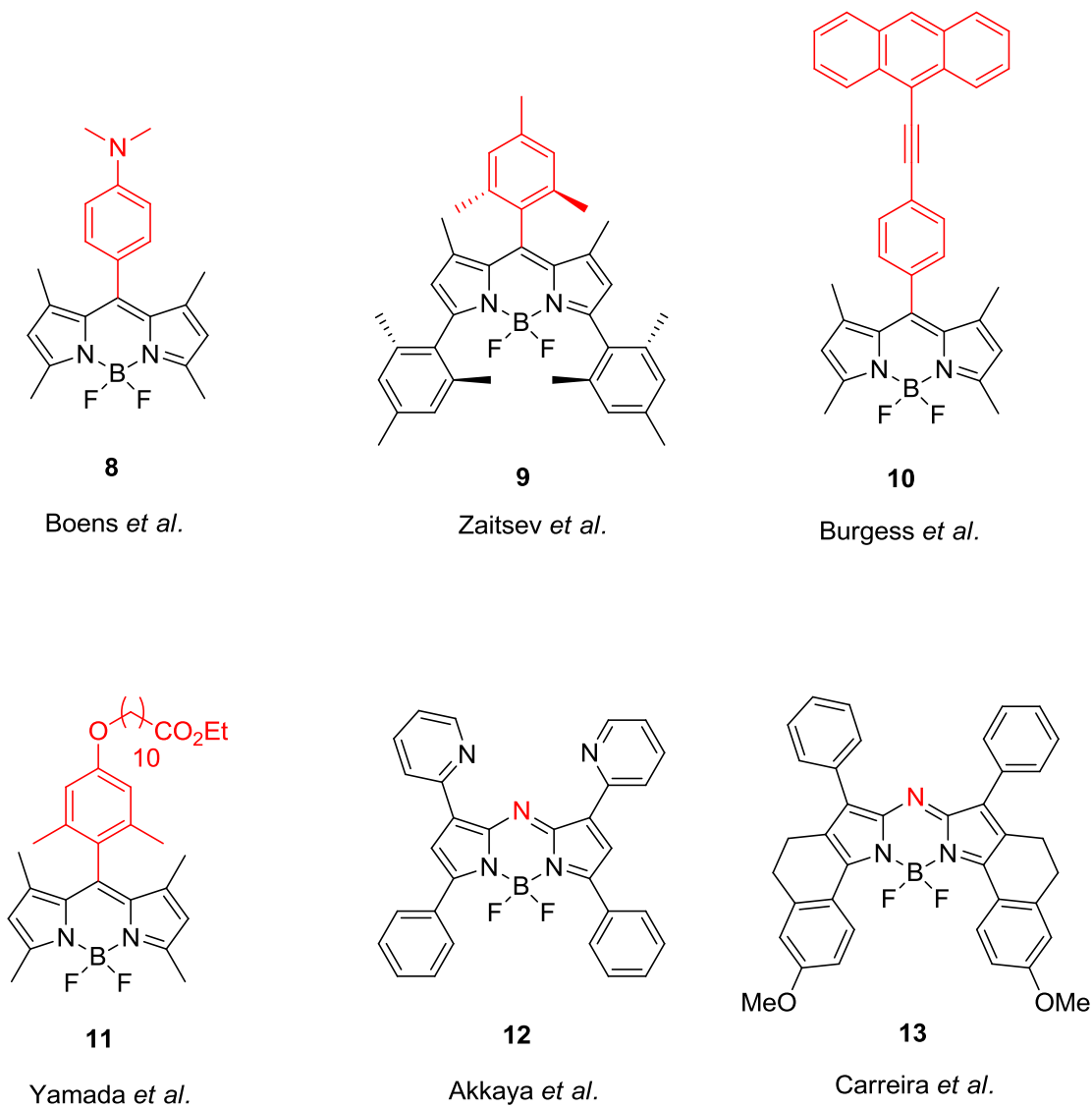


**Figure 1.3:** Chemical structures of various *meso*-substituted BODIPYs from literature: **8**,<sup>50</sup> **9**,<sup>57</sup> **10**,<sup>58</sup> **11**,<sup>59</sup> **12**<sup>53</sup> and **13**<sup>44</sup>

### 1.3.2: Functionalization at the 2,6-positions

Simple consideration of mesomeric structures of BODIPY reveal that the 2 and/or 6-positions of the BODIPY core bear the least positive charge and hence are more susceptible to electrophilic attack (Figure 1.4). Surprisingly only limited electrophilic substitution reactions have been reported including sulfonation,<sup>18</sup> nitration,<sup>60</sup> halogenation,<sup>61</sup> and formylation<sup>46</sup> into the BODIPY backbone through the electron-rich 2,6-positions. While sulfonate groups impart water-solubility to the hydrophobic BODIPY core without affecting the absorption and emission maxima significantly, the introduction of nitro or halo groups drastically decrease the fluorescence quantum yields with respect to the parent dye (Figure 1.5, structure 14). The decrease in the fluorescence quantum yield for bromo and iodo groups is attributed to the internal heavy-atom effect.<sup>62</sup> Recently, a myriad of diphenylethynyl-BODIPY oligomers have been generated from 2,6-diiodo BODIPYs to serve as potential building blocks in the construction of several light-emitting conjugated polymers and functional supramolecular assemblies (e.g. 15).<sup>63</sup>

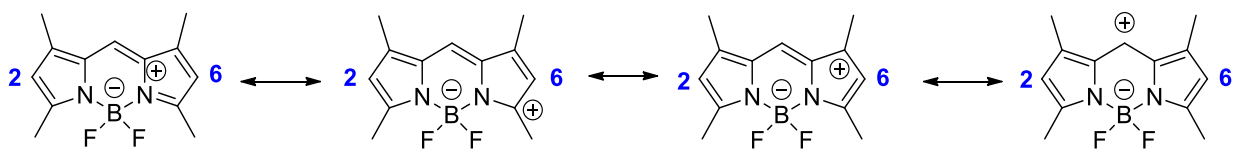


**Figure 1.4:** Susceptible positions for the electrophilic attack on 1,3,5,7-tetramethyl BODIPY dye

Another direct approach for  $\pi$ -conjugation extension at the 2,6-positions of BODIPY molecules involve palladium-mediated C-H functionalization (e.g. 16). As reported by Thivierge and co-workers,<sup>12b</sup> the halogenated or metalated intermediates, generate both mono- and di-

substitution products with fluorescence emissions in the range of 525-570 nm. This methodology can be employed for the syntheses of hydrophilic BODIPY systems with functional groups to act as “tags” for bioconjugation.

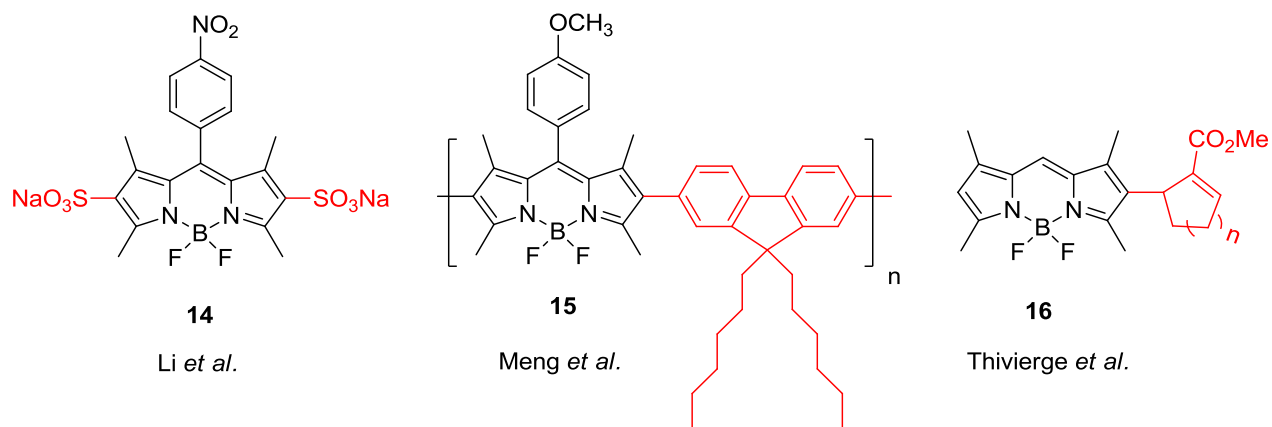


**Figure 1.5:** Chemical structures of various 2- and/or 6-substituted BODIPYs from literature: **14**,<sup>64</sup> **15**<sup>63d</sup> and **16**<sup>65</sup>

### 1.3.3: Functionalization at the 1,3-positions

The 3,5-Dimethyl substituents on electron-deficient BODIPYs are acidic enough to undergo base-catalyzed Knoevenagel-type condensations.<sup>3b</sup> A variety of electron-donating and recently electron-withdrawing aromatic aldehydes have been used to introduce different styryl moieties at the 3- and/or 5-positions, in order to bring significant red-shifts in the optical spectra with respect to the parent chromophore (Figure 1.6, structure 17). Styryl-derivatization of BODIPYs is often a more convenient and less time consuming approach over the analogous lengthy synthetic routes,<sup>2d</sup> and highly functionalized BODIPY derivatives can be generated in a single step by controlling the reaction conditions.

The presence of good leaving groups (such as iodine or chlorine atoms) at the 3- and/or 5- positions allow electron-deficient BODIPYs to undergo nucleophilic aromatic substitution (S<sub>N</sub>Ar)<sup>66</sup> and transition metal-catalyzed coupling reactions (Heck, Sonogashira, Stille and

Suzuki, e.g. **18** and **19**).<sup>67</sup> As reported by Dehaen and Boens, 3,5-dichloroBODIPYs can be easily modified by substitution with carbon, nitrogen, oxygen and sulfur nucleophiles to induce large bathochromic shifts of the absorption and emission maxima. Various aryl, ethenylaryl and ethynylaryl substituents can be grafted on the BODIPY fluorophore using palladium-catalyzed Stille, Suzuki, Heck and Sonogashira coupling reactions. These strategies have been richly explored in the synthesis of novel BODIPY-based fluorescent materials for biosensing and labeling applications.<sup>48a, 68</sup>

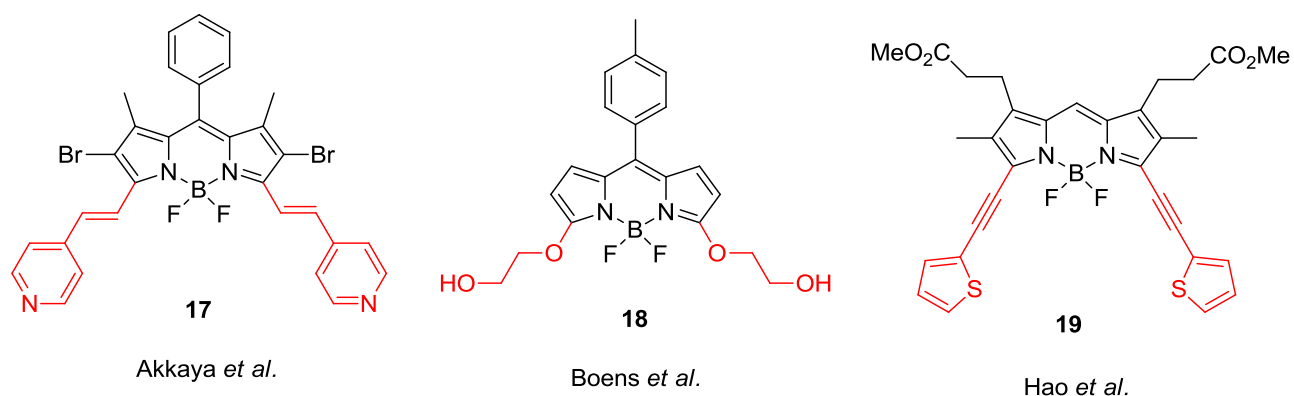


**Figure 1.6:** Chemical structures of various 3,5-substituted BODIPYs from literature: **17**,<sup>69</sup> **18**<sup>66</sup> and **19**<sup>40b</sup>

### 1.3.4: Modification at the boron center

Replacement of the two fluorine atoms in BODIPYs by aryl, ethynyl (or ethynylaryl) and alkoxide groups, generates a new family of highly luminescent, redox-active and photostable dyes called C-BODIPYs, E-BODIPYs and O-BODIPYs, respectively (Figure 1.7, structures **20-22**).<sup>3a</sup> This strategy provides a platform to overcome the problems commonly associated with BODIPYs, i.e. small Stokes shifts and fluorescence quenching. Enhancement of the virtual Stokes shift ( $>10\ 000\ \text{cm}^{-1}$ ) can be realized by attaching one or more aromatic polycycles to the

BODIPY fluorophore. The main strategy here is to attach many light absorbing units in one molecule, so that there are many energy-donors but a single energy-acceptor, i.e. the BODIPY nucleus. In such “energy-cassettes”, illumination into the appended polycycle leads to rapid through-space energy-transfer from donor to the acceptor due to the significant overlap of the donor emission and acceptor absorption spectra. Furthermore, the substituents on E-BODIPYs do not affect the photophysical properties, unlike the case of BODIPYs, in which the spectral properties can be tuned over a wide range. The attached donors merely function as near UV-photon collectors. This method of  $\pi$ -conjugation extension of BODIPY dyes is currently being explored by Ziessel, Ulrich and Harriman, and many BODIPY scaffold-based molecular dyads, photovoltaics, electroluminescent devices, energy transfer cassettes and supramolecular assemblies have been realized so far.<sup>70</sup>

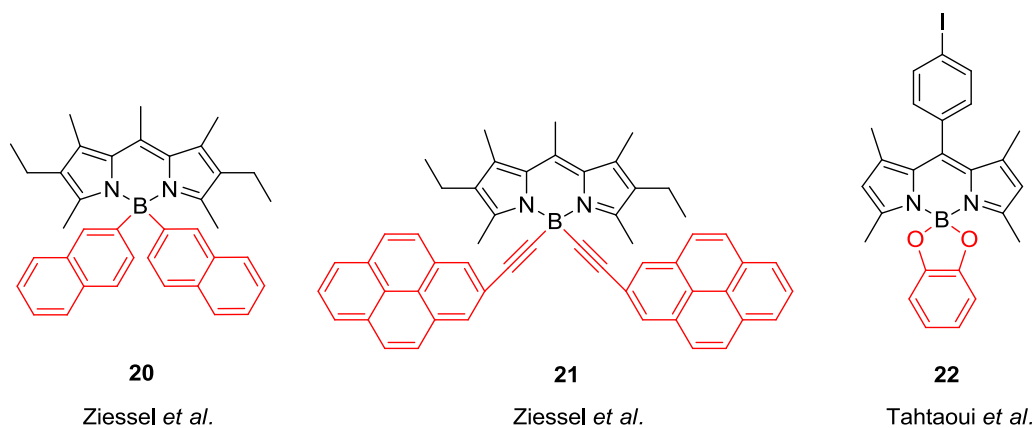


**Figure 1.7:** Chemical structures of various boron atom substituted BODIPYs from literature: **20**,<sup>3a</sup> **21**<sup>25a</sup> and **22**<sup>71</sup>

### 1.3.5: Rigidification by the ring fusion

Aromatic ring fusion is a promising strategy towards the generation of long emission BODIPY-based dyes with many possibilities for further functionalization.<sup>72</sup> The pioneer work in this field was carried out by Burgess et al. as they reported the synthesis of five conformationally

rigid BODIPY derivatives with heteroatom or ethylene bridge linkages (Figure 1.8, structure 23).<sup>73</sup> As the emission behavior of luminogens is greatly enhanced by the restricted intramolecular rotations and steric hindrance, these structurally constrained molecules were found to be more emissive than their unconstrained analogues.<sup>16</sup> Highly annelated-BODIPY dyes could also be generated by aromatic ring annulation at the  $\beta,\beta'$ -positions of the BODIPY core. This strategy has been exploited to generate BODIPYs fused with benzene,<sup>6</sup> substituted benzene,<sup>74</sup> phenanthrene<sup>72</sup>, dihydronaphthalene<sup>5</sup>, and spiro-fluorene moieties<sup>75</sup> starting from either aryl-fused pyrroles or 2-acetyl-phenols (e.g. 24 and 25).<sup>74</sup>

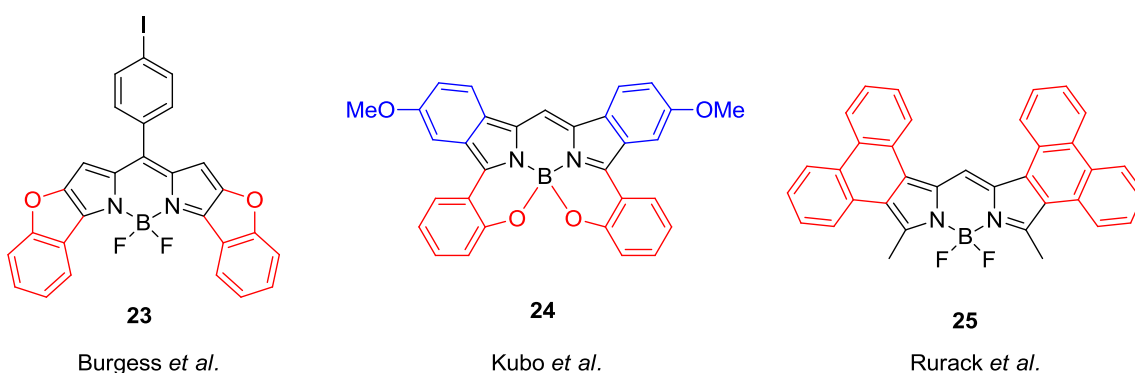


**Figure 1.8:** Chemical structures of rigidified BODIPYs from literature: 23,<sup>73</sup> 24,<sup>76</sup> and 25<sup>72</sup>

#### 1.4: Biological applications of the BODIPY dyes

A fluorescent dye (fluorophore) can act as an important reporting molecule when tagged to various analytes (proton or metal ions) or biomolecules (proteins, peptides, lipid membranes or nucleic acids). Fluorescent organic dyes are widely used as nonradioactive ligands in biological analysis or as biomarkers in *in vivo* imaging.<sup>77</sup> Dyes that fluoresce in the red or NIR region have attracted much attention over the past few decades because of rapid advancements in various bioanalytical and optical imaging techniques, such as DNA sequencing,



gel electrophoresis, nucleic acid detection, *in vivo* imaging, vascular mapping and tissue perfusion.<sup>19e</sup>

There are several advantages of working in the red/NIR region of the spectrum. Endogenous chromophores present in living tissues, such as water, lipids, oxy- and deoxyhemoglobin and other chemical compounds, absorb and scatter visible light, limiting its penetration to only a few millimeters. Due to this phenomenon of “tissue auto-fluorescence” a high background noise appears in the detection of biological samples, which obscures the signal collection and quantification, as demonstrated in Figure 1.9. Fortunately, the absorption coefficient of tissue is much lower for the NIR light, which permits its deeper penetration to depths of several centimeters.<sup>2c</sup>

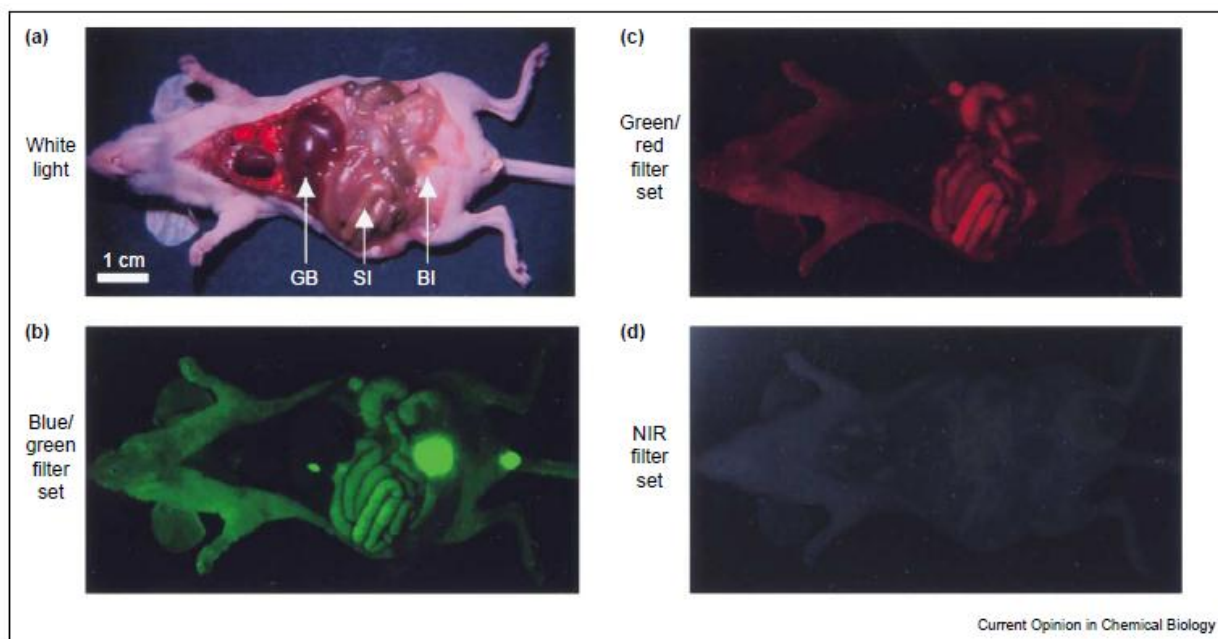


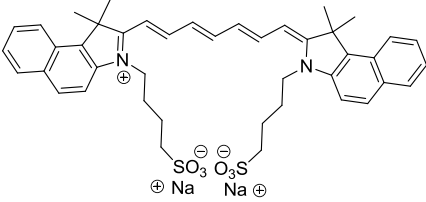
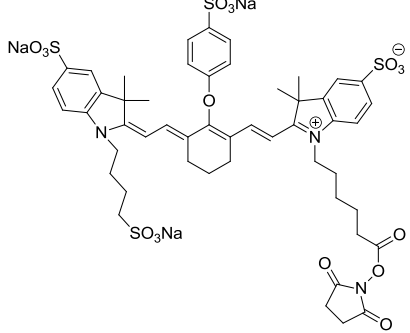
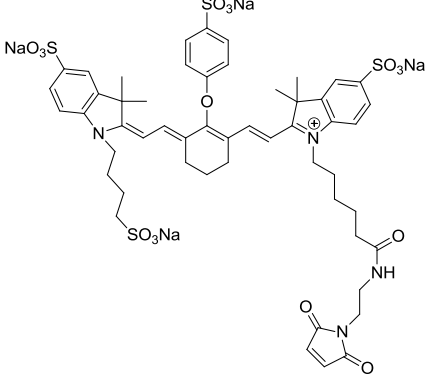
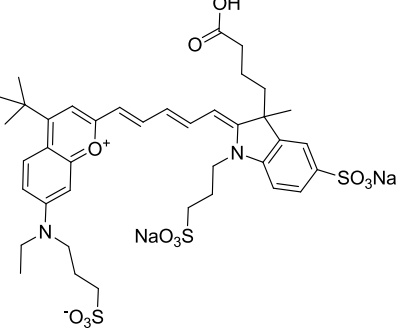
**Figure 1.9:** Tissue auto-fluorescence in the mouse using different excitation/emission filters; (GB: gall bladder, SI: small intestines, BI: bladder).<sup>78</sup> Reprinted with permission from [78] Copyright (2002) Elsevier

Additionally, the scattered light from the excitation source is greatly reduced in the NIR region since the scattering intensity is proportional to the inverse fourth power of the wavelength. Low background noise and low scattering of the NIR radiations result in a high signal to noise ratio, thereby allowing highly sensitive detection. Further advantages of red/NIR radiations include low interferences from Raman scattering and reduced possibility of sample degradation. Due to these combined attributes, this region of the electromagnetic spectrum (ca. 700-900 nm) is often referred to as the “Biological window.” These advantages along with the availability and low cost of long-wavelength diode lasers and detectors for the red/NIR light, has led to increasing research interest in the design, development, spectroscopic characterization and application of novel red/NIR-fluorescent labels, probes or indicators.

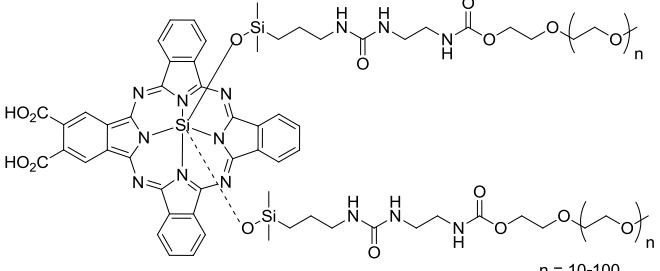
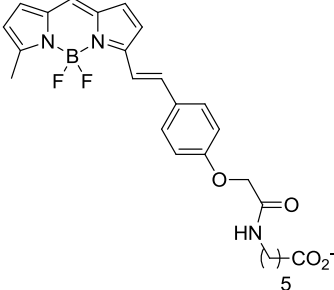
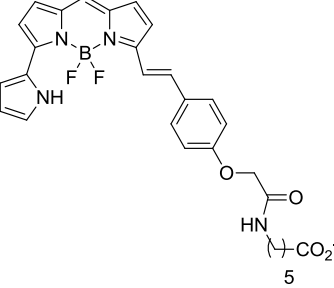
Besides the absorption and emission in the red or NIR region, an ideal NIR dye should possess high molar absorption coefficients, high fluorescence quantum yields, robustness against light and chemicals, good solubility, resistance towards self-aggregation, straightforward synthetic routes and possibility for further and facile functionalization for construction of fluorescent probes or indicators.<sup>1</sup>

Significant progress has been made towards the development of NIR fluorescent dyes based on cyanines, squaraine, phthalocyanine, porphyrin and BODIPY scaffolds, with improved photostability and fluorescence maxima ranging from 600-800 nm (Table 1.1). The principle limitations of most of these dyes are low quantum yields, poor photo- and/or chemical- stability and limited solubility in the aqueous media. So far, cyanine dyes form the main group of long-wavelength fluorophores pursued for use in biological systems and to date, indocyanine green [ICG: cardiogreen] is the only FDA and EMA-approved NIR imaging dye for medical use. It has been used for decades as an angiographic contrast agent with low toxicity and negligible side

**Table 1.1:** Some commercially available NIR dyes for conjugation to biomolecular targets

Dye name	Chemical Structure	Absorption max (nm)	Emission max (nm)
ICG (Sigma-Aldrich)		800	810
IRDye800CW NHS ester (LI-COR Biosciences)		778	794
IRDye800CW maleimide (LI-COR Biosciences)		778	794
DY-783 NHS ester (Dyomics GmbH.)		783	800

**Table 1.1:** (continued)

La Jolla Blue (Hyperion Inc.)		680	700
BODIPY 630/650 (Life Technologies Inc.)		625	640
BODIPY 650/665 (Life Technologies Inc.)		646	660

effects. Unfortunately, like other cyanine-based dyes, ICG also has a low quantum yield (0.3% in water and 1.2% in blood) and lacks additional functional group for conjugation to biomolecules.<sup>79</sup> IRDye<sup>®</sup>800CW is another promising next-generation NIR-fluorescent imaging dye. It is a reactive dye which is functionalized with either an NHS or a maleimide reactive group, allowing it to be attached to numerous targeting biomolecules.<sup>80</sup> This dye has been evaluated in several preclinical studies however, it lacks any clinical investigations.

As an emerging new class of fluorophores, BODIPY dyes have gained strong popularity as small molecule fluorescent stains, labels and indicators. Highly fluorescent BODIPY dyes combine many advantageous properties of NIR dyes such as high molar absorption coefficients

(typically  $\log \epsilon_{\max} < 8.8$ ), narrow and structured emission bandwidths (important in multicolor applications), negligible dependence on solvent polarity and small Stokes shifts. BODIPY dyes offer improved spectral characteristics compared with other conventional dyes. For instance, when compared with the positively charged cyanines and rhodamines, BODIPY dyes are electrically neutral and have relatively nonpolar structures.<sup>81</sup> The lack of a net ionic charge enhances the affinity of the BODIPY-labeled probes towards the targeted analyte or receptors. Fluorophores based on BODIPY scaffold have been developed for various biological applications, such as labels for biomolecules, indicators for proton and metal ions, stains for organelles and substrates for enzymes (Figure 1.10).

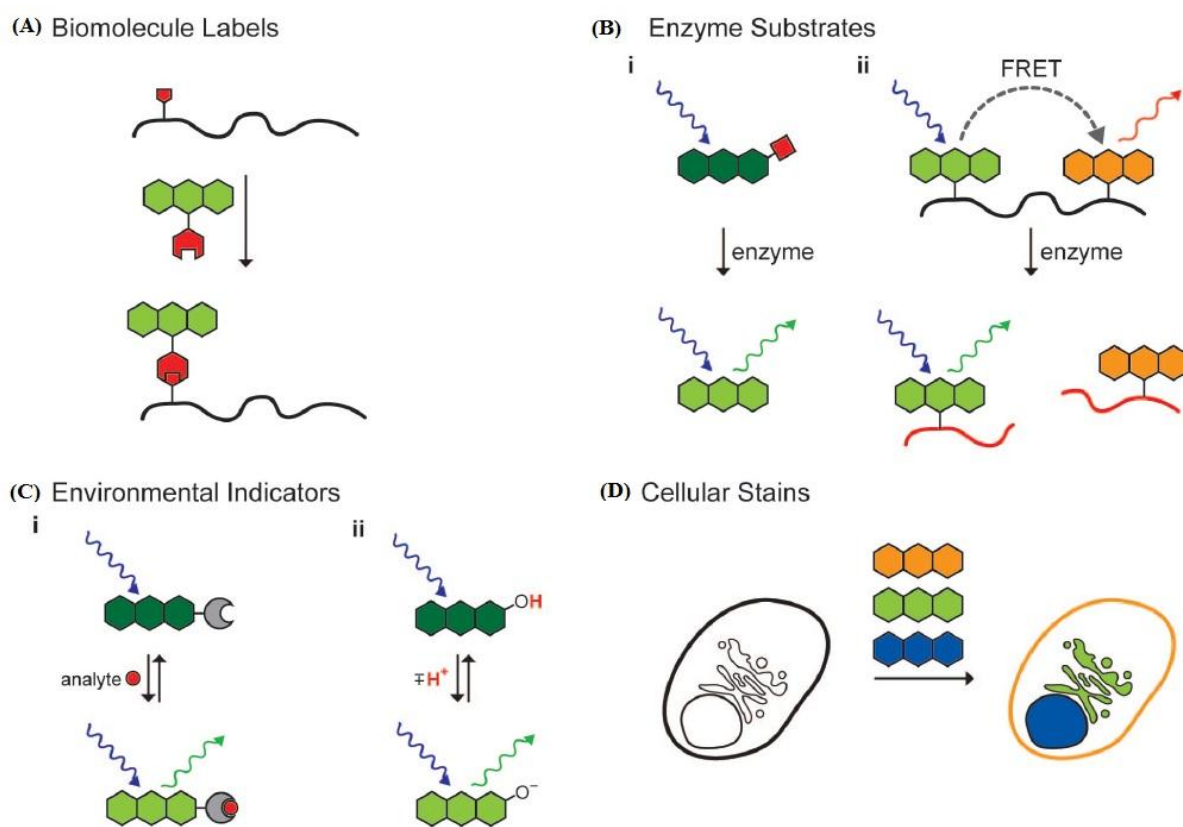


**Figure 1.10:** Various biological applications of small molecule fluorescent probes.<sup>82</sup> Reprinted with permission from [82] Copyright (2008) American Chemical Society

### 1.4.1: Biological Labels

There is a growing need for visualization and investigations of interactions between the proteins, enzymes and other biomolecules in living cells. As an organism lacks selective detectable signals, fluorescent labeling of biomolecules is often a powerful tool for this purpose. For example, labels can be attached to proteins for imaging events in cells and whole-organisms.

BODIPY dyes, due to their excellent physicochemical properties and low dark toxicities,<sup>40b</sup> are among the most promising candidates for fluorescent labels and probes. Also, these organic dyes do not significantly influence the biological functions, on account of their small molecular size. Numerous BODIPY-based fluorescent labels have been widely used to target biological compounds such as DNAs, RNAs, nucleotides, amino acids, lipids, polystyrene microspheres, dextran, and proteins.<sup>83 19c, 84</sup> In general, BODIPY-based probes are functionalized with reactive ligand/anchor groups at the end (such as carboxylic acids, sulphonic acids, polyethylene glycol, polysaccharides, oligonucleotides), for effective bio-conjugation.<sup>2d</sup> Ligand targeted BODIPYs have been developed for detection and visualization of various proteins including  $\beta$ -amyloid plaques,<sup>85</sup> unordered or ordered A $\beta$ 1-42 soluble oligomers<sup>86</sup> and neurofibrillary tangles (NFTs) tau proteins (Figure 1.11, structures 26 and 27).<sup>87</sup>

Due to their high peak intensity, fluorescent BODIPY probes are among the most readily detectable fluorophores available for various analytical techniques such as gel electrophoresis and DNA sequencing. Oligonucleotide conjugates of BODIPY fluorophores have been used in DNA sequencing as the small molecule fluorescent dye exhibits a minimal effect on the fragment mobility during electrophoresis.<sup>81</sup>

More recently, BODIPY derivatives have been evaluated as a totally new class of potent photodynamic therapy agents,<sup>14, 88</sup> an application more commonly associated with porphyrins

and phthalocyanines. These photosensitizers are based on the  $\text{BF}_2$ -chelated azadipyrromethene core structure with bromo and polyethylene glycol moieties to promote singlet oxygen generation (e.g. **28**).

Additionally, many fluorescent probes based on BODIPY platform are being employed in live cell labeling of biomolecules. A handful of potential BODIPY-based probes have been reported for both single and two photon microscopic imaging for much deeper analysis of the living tissue.<sup>89</sup> Wolfbeis et al.<sup>90</sup> reported the *in vivo* cellular labeling of biomolecules such as sugars, amino acids and nucleotides using a combination of copper free and copper-mediated click chemistry. In this approach, BODIPY-based clickable fluorophores were designed as non-native, non-perturbing “Bioorthogonal reporters” and used for labeling the azide modified surface glycans of CHO cells. In another report by Meijler and colleagues,<sup>91</sup> live cell fluorescent labeling of proteins (QS receptors) was carried out in a two-step bio-orthogonal labeling strategy using aniline-catalyzed oxime formation between the receptor and the BODIPY fluorophore (e.g. **29**).

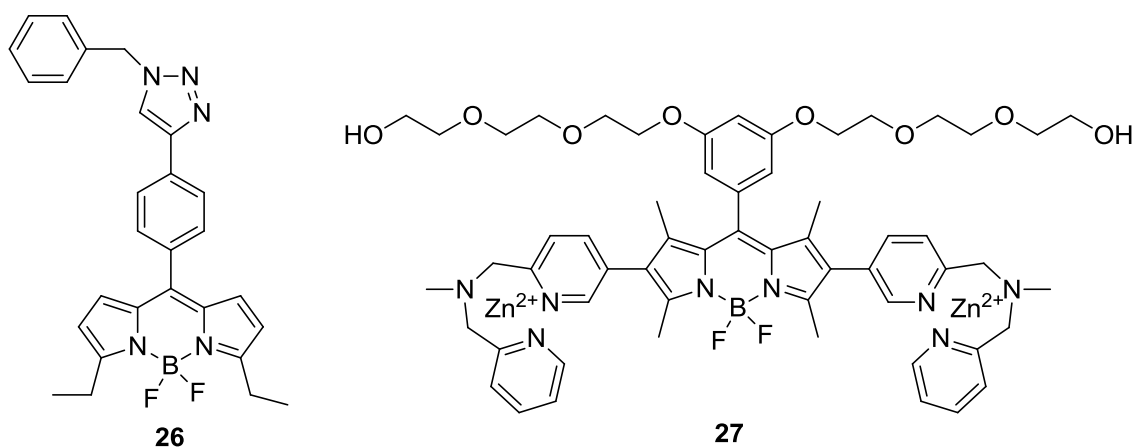


**Figure 1.11:** Some known examples of fluorescent BODIPY probes as biological labels, from the literature

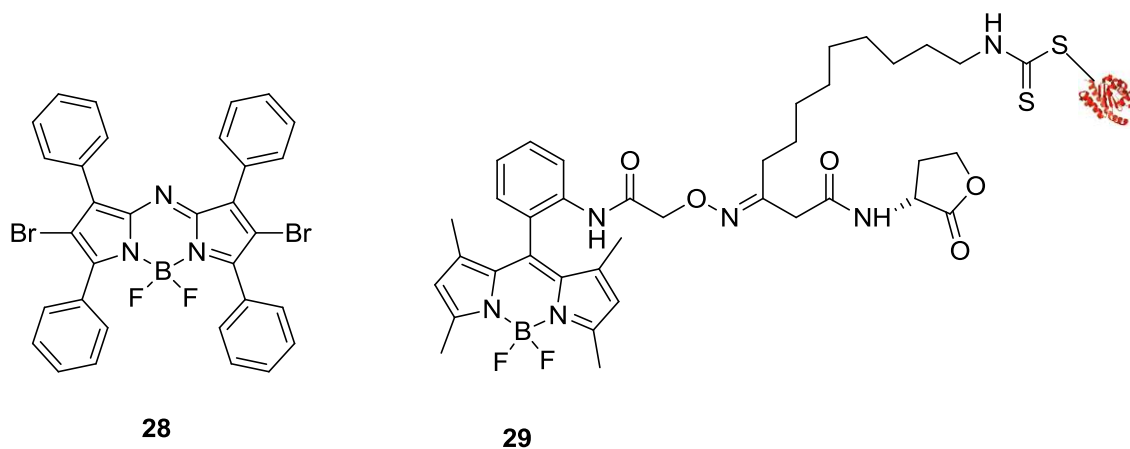


**Figure 1.11:** (continued)

### 1.4.2: Enzyme Substrates

Enzyme activity is often analyzed using fluorometric assays, which use the difference between the fluorescence of the substrate from the product to measure the enzymatic activities. Enzyme-substrates that contain BODIPY fluorophore have been employed in several fluorometric assays for measuring enzymatic activities of proteases, phospholipases, chloramphenicol acetyltransferases, amylase and other enzymes (Figure 1.12).<sup>92</sup> In 2009, Saba and co-workers<sup>93</sup> reported a new Sphingosine-1-phosphate lyase (SPL) assay to replace the standard radioactive SPL assay. In this fluorescent assay,  $\omega$ -labeled BODIPY-sphingosine-1-phosphate substrate was used to effectively measure the activity of the sphingosine-1-phosphate lyase in biological samples. BODIPY fluorophore has also been employed in designing of fluorometric assays for proteases based on Fluorescence Resonance Energy Transfer (FRET). The protease substrate in such assays is non-fluorescent due to phenomenon of “self-quenching”. Hydrolysis of the protein to smaller fragments is accompanied by a dramatic increase in the fluorescence due to disruption of intramolecular FRET quenching.<sup>94</sup> This forms the basis of a simple and continuum assay for a variety of proteases.



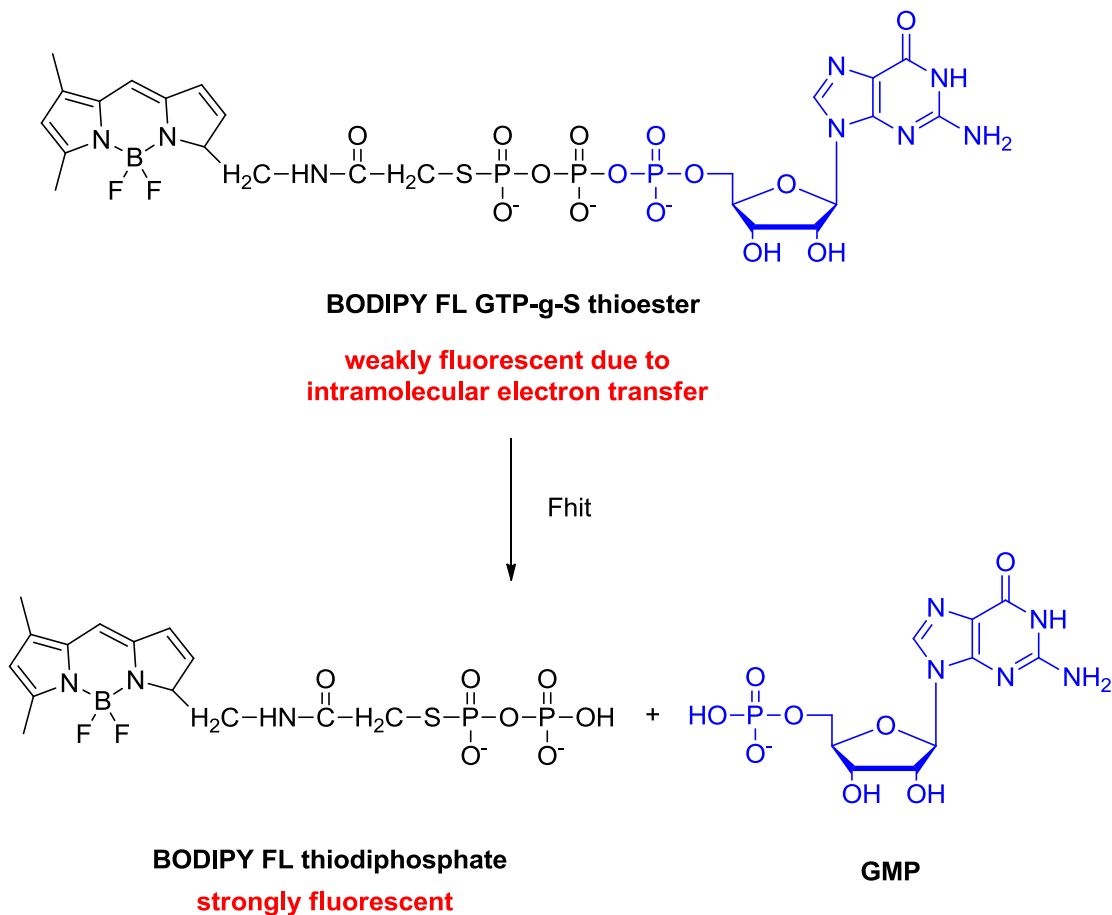


**Figure 1.12:** BODIPY dyes as enzyme substrate for the detection of Fhit, a nucleotide-binding protein<sup>92</sup>

### 1.4.3: Environmental Indicators

Intracellular pH and metal ions play a diverse and crucial role in several biological processes and disorders. As a result, design and construction of selective and sensitive fluorescent chemosensors have gained considerable research interest over the past decade.

Many fluorescent sensors are either constructed as fluorophore-spacer-receptor or as intrinsic fluorescent probes (where the receptor is part of the  $\pi$ -electron system of the fluorophore). Fluorophore-spacer-receptor systems operate on the basis of photoinduced electron transfer (PET) and internal charge transfer (ICT) processes, respectively. Binding of the analyte

(a metal or a proton) to the sensor is monitored by recording the alterations in either the fluorescence intensity or wavelength. In both sensors, the absence of the analyte quenches the luminescence due to PET or ICT in the excited state.<sup>83c</sup> In PET sensors, binding of the analyte inhibits the PET while increasing the fluorescence intensity, without much change in the spectral shift. In contrast, ICT sensor molecules show a moderate increase in their emission intensity accompanied with significant shifts in their optical spectra. Hence, in most cases, for sensitivity reasons, the interaction with the analyte is associated with the fluorescence “OFF/ON” switching. Though many PET sensor molecules have been developed based on fluorescence “ON/OFF” switching upon interaction with an analyte.<sup>48a</sup>

Organoboron compounds such as BODIPY dyes, have often displayed high potential as building blocks in synthesis of novel chemosensors for various colorimetric and fluorimetric assays.<sup>68b, 95</sup> A series of small molecule fluorescent BODIPY-based sensors have been reported for detection of protons, metal cations, anions and reactive-oxygen species.<sup>15</sup> These sensors are crucial for sensing and imaging pH,<sup>96</sup> K<sup>+</sup>,<sup>97</sup> Ni<sup>2+</sup>,<sup>98</sup> Cu<sup>2+</sup>,<sup>40c</sup> Zn<sup>2+</sup>,<sup>99</sup> Hg<sup>2+</sup>,<sup>28a</sup> etc metal ions in living cells (Figure 1.13). There are many examples of crown,<sup>97, 100</sup> cryptand,<sup>101</sup> podand,<sup>102</sup> 2,2'-dipyridyl,<sup>103</sup> calixarene,<sup>104</sup> p-(N,N-dialkyl)aniline<sup>41</sup>-based PET sensors for detection of protons, sodium, calcium, potassium and transition metal ions, respectively.

#### 1.4.4: Cellular Stains

Many biological samples, particularly cells are quite transparent when seen under the microscope. The internal parts of the cells, such as the organelles are so transparent that they are often difficult to see. Thus, visualization of the cell and its organelles with organelle specific antibodies or organelle specific stains, provide a better understanding of cellular morphology and

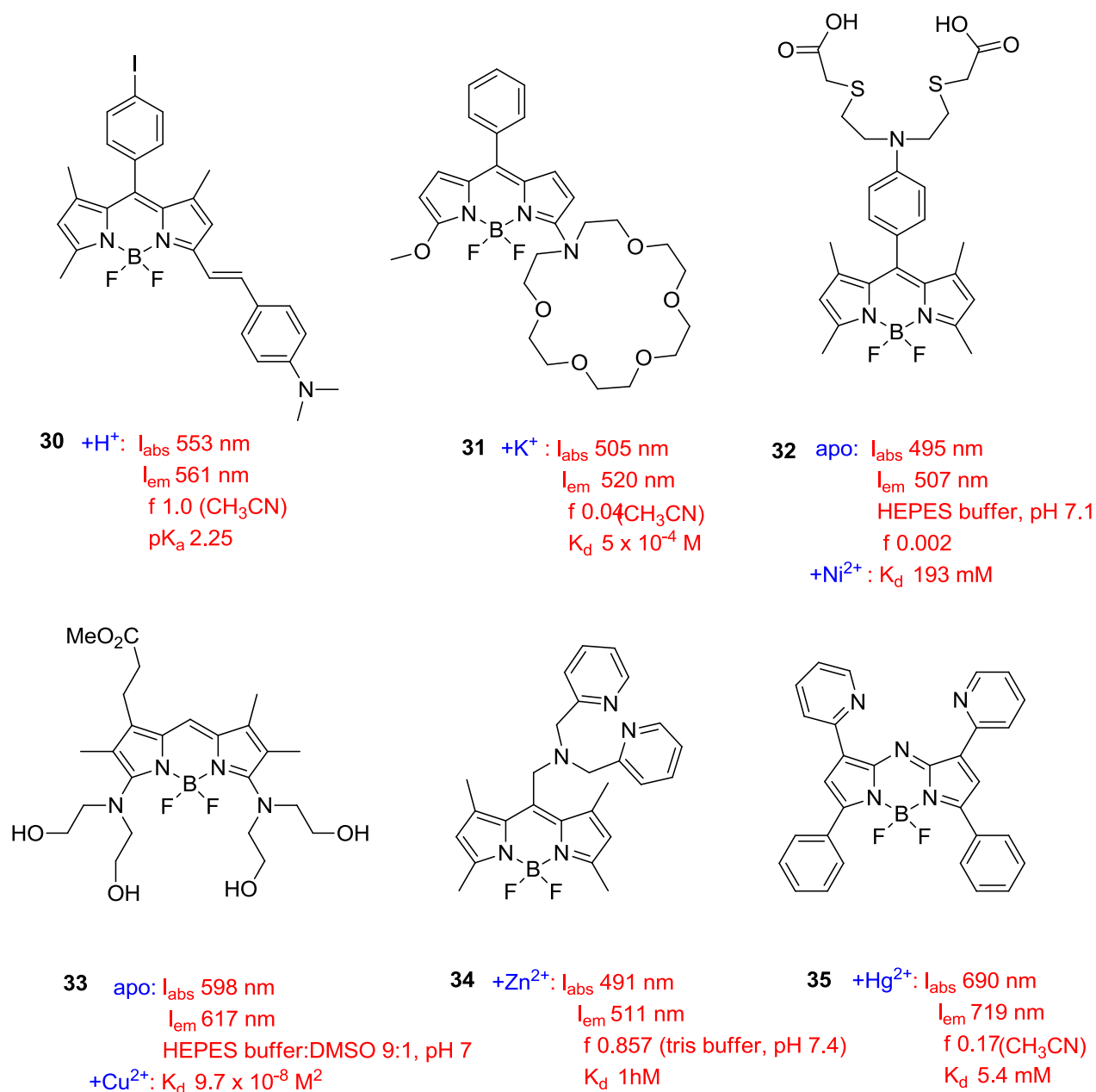


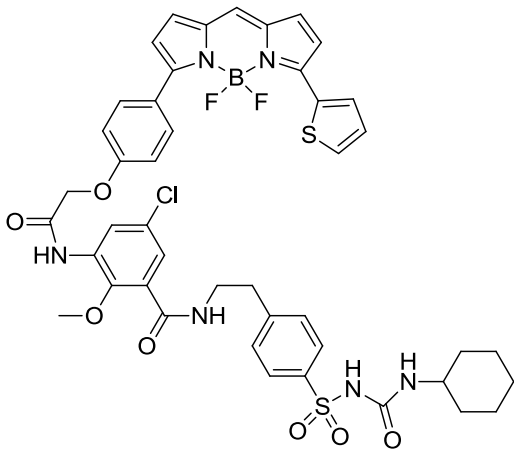
**Figure 1.13:** BODIPY based chemosensors<sup>1</sup> for H<sup>+</sup>, K<sup>+</sup>, Ni<sup>2+</sup>, Cu<sup>2+</sup>, Zn<sup>2+</sup> and Hg<sup>2+</sup>

functioning. Among the organelle specific stains, especially appealing are the small neutral dyes such as BODIPY derivatives that can pass through a viable cell membrane more efficiently than large molecules, and remain inside the cell depending on their reactivity and hydrophilicity.

A range of cell-permeant BODIPY dyes either as “conjugate” or as “reactive fluorophore”, have been employed for *in vitro* and *in vivo* visualization of intracellular organelles. For instance, the red fluorescent BODIPY TR-glibenclamide and BODIPY TR-ceramide (Life Technologies Inc., Figure 1.14, structures 36 and 37), are the best known commercially available structural markers for endoplasmic reticulum and Golgi apparatus, respectively. Additionally, numerous yellow or green fluorescent BODIPY-conjugates such as BODIPY FL-ceramide (e.g. 38), BODIPY FL C<sub>5</sub>-sphingomyelin (e.g. 39) and BODIPY-brefeldin A conjugates (e.g. 40), for live cell or fixed cell imaging and for flow cytometry, are covered by several patents issued to Life Technologies Inc. In general, these dyes absorb and emit at different wavelength ranges and the fluorescence emission of the dye does not change with its intracellular environment.<sup>105</sup> Low molecular weight BODIPY conjugates are often found to be more permanent in living cells than the conjugates of charged fluorophores and the staining at low concentrations, in general, does not appear to be toxic to the cells.<sup>92</sup>

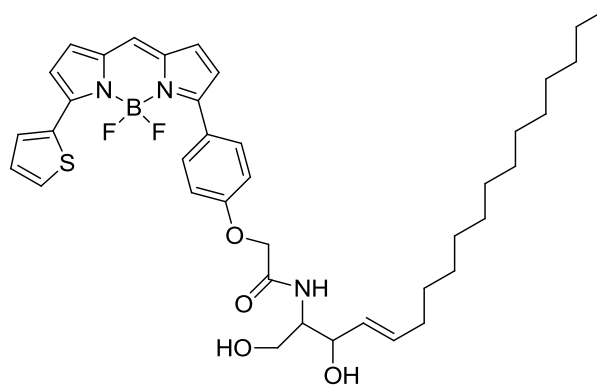
## 1.5: Research Outlook

Despite the innumerable advancements in the BODIPY-field, these fluorophores are far from being mature. The synthesis of BODIPY derivatives that absorb and emit in the red or NIR region of the electromagnetic spectrum and their conjugation to various target biomolecules, represent a long-standing challenge in the BODIPY biomarker community. For instance, most of the available BODIPY dyes and bioconjugates emit in the visible region (< 600 nm) and very few water-soluble BODIPY fluorophores have been reported in the literature. With these facts in mind, the synthesis, characterization and *in vitro* evaluations of novel red and NIR emissive BODIPY dyes and their bioconjugates will be discussed in the next Chapters.



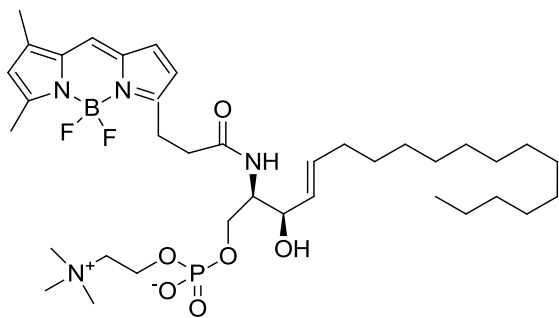
31

**BODIPY TR-glibenclamide**  
Abs/Ems = 587/615 nm



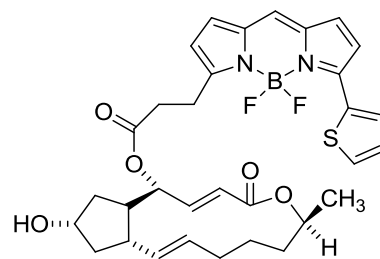
32

**BODIPY TR-ceramide**  
Abs/Ems = 592/618 nm



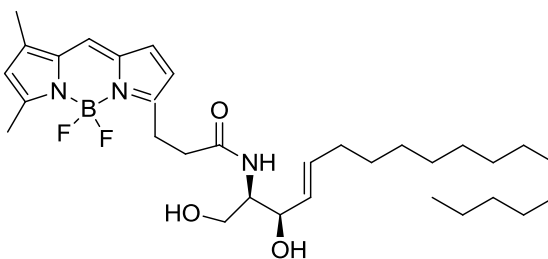
33

**BODIPY FL C<sub>5</sub>-sphingomyelin**



34

**BODIPY-brefeldin A**  
Abs/Ems = 558/568 nm



35

**BODIPY FL ceramide**  
Abs/Ems = 505/620 nm

**Figure 1.14:** Commercially available red fluorescent BODIPY probes for ER and Golgi apparatus labeling

## 1.6: References

1. Boens, N.; Leen, V.; Dehaen, W., Fluorescent indicators based on BODIPY. *Chemical Society Reviews* **2012**, *41* (3), 1130-1172.
2. (a) Escobedo, J. O.; Rusin, O.; Lim, S.; Strongin, R. M., NIR dyes for bioimaging applications. *Curr Opin Chem Biol* **2010**, *14* (1), 64-70; (b) Ntziachristos, V.; Bremer, C.; Weissleder, R., Fluorescence imaging with near-infrared light: new technological advances that enable in vivo molecular imaging. *Eur Radiol* **2003**, *13* (1), 195-208; (c) Amiot, C.; Xu, S.; Liang, S.; Pan, L.; Zhao, J., Near-Infrared Fluorescent Materials for Sensing of Biological Targets. *Sensors* **2008**, *8* (5), 3082-3105; (d) Niu, S. L.; Massif, C.; Ulrich, G.; Ziessel, R.; Renard, P. Y.; Romieu, A., Water-solubilisation and bio-conjugation of a red-emitting BODIPY marker. *Org Biomol Chem* **2011**, *9* (1), 66-9.
3. (a) Ziessel, R.; Ulrich, G.; Harriman, A., The chemistry of Bodipy: A new El Dorado for fluorescence tools. *New Journal of Chemistry* **2007**, *31* (4), 496-501; (b) Loudet, A.; Burgess, K., BODIPY dyes and their derivatives: syntheses and spectroscopic properties. *Chem Rev* **2007**, *107* (11), 4891-932.
4. Ulrich, G.; Ziessel, R.; Harriman, A., The Chemistry of Fluorescent Bodipy Dyes: Versatility Unsurpassed. *Angewandte Chemie International Edition* **2008**, *47* (7), 1184-1201.
5. Wang, Y. W.; Descalzo, A. B.; Shen, Z.; You, X. Z.; Rurack, K., Dihydronaphthalene-fused boron-dipyrromethene (BODIPY) dyes: insight into the electronic and conformational tuning modes of BODIPY fluorophores. *Chemistry* **2010**, *16* (9), 2887-903.
6. Shen, Z.; Rohr, H.; Rurack, K.; Uno, H.; Spieles, M.; Schulz, B.; Reck, G.; Ono, N., Boron-diindomethene (BDI) dyes and their tetrahydrobicyclo precursors--en route to a new class of highly emissive fluorophores for the red spectral range. *Chemistry* **2004**, *10* (19), 4853-71.
7. Zheng, Q.; Xu, G.; Prasad, P. N., Conformationally Restricted Dipyrromethene Boron Difluoride (BODIPY) Dyes: Highly Fluorescent, Multicolored Probes for Cellular Imaging. *Chemistry – A European Journal* **2008**, *14* (19), 5812-5819.
8. Qin, W.; Baruah, M.; De Borggraeve, W. M.; Boens, N., Photophysical properties of an on/off fluorescent pH indicator excitable with visible light based on a borondipyrromethene-linked phenol. *Journal of Photochemistry and Photobiology A: Chemistry* **2006**, *183* (1-2), 190-197.
9. Tram, K.; Yan, H.; Jenkins, H. A.; Vassiliev, S.; Bruce, D., The synthesis and crystal structure of unsubstituted 4,4-difluoro-4-bora-3a,4a-diaza-s-indacene (BODIPY). *Dyes and Pigments* **2009**, *82* (3), 392-395.
10. Arroyo, I. J.; Hu, R.; Merino, G.; Tang, B. Z.; Pena-Cabrera, E., The smallest and one of the brightest. Efficient preparation and optical description of the parent borondipyrromethene system. *J Org Chem* **2009**, *74* (15), 5719-22.

11. Schmitt, A.; Hinkeldey, B.; Wild, M.; Jung, G., Synthesis of the core compound of the BODIPY dye class: 4,4'-difluoro-4-bora-(3a,4a)-diazas-indacene. *Journal of fluorescence* **2009**, *19* (4), 755-8.
12. (a) Li, L.; Nguyen, B.; Burgess, K., Functionalization of the 4,4-difluoro-4-bora-3a,4a-diazas-indacene (BODIPY) core. *Bioorganic & medicinal chemistry letters* **2008**, *18* (10), 3112-6; (b) Thivierge, C.; Bandichhor, R.; Burgess, K., Spectral dispersion and water solubilization of BODIPY dyes via palladium-catalyzed C-H functionalization. *Organic letters* **2007**, *9* (11), 2135-8.
13. Shen, Z.; Röhr, H.; Rurack, K.; Uno, H.; Spieles, M.; Schulz, B.; Reck, G.; Ono, N., Boron-Diindomethene (BDI) Dyes and Their Tetrahydrobicyclo Precursors—en Route to a New Class of Highly Emissive Fluorophores for the Red Spectral Range. *Chemistry – A European Journal* **2004**, *10* (19), 4853-4871.
14. Yogo, T.; Urano, Y.; Ishitsuka, Y.; Maniwa, F.; Nagano, T., Highly Efficient and Photostable Photosensitizer Based on BODIPY Chromophore. *Journal of the American Chemical Society* **2005**, *127* (35), 12162-12163.
15. Boens, N.; Leen, V.; Dehaen, W., Fluorescent indicators based on BODIPY. *Chem Soc Rev* **2012**, *41* (3), 1130-72.
16. Hu, R.; Lager, E.; Aguilar-Aguilar, A. I.; Liu, J.; Lam, J. W. Y.; Sung, H. H. Y.; Williams, I. D.; Zhong, Y.; Wong, K. S.; Peña-Cabrera, E.; Tang, B. Z., Twisted Intramolecular Charge Transfer and Aggregation-Induced Emission of BODIPY Derivatives. *The Journal of Physical Chemistry C* **2009**, *113* (36), 15845-15853.
17. Treibs, A.; Kreuzer, F.-H., Difluoroboryl-Komplexe von Di- und Tripyrrylmethenen. *Justus Liebigs Annalen der Chemie* **1968**, *718* (1), 208-223.
18. Wories, H. J.; Koek, J. H.; Lodder, G.; Lugtenburg, J.; Fokkens, R.; Driessen, O.; Mohn, G. R., A novel water-soluble fluorescent probe: Synthesis, luminescence and biological properties of the sodium salt of the 4-sulfonato-3,3',5,5'-tetramethyl-2,2'-pyrromethen-1,1'-BF<sub>2</sub> complex. *Recueil des Travaux Chimiques des Pays-Bas* **1985**, *104* (11), 288-291.
19. (a) Sathyamoorthi, G.; Boyer, J. H.; Allik, T. H.; Chandra, S., Laser active cyanopyrromethene-BF<sub>2</sub> complexes. *Heteroatom Chemistry* **1994**, *5* (4), 403-407; (b) Johnson, I. D.; Kang, H. C.; Haugland, R. P., Fluorescent membrane probes incorporating dipyrrometheneboron difluoride fluorophores. *Analytical Biochemistry* **1991**, *198* (2), 228-237; (c) Karolin, J.; Johansson, L. B. A.; Strandberg, L.; Ny, T., Fluorescence and Absorption Spectroscopic Properties of Dipyrrometheneboron Difluoride (BODIPY) Derivatives in Liquids, Lipid Membranes, and Proteins. *Journal of the American Chemical Society* **1994**, *116* (17), 7801-7806; (d) Schade, S. Z.; Jolley, M. E.; Sarauer, B. J.; Simonson, L. G., BODIPY- $\alpha$ -Casein, a pH-Independent Protein Substrate for Protease Assays Using Fluorescence Polarization. *Analytical Biochemistry* **1996**, *243* (1), 1-7; (e) Haugland, R. P., *The Handbook, A Guide to Fluorescent Probes and Labeling Technologies*. 10th ed.; Invitrogen Corp.: Eugene, OR, 2005.

20. (a) Ariano, M. A.; Monsma, F. J., Jr.; Barton, A. C.; Kang, H. C.; Haugland, R. P.; Sibley, D. R., Direct visualization and cellular localization of D1 and D2 dopamine receptors in rat forebrain by use of fluorescent ligands. *Proceedings of the National Academy of Sciences of the United States of America* **1989**, *86* (21), 8570-4; (b) Monsma, F. J., Jr.; Barton, A. C.; Kang, H. C.; Brassard, D. L.; Haugland, R. P.; Sibley, D. R., Characterization of novel fluorescent ligands with high affinity for D1 and D2 dopaminergic receptors. *Journal of neurochemistry* **1989**, *52* (5), 1641-4.
21. (a) Benniston, A. C.; Copley, G., Lighting the way ahead with boron dipyrromethene (Bodipy) dyes. *Physical chemistry chemical physics : PCCP* **2009**, *11* (21), 4124-31; (b) Descalzo, A. B.; Xu, H. J.; Shen, Z.; Rurack, K., Red/near-infrared boron-dipyrromethene dyes as strongly emitting fluorophores. *Annals of the New York Academy of Sciences* **2008**, *1130*, 164-71.
22. (a) Mula, S.; Ray, A. K.; Banerjee, M.; Chaudhuri, T.; Dasgupta, K.; Chattopadhyay, S., Design and development of a new pyrromethene dye with improved photostability and lasing efficiency: theoretical rationalization of photophysical and photochemical properties. *J Org Chem* **2008**, *73* (6), 2146-54; (b) Chen, T.; Boyer, J. H.; Trudell, M. L., Synthesis of 2,6-diethyl-3-methacroyloxymethyl-1,5,7,8-tetramethylpyrromethene-BF<sub>2</sub> for the preparation of new solid-state laser dyes. *Heteroatom Chemistry* **1997**, *8* (1), 51-54; (c) Sathyamoorthi, G.; Wolford, L. T.; Haag, A. M.; Boyer, J. H., Selective side-chain oxidation of peralkylated pyrromethene-BF<sub>2</sub> complexes. *Heteroatom Chemistry* **1994**, *5* (3), 245-249.
23. (a) Merino, E. J.; Weeks, K. M., Facile Conversion of Aptamers into Sensors Using a 2'-Ribose-Linked Fluorophore. *Journal of the American Chemical Society* **2005**, *127* (37), 12766-12767; (b) Meng, Q.; Kim, D. H.; Bai, X.; Bi, L.; Turro, N. J.; Ju, J., Design and Synthesis of a Photocleavable Fluorescent Nucleotide 3'-O-Allyl-dGTP-PC-Bodipy-FL-510 as a Reversible Terminator for DNA Sequencing by Synthesis. *The Journal of Organic Chemistry* **2006**, *71* (8), 3248-3252.
24. (a) Peters, C.; Billich, A.; Ghobrial, M.; Högenauer, K.; Ullrich, T.; Nussbaumer, P., Synthesis of Borondipyrromethene (BODIPY)-Labeled Sphingosine Derivatives by Cross-metathesis Reaction. *The Journal of Organic Chemistry* **2007**, *72* (5), 1842-1845; (b) Li, Z.; Mintzer, E.; Bittman, R., First Synthesis of Free Cholesterol-BODIPY Conjugates. *The Journal of Organic Chemistry* **2006**, *71* (4), 1718-1721; (c) Merino, E. J.; Weeks, K. M., Facile Conversion of Aptamers into Sensors Using a 2'-Ribose-Linked Fluorophore. *Journal of the American Chemical Society* **2005**, *127* (37), 12766-12767.
25. (a) Ulrich, G.; Goze, C.; Guardigli, M.; Roda, A.; Ziessel, R., Pyrromethene Dialkynyl Borane Complexes for "Cascatelle" Energy Transfer and Protein Labeling. *Angewandte Chemie International Edition* **2005**, *44* (24), 3694-3698; (b) Loudet, A.; Bandichhor, R.; Wu, L.; Burgess, K., Functionalized BF<sub>2</sub> chelated azadipyrromethene dyes. *Tetrahedron* **2008**, *64* (17), 3642-3654; (c) Tan, K.; Jaquinod, L.; Paolesse, R.; Nardis, S.; Di Natale, C.; Di Carlo, A.; Prodi, L.; Montalti, M.; Zaccheroni, N.; Smith, K. M., Synthesis and characterization of  $\beta$ -fused porphyrin-BODIPY® dyads. *Tetrahedron* **2004**, *60* (5), 1099-1106; (d) Li, F.; Yang, S. I.; Ciringh, Y.; Seth, J.; Martin, C. H.; Singh, D. L.; Kim, D.; Birge, R. R.; Bocian, D. F.; Holten, D.; Lindsey, J. S., Design, Synthesis, and Photodynamics of Light-Harvesting Arrays Comprised



of a Porphyrin and One, Two, or Eight Boron-Dipyrin Accessory Pigments. *Journal of the American Chemical Society* **1998**, *120* (39), 10001-10017.

26. (a) He, H.; Lo, P. C.; Yeung, S. L.; Fong, W. P.; Ng, D. K., Synthesis and in vitro photodynamic activities of pegylated distyryl boron dipyrromethene derivatives. *J Med Chem* **2011**, *54* (8), 3097-102; (b) Bura, T.; Retailleau, P.; Ulrich, G.; Ziessel, R., Highly substituted Bodipy dyes with spectroscopic features sensitive to the environment. *J Org Chem* **2011**, *76* (4), 1109-17; (c) Erbas, S.; Gorgulu, A.; Kocakusakogullari, M.; Akkaya, E. U., Non-covalent functionalized SWNTs as delivery agents for novel Bodipy-based potential PDT sensitizers. *Chem Commun* **2009**, *7* (33), 4956-8.

27. (a) Lammi, R. K.; Ambroise, A.; Balasubramanian, T.; Wagner, R. W.; Bocian, D. F.; Holten, D.; Lindsey, J. S., Structural Control of Photoinduced Energy Transfer between Adjacent and Distant Sites in Multiporphyrin Arrays. *Journal of the American Chemical Society* **2000**, *122* (31), 7579-7591; (b) Ambroise, A.; Kirmaier, C.; Wagner, R. W.; Loewe, R. S.; Bocian, D. F.; Holten, D.; Lindsey, J. S., Weakly Coupled Molecular Photonic Wires: Synthesis and Excited-State Energy-Transfer Dynamics. *The Journal of Organic Chemistry* **2002**, *67* (11), 3811-3826.

28. (a) Coskun, A.; Akkaya, E. U., Ion Sensing Coupled to Resonance Energy Transfer: A Highly Selective and Sensitive Ratiometric Fluorescent Chemosensor for Ag(I) by a Modular Approach. *Journal of the American Chemical Society* **2005**, *127* (30), 10464-10465; (b) Zeng, L.; Miller, E. W.; Pralle, A.; Isacoff, E. Y.; Chang, C. J., A Selective Turn-On Fluorescent Sensor for Imaging Copper in Living Cells. *Journal of the American Chemical Society* **2005**, *128* (1), 10-11; (c) Peng, X.; Du, J.; Fan, J.; Wang, J.; Wu, Y.; Zhao, J.; Sun, S.; Xu, T., A Selective Fluorescent Sensor for Imaging Cd<sup>2+</sup> in Living Cells. *Journal of the American Chemical Society* **2007**, *129* (6), 1500-1501.

29. (a) Krumova, K.; Oleynik, P.; Karam, P.; Cosa, G., Phenol-Based Lipophilic Fluorescent Antioxidant Indicators: A Rational Approach. *The Journal of Organic Chemistry* **2009**, *74* (10), 3641-3651; (b) Yuan, M.; Zhou, W.; Liu, X.; Zhu, M.; Li, J.; Yin, X.; Zheng, H.; Zuo, Z.; Ouyang, C.; Liu, H.; Li, Y.; Zhu, D., A Multianalyte Chemosensor on a Single Molecule: Promising Structure for an Integrated Logic Gate. *The Journal of Organic Chemistry* **2008**, *73* (13), 5008-5014; (c) Wang, J.; Qian, X., A Series of Polyamide Receptor Based PET Fluorescent Sensor Molecules: Positively Cooperative Hg<sup>2+</sup> Ion Binding with High Sensitivity. *Organic letters* **2006**, *8* (17), 3721-3724.

30. (a) Kim, B.; Ma, B.; Donuru, V. R.; Liu, H.; Frechet, J. M. J., Bodipy-backboned polymers as electron donor in bulk heterojunction solar cells. *Chemical Communications* **2010**, *46* (23), 4148-4150; (b) Rousseau, T.; Cravino, A.; Bura, T.; Ulrich, G.; Ziessel, R.; Roncali, J., BODIPY derivatives as donor materials for bulk heterojunction solar cells. *Chemical Communications* **2009**, (13), 1673-1675.

31. (a) Rousseau, T.; Cravino, A.; Ripaud, E.; Leriche, P.; Rihn, S.; De Nicola, A.; Ziessel, R.; Roncali, J., A tailored hybrid BODIPY-oligothiophene donor for molecular bulk heterojunction solar cells with improved performances. *Chem Commun* **2010**, *46* (28), 5082-4; (b) Wang, J.-B.; Fang, X.-Q.; Pan, X.; Dai, S.-Y.; Song, Q.-H., New 2, 6-Modified Bodipy Sensitizers for Dye-Sensitized Solar Cells. *Chemistry – An Asian Journal* **2012**, *7* (4), 696-700.

32. Peña-Cabrera, E.; Aguilar-Aguilar, A.; González-Domínguez, M.; Lager, E.; Zamudio-Vázquez, R.; Godoy-Vargas, J.; Villanueva-García, F., Simple, General, and Efficient Synthesis of Meso-Substituted Borondipyrromethenes from a Single Platform. *Organic letters* **2007**, *9* (20), 3985-3988.
33. Goud, T. V.; Tutar, A.; Biellmann, J.-F., Synthesis of 8-heteroatom-substituted 4,4-difluoro-4-bora-3a,4a-diaza-s-indacene dyes (BODIPY). *Tetrahedron* **2006**, *62* (21), 5084-5091.
34. Wood, T. E.; Thompson, A., Advances in the chemistry of dipyrins and their complexes. *Chem Rev* **2007**, *107* (5), 1831-61.
35. (a) Jackson, A. H.; Pandey, R. K.; Nagaraja Rao, K. R.; Roberts, E., Reactions on solid supports part II: a convenient method for synthesis of pyrromethanes using a montmorillonite clay as catalyst. *Tetrahedron Letters* **1985**, *26* (6), 793-796; (b) Bari, S. E.; Iturraspe, J.; Frydman, B., Synthesis of biliverdins with stable extended conformations. Part II. *Tetrahedron* **1995**, *51* (8), 2255-2266.
36. Wu, L.; Burgess, K., A new synthesis of symmetric boraindacene (BODIPY) dyes. *Chem Commun* **2008**, *28* (40), 4933-5.
37. Wood, T. E.; Thompson, A., Advances in the Chemistry of Dipyrins and Their Complexes. *Chemical Reviews* **2007**, *107* (5), 1831-1861.
38. Umezawa, K.; Matsui, A.; Nakamura, Y.; Citterio, D.; Suzuki, K., Bright, color-tunable fluorescent dyes in the Vis/NIR region: establishment of new "tailor-made" multicolor fluorophores based on borondipyrromethene. *Chemistry* **2009**, *15* (5), 1096-106.
39. Li, L.; Han, J.; Nguyen, B.; Burgess, K., Syntheses and spectral properties of functionalized, water-soluble BODIPY derivatives. *J Org Chem* **2008**, *73* (5), 1963-70.
40. (a) Uppal, T.; Hu, X.; Fronczek, F. R.; Maschek, S.; Bobadova-Parvanova, P.; Vicente, M. G. H., Synthesis, Computational Modeling, and Properties of Benzo-Appended BODIPYs. *Chemistry – A European Journal* **2012**, *18* (13), 3893-3905; (b) Jiao, L.; Yu, C.; Uppal, T.; Liu, M.; Li, Y.; Zhou, Y.; Hao, E.; Hu, X.; Vicente, M. G. H., Long wavelength red fluorescent dyes from 3,5-diiodo-BODIPYs. *Organic & Biomolecular Chemistry* **2010**, *8* (11), 2517-2519; (c) Jiao, L.; Li, J.; Zhang, S.; Wei, C.; Hao, E.; Vicente, M. G. H., A selective fluorescent sensor for imaging Cu<sup>2+</sup> in living cells. *New Journal of Chemistry* **2009**, *33* (9), 1888-1893.
41. Rurack, K.; Kollmannsberger, M.; Daub, J., Molecular Switching in the Near Infrared (NIR) with a Functionalized Boron-Dipyrromethene Dye. *Angewandte Chemie International Edition* **2001**, *40* (2), 385-387.
42. Atilgan, S.; Ozdemir, T.; Akkaya, E. U., Selective Hg(II) sensing with improved Stokes shift by coupling the internal charge transfer process to excitation energy transfer. *Organic letters* **2010**, *12* (21), 4792-5.
43. Murtagh, J.; Frimannsson, D. O.; O'Shea, D. F., Azide conjugatable and pH responsive near-infrared fluorescent imaging probes. *Organic letters* **2009**, *11* (23), 5386-9.

44. Zhao, W.; Carreira, E. M., Conformationally restricted aza-BODIPY: highly fluorescent, stable near-infrared absorbing dyes. *Chemistry* **2006**, *12* (27), 7254-63.
45. Baruah, M.; Qin, W.; Flors, C.; Hofkens, J.; Vallée, R. A. L.; Beljonne, D.; Van der Auweraer, M.; De Borggraeve, W. M.; Boens, N., Solvent and pH Dependent Fluorescent Properties of a Dimethylaminostyryl Borondipyrromethene Dye in Solution. *The Journal of Physical Chemistry A* **2006**, *110* (18), 5998-6009.
46. Jiao, L.; Yu, C.; Li, J.; Wang, Z.; Wu, M.; Hao, E.,  $\beta$ -Formyl-BODIPYs from the Vilsmeier–Haack Reaction. *The Journal of Organic Chemistry* **2009**, *74* (19), 7525-7528.
47. Ulrich, G.; Ziessel, R., Convenient and efficient synthesis of functionalized oligopyridine ligands bearing accessory pyrromethene-BF<sub>2</sub> fluorophores. *J Org Chem* **2004**, *69* (6), 2070-83.
48. (a) Móczár, I.; Huszthy, P.; Maidics, Z.; Kádár, M.; Klára, T., Synthesis and optical characterization of novel enantiopure BODIPY linked azacrown ethers as potential fluorescent chemosensors. *Tetrahedron* **2009**, *65* (39), 8250-8258; (b) Gossauer, A.; Nydegger, F.; Kiss, T.; Slezniak, R.; Stoeckli-Evans, H., Synthesis, chiroptical properties, and solid-state structure determination of two new chiral dipyrin difluoroboryl chelates. *Journal of the American Chemical Society* **2004**, *126* (6), 1772-80.
49. (a) Zrig, S.; Remy, P.; Andrioletti, B.; Rose, E.; Asselberghs, I.; Clays, K., Engineering tuneable light-harvesting systems with oligothiophene donors and mono- or bis-bodipy acceptors. *J Org Chem* **2008**, *73* (4), 1563-6; (b) Ziessel, R.; Bonardi, L.; Ulrich, G., Boron dipyrromethene dyes: a rational avenue for sensing and light emitting devices. *Dalton Trans* **2006**, *21* (23), 2913-8; (c) Wu, L.; Loudet, A.; Barhoumi, R.; Burghardt, R. C.; Burgess, K., Fluorescent cassettes for monitoring three-component interactions in vitro and in living cells. *Journal of the American Chemical Society* **2009**, *131* (26), 9156-7.
50. Baruah, M.; Qin, W.; Basaric, N.; De Borggraeve, W. M.; Boens, N., BODIPY-based hydroxyaryl derivatives as fluorescent pH probes. *J Org Chem* **2005**, *70* (10), 4152-7.
51. McDonnell, S. O.; O'Shea, D. F., Near-infrared sensing properties of dimethylamino-substituted BF<sub>2</sub>-azadipyrromethenes. *Organic letters* **2006**, *8* (16), 3493-6.
52. Loudet, A.; Bandichhor, R.; Burgess, K.; Palma, A.; McDonnell, S. O.; Hall, M. J.; O'Shea, D. F., B,O-chelated azadipyrromethenes as near-IR probes. *Organic letters* **2008**, *10* (21), 4771-4.
53. Coskun, A.; Yilmaz, M. D.; Akkaya, E. U., Bis(2-pyridyl)-substituted borotriazaindacene as an NIR-emitting chemosensor for Hg(II). *Organic letters* **2007**, *9* (4), 607-9.
54. (a) Gresser, R.; Hartmann, H.; Wrackmeyer, M.; Leo, K.; Riede, M., Synthesis of thiophene-substituted aza-BODIPYs and their optical and electrochemical properties. *Tetrahedron* **2011**, *67* (37), 7148-7155; (b) Adarsh, N.; Avirah, R. R.; Ramaiah, D., Tuning photosensitized singlet oxygen generation efficiency of novel aza-BODIPY dyes. *Organic letters* **2010**, *12* (24), 5720-3.

55. Li, Y.; Dolphin, D.; Patrick, B. O., Synthesis of a BF<sub>2</sub> complex of indol-2-yl-isoindol-1-ylidene-amine: a fully conjugated azadipyrromethene. *Tetrahedron Letters* **2010**, *51* (5), 811-814.
56. (a) Palma, A.; Tasiar, M.; Frimannsson, D. O.; Vu, T. T.; Meallet-Renault, R.; O'Shea, D. F., New on-bead near-infrared fluorophores and fluorescent sensor constructs. *Organic letters* **2009**, *11* (16), 3638-41; (b) Yoshii, R.; Nagai, A.; Chujo, Y., Highly near-infrared photoluminescence from aza-borondipyrromethene-based conjugated polymers. *Journal of Polymer Science Part A: Polymer Chemistry* **2010**, *48* (23), 5348-5356.
57. Zaitsev, A. B.; Méallet-Renault, R.; Schmidt, E. Y.; Mikhaleva, A. b. I.; Badré, S.; Dumas, C.; Vasil'tsov, A. M.; Zorina, N. V.; Pansu, R. B., Synthesis of 2-mesityl-3-methylpyrrole via the Trofimov reaction for a new BODIPY with hindered internal rotation. *Tetrahedron* **2005**, *61* (10), 2683-2688.
58. Wan, C.-W.; Burghart, A.; Chen, J.; Bergström, F.; Johansson, L. B. Å.; Wolford, M. F.; Kim, T. G.; Topp, M. R.; Hochstrasser, R. M.; Burgess, K., Anthracene–BODIPY Cassettes: Syntheses and Energy Transfer. *Chemistry – A European Journal* **2003**, *9* (18), 4430-4441.
59. Yamada, K.; Toyota, T.; Takakura, K.; Ishimaru, M.; Sugawara, T., Preparation of BODIPY probes for multicolor fluorescence imaging studies of membrane dynamics. *New Journal of Chemistry* **2001**, *25* (5), 667-669.
60. Pavlopoulos, T. G.; Boyer, J. H.; Shah, M.; Thangaraj, K.; Soong, M.-L., Laser action from 2,6,8-position trisubstituted 1,3,5,7-tetramethylpyrromethene-BF<sub>2</sub> complexes: part 1. *Appl. Opt.* **1990**, *29* (27), 3885-3886.
61. Haugland, R. P.; Kang, H. C. Reactive fluorescent dipyrrometheneboron difluoride dyes as molecular probes for biopolymers. 1988.
62. Zhou, C.; Nagy, G.; Walker, A. V., Toward molecular electronic circuitry: selective deposition of metals on patterned self-assembled monolayer surfaces. *Journal of the American Chemical Society* **2005**, *127* (35), 12160-1.
63. (a) Cakmak, Y.; Akkaya, E. U., Phenylethynyl-BODIPY oligomers: bright dyes and fluorescent building blocks. *Organic letters* **2009**, *11* (1), 85-8; (b) Thivierge, C.; Loudet, A.; Burgess, K., Brilliant BODIPY-fluorene Copolymers With Dispersed Absorption and Emission Maxima. *Macromolecules* **2011**, *44* (10), 4012-4015; (c) Chase, D. T.; Young, B. S.; Haley, M. M., Incorporating BODIPY fluorophores into tetrakis(arylethynyl)benzenes. *J Org Chem* **2011**, *76* (10), 4043-51; (d) Lee, J.-I.; Klaerner, G.; Davey, M. H.; Miller, R. D., Color tuning in polyfluorenes by copolymerization with low band gap comonomers. *Synthetic Metals* **1999**, *102* (1–3), 1087-1088.
64. Li, L.; Han, J.; Nguyen, B.; Burgess, K., Syntheses and Spectral Properties of Functionalized, Water-Soluble BODIPY Derivatives. *The Journal of Organic Chemistry* **2008**, *73* (5), 1963-1970.

65. Thivierge, C.; Bandichhor, R.; Burgess, K., Spectral Dispersion and Water Solubilization of BODIPY Dyes via Palladium-Catalyzed C–H Functionalization. *Organic letters* **2007**, *9* (11), 2135-2138.
66. Rohand, T.; Baruah, M.; Qin, W.; Boens, N.; Dehaen, W., Functionalisation of fluorescent BODIPY dyes by nucleophilic substitution. *Chemical Communications* **2006**, (3), 266-268.
67. Rohand, T.; Qin, W.; Boens, N.; Dehaen, W., Palladium-Catalyzed Coupling Reactions for the Functionalization of BODIPY Dyes with Fluorescence Spanning the Visible Spectrum. *European Journal of Organic Chemistry* **2006**, *2006* (20), 4658-4663.
68. (a) Domaille, D. W.; Zeng, L.; Chang, C. J., Visualizing ascorbate-triggered release of labile copper within living cells using a ratiometric fluorescent sensor. *Journal of the American Chemical Society* **2010**, *132* (4), 1194-5; (b) Yin, S.; Leen, V.; Van Snick, S.; Boens, N.; Dehaen, W., A highly sensitive, selective, colorimetric and near-infrared fluorescent turn-on chemosensor for Cu<sup>2+</sup> based on BODIPY. *Chem Commun (Camb)* **2010**, *46* (34), 6329-31.
69. Deniz, E.; Isbasar, G. C.; Bozdemir, O. A.; Yildirim, L. T.; Siemiarczuk, A.; Akkaya, E. U., Bidirectional Switching of Near IR Emitting Boradiazaindacene Fluorophores. *Organic letters* **2008**, *10* (16), 3401-3403.
70. (a) Harriman, A.; Izzet, G.; Ziessel, R., Rapid energy transfer in cascade-type bodipy dyes. *Journal of the American Chemical Society* **2006**, *128* (33), 10868-75; (b) Goze, C.; Ulrich, G.; Ziessel, R., Tetrahedral boron chemistry for the preparation of highly efficient "cascatelle" devices. *J Org Chem* **2007**, *72* (2), 313-22.
71. Tahtaoui, C.; Thomas, C.; Rohmer, F.; Klotz, P.; Duportail, G.; Mely, Y.; Bonnet, D.; Hibert, M., Convenient method to access new 4,4-dialkoxy- and 4,4-diaryloxy-diaza-s-indacene dyes: Synthesis and spectroscopic evaluation. *J Org Chem* **2007**, *72* (1), 269-72.
72. Descalzo, A. B.; Xu, H. J.; Xue, Z. L.; Hoffmann, K.; Shen, Z.; Weller, M. G.; You, X. Z.; Rurack, K., Phenanthrene-fused boron-dipyrrromethenes as bright long-wavelength fluorophores. *Organic letters* **2008**, *10* (8), 1581-4.
73. Chen, J.; Burghart, A.; Derecskei-Kovacs, A.; Burgess, K., 4,4-Difluoro-4-bora-3a,4a-diaza-s-indacene (BODIPY) dyes modified for extended conjugation and restricted bond rotations. *J Org Chem* **2000**, *65* (10), 2900-6.
74. Ulrich, G.; Goeb, S.; De Nicola, A.; Retailleau, P.; Ziessel, R., Chemistry at boron: synthesis and properties of red to near-IR fluorescent dyes based on boron-substituted diisoindolomethene frameworks. *J Org Chem* **2011**, *76* (11), 4489-505.
75. Kowada, T.; Yamaguchi, S.; Ohe, K., Highly fluorescent BODIPY dyes modulated with spirofluorene moieties. *Organic letters* **2010**, *12* (2), 296-9.

76. Kubo, Y.; Minowa, Y.; Shoda, T.; Takeshita, K., Synthesis of a new type of dibenzopyrromethene–boron complex with near-infrared absorption property. *Tetrahedron Letters* **2010**, *51* (12), 1600-1602.
77. Niu, S. L.; Ulrich, G.; Ziessel, R.; Kiss, A.; Renard, P. Y.; Romieu, A., Water-soluble BODIPY derivatives. *Organic letters* **2009**, *11* (10), 2049-52.
78. Frangioni, J. V., In vivo near-infrared fluorescence imaging. *Curr Opin Chem Biol* **2003**, *7* (5), 626-34.
79. Marshall, M.; Draney, D.; Sevick-Muraca, E.; Olive, D., Single-Dose Intravenous Toxicity Study of IRDye 800CW in Sprague-Dawley Rats. *Molecular Imaging and Biology* **2010**, *12* (6), 583-594.
80. Cohen, R.; Stammes, M. A.; de Roos, I. H.; Stigter-van Walsum, M.; Visser, G. W.; van Dongen, G. A., Inert coupling of IRDye800CW to monoclonal antibodies for clinical optical imaging of tumor targets. *EJNMMI research* **2011**, *1* (1), 31.
81. Goncalves, M. S., Fluorescent labeling of biomolecules with organic probes. *Chem Rev* **2009**, *109* (1), 190-212.
82. Lavis, L. D.; Raines, R. T., Bright ideas for chemical biology. *ACS chemical biology* **2008**, *3* (3), 142-55.
83. (a) Ehenschwender, T.; Wagenknecht, H. A., 4,4-Difluoro-4-bora-3a,4a-diaza-s-indacene as a bright fluorescent label for DNA. *J Org Chem* **2011**, *76* (7), 2301-4; (b) Gießler, K.; Griesser, H.; Göhringer, D.; Sabirov, T.; Richert, C., Synthesis of 3'-BODIPY-Labeled Active Esters of Nucleotides and a Chemical Primer Extension Assay on Beads. *European Journal of Organic Chemistry* **2010**, *2010* (19), 3611-3620; (c) Kálai, T.; Hideg, K., Synthesis of new, BODIPY-based sensors and labels. *Tetrahedron* **2006**, *62* (44), 10352-10360.
84. Namkung, W.; Padmawar, P.; Mills, A. D.; Verkman, A. S., Cell-Based Fluorescence Screen for K<sup>+</sup> Channels and Transporters Using an Extracellular Triazacryptand-Based K<sup>+</sup> Sensor. *Journal of the American Chemical Society* **2008**, *130* (25), 7794-7795.
85. (a) Parhi, A. K.; Kung, M. P.; Ploessl, K.; Kung, H. F., Synthesis of Fluorescent Probes based on Stilbenes and Diphenylacetylenes targeting beta-Amyloid Plaques. *Tetrahedron Lett* **2008**, *49* (12), 3395-3399; (b) Ono, M.; Ishikawa, M.; Kimura, H.; Hayashi, S.; Matsumura, K.; Watanabe, H.; Shimizu, Y.; Cheng, Y.; Cui, M.; Kawashima, H.; Saji, H., Development of dual functional SPECT/fluorescent probes for imaging cerebral beta-amyloid plaques. *Bioorganic & medicinal chemistry letters* **2010**, *20* (13), 3885-8.
86. Smith, N. W.; Alonso, A.; Brown, C. M.; Dzyuba, S. V., Triazole-containing BODIPY dyes as novel fluorescent probes for soluble oligomers of amyloid Abeta1-42 peptide. *Biochemical and biophysical research communications* **2010**, *391* (3), 1455-8.
87. Ojida, A.; Sakamoto, T.; Inoue, M. A.; Fujishima, S. H.; Lippens, G.; Hamachi, I., Fluorescent BODIPY-based Zn(II) complex as a molecular probe for selective detection of

neurofibrillary tangles in the brains of Alzheimer's disease patients. *Journal of the American Chemical Society* **2009**, *131* (18), 6543-8.

88. (a) Byrne, A. T.; O'Connor, A. E.; Hall, M.; Murtagh, J.; O'Neill, K.; Curran, K. M.; Mongrain, K.; Rousseau, J. A.; Lecomte, R.; McGee, S.; Callanan, J. J.; O'Shea, D. F.; Gallagher, W. M., Vascular-targeted photodynamic therapy with BF<sub>2</sub>-chelated Tetraaryl-Azadipyromethene agents: a multi-modality molecular imaging approach to therapeutic assessment. *British journal of cancer* **2009**, *101* (9), 1565-73; (b) He, H.; Lo, P.-C.; Yeung, S.-L.; Fong, W.-P.; Ng, D. K. P., Synthesis and in Vitro Photodynamic Activities of Pegylated Distyryl Boron Dipyrromethene Derivatives. *Journal of Medicinal Chemistry* **2011**, *54* (8), 3097-3102; (c) Gorman, A.; Killoran, J.; O'Shea, C.; Kenna, T.; Gallagher, W. M.; O'Shea, D. F., In Vitro Demonstration of the Heavy-Atom Effect for Photodynamic Therapy. *Journal of the American Chemical Society* **2004**, *126* (34), 10619-10631.

89. Zhang, D.; Wang, Y.; Xiao, Y.; Qian, S.; Qian, X., Long-wavelength boradiazaindacene derivatives with two-photon absorption activity and strong emission: versatile candidates for biological imaging applications. *Tetrahedron* **2009**, *65* (39), 8099-8103.

90. Kele, P.; Li, X.; Link, M.; Nagy, K.; Herner, A.; Lorincz, K.; Beni, S.; Wolfbeis, O. S., Clickable fluorophores for biological labeling--with or without copper. *Org Biomol Chem* **2009**, *7* (17), 3486-90.

91. Rayo, J.; Amara, N.; Krief, P.; Meijler, M. M., Live cell labeling of native intracellular bacterial receptors using aniline-catalyzed oxime ligation. *Journal of the American Chemical Society* **2011**, *133* (19), 7469-75.

92. Haugland, R. P., *The Handbook A Guide to Fluorescent Probes and Labeling Technologies*. Tenth ed.; United States of America, 2005.

93. Bandhuvula, P.; Li, Z.; Bittman, R.; Saba, J. D., Sphingosine 1-phosphate lyase enzyme assay using a BODIPY-labeled substrate. *Biochemical and biophysical research communications* **2009**, *380* (2), 366-70.

94. (a) Jones, L. J.; Upson, R. H.; Haugland, R. P.; Panchuk-Voloshina, N.; Zhou, M., Quenched BODIPY dye-labeled casein substrates for the assay of protease activity by direct fluorescence measurement. *Anal Biochem* **1997**, *251* (2), 144-52; (b) Olsen, M. J.; Stephens, D.; Griffiths, D.; Daugherty, P.; Georgiou, G.; Iverson, B. L., Function-based isolation of novel enzymes from a large library. *Nature biotechnology* **2000**, *18* (10), 1071-4.

95. Hudnall, T. W.; Gabbai, F. P., A BODIPY boronium cation for the sensing of fluoride ions. *Chemical Communications* **2008**, (38), 4596-4597.

96. Ziessel, R.; Ulrich, G.; Harriman, A.; Alamiry, M. A.; Stewart, B.; Retailleau, P., Solid-state gas sensors developed from functional difluoroboradiazaindacene dyes. *Chemistry* **2009**, *15* (6), 1359-69.

97. Baruah, M.; Qin, W.; Vallee, R. A.; Beljonne, D.; Rohand, T.; Dehaen, W.; Boens, N., A highly potassium-selective ratiometric fluorescent indicator based on BODIPY azacrown ether excitable with visible light. *Organic letters* **2005**, 7 (20), 4377-80.
98. Dodani, S. C.; He, Q.; Chang, C. J., A Turn-On Fluorescent Sensor for Detecting Nickel in Living Cells. *Journal of the American Chemical Society* **2009**, 131 (50), 18020-18021.
99. Wu, Y.; Peng, X.; Guo, B.; Fan, J.; Zhang, Z.; Wang, J.; Cui, A.; Gao, Y., Boron dipyrromethene fluorophore based fluorescence sensor for the selective imaging of Zn(II) in living cells. *Org Biomol Chem* **2005**, 3 (8), 1387-92.
100. Yamada, K.; Nomura, Y.; Citterio, D.; Iwasawa, N.; Suzuki, K., Highly sodium-selective fluoroionophore based on conformational restriction of oligoethyleneglycol-bridged biaryl boron-dipyrromethene. *Journal of the American Chemical Society* **2005**, 127 (19), 6956-7.
101. de Silva, A. P.; Nimal Gunaratne, H. Q.; Samankumara Sandanayake, K. R. A., A new benzo-annelated cryptand and a derivative with alkali cation-sensitive fluorescence. *Tetrahedron Lett* **1990**, 31 (36), 5193-5196.
102. Arunkumar, E.; Ajayaghosh, A., Proton controlled intramolecular photoinduced electron transfer (PET) in podand linked squaraine-aniline dyads. *Chem Commun (Camb)* **2005**, (5), 599-601.
103. (a) Turfan, B.; Akkaya, E. U., Modulation of boradiazaindacene emission by cation-mediated oxidative PET. *Organic letters* **2002**, 4 (17), 2857-9; (b) Ziessel, R.; Bonardi, L.; Retailleau, P.; Ulrich, G., Isocyanate-, isothiocyanate-, urea-, and thiourea-substituted boron dipyrromethene dyes as fluorescent probes. *J Org Chem* **2006**, 71 (8), 3093-102.
104. Kim, S. K.; Lee, S. H.; Lee, J. Y.; Bartsch, R. A.; Kim, J. S., An excimer-based, binuclear, on-off switchable calix[4]crown chemosensor. *Journal of the American Chemical Society* **2004**, 126 (50), 16499-506.
105. Loudet, A.; Ueno, Y.; Wu, L.; Jose, J.; Barhoumi, R.; Burghardt, R.; Burgess, K., Organelle-selective energy transfer: a fluorescent indicator of intracellular environment. *Bioorganic & medicinal chemistry letters* **2011**, 21 (6), 1849-51.



## CHAPTER 2: SYNTHESIS, COMPUTATIONAL STUDIES AND BIOLOGICAL EVALUATION OF NOVEL SYMMETRICAL AND UNSYMMETRICAL BENZO-APPENDED BODIPYS<sup>[a]</sup>

### 2.1: Introduction

Over the past decade, interest in the BODIPY dyes fused with external aromatic rings at the  $\beta$ -carbon atoms has attracted considerable research interest.<sup>1</sup> Often, referred to as “ $\pi$ -extended BODIPYs” these dye systems possess many interesting properties, inviting applications in many branches of material research and biomedical technology.<sup>2</sup> Due to their high planarity, extended  $\pi$ -conjugation and rigidified molecular framework, the spectral features of this class of annelated BODIPY dyes are much sharper and well-defined, with their absorption and emission wavelengths shifted considerably farthest to the infrared.<sup>3</sup>

Structurally constrained BODIPY dyes exhibit more favorable fluorescence emission characteristics when compared with their unconstrained analogues.<sup>4</sup> In general, the fluorescence quantum yield of a fluorescent dye drops rapidly with an increase in the number of flexible bonds in the molecule. This is attributed to the twisting of the single and/or double bonds that act as an effective channel for dissipation of excitation energy by nonradiative decay of excited states. Therefore, a complete fixation of the chromophoric system seems to guarantee an intrinsically high conversion of the absorbed photons into emitted light, leading to an increased fluorescence emission or brightness of the dye.<sup>1a</sup>

Among the rigid ring extended BODIPY systems, molecules such as dibenzo-fused BODIPYs (hereafter abbreviated as db-BODIPYs) have become one of the most widely used

---

[a] This Chapter originally appeared as Uppal, T.; Hu, X.; Fronczek, F. R.; Maschek, S.; Bobadova-Parvanova, P.; Vicente, M. G. H., Synthesis, Computational Modeling, and Properties of Benzo-Appended BODIPYs. *Chemistry – A European Journal* **2012**, *18* (13), 3893-3905. Reprinted with permission from [2] Copyright (2012) John Wiley and Sons.

building blocks for the construction of molecular switches and light-emitting polymers,<sup>5</sup> biolabeling reagents,<sup>1b</sup> pH sensors,<sup>1c</sup> and photovoltaic cells.<sup>6</sup> Benzo-fused BODIPY dyes often possess high rigidity in their structure which leads to a high fluorescence quantum yield in solution as well as strong intermolecular  $\pi$ - $\pi$  interactions in the solid state, the factors beneficial for their applications as  $\pi$ -functional materials.<sup>7</sup> In structural terms, these ring expanded and annelated BODIPY dyes are closely related to the tetrabenzoporphyrins (TBPs) and can be conveniently referred to as “half-TBP’s” (Figure 2.1)

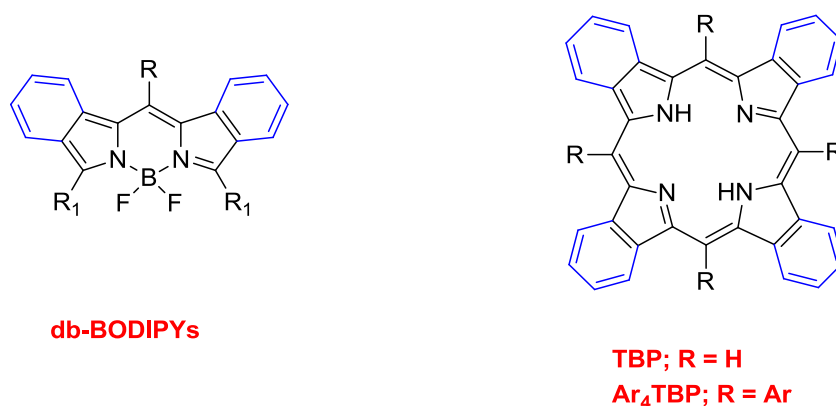
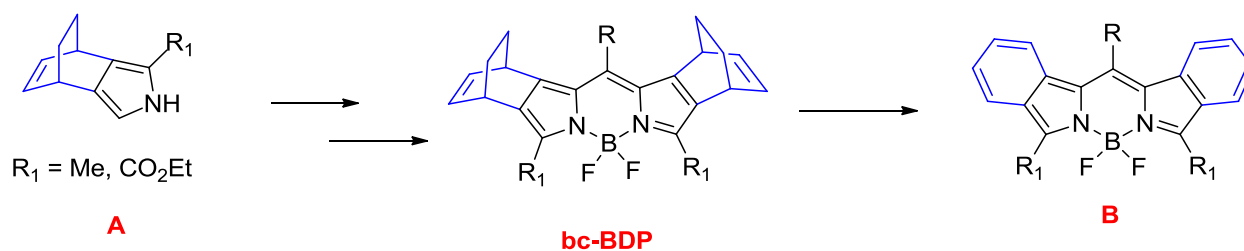


**Figure 2.1:** The general structure of **db-BODIPYs**, **TBP** and **Ar<sub>4</sub>TBP**

Currently, the main synthetic approaches to the *meso*-substituted db-BODIPYs **B** (Scheme 2.1) includes the Ono et al. method,<sup>1a</sup> which is based on the strategy of TBPs synthesis and centers around the “masked” isoindoles i.e. bicyclo octadiene-fused pyrroles **A**. Such pyrroles fused with non-aromatic rings are readily available from “Barton-Zard isocyanoacetate chemistry” and appear to be useful synthons for other  $\pi$ -extended pyrrole-based macrocycles.<sup>3</sup> In this approach, the precursor pyrrole **A**, is condensed with aromatic aldehyde under typical Lindsey conditions, followed by the treatment with N-ethyl-N, N-diisopropyl amine and  $\text{BF}_3 \cdot \text{OEt}_2$  to generate the bicycle [2.2.2] octadiene-fused BODIPY system (**bc-BDP**).

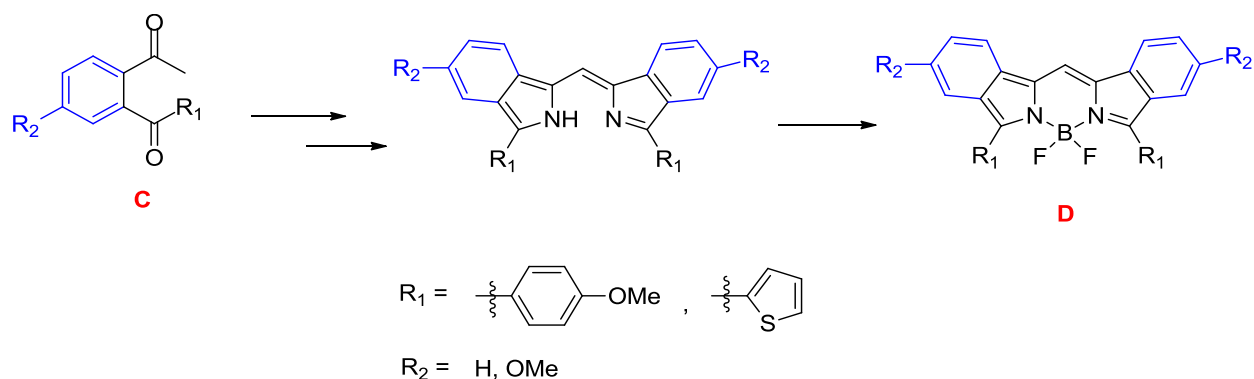
Subsequently, the *meso*-substituted db-BODIPY **B** is generated by the retro Diels-Alder reaction upon heating the “masked” BODIPY system to 220 °C under reduced pressure (30 mmHg) for 30 minutes. Though this approach enables the fast expansion of the scope and preparative value of the benzo-fused BODIPYs, the major drawback of this methodology includes the severe reaction conditions required for the final aromatization step to effect the ethylene extrusion, which often leads to considerable loss of the product at final stage of the long synthesis. As a result, the full potential of this approach has been so far largely unexplored, resulting in only a handful of annelated BODIPY dyes that have been reported using this method.<sup>4</sup>



**Scheme 2.1:** Synthetic route to db-BODIPY **B** from bicyclooctadiene-fused pyrrole **A**

In direct connection with the present work, another approach to *meso*-unsubstituted db-BODIPYs **D**, initially developed by Kang and Haugland,<sup>8</sup> utilizes the substituted 2-acylacetophenones **C** (Scheme 2.2) as the building units to db-BODIPY derivatives.<sup>6, 9</sup> Compound **C** is first condensed with ammonia to generate the dibenzo-fused dipyrin, which after treatment with Hunig’s base and  $\text{BF}_2$ -chelation, affords the constrained db-BODIPY dyes in good overall yields. This synthetic methodology is unique as it allows the introduction of various functional groups at the 5-position on the isoindole ring for further derivatization of the BODIPY dyes. Though considerable efforts for the development of new methodologies for the synthesis of

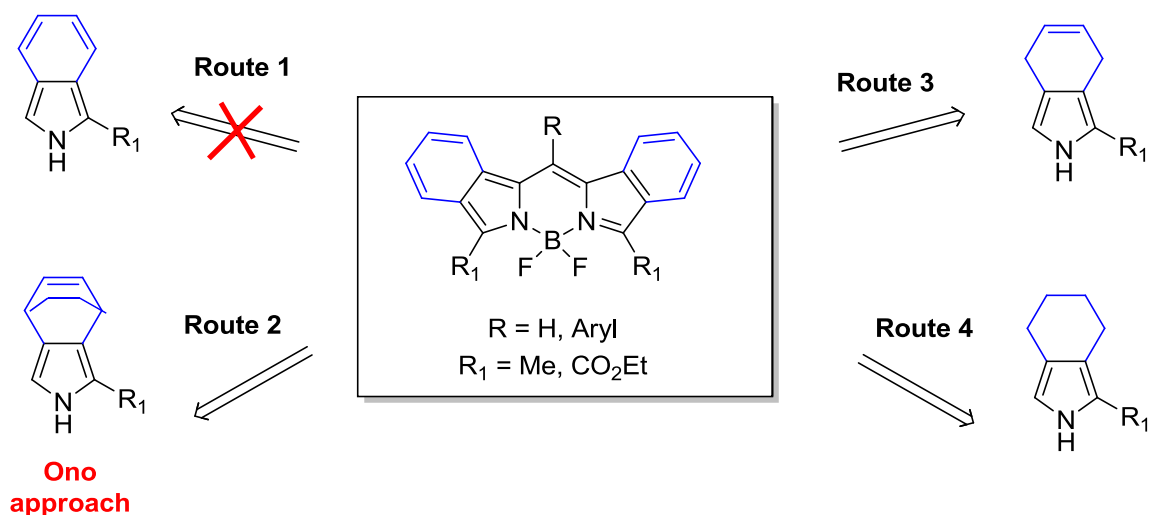
constrained benzo-fused BODIPYs have been investigated, however, there still remains a scope for shorter and more efficacious approaches to contribute towards achieving the synthesis of these systems in a synthetically useful manner.



**Scheme 2.2:** Synthetic route to db-BODIPYs **D** from 2-acetylacetophenone **C**

Given an overwhelming array of applications, it appears interesting and relevant to search for more reliable and practical approaches to  $\pi$ -extended BODIPYs. Starting from the closely related pyrrolic precursors to isoindole, some plausible synthetic routes to db-BODIPYs are depicted in Scheme 2.3.<sup>10</sup> For db-BODIPY synthesis, the most straightforward method of acid-catalyzed condensation of aromatic aldehyde with 2H-isoindole (Scheme 2.3, Route 1) is not possible due to the high reactivity and instability associated with the precursor pyrrole. Another approach utilizing bicyclooctadiene-fused pyrrole (Scheme 2.3, Route 2) represents the classical “Ono et al.” method and suffers from certain drawbacks, as discussed before. Alternatively, the db-BODIPY system can be assembled by the use of stable pyrrolic compounds such as 4,7-dihydroisoindole and 4,5,6,7-tetrahydroisoindole (Scheme 2.3, Route 3 and 4, respectively), as explored for the synthesis of TBPs, where the final aromatization step can be performed by oxidative dehydrogenation with DDQ. These approaches, so far, have not been developed into a

general method of db-BODIPY synthesis, despite the preparation of  $\pi$ -extended dipyrrens from 4,7-dihydroisindole, as recently reported by Filatov and co-workers.<sup>11</sup>



**Scheme 2.3:** Synthetic routes to symmetrical db-fused BODIPYs

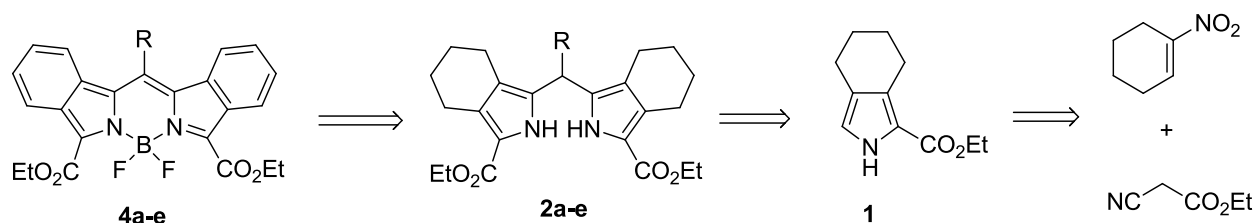
Therefore, in search of a facile and reliable method for the synthesis of  $\pi$ -extended benzo-fused BODIPYs, two synthetic pathways starting from thermodynamically stable 4,5,6,7-tetrahydroisindole ester were investigated. While we were hopeful that these new systems would exhibit red-shifted spectral features, the principle motivation for this work was to study the structural variations on the BODIPY chromophoric core, including the effect of; (1) benzannulation of pyrroles, (2) number of fused-benzene rings, and (3) the nature of *meso*-substituent (R) on the physicochemical and *in vitro* biological properties of the db-BODIPY dyes.

## 2.2: Results and Discussion

### 2.2.1: Syntheses

The C-8 or *meso*-position of the BODIPY chromophore has often been used to attach several aryl substituents with various functionalities for increased solubility and/or conjugation

to target-specific molecules. Although *meso*-arylation on the BODIPY chromophoric core doesn't lead to pronounced effect on the linear absorption and fluorescence emission wavelengths, the steric hindrance between the *meso*-aryl group and the 1,7-substituents on BODIPY core is known to significantly enhance the fluorescence quantum yields due to the restricted rotational motion of the aryl group at the *meso*-position, and reduced rate of fluorescence quenching in such ring constrained, rigidified molecules.<sup>12</sup>

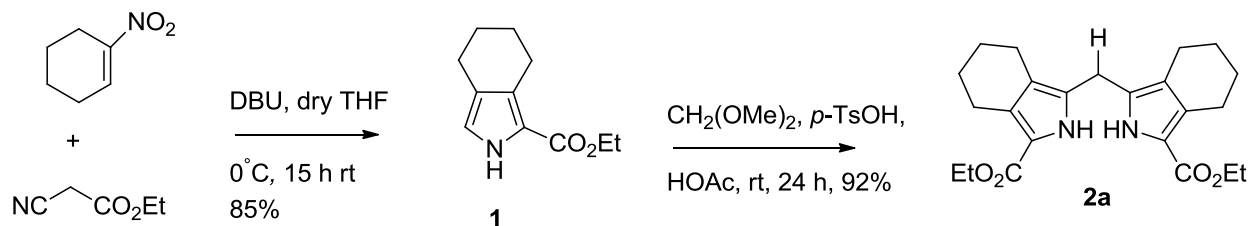


**Scheme 2.4:** Retrosynthetic route to db-BODIPYs **4a-e**

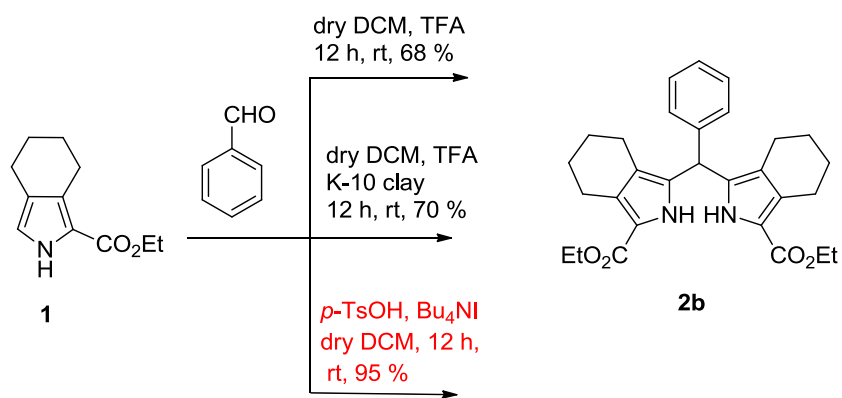
Bearing this apparent analogy in mind, the structure of target db-BODIPY dyes **4a-e**, along with the retrosynthetic analysis is depicted in Scheme 2.4. The key starting material of the entire reaction sequence is 4,5,6,7-tetrahydroisindole ester **1**. Such cyclohexenyl-fused pyrroles can be conveniently prepared in bulk quantities from commercially available 1-nitroarenes and ethyl isocyanoacetate, in the presence of a base (such as DBU) via Barton-Zard synthesis.<sup>13</sup> Another useful precursor, *meso*-unsubstituted dipyrromethane **2a**, was prepared in excellent yields (92%) in one step by acid-mediated condensation of pyrrole **1** and dimethoxymethane, dissolved in acetic acid at room temperature, using a published literature procedure (Scheme 2.5).<sup>14</sup>

*Meso*-substituted dipyrromethanes, which in principle are key synthons in this db-BODIPY synthesis, are usually prepared via a one-flask method based on the acid-catalyzed condensation (trifluoroacetic acid or trifluoroacetic acid/K-10 clay) of an appropriate aldehyde

with two equiv. of pyrrole-2-carboxylates, under well-established Lindsey chemistry.<sup>15</sup> However, in our hands, this classical approach when applied to the synthesis of dipyrromethane **2b**, afforded the target compound in moderate yields of 68% and 70% respectively, (Scheme 2.6) due to side reactions promoted by the action of strong acid in the presence of liberated water.



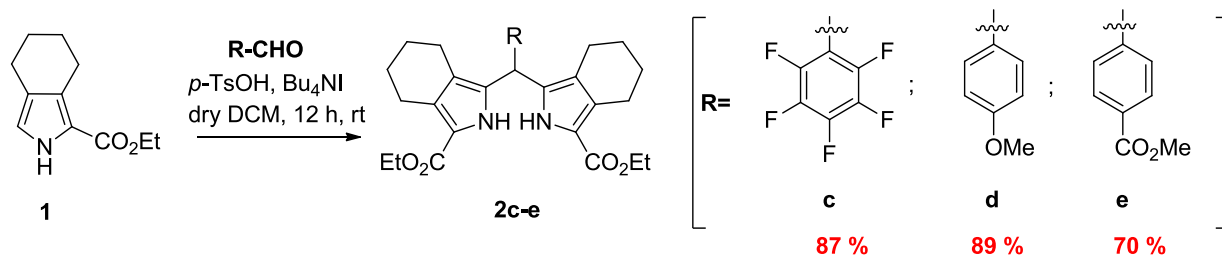
**Scheme 2.5:** Synthetic route to 4,5,6,7-tetrahydroisindole ester **1** and dipyrromethane **2a**



**Scheme 2.6:** Synthetic route to dipyrromethane **2b**

Recently, according to the modified protocol described by Vinogradov et al., the yields of dipyrromethane synthesis from the pyrroles with aromatic aldehydes can be significantly improved in the presence of mild acids, such as *p*-toluene sulfonic acid and anhydrous tetrabutylammonium halide, a highly hygroscopic salt that facilitates the salt-effected water scavenging.<sup>14</sup> Hence, the synthesis of dipyrromethane **2b** was repeated using this modified approach to ensure an optimal yield (~ 95%) of the desired compound **2b**. This strategy was later

extended to the synthesis of a series of *meso*-substituted dipyrromethanes **2c-e**, by condensation of pyrrole **1** with pentafluorobenzaldehyde, *p*-anisaldehyde and methyl 4-formyl benzoate respectively, followed by flash column chromatography, affording the target compounds in moderate to excellent yields, as shown in scheme 2.7.



**Scheme 2.7:** Synthetic routes to dipyrromethanes **2c-e**

All the synthesized dipyrromethanes were analyzed by NMR ( $^1\text{H}$ ,  $^{13}\text{C}$ ) and mass spectrometry. Well-resolved  $^1\text{H}$ -NMR spectra of **2a-e** showed a peak due to NH protons at  $\sim 8.7$  ppm, the *meso*-proton as a sharp singlet at  $\sim 5.5$  ppm, *ortho* and *meta*-protons as doublets in the aromatic region (for **2b**, **2d** and **2e**). The 16 protons of the two cyclohexenyl rings appeared as three sets of triplet due to 4, 4 and 8 protons at  $\sim 2.7$ , 2.2 and 1.6 ppm, respectively. The large difference in the chemical shifts between the  $\alpha$ -protons on the cyclohexenyl rings is attributed to the ring current of the *meso*-aryl group which is roughly perpendicular to the effective indacene plane, leading to shielding of the  $\alpha$ -protons in the *meso*-substituted area. A typical  $^1\text{H}$ -NMR spectrum for dipyrromethane **2d** is shown in Figure 2.2. MS-ESI analysis gave a molecular ion peak at  $m/z$  **2a**: 398.49; **2b**: 474.25; **2c**: 587.19; **2d**: 504.26 and **2e**: 533.26. X-ray crystal structures were obtained for dipyrromethanes **2a-d** by slow evaporation of the solvent from dichloromethane solution of these compounds (discussed in Section 2.2.3).



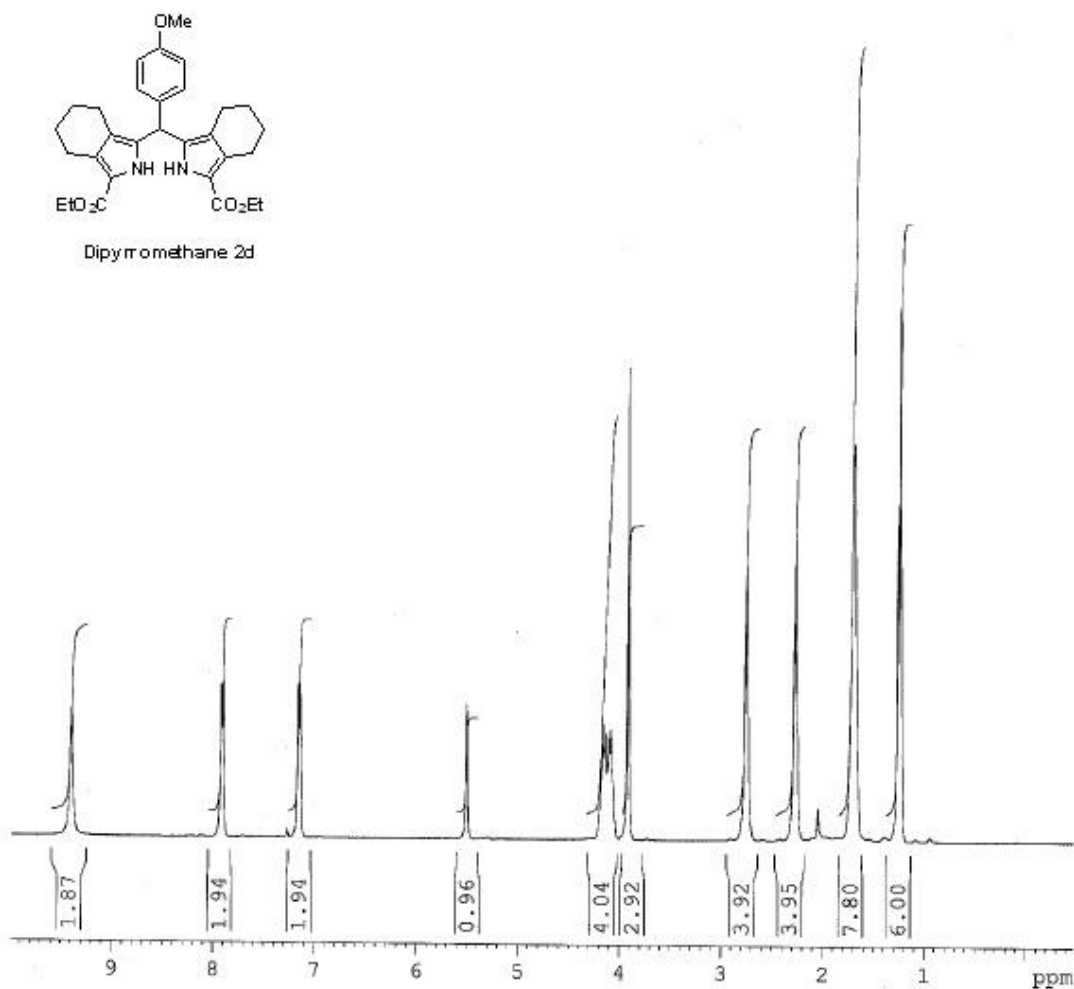
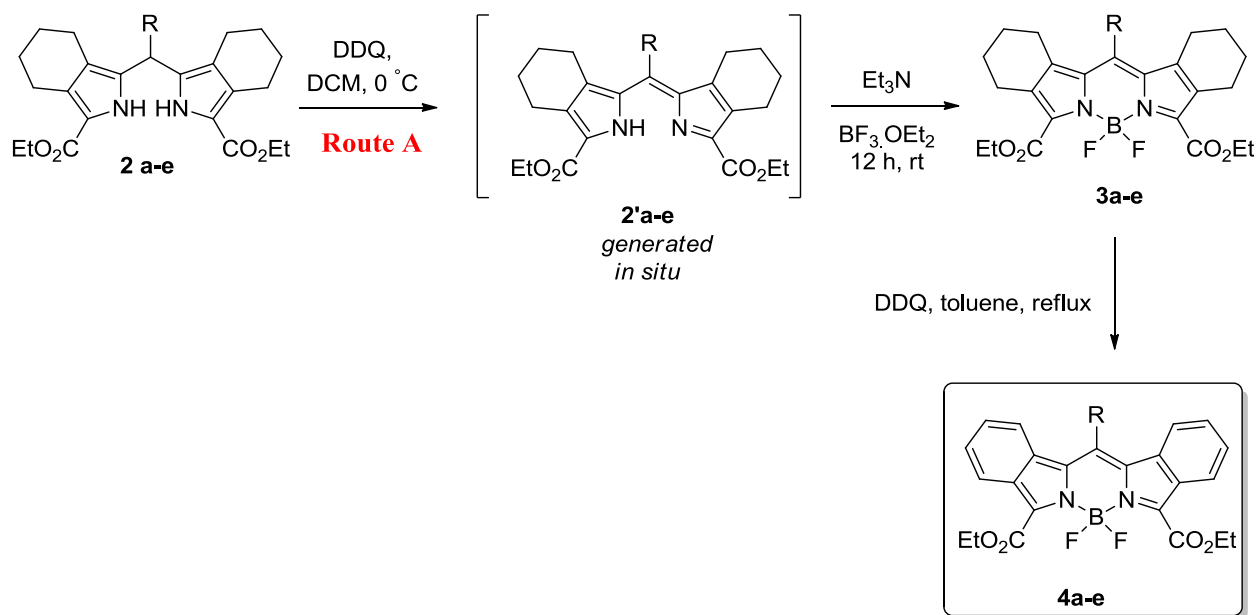


**Figure 2.2:** <sup>1</sup>H-NMR spectrum of dipyromethane **2d** in CDCl<sub>3</sub> at 400 MHz

Two pathways for the conversion of dipyromethanes **2a-e** to fully aromatized db-BODIPYs **4a-e** were investigated; namely bicyclo-BODIPYs pathway (Route **A**) and dibenzodipyrins pathway (Route **B**), as depicted in Scheme **2.8** and Scheme **2.11**. In Route **A**, the BODIPY chromophore was assembled first from the dipyromethanes **2a-e**, followed by oxidative aromatization similar to TBPs synthetic methodology. In alternative Route **B**, the aromatization step was performed prior to the construction of the BODIPY core.



**Scheme 2.8:** Synthetic route to db-BODIPYs **4a-e** following Route A

In Route A, the bicyclo-BODIPYs **3a-e** (abbreviated hereafter as bc-BODIPYs) was synthesized from corresponding dipyrromethanes **2a-e** via two-step one-flask procedure. In the first step, dipyrromethenes **2a-e** was oxidized with 1.2 equiv. of DDQ in THF (for **2a**) or dichloromethane (for **2b-e**) at 0 °C. The progress of the reaction was monitored by TLC analysis, which clearly indicated the formation of corresponding dipyrromethenes **2'a-e** as the sole products within 15-20 minutes. Without isolation, compounds **2'a-e** were treated with triethylamine (6 equiv.) and  $\text{BF}_3 \cdot \text{OEt}_2$  (10 equiv.), first at 0 °C for 30 min. followed by stirring overnight at room temperature. TLC and absorption spectral analysis of the crude reaction mixture indicated the formation of bc-BODIPYs **3a-e**. The crude product was then subjected to silica gel column chromatographic purification and afforded bc-BODIPYs **3a-e** as shiny green solids in 60-80% overall yields (**3a**: 67 %; **3b**: 80 %; **3c**: 75 %; **3d**: 73 % and **3e**: 60 % respectively). Single crystal of BODIPYs **3b-e** was obtained by slow evaporation of n-hexane

into a solution of compounds in dichloromethane over a period of 2 days (see Section 2.2.3 for details). Trace amounts of intermediate dipyrromethenes **2'b-e** were also isolated in all these reactions in < 5% yield. The formation of BODIPYs **3a-e** was confirmed by molecular ion peaks in ESI-MS at *m/z* **3a**: 444.20; **3b**: 520.23; **3c**: 610.19; **3d**: 550.25 and **3e**: 577.22 respectively. The absorption spectrum of bc-BODIPYs **3a-e** showed one strong  $S_0$ - $S_1$  absorption band at  $\lambda_{\text{max}}$  = 553, 540, 563, 539 and 542 nm due to **3a**, **3b**, **3c**, **3d** and **3e** respectively.  $^1\text{H-NMR}$  spectra for **3a-e** (as shown in Figure 2.3 for **3d**) when compared to their precursor dipyrromethanes **2-e**, in general, indicated the absence of signals corresponding to NH protons because of their complexation with boron of the  $\text{BF}_3$  molecule.

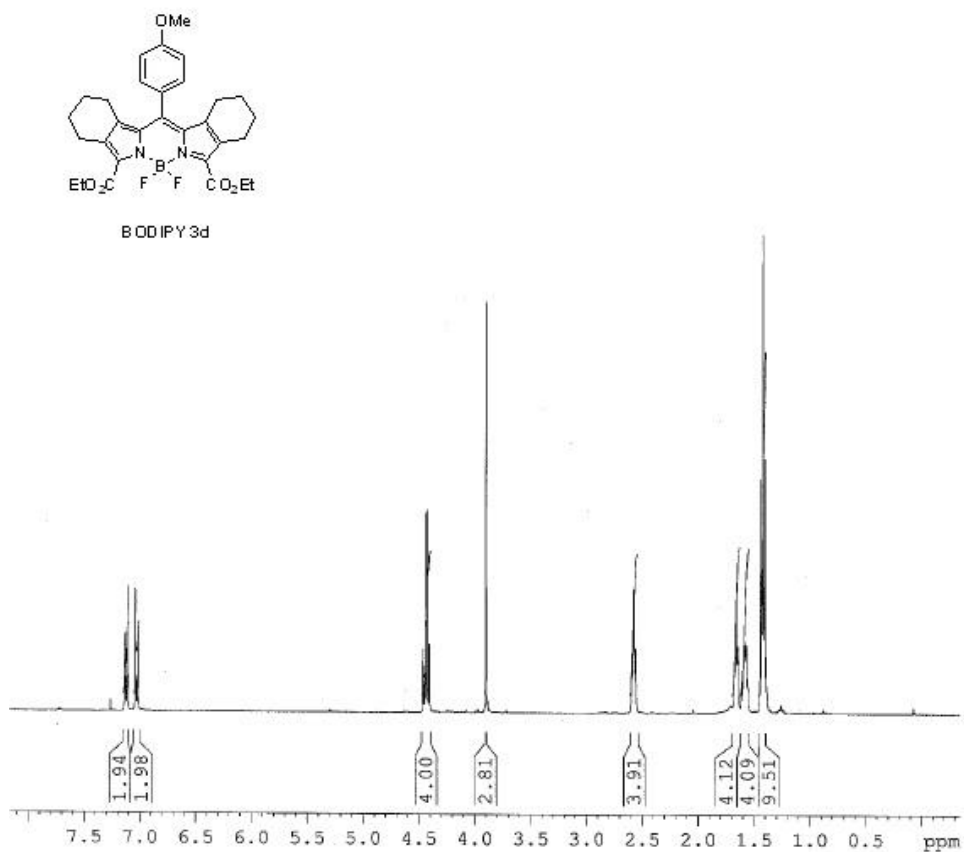
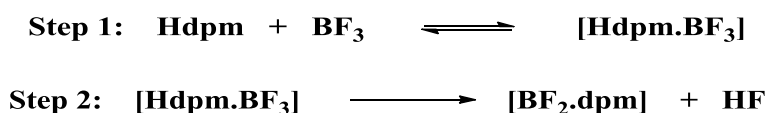
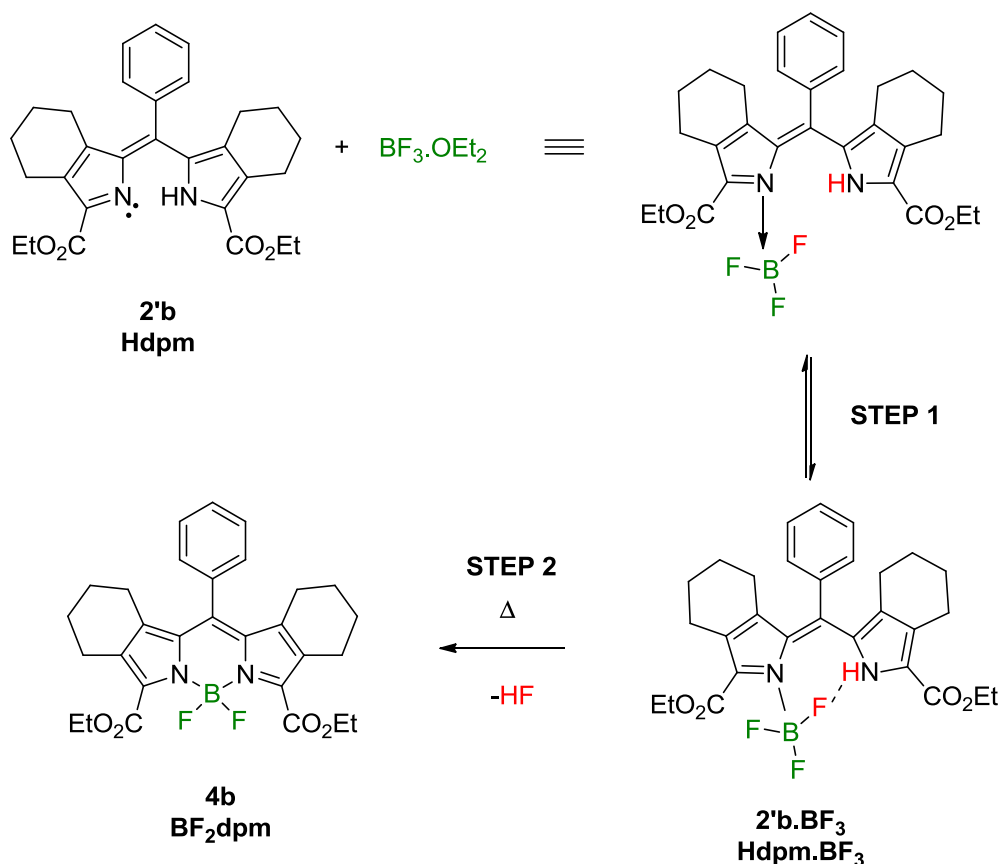


**Figure 2.3:**  $^1\text{H-NMR}$  spectrum of BODIPY **3d** in  $\text{CDCl}_3$  at 400 MHz

Though the use of dipyrromethenes as effective chelating ligands is well-known, little attention has been paid so far, to the studies of reaction mechanism or intermediates formed in the synthesis of BODIPY dyes. This is partly attributed to the high rates involved in establishing of equilibrium in such complexes, which makes the kinetics studies much difficult to monitor. Recently, Rumyantsev et al.<sup>16</sup> had defined BODIPY dyes as the boron fluoride complex of dipyrromethene, formed by interaction of dipyrromethene (Hdpm, donor) and BF<sub>3</sub> (acceptor) in a 1:1 ratio according to the following two-step mechanism:



The first step of the BODIPY synthesis is the formation of a stable donor-acceptor complex (DAC) due to strong donor-acceptor interactions between the lone pair of electrons on pyrroline nitrogen atom of the donor with the vacant *p*-orbital of the boron atom in the BF<sub>3</sub> molecule (Scheme 2.9). This step is accompanied by the change in the geometry of the BF<sub>3</sub> molecule from planar to tetrahedral, which places one of the fluorine atoms on BF<sub>3</sub> molecule in close proximity to the NH group of the donor. The second step then involves the hydrogen bond formation between the hydrogen atom of the NH group of the dipyrromethene and the nearest fluorine atom in the BF<sub>3</sub> molecule. The hydrogen bonding [N-H.....F-B] stabilizes the donor-acceptor complex and further promotes the elimination of HF in the final step of the BODIPY core formation. In general, the BF<sub>2</sub>-complexation reactions are carried out in moderately polar solvents such as toluene and dichloromethane as the BF<sub>3</sub> molecule is only slightly solvated under these conditions. The use of more polar solvents such as DMF and DMSO is generally avoided as BF<sub>3</sub> is known to form quite stable complexes with these polar electron donor molecules.



**Scheme 2.9:** Mechanism of BODIPY **4b** synthesis from dipyrromethene **2'b** and  $\text{BF}_3 \cdot \text{OEt}_2$

The next step of this route is the aromatization of bc-BODIPYs **3a-e** to db-BODIPYs **4a-e**, which required the removal of 8 hydrogens by the ways of oxidative dehydrogenation. Fully aromatized db-BODIPYs **4a**, **4b**, **4d** and **4e** (with an exception of **4c**) were synthesized by heating the solution of corresponding bc-BODIPYs **3a**, **3b**, **3d** and **3e** in toluene with 9 equiv. of DDQ at 110 °C. TLC analysis initially showed more number of spots corresponding to partially oxidized BODIPYs, but with the progress of the reaction, these spots disappeared and one major highly fluorescent spot corresponding to fully oxidized db-BODIPYs was observed. The progress of the reaction was also judged by the color change of the reaction mixture from fluorescent orange-red to a deep blue fluorescent solution and also by spectrometric monitoring of the reaction (i.e. intensive maximum at  $\lambda_{\text{max}} = 642, 643, 643$  and  $644$  nm due to **4a**, **4b**, **4d** and

**4e** respectively). The crude mixture was purified by silica gel column chromatography to afford **4a**, **4b**, **4d** and **4e** as shiny deep blue crystals in 67-92% yields (Table 2.1).

**Table 2.1:** Synthesis of db-BODIPYs **4a**, **4b**, **4d** and **4e** from corresponding bc-BODIPYs **3a**, **3b**, **3d** and **3e** via Route A

db-BODIPYs	Time (h)	Yield (%)
<b>4a</b>	3-4	69
<b>4b</b>	6	67
<b>4c</b>	-	-
<b>4d</b>	2	92
<b>4e</b>	8	68

The reaction appears to be quite general. From Table 2.1, it can be seen that for BODIPYs with electron withdrawing *meso*-aryl groups (BODIPY **4e**), longer reaction time (~ 8h) are required for complete aromatization, while for BODIPY **4d**, a much shorter reaction time of ~ 2 h was required. In the case of BODIPY **4c** bearing a *meso*-pentafluorophenyl group, no progress could be observed even after several hours/days of refluxing. Analysis of the reaction mixture revealed that the aromatization of BODIPY **3c** to BODIPY **4c** occurred very slowly and never came to completion, making it clear that the bc-BODIPY **3c** is totally inactive in aromatization. Well-resolved <sup>1</sup>H-NMR spectra of **4a**, **4b**, **4d** and **4e** showed additional peaks in the aromatic region, corresponding to the newly annelated benzo rings, as shown in Figure 2.4 for db-BODIPY **4d**. The 8 protons of the two benzo rings appeared in between 7.2-8.4 ppm, as four triplets due to two protons each. Once again, the large difference in chemical shifts between the  $\alpha$ -protons of the benzo rings is attributed to the superposition of the ring currents of BODIPY core plus the benzo rings and the ring current of the *meso*-aryl group (shielding of the  $\alpha$ -protons in the *meso*-substituted bay with respect to those in the *meso*-unsubstituted bay). MS-ESI

analysis gave a molecular ion peak at  $m/z$  **4a**: 436.20; **4b**: 512.17; **4d**: 542.18 and **4e**: 570.18 respectively.

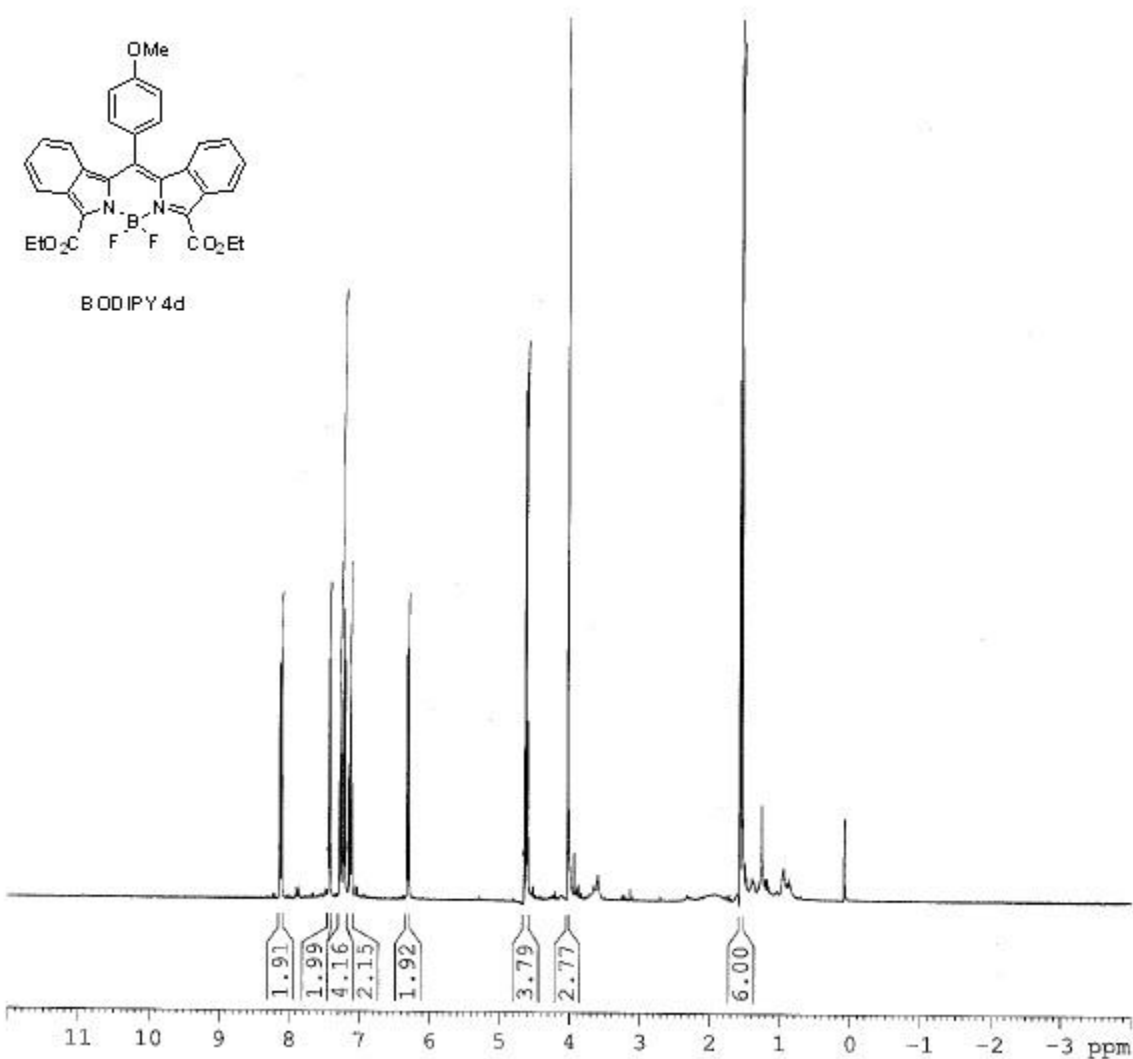


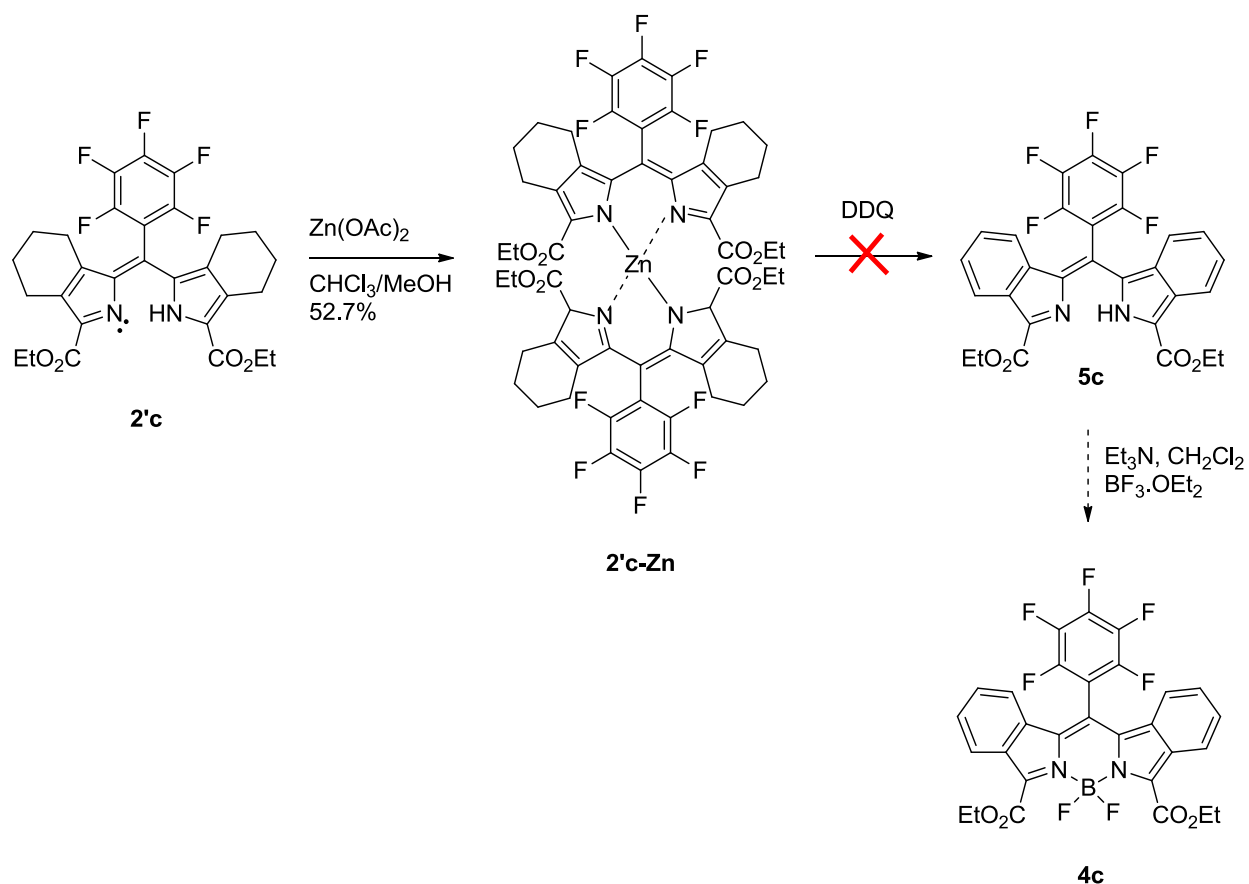
**Figure 2.4:**  $^1\text{H-NMR}$  spectrum of BODIPY **4d** in  $\text{CDCl}_3$  at 400 MHz

Since the oxidative aromatization is an important step to db-BODIPYs synthesis, it is interesting to consider the possible mechanism for this transformation. Oxidations by DDQ are usually regarded within the framework of the SET/hydride abstraction mechanistic dualism.<sup>3</sup> The most plausible mechanism involves the single-electron transfer (SET) from the bc-BODIPYs to

DDQ with the formation of an ion-radical pair [bc-BODIPYs<sup>+</sup>/DDQ<sup>-</sup>] at the first stage. The semiquinone anion-radical DDQ<sup>-</sup> further facilitates the stepwise abstraction of a hydrogen atom and a proton, with the net result of dehydrogenation. Alternatively, this sequence can be presented as an abstraction of a hydride from bc-BODIPY followed by the proton transfer. Further, when applied to the case of BODIPY **3c**, it is possible that electron-withdrawing pentafluorophenyl group has a much slower rate of oxidation due to its lower tendency to form benzylic cation intermediate, either by SET/hydride abstraction by DDQ.<sup>2</sup>

We further attempted to carry out the synthesis of BODIPY **4c** by carrying out oxidation using “pre-metalation” - a strategy developed for the synthesis of *meso*-substituted Ar<sub>4</sub>TBPs from their precursor tetracyclohexenoporphyrins (Ar<sub>4</sub>TCHPs). Ar<sub>4</sub>TBPs are often synthesized by oxidizing metalated Ar<sub>4</sub>TCHPs (MAr<sub>4</sub>TCHPs, where M = Zn, Cu, Ni etc) upon treatment with DDQ in refluxing solvents. After aromatization, the MAr<sub>4</sub>TBPs are demetalated to give the corresponding Ar<sub>4</sub>TBPs as free bases. As dipyrromethenes are known to form stable and isolable complexes with Zn and other bivalent metal cations, we anticipated that a similar methodology when applied to dipyrromethene **2’c**, could generate the desired db-BODIPY **4c** as depicted in Scheme **2.10**. A mixture containing **2’c** and an excess of Zn(OAc)<sub>2</sub> [in 3:2 ratio] was stirred overnight at room temperature in CHCl<sub>3</sub>/MeOH, under standard dipyrromethene-Zn complexation conditions.<sup>17</sup> The reaction mixture was filtered off using celite and the solvent was evaporated *in vacuo* to afford the deep-red neutral homoleptic dipyrromethene-Zn complex (**2’c-Zn**) in 52.7% yield. **2’c-Zn** complex was then treated with DDQ (16 equiv.) in boiling organic solvents such as toluene, acetonitrile, dichloromethane and DMF. However, all our attempts to oxidize the cyclohexyl rings in the metalated dipyrromethene complex, turned out unsuccessful as the more labile complex rapidly lost its metal under the employed aromatization conditions, yielding the dipyrromethene **2’c** which was recovered by column chromatography.



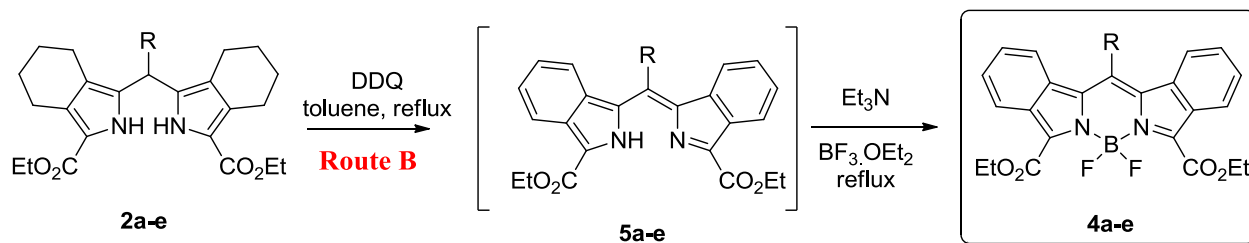


**Scheme 2.10:** Alternate synthetic route to db-BODIPY **4c**

In another attempt to generate db-BODIPY **4c**, the aromatization of BODIPY **3c** was studied using various inorganic oxidizing agents. In a typical procedure, a solution of BODIPY **3c** in dichloromethane was treated with a methanolic solution of the oxidizing agent. The resulting reaction mixture was first stirred at room temperature for 6 h and then heated at reflux for additional 3 h. The progress of the reaction was monitored by MALDI MS and UV-vis spectroscopy (Table 2.2). All attempts to oxidize BODIPY **3c** using inorganic oxidizing agents failed to generate/isolate the desired product in decent or lower yields.

**Table 2.2:** Aromatization of BODIPY **3c** using inorganic oxidation approach

Oxidizing agent	MALDI-MS ( $m/z = 531$ )	UV-Vis data (nm)
AgNO <sub>3</sub>	-	533
KMnO <sub>4</sub>	+	537
Cu(NO <sub>3</sub> ) <sub>2</sub>	-	536
MnO <sub>2</sub>	+	546
CuCl <sub>3</sub>	-	534
RuCl <sub>3</sub>	-	533
I <sub>2</sub> -MeOH	+	537
Pd-C	-	537
CAN	-	-
FeCl <sub>3</sub>	-	537

**Scheme 2.11:** Synthetic route to db-BODIPYs **4a-e** following Route **B**

We next focused on to the synthesis of db-BODIPYs **4a-e** via Route **B**, which commenced with the synthesis of dibenzo-dipyrrins (db-dipyrrins) **5a-e** from dipyrromethanes **2a-e**. Aromatization of **2a-e** into db-dipyrrins **5a-e** was realized by oxidation with 10 equiv. of DDQ in refluxing toluene. Progress of the reaction was monitored from clear color change of the reaction mixture (i.e. orange-red to deep purple solution) and by absorption spectroscopy ( $\lambda_{\text{max}}$  at 568, 569, 583, 569 and 572 nm for **5a**, **5b**, **5c**, **5d** and **5e** respectively). Interestingly, in spite of

the overall facile reaction, once again the effect of *meso*-aryls was much more pronounced as electron-withdrawing groups in *meso*-aryls considerably decreased the rate of the aromatization and the product yield (Table 2.3). For e.g. aromatization of **2c** and **2e** required a longer reaction time (~ 10 and 8 h respectively), while **2b** was oxidized completely in 3 h upon bringing their solution with DDQ to reflux. **2a** and **2d** (with *meso*-H and *meso-p*-methoxyphenyl group) had to be refluxed for 2 h only. Nevertheless, in all these cases, aromatization could be drive to completion and gave the target db-dipyrins **5a-e** in moderate yields, after careful column chromatography and recrystallization using dichloromethane/hexane solvent mixture. All the db-fused dipyrins **5a-e** were analyzed by NMR and high resolution MS. <sup>1</sup>H-NMR spectrum for **5d** (and related compounds), as displayed in Figure 2.5, showed the absence of the cyclohexenyl peaks (in between 2-3 ppm) and presence of additional peaks in the aromatic region.

**Table 2.3:** Synthesis of db-dipyrins **5a-e** from dipyrromethanes **2a-e** via Route **B**

db-dipyrins	Time (h)	Yield (%)
<b>5a</b>	2	56
<b>5b</b>	3	66
<b>5c</b>	10	62
<b>5d</b>	2	69
<b>5e</b>	8	58

Reactions of db-dipyrins **5a-e** with BF<sub>3</sub>.OEt<sub>2</sub> in the presence of Et<sub>3</sub>N, in refluxing toluene, gave rise to the formation of the corresponding db-BODIPYs **4a-e** in 55-90% yields (Table 2.4), after flash column chromatography by using dichloromethane or dichloromethane/ethyl acetate as the eluent and silica gel as the absorbent, in analogy to standard procedure reported in the literature,<sup>18</sup> In general, DDQ oxidation of **2a-e** to the corresponding

fully aromatized db-dipyrrins **5a-e** gave lower yields of 56-69%, when compared to oxidative-dehydrogenation of BODIPYs **3a**, **3b**, **3d** and **3e** to BODIPYs **4a**, **4b**, **4d** and **4e** (67-92%). This could be attributed to the higher stability of BODIPYs when compared to the corresponding dipyrromethanes under oxidative reaction conditions. However, the BF<sub>2</sub>-complexation of **2a-e** (to **3a-e**) and **5a-e** (to **4a-e**) gave nearly similar reaction yields. Overall, Route **A** is far by the method of choice for the synthesis of db-BODIPYs affording the target products in higher yields due to the ease of aromatization of BODIPYs over corresponding dipyrromethanes. However, Route **B** could be followed to synthesize  $\pi$ -extended BODIPYs with highly electron-deficient *meso*-aryl groups (such as **4c**) due to slow oxidation of their corresponding BODIPY precursors.

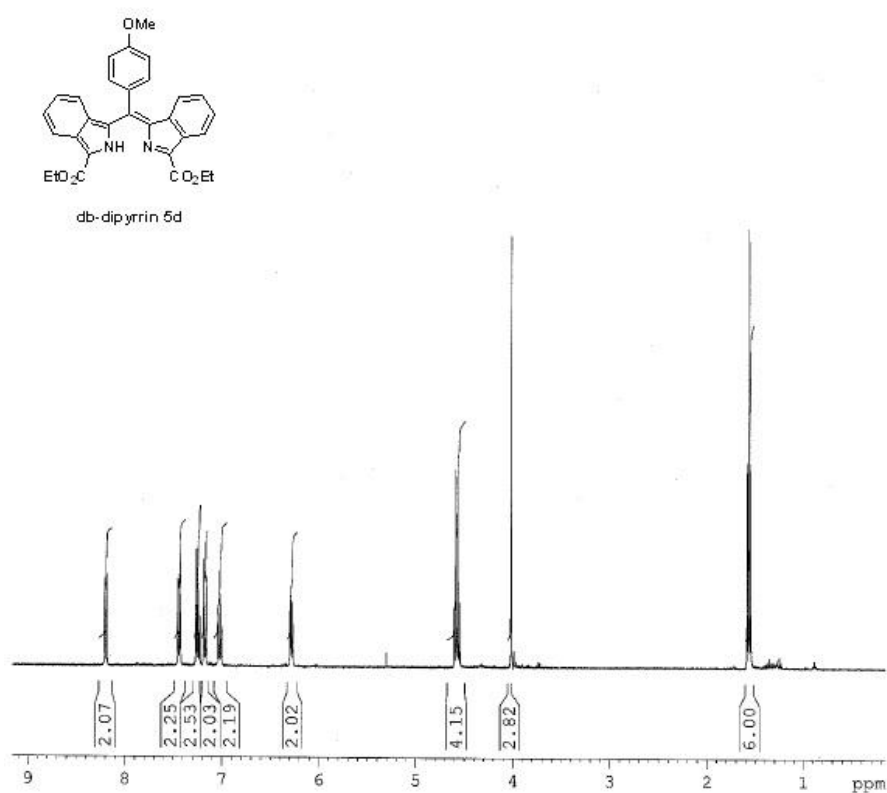


**Figure 2.5:** <sup>1</sup>H-NMR spectrum of BODIPY **5d** in CDCl<sub>3</sub> at 400 MHz

**Table 2.4:** Synthesis of db-BODIPYs **4a-e** from db-dipyrrins **5a-e** via Route **B**

db-BODIPYs	Time (h)	Yield (%)
<b>4a</b>	3	55
<b>4b</b>	4-5	80
<b>4c</b>	overnight	56
<b>4d</b>	2	90
<b>4e</b>	overnight	75

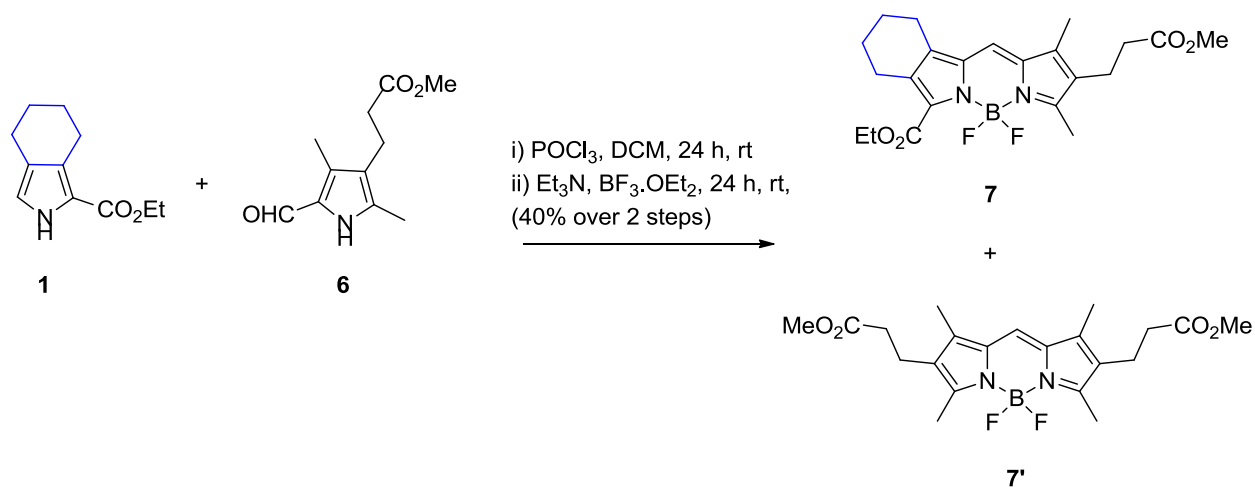
In order to investigate the synthesis of bc-BODIPYs **3b-e** and db-dipyrrins **5b-e** from dipyrromethenes **2'b-e**, a dichloromethane solution of dipyrromethanes **2b-e** was treated with 1.2 equiv. of DDQ at 0 °C, causing a color change of the solution to deep orange. Further column chromatographic separation on a silica gel eluting with petroleum ether/ethyl acetate (7/3, v/v) solvent mixture and recrystallization from pure dichloromethane afforded dipyrromethenes **2'b-e** in overall moderate yields (**2'b**: 75 %; **2'c**: 70 %; **2'd**: 82 %; **2'e**: 68 %). Further BF<sub>2</sub>-complexation and DDQ oxidation reactions were performed using the same protocol as developed above for dipyrromethanes **2a-e**. The results obtained from these reactions are listed in Table 2.5.

**Table 2.5:** Synthesis of bc-BODIPYs **3b-e** and db-dipyrrins **5b-e** from dipyrromethenes **2'b-e**

Dipyrromethene	bc-BODIPYs <b>3</b> Yield (%)	db-dipyrrins <b>5</b> Yield (%)
<b>2'b</b>	66	53
<b>2'c</b>	62	48
<b>2'd</b>	60	65
<b>2'e</b>	52	45

As can be seen, the yields of bc-BODIPYs **3b-e** obtained from **2'b-e** decreased significantly, when compared to their synthesis from dipyrromethanes **2a-e**. On the other hand, the yields for the db-dipyrins **5a-e**, were nearly similar to those obtained from **2a-e**. Hence, it can be concluded, that the generation of **2'b-e** in situ, during the formation of db-BODIPYs is much more beneficial as it increases the product yield by reducing an additional purification step in the synthesis.

A second goal of this study was to prepare monobenzo-fused BODIPYs, in order to study the effect of the number of fused rings on the optical properties of the ring-fused BODIPYs. Scheme 2.12 and 2.13, depicts the synthesis of monobenzo-fused BODIPY **8** from mono-cyclohexenyl BODIPY **7**, which in turn is prepared from pyrrole **6**, following BF<sub>2</sub>-complexation and oxidation procedure similar to Route A in Scheme 2.8. Compound **6** was synthesized from its *tert*-butyl protected pyrrole precursor (**A**) in two steps involving deprotection of ester with trifluoroacetic acid, followed by formylation with triethyl orthoformate.



**Scheme 2.12:** Synthetic route to mono-cyclohexenyl BODIPY **7**

Pyrrole **6** was dissolved in a solvent mixture of dry dichloromethane and trifluoroacetic acid at 0 °C under argon. This mixture was stirred for 20 min. while cooling with an ice bath. Next, 5 equiv. of triethyl orthoformate were added at 4 °C and stirring was continued until TLC indicated reaction completion. The reaction mixture was then quenched by pouring it into ice-cold water and was subsequently neutralized with 10N NaOH solution. The product separated out as green droplets and was extracted into dichloromethane. Combined organic extracts were washed with 5% NaHCO<sub>3</sub>, brine and dried over anhydrous Na<sub>2</sub>SO<sub>4</sub>. The solvent was removed under reduced pressure and crude brown product was purified on a silica gel column eluting with dichloromethane/ethyl acetate (10/1, v/v) to give pale green crystals of the desired product **6** in 84% yield. The product was characterized by <sup>1</sup>H-NMR (aldehyde peak at 10.2 ppm and a broad NH singlet peak at 9.43 ppm) and MS-ESI (a peak at m/z 209.11). The structure of the compound **6** was also confirmed by X-ray analysis as shown in Figure 2.6.

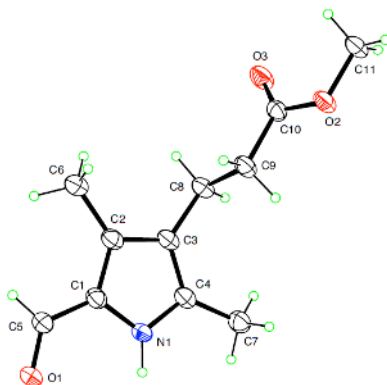
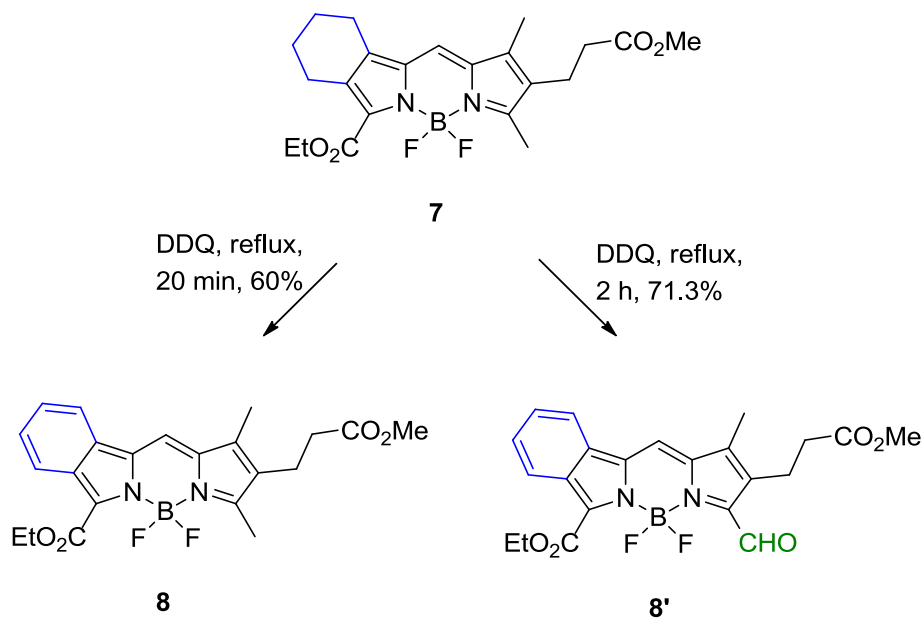


**Figure 2.6:** X-ray crystal structure of pyrrole-2-carbaldehyde **6**

To an equimolar solution of pyrroles **1** and **6** in dry dichloromethane at 0 °C under argon, phosphorus oxychloride (POCl<sub>3</sub>) was added dropwise over a period of 5 min. The reaction mixture was stirred at room temperature overnight and then treated with Et<sub>3</sub>N base and BF<sub>3</sub>.OEt<sub>2</sub>. After the addition was over, the reaction was stirred at room temperature (16 h) and followed-up

by silica gel TLC. Two well-separated fluorescent yellow spots due to their different R<sub>f</sub> values were observed on the TLC. The solvent was removed under reduced pressure and residue was taken up in pure dichloromethane and washed with 10% aq. NaHCO<sub>3</sub>, brine and dried over Na<sub>2</sub>SO<sub>4</sub>. The solvent was evaporated to dryness and residue was purified by column chromatography (hexane/ethyl acetate, 3/2, v/v). Two fluorescent fractions were collected, dried *in vacuo* and recrystallized from CH<sub>2</sub>Cl<sub>2</sub>/hexane to obtain the pure compounds, (later identified as BODIPY **7** and BODIPY **7'**) as lustrous green solids in 40% and 15% yield respectively. The structure of both the BODIPYs was unambiguously determined by NMR and mass spectrometry. Formation of BODIPY **7'**, under these reaction conditions can be attributed to the self-condensation of pyrrole **6** as triggered by phosphorus oxychloride.



**Scheme 2.13:** Synthetic route to BODIPYs **8** and **8'**



The final aromatization step was performed by treating a solution of BODIPY **7** in refluxing toluene with a solution of DDQ (5 equiv.) in toluene for a few minutes. The aromatization took place instantaneously (within 5-10 min). Two fluorescent magenta spots with marked difference in their  $R_f$  values were observed on silica gel TLC, one polar spot became prominent after 2 h. After 2 h, the reaction mixture was cooled down to room temperature and the solvent was removed under the reduced pressure. The residue was taken in dichloromethane and washed with saturated  $\text{NaHCO}_3$ , brine and dried over  $\text{Na}_2\text{SO}_4$ . The solution was evaporated to dryness and the residue was purified by column chromatography eluting with hexane/EtOAc, 3/2, v/v. The magenta fluorescent fractions were collected separately, dried *in vacuo* and recrystallized from  $\text{CH}_2\text{Cl}_2$ /hexane to obtain the pure BODIPY **8** and BODIPY **8'** as lustrous green solid in 4% and 71.3% yield. The percent yield of BODIPY **8** improved drastically (from 4% to 60%), on stopping the reaction after 10 min. The DDQ oxidation of the side chain methyl group (in the substitution position 3) of BODIPY **8** can be explained by the initial abstraction of hydride anion from the benzylic position, leading to a carbenium ion intermediate. Subsequent trapping with water, followed by oxidation then generates the 3-formyl BODIPY **8'**.<sup>19</sup> Full confirmation of the nature of BODIPYs **8** and **8'** was obtained using  $^1\text{H-NMR}$ , MS-MALDI and X-ray crystal structure analysis (Figure 2.7).

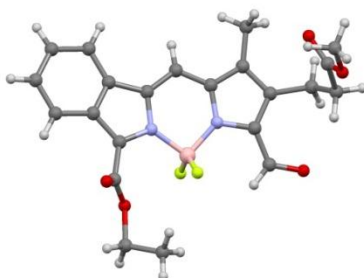


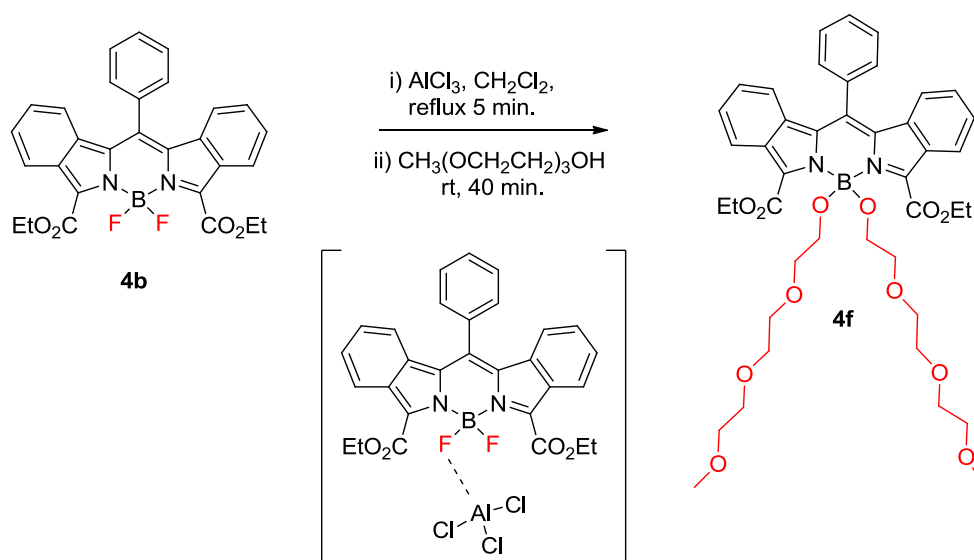
**Figure 2.7:** X-ray crystal structure of BODIPY **8** and **8'**

Peripheral substituents on the BODIPY core can be used to impart desired physicochemical and biological properties to the BODIPY dye. For example, these substituents can be used to target the chromophore to various biological materials, modulate the electronic properties such as absorption and emission or serve as scaffold for further synthetic modifications. In addition, it is noteworthy that the aromatic ring fusion to the  $\beta$ -pyrrolic positions on BODIPY chromophore is often considered to be a promising strategy, as it leaves other positions such as *meso*-, 3,5-positions or boron center) for further synthetic modifications. Hence, with the aim to further functionalize the designed db-BODIPYs, two different ways of derivatization were investigated.

In our first attempt towards post-functionalization of db-BODIPYs, we targeted the derivatization of the BODIPY at the boron center. Recently, Tahtaoui et al.<sup>20</sup> had described the synthesis of a series of BODIPY derivatives obtained by nucleophilic displacement of the fluorine atom at the boron center with various alcohols, in the presence of aluminium chloride. A similar strategy was followed to obtain PEGylated-BODIPY **4f** by replacing the fluorine atoms on BODIPY **4b** using 2-[2-(2-methoxyethoxy)ethoxy]ethanol, as depicted in Scheme 2.14.

A deep-blue solution of BODIPY **4b** (1 equiv.) in dry dichloromethane was refluxed in the presence of aluminium chloride (3 equiv.) under argon for 5 min, followed by addition of 2-[2-(2-methoxyethoxy)ethoxy]ethanol and stirring at room temperature. TLC monitoring of the reaction revealed the disappearance of the starting material and the formation of a more polar green product, which was subsequently converted into a blue spot corresponding to BODIPY **4f**. Spectroscopic analysis of the reaction mixture indicated an absorption band similar to that of parent BODIPY **4b**. MALDI-analysis of the reaction mixture gave a molecular ion peak at  $m/z$  888.42, indicating a total substitution of the two fluorine atoms on BODIPY **4b**. However, all the

attempts to isolate the highly polar BODIPY **4f** on a deactivated basic alumina failed and as a result, the product could not be isolated and/or characterized.

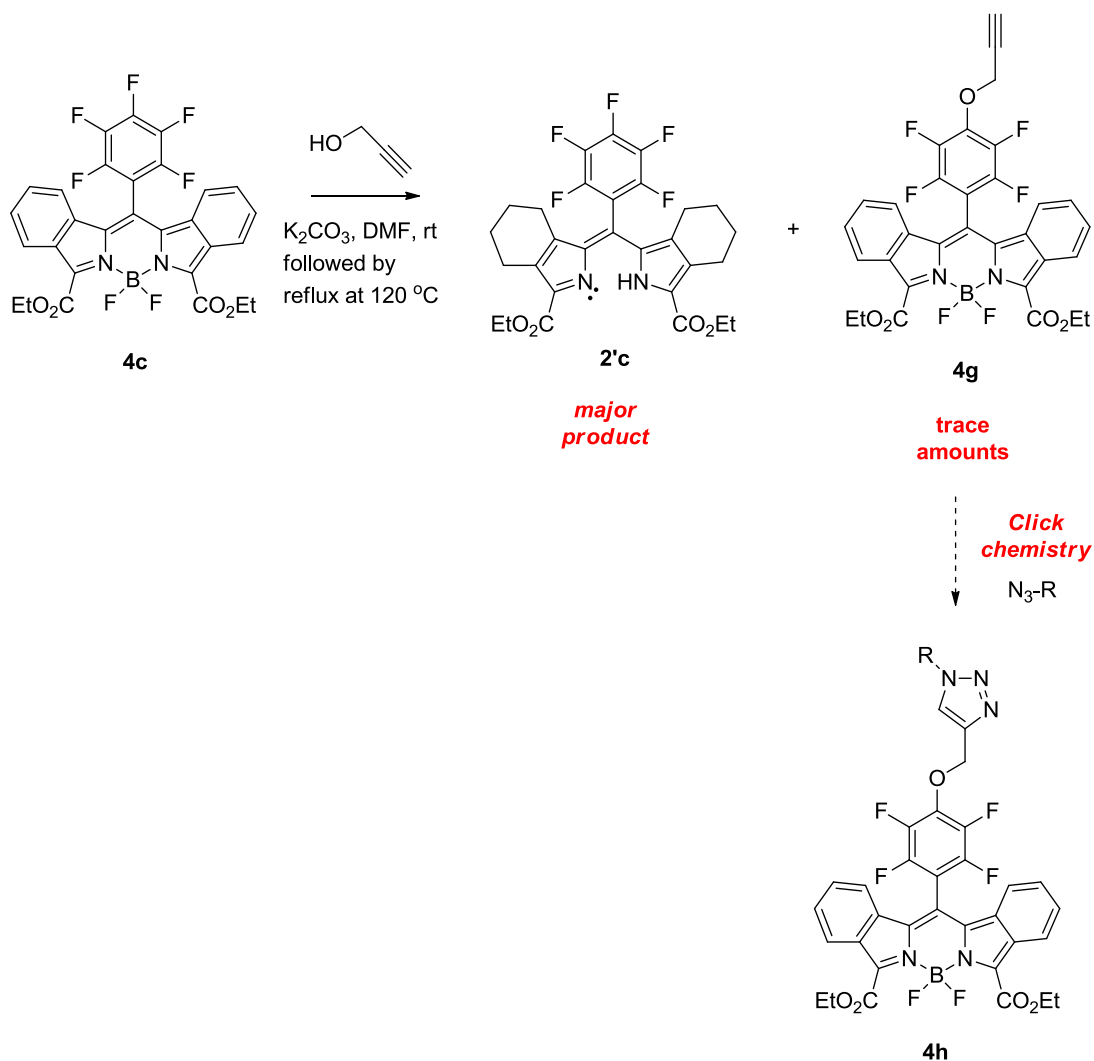


**Scheme 2.14:** Synthetic route to PEGylated-BODIPY **4f**

Nucleophilic substitution reactions of the perfluorinated ring are well-documented, and offer an effective way to generate C-S, C-N and C-O bonds to graft a variety of biological molecules or water-solubilizing groups on a chromophore. The *p*-fluoro group on the pentafluorophenyl moiety is known to react with a variety of primary nucleophiles such as  $\text{HS-CH}_2\text{R}$ ,  $\text{H}_2\text{N-CH}_2\text{R}$  and  $\text{HO-CH}_2\text{R}$ .<sup>21</sup> Thus, selective nucleophilic substitution on a pentafluorophenyl moiety of BODIPY **4c** using a primary alcohol was studied with a goal to tether an “alkyne tag” on BODIPY **4c** for alkyne/azide cycloaddition via click chemistry, following the synthetic route shown in Scheme **2.15**.

A solution of BODIPY **4c** in DMF was treated with 1.4 equiv of propyne-2-ol in the presence of  $\text{K}_2\text{CO}_3$  at room temperature. MALDI analysis of the reaction mixture indicated two strong peaks at  $\text{M}^+ - 19$  and  $\text{M}^+ - \text{BF}_2$ , corresponding to the loss of a fluorine atom (borenium cation), and decomposition of the boron complex respectively, indicating that the lewis acid

boron center is susceptible to an attack from a strong base. Though trace amounts of BODIPY **4g** could be detected as traces on TLC analysis as bright red-spot but could not be recovered after several tedious silica gel purifications.



**Scheme 2.15:** Synthetic route to BODIPY **4h**

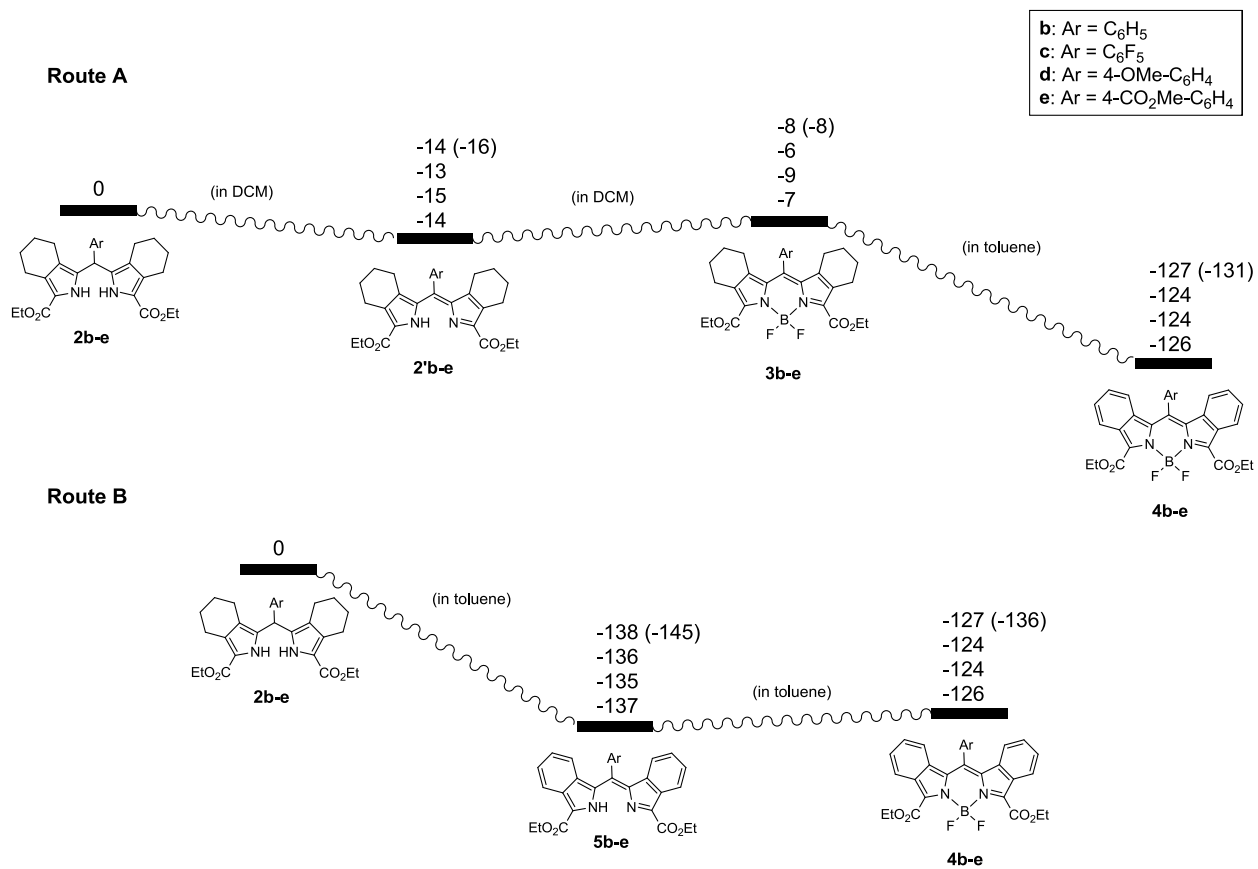
### 2.2.2: Computational Analysis

As can be seen, experimentally the yields of the oxidation reaction depend significantly on the *meso*-aryl substituent (**R**). The reaction yields are higher with  $\text{R} = 4\text{-OMe-C}_6\text{H}_4$  and  $4\text{-CO}_2\text{Me-C}_6\text{H}_4$ , when compared to  $\text{R} = \text{C}_6\text{H}_5$  and  $\text{C}_6\text{F}_5$ . In order to theoretically explain the effect

of different *meso*-substituents on the synthesis of db-BODIPYs, computational studies were performed using Density Functional Theory (DFT) B3LYP potential and the 6-31G (d,p) basis set. Four different aryl substituents, i.e. C<sub>6</sub>H<sub>5</sub>, C<sub>6</sub>F<sub>5</sub>, 4-OMe-C<sub>6</sub>H<sub>4</sub>, and 4-CO<sub>2</sub>Me-C<sub>6</sub>H<sub>4</sub> corresponding to structures **2b-e**, **2'b-e**, **3b-e**, **4b-e**, and **5b-e** respectively, were used for the calculation of the reaction energetics (expressed in kcal mol<sup>-1</sup>). The results obtained are shown in Scheme **2.16** and summarized in Table **2.6**. As can be seen, thermodynamically, there is no substantial difference observed on introducing different *meso*-aryl substituents on the BODIPY chromophore. The calculated relative activation energies are between 2-4 kcal mol<sup>-1</sup>, which is close to the calculation error (1-2 kcal mol<sup>-1</sup>). These results thus indicate that the significant differences in the experimental yields obtained for the db-BODIPYs **4b-e** could be tentatively attributed to their different potential energy barriers.

**Table 2.6:** Relative activation energies (kcal mol<sup>-1</sup>) of BODIPY reaction species following two different routes (Routes **A** and **B**) when different *meso*-aryl substituents are used.

	<b>BODIPY</b>	<b>C<sub>6</sub>H<sub>5</sub></b>	<b>C<sub>6</sub>F<sub>5</sub></b>	<b>4-OMe-C<sub>6</sub>H<sub>4</sub></b>	<b>4-CO<sub>2</sub>Me-C<sub>6</sub>H<sub>4</sub></b>
<b>ROUTE A</b>					
reactant	<b>2</b>	0	0	0	0
intermediate	<b>2'</b>	-14	-13	-15	-14
intermediate	<b>3</b>	-8	-6	-9	-7
product	<b>4</b>	-127	-124	-124	-126
<b>ROUTE B</b>					
reactant	<b>2</b>	0	0	0	0
intermediate	<b>5</b>	-138	-136	-135	-137
product	<b>4</b>	-127	-124	-124	-126



**Scheme 2.16:** Potential energy surface (kcal mol<sup>-1</sup>) as calculated at B3LYP/6-31G(d,p) level

As can be seen, the BF<sub>2</sub>-complexation reactions **2** → **2'** and **2'** → **3** were carried out in dichloromethane, while reactions **2** → **5**, **3** → **4**, and **5** → **4** were performed in toluene. Therefore, to examine the effect of different solvents on the reaction energetics, structures **2b**, **2'b**, **3b**, **4b**, and **5b** were re-optimized in dichloromethane and toluene, respectively. The presence of the solvent was found to stabilize all the structures and the results obtained are listed in Table 2.7. As a result of different solvents, the energies for Route A shifted by 4-6 kcal mol<sup>-1</sup>, however the relative energies remain approximately same and the potential energy is similar. On the other hand, for Route B the solvent-effect is much more pronounced, especially in the case of step 2. The presence of toluene shifts the energetics of step 2 by only 2 kcal mol<sup>-1</sup>, but that of

step 1 by 7 kcal mol<sup>-1</sup>. Therefore, Route B leads to a more exothermic reaction in toluene solvent than in gas phase mainly due to the increased exothermicity of step 1. These results suggest that calculations in gas phase would give a more realistic description of the mechanism. However, care must be taken when step 1 (Route B) is studied as solvent effects are more pronounced for this step, which often results in higher exothermicity of the overall reaction than in gas phase.

**Table 2.7:** Relative activation energies (kcal mol<sup>-1</sup>) of BODIPY reaction species following two different routes (Routes **A** and **B**) in gas and solvent phase.

	<b>BODIPY</b>	<b>In solvent</b>	<b>In gas-phase</b>
<b>ROUTE A</b>			
reactant	<b>2b</b>	0	0
intermediate	<b>2'b</b>	-16	-14
intermediate	<b>3b</b>	-8	-8
product	<b>4b</b>	-131	-127
<b>ROUTE B</b>			
reactant	<b>2b</b>	0	0
intermediate	<b>5b</b>	-145	-138
product	<b>4b</b>	-136	-145

The molecular electrostatic potential (MEP) at a given point  $p(x,y,z)$  in the vicinity of a molecule is defined as the force acting on a positive test charge (for instance, a proton) located at  $p$  through the electrical charge cloud generated through the molecules electrons and nuclei. Despite the fact that the molecular charge distribution remains unperturbed through the external test charge (no polarization occurs) the electrostatic potential of a molecule is still a good guide in assessing the molecules reactivity towards positively or negatively charged reactants. Thus, to account for the different reactivity observed between **2b-e** (or **2'b-e**) and **3b-e**, the feasibility of the cyclohexenyl hydrogens towards oxidation reaction was investigated by calculating the

average molecular electrostatic potentials at their nuclei (MEPN). The results obtained are summarized in Table 2.8. The calculated MEPN showed significant differences when different *meso*-aryl substituents were used. In general, dipyrromethenes **2'** were found to have more negative MEPNs when compared with the corresponding BODIPYs **3**, making them less electron-deficient and thus more prone to oxidation. As a result, the higher yields obtained from oxidation of **3b,d,e** compared with **2b,d,e** and **2'b,d,e** are presumably due to the higher stability and lower tendency of BODIPYs to undergo side reactions. Interestingly, BODIPY **3c** had the highest value of MEPN among all the other BODIPYs, suggesting that this compound is too electron-deficient to undergo oxidation, which is in line with the experimental observations.

**Table 2.8:** Average molecular electrostatic potential at nuclei (MEPN) at the cyclohexenyl hydrogens of **2'b-e**, **3b-e**, and **2b-e**.

Dipyrromethane <b>e</b>	MEPN <sub>H</sub>	Dipyrromethene	MEPN <sub>H</sub>	BODIPY	MEPN <sub>H</sub>
<b>2b</b>	-1.137	<b>2'b</b>	-1.136	<b>3b</b>	-1.128
<b>2c</b>	-1.132	<b>2'c</b>	-1.128	<b>3c</b>	-1.120
<b>2d</b>	-1.138	<b>2'd</b>	-1.138	<b>3d</b>	-1.130
<b>2e</b>	-1.135	<b>2'e</b>	-1.134	<b>3e</b>	-1.126

### 2.2.3: X-ray Structure Determinations

Full confirmation of the nature of all compounds was obtained from the X-ray crystal structures. Single crystals suitable for X-ray structural analysis could be obtained for compounds **2a-d**, **2b'-d'**, **3b-e**, **4b-d**, **8** and **5b-d** by recrystallization from either pure dichloromethane or mixed solvents of dichloromethane/hexane or dichloromethane/ethyl acetate (Figures 2.8 to



**2.11**). The cell parameters and refinement details are reported in the Section **2.4.3** in the experimental details.

X-ray analysis of these compounds confirmed the identity expected on the basis of their synthesis and defined the effect of benz-annulation and boron substituent on the planarity of the ring system. In the case of dipyrromethanes **2a-d**, the two pyrrole rings showed significant distortion from planarity, which is probably caused by the central C<sub>sp3</sub>-atom and two pyrrole rings (average dihedral angle = 68.5°). Interestingly, the intramolecular hydrogen-bonding as seen in the case of dipyrromethenes **2'b-d** and db-dipyrins **5b-d**, caused the two pyrrole rings to be more conjugated and coplanar as indicated by the decrease in their average dihedral angle values of 8.6° and 7.0° respectively. Additionally, coordination of free-pyrroles to boron moiety (for instance BODIPYs **3b-e**, **4b-d** and **8**) indicated a tetra-coordination state on the central boron atom and high planarity of the boron-coordinated ligand moiety.

There is a strong  $\pi$ -electron delocalization between the central six-membered ring and the two adjacent pyrrole rings. However, no  $\pi$ -electron delocalization is observed between the *meso*-aryl group and the BODIPY core, due to planar indacene framework and orthogonal *meso*-phenyl rings, as reported earlier for alkyl pyrroles and isoindole-BODIPYs.<sup>1b, c</sup> The bond angles and bond lengths of the indacene ring system are very close to the values of previously reported BODIPYs.<sup>1a, 12</sup> Thus from the observed trends, it can be concluded, benzannulation and BF<sub>2</sub>-complexation indeed induces increased conjugation and enhanced planarity in the molecule than the corresponding saturated and free-pyrrole analogues.<sup>2</sup> The extended conjugation and higher ring-coplanarity are two important features of the BODIPY chromophore, with respect to its spectroscopic properties and biological efficacy.

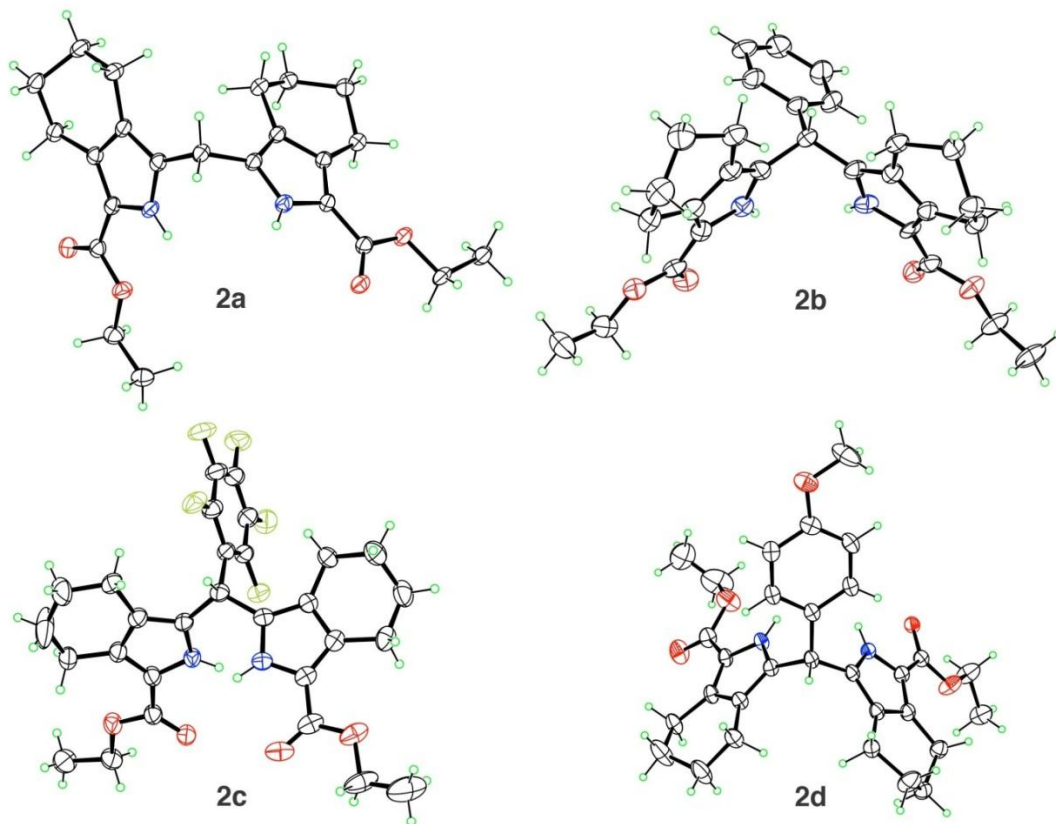


**Figure 2.8:** ORTEP plots of dipyrromethanes **2a-d**

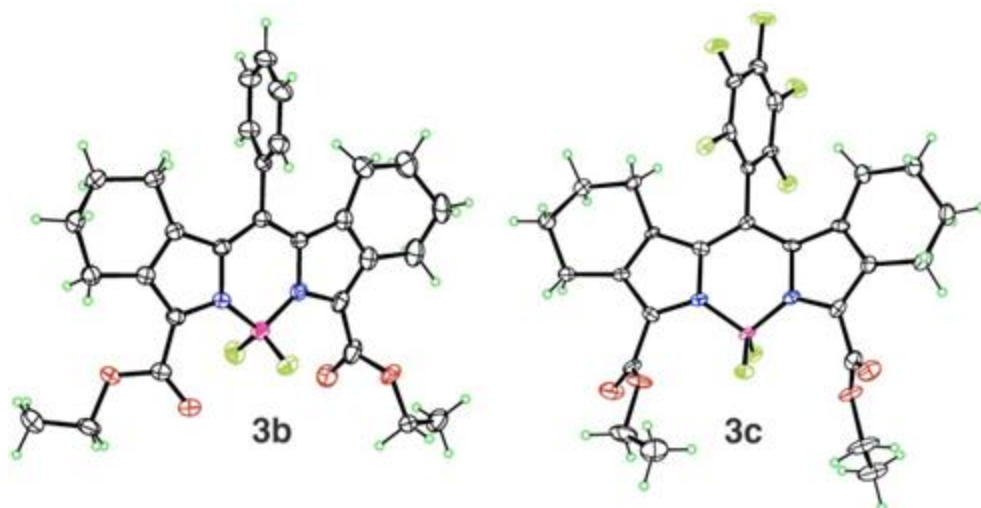


**Figure 2.9:** ORTEP plots of BODIPYs **3b-e**

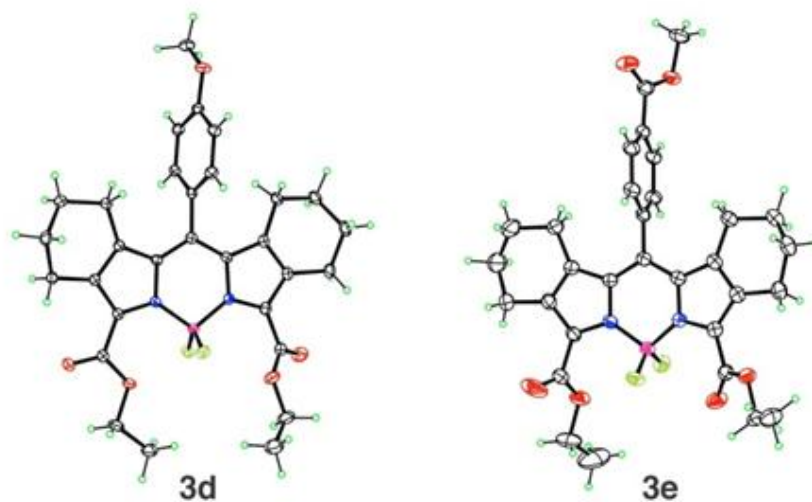


Figure 2.9: (continued)

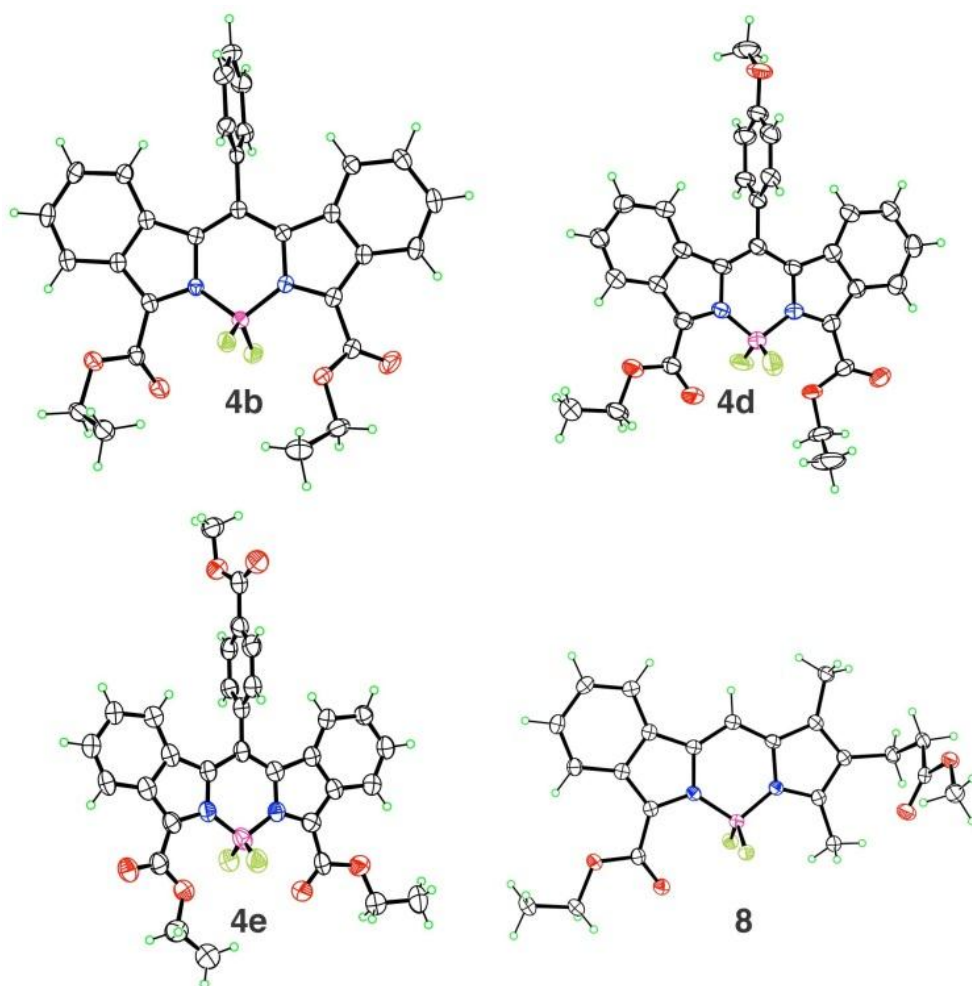
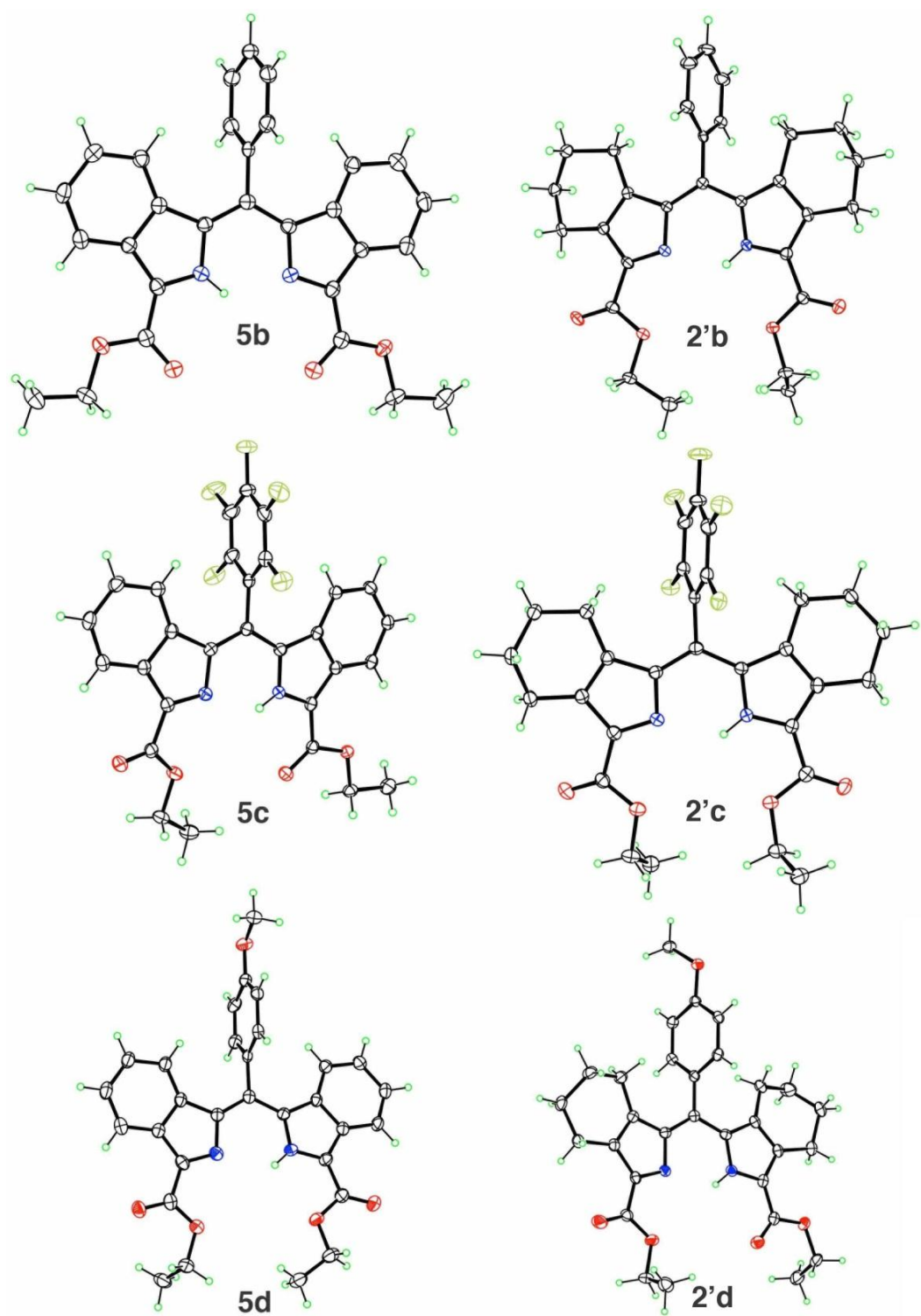


Figure 2.10: ORTEP plots of BODIPYs 8, 4, 4d and 4e



**Figure 2.11:** ORTEP plots of saturated dipyrromethenes **2b'-d'** and db-dipyririns **5b-d**

## 2.2.4: Photophysical Studies

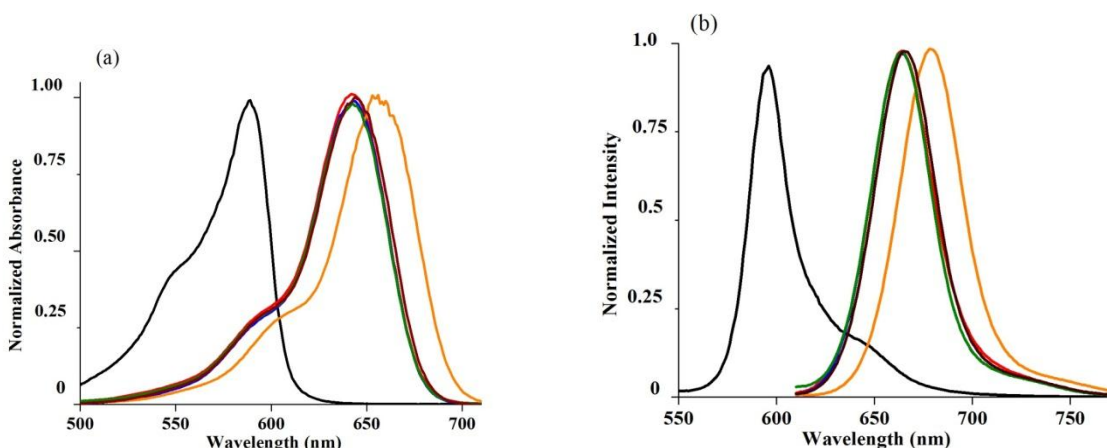
Comparative studies were performed for several cyclohexenyl-fused BODIPYs (**7**, **3a-e**) and benzo-fused BODIPYs (**8**, **4a-e**) in solvents of different polarities (toluene, dichloromethane, and methanol), in order to study the effect of molecular configurations including number of benzo-rings, benzannulation and effect of *meso*-substituent on the spectroscopic properties of BODIPY dyes. The results are compiled in Table **2.9** to **2.12**, and the normalized absorbance and emission spectra in three different solvents are shown in Figures **2.12** to **2.14**.

**Table 2.9:** Spectral properties of BODIPYs **7** and **3a-e** in dichloromethane and methanol at room temperature

BODIPY	Solvent	Absorbance $\lambda_{\max}/\text{nm}$	$\log \epsilon(\text{M}^{-1} \cdot \text{cm}^{-1})$	Emission $\lambda_{\max}/\text{nm}$	$\Phi_f^{[a]}$	Stokes Shift (nm)
<b>7</b>	DCM	530	4.3165	541	0.53	11
	MeOH	523	4.4553	536	0.32	13
<b>3a</b>	DCM	553	4.0289	567	0.35	14
	MeOH	545	4.0523	562	0.23	17
<b>3b</b>	DCM	540	4.3079	561	0.34	21
	MeOH	535	4.3358	555	0.29	20
<b>3c</b>	DCM	563	4.0297	586	0.18	23
	MeOH	557	4.0965	579	0.06	22
<b>3d</b>	DCM	539	4.2467	559	0.34	20
	MeOH	535	4.3582	556	0.20	21
<b>3e</b>	DCM	542	4.2373	562	0.30	20
	MeOH	538	4.3182	560	0.22	22

[a] Fluorescence quantum yields for BODIPY **7** ( $\lambda_{\text{exc}} = 481$  nm) and BODIPYs **3a-e** ( $\lambda_{\text{exc}} = 500$  nm) were calculated using Rhodamine 6G (0.80 in methanol) as the reference,<sup>[28]</sup> respectively.

All these compounds possess characteristic features of BODIPYs including narrow spectral bands with two absorption maxima—an intense  $S_0$ - $S_1$  transition and a weak shoulder at high energy side due to 0-1 vibrational transition.<sup>22</sup> The fluorescence emission spectra were almost mirror-images of the corresponding absorption spectra. Absorption maxima for the BODIPY core, monobenzo- and db-BODIPYs were centered at 540, 590 and 640 nm, and the emission maxima at about 560, 595 and 665 nm, respectively. Benzannulation caused a pronounced red-shift in the absorption and emission profiles of BODIPYs (~ 50-60 nm per appended aromatics). Aromatization of monocyclo-BODIPY **7** to produce monobenzo-BODIPY **8** caused a bathochromic shift of ~ 60 nm in absorption and emission bands, whereas benzannulation of bc-BODIPYs **3a-e** to db-BODIPYs **4a-e** resulted in nearly 90-104 nm red-shift in the optical spectra.<sup>2</sup>

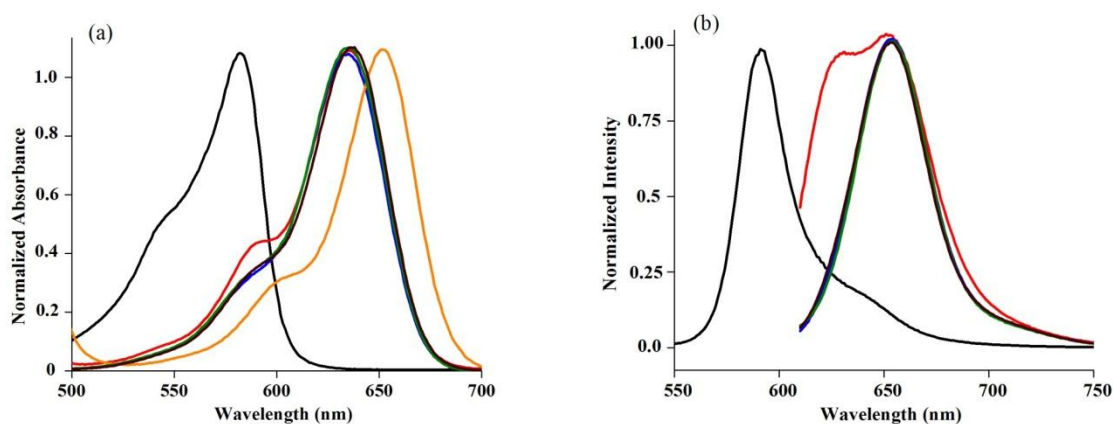


**Figure 2.12:** Normalized fluorescence spectra of BODIPYs **8** (black), **4a** (red), **4b** (blue), **4c** (orange), **4d** (green), **4e** (brown) in dichloromethane at 25 °C.

**Table 2.10:** Spectral properties of BODIPYs **8** and **4a-e** in dichloromethane at room temperature

BODIPY	Absorbance $\lambda_{\max}/\text{nm}$	$\log \epsilon(\text{M}^{-1} \cdot \text{cm}^{-1})$	Emission $\lambda_{\max}/\text{nm}$	$\Phi_f^{[a]}$	Stokes shift (nm)
<b>4a</b>	642	4.2971	664	0.38	22
<b>4b</b>	643	4.3881	665	0.38	22
<b>4c</b>	658	4.2826	680	0.31	22
<b>4d</b>	643	4.1858	664	0.43	21
<b>4e</b>	644	4.4196	666	0.43	22
<b>8</b>	589	4.1723	596	0.99	7

[a] Fluorescence quantum yields for BODIPY **8** ( $\lambda_{\text{exc}} = 530$  nm) and BODIPYs **4a-e** ( $\lambda_{\text{exc}} = 600$  nm) were calculated using cresyl violet perchlorate (0.54 in ethanol) and methylene blue (0.03 in methanol) as the reference,<sup>[28]</sup> respectively using Fluorolog®-3 Modular spectrofluorometer.

**Figure 2.13:** Normalized fluorescence spectra of BODIPYs **8** (black), **4a** (red), **4b** (blue), **4c** (orange), **4d** (green), **4e** (brown) in methanol at 25 °C.

It is noteworthy, that the spectral properties of BODIPYs **3c** and **4c** bearing electron-withdrawing pentafluorophenyl group differ significantly than those bearing the *meso*-aryl groups. The absorption and emission bands for **3c** and **4c** showed a marked red-shift by 20 nm,

indicating a better stabilization of HOMO/LUMO energy gap, as described recently by Galangau and co-workers.<sup>23</sup>

**Table 2.11:** Spectral properties of BODIPYs **8** and **4a-e** in methanol at room temperature

BODIPY	Absorbance $\lambda_{\max}/\text{nm}$	$\log \epsilon(\text{M}^{-1} \cdot \text{cm}^{-1})$	Emission $\lambda_{\max}/\text{nm}$	$\Phi_f^{[a]}$	Stokes shift (nm)
<b>4a</b>	635	3.5182	651	0.11	16
<b>4b</b>	635	4.2363	654	0.45	19
<b>4c</b>	652	nd	nd	nd	nd
<b>4d</b>	635	4.2697	655	0.38	20
<b>4e</b>	636	3.9434	654	0.36	18
<b>8</b>	582	4.2219	591	0.77	9

[a] Fluorescence quantum yields for BODIPY **8** ( $\lambda_{\text{exc}} = 530 \text{ nm}$ ) and BODIPYs **4a-e** ( $\lambda_{\text{exc}} = 600 \text{ nm}$ ) were calculated using cresyl violet perchlorate (0.54 in ethanol) and methylene blue (0.03 in methanol) as the reference,<sup>[28]</sup> respectively using Fluorolog®-3 Modular spectrofluorometer

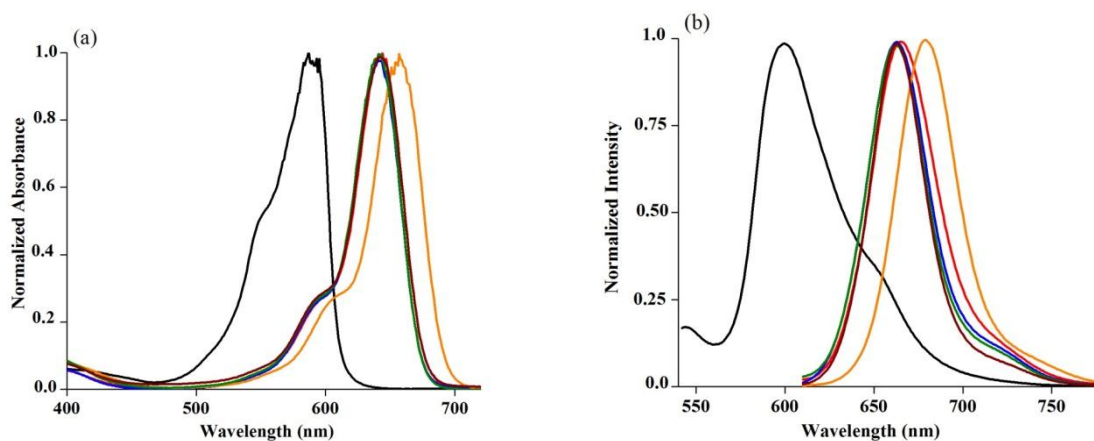


**Figure 2.14:** Normalized fluorescence spectra of BODIPYs **8** (black), **4a** (red), **4b** (blue), **4c** (orange), **4d** (green), **4e** (brown) in toluene at 25 °C.



**Table 2.12:** Spectral properties of BODIPYs **8** and **4a-e** in toluene at room temperature

BODIPY	Absorbance $\lambda_{\text{max}}/\text{nm}$	$\log \epsilon$ ( $\text{M}^{-1} \cdot \text{cm}^{-1}$ )	Emission $\lambda_{\text{max}}/\text{nm}$	$\Phi_{\text{f}}^{[\text{a}]}$	Stokes shift (nm)
<b>4a</b>	644	4.1100	665	0.91	21
<b>4b</b>	643	4.000	663	0.83	20
<b>4c</b>	658	3.8560	679	0.60	21
<b>4d</b>	643	3.9150	662	0.81	19
<b>4e</b>	643	4.3999	663	0.82	20
<b>8</b>	587	4.1030	600	0.96	13

[a] Fluorescence quantum yields for BODIPY **8** ( $\lambda_{\text{exc}} = 530$  nm) and BODIPYs **4a-e** ( $\lambda_{\text{exc}} = 600$  nm) were calculated using cresyl violet perchlorate (0.54 in ethanol) and methylene blue (0.03 in methanol) as the reference,<sup>[28]</sup> respectively using Fluorolog®-3 Modular spectrofluorometer.

However, the electron-donating/withdrawing nature of the *para*-substituent on the benzene ring of BODIPYs **4b**, **4d** and **4e** was shown to have negligible influence on the absorption and fluorescence emission properties of the BODIPYs.<sup>24</sup> The absorption and emission solvatochromism of all BODIPYs (except **4c**) indicated only a weak dependence on the polarity of the solvents, nearly 4-7 nm blue-shifts on changing solvent polarity from dichloromethane to methanol, due to the increase in the non-radiative deactivation process in the more polar solvents. In comparison, the fluorescence properties of BODIPY **4c** were highly dependent on the polarity of the solvent. In apolar solvents such as dichloromethane and toluene, intense fluorescence was observed for **4c**, however, in polar protic solvent such as methanol, hydrogen bonding interactions due to pentafluorophenyl group induced the photoinduced electron transfer between the excited BODIPY and the pentafluorophenyl moiety, resulting in significant fluorescence quenching which lead to difficulty in recording its fluorescence spectrum and quantum yield.<sup>22</sup> Additionally, lower quantum yields were obtained for BODIPYs **3c** and **4c**,

when compared to their analogues, presumably due to the additional aryl group rotation<sup>25</sup> and/or the heavy atom effect.<sup>26</sup>

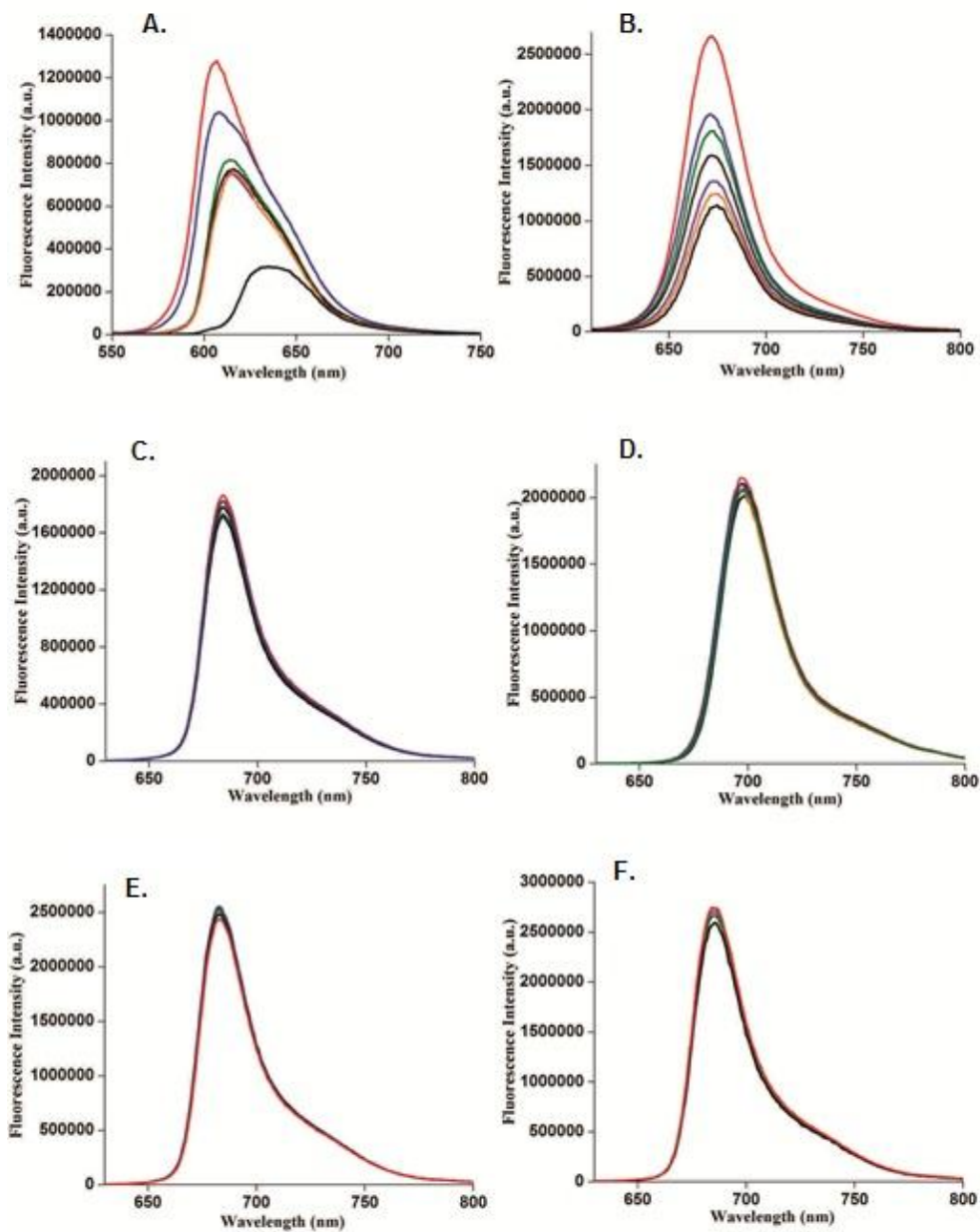


**Figure 2.15:** Time-dependent fluorescence spectra of 0.32 mM DMSO solutions of BODIPYs **8** (a), **4a** (b), **4b** (c), **4c** (d), **4d** (e) and **4e** (f), respectively, at 0 min (red), 15 min (blue), 30 min (green), 45 min (brown), 60 min (purple), 120 min (orange) and 24 h (black) after solution preparation, at room temperature. The excitation wavelengths for BODIPY **8** and BODIPYs **4(a-e)** were 530 nm and 610 nm, respectively.

The fluorescence quantum yields for benzo-fused BODIPYs **4a-e** were found to be higher than those for cyclohexyl-BODIPYs **3a-e**, as measured in dichloromethane. It is worth noting that the presence of 3,5-methyl groups in BODIPYs **7** and **8** increased their fluorescence quantum yields appreciably (0.53 and 0.99), as compared to the 3,5-ethoxycarbonyls in BODIPYs **3a-e** and **4a-e**, due to the “push-pull” electronic effect caused by the methyl groups at the 3,5-positions.<sup>4, 27</sup> All these results are in line with the behaviour of the other methyl-BODIPYs reported previously.

As high photostability is an important characteristic for various practical applications of BODIPYs dyes, hence in order to study the effect of *meso*-substituents on BODIPY dye, photofading process was studied for benzo-fused BODIPYs **8** and **4a-e** in DMSO, over a period of 24 h.<sup>27a</sup> As seen in Figure **2.15**, significant decrease in the fluorescence emission maxima was observed in the case of *meso*-free BODIPYs **8** and **4a**. However, no fluorescence quenching was observed for *meso*-substituted BODIPYs **4b-e**, indicating that these dyes are much more stable than dyes **8** and **4a**.

## **2.2.5: In Vitro Cellular Studies**

**2.2.5.1: Cytotoxicity.** The *in vitro* photocytotoxic activity of mono-(**8**) and db- BODIPYs (**4a-e**) was evaluated against HEP2 cells exposed to increasing concentration of each compound up to 400  $\mu$ M for 24 h, using Cell Titer Blue assay and irradiation with 1.5 J/cm<sup>2</sup> of broad spectrum light. Parallel assays without light irradiation were also carried out to determine the cytotoxicity in the absence of light. Compounds stock solution was prepared in DMSO and Cremophor (< 0.9% DMSO/0.1% Cremophor). The dose-dependent survival curves for these BODIPYs are shown in Figure **2.16** and **2.17** and the results are summarized in Table **2.13**. Results were expressed as IC<sub>50</sub>, defined as the concentration of dye (in  $\mu$ M) required to kill 50% of the cells.

All BODIPYs were found to have very low dark cytotoxicities with  $IC_{50} > 200 \mu\text{M}$ . All the cellular studies were performed by Dr. Xiaoke Hu, from Vicente research group.

**Table 2.13:** Cytotoxicity (Hep2 cells) using Cell Titer Blue assay for benzo-appended-BODIPYs **8** and **4a-e**.

Compound	Dark toxicity ( $IC_{50}$ , $\mu\text{M}$ )	Phototoxicity ( $IC_{50}$ , $\mu\text{M}$ )
<b>8</b>	400	> 100
<b>4a</b>	> 400	> 100
<b>4b</b>	236	> 100
<b>4c</b>	> 400	> 100
<b>4d</b>	> 400	> 100
<b>4e</b>	373.5	> 100

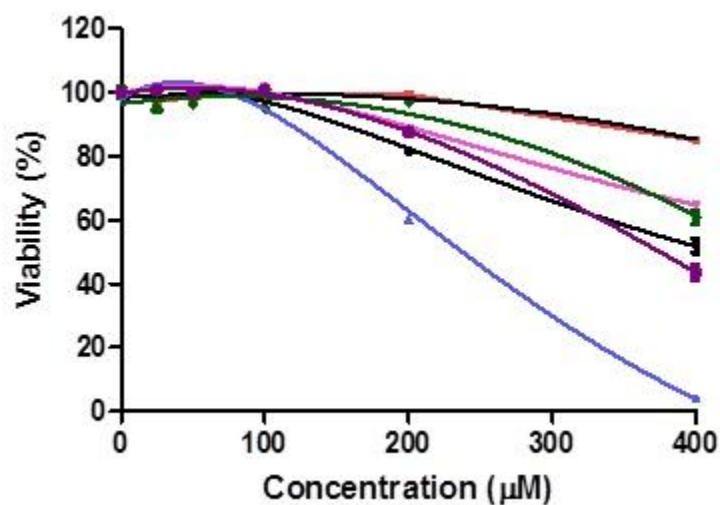


**Figure 2.16:** Dark toxicity of BODIPYs **4a-e** and **8** toward HEp2 cells using Cell Titer Blue assay

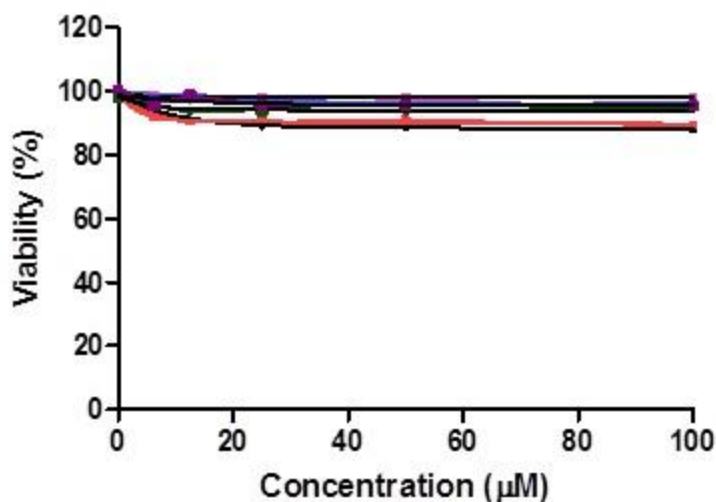


**Figure 2.17:** Photo cytotoxicity of BODIPYs **4a-e** and **8** toward HEP2 cells using using  $1 \text{ J/cm}^2$  light dose and the Cell Titer Blue assay

except for BODIPY **4b**, which showed the highest dark toxicity presumably due to its lower solubility in the biological media. Upon exposure to a low light dose ( $1.5 \text{ J/cm}^2$ ), all BODIPY derivatives were essentially non-phototoxic to HEP2 cells. The observed results are in good agreement with previously reported *in vitro* photocytotoxicity investigations for various *meso*-substituted BODIPYs.<sup>28, 29</sup>

**2.2.5.2: Time-Dependent Cellular Uptake.** The results obtained for the time-dependent uptake of BODIPYs **8** and **4a-e** at a concentration of  $10 \text{ }\mu\text{M}$  in human HEP2 cells, over a period of 24 h, are shown in Figure **2.18**. Significant differences were observed in the cellular uptake of these BODIPYs and can be categorized on the basis of *meso*-free, *meso*-phenyl and *meso*-pentafluorophenyl ( $\text{C}_6\text{H}_5$ )-BODIPY derivatives. BODIPY **4c** with *meso*- $\text{C}_6\text{H}_5$  functional group, accumulated the most within the cells than the *meso*-free and *meso*-phenyl BODIPYs, at all time points studied. The higher cellular uptake for BODIPY **4c** can be attributed to its polar hydrophilicity which introduces charge and hydrogen bonding interactions that influence its

ability to interact with cellular membrane and leads to increased uptake by the cells. It is interesting to note that similar uptake results were obtained for all *meso*-aryl BODIPYs **4b**, **4d** and **4e**. On the other hand, the *meso*-free monobenzo- and db-BODIPYs **8** and **4a** were least taken up by the cells, presumably due to their lower photostability and significant fluorescence self-quenching. These findings are in agreement with previous reports, indicating that the presence of *meso*-aryl group increases the photostability of BODIPYs over *meso*-unsubstituted BODIPYs.<sup>27b</sup>

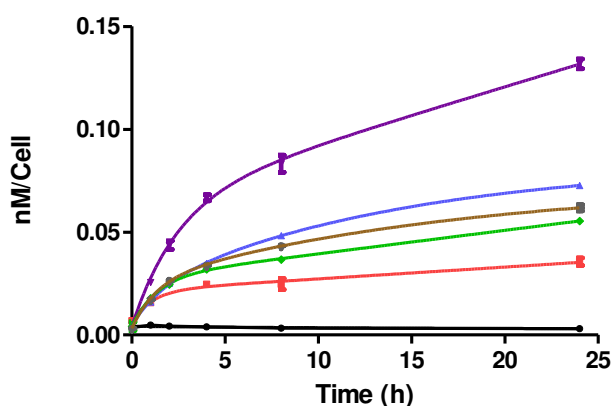


**Figure 2.18:** Time-dependent uptake of BODIPYs **8** (black), **4a** (red), **4b** (blue), **4c** (purple), **4d** (green) and **4e** (brown) at 10  $\mu$ M by HEP2 cells

**2.2.5.3: Intracellular Localization.** The preferential sites of intracellular localization of BODIPY **8** were evaluated using Leica DMRXA fluorescence microscope. First the HEP2 cells were observed using 40X NA 0.8dip objective lens in the phase-contrast mode, followed by exposure to UV-visible light using a Texas-red filter, DAPI and GFP filter (to check the background autofluorescence, Figure **2.19a**). Next, the cells were exposed to 10  $\mu$ M compound concentration for 6 h. and observed under microscope using the Texas-red filter (Figure **2.19b**). Later on, the cell cultures with BODIPY **8** were incubated with ER Tracker Blue/White, Mitotracker Green, BODIPY FL C5 ceramide and LysoSensor Green, i.e ER, Mitochondria, Golgi apparatus and Lysosome specific tracker dye respectively. The signals obtained were first imaged using the

DAPI/GFP filter set (to record emission by organelle-specific dye, Figures **2.19c, e, g** and **i**) and then using Texas-red filter (to record the emission by BODIPY **8**). Finally the two images obtained in each case were overlapped to obtain images shown in Figure **2.19d, f, h** and **j** in order to explore the sites of preferential localization of BODIPY **8** in HEp2 cells. The results obtained from these studies are shown in Figure **2.19** and are summarized in Table **2.14**.

The intracellular localization studies were extended to BODIPYs **4a-e** using the same method and instrumentation. The fluorescence patterns obtained from these studies are shown in Figure **2.20** to **2.24** and summarized in Table **2.14**. As can be seen, all BODIPYs investigated were found to localize preferentially in the endoplasmic reticulum of the cell. Furthermore, all the BODIPYs were found in other cell organelles, for instance BODIPY **4a-d** and **8** were found in mitochondria, **4a** and **4c-e** in the lysosomes and **4a, 4d** and **4e** in the Golgi. Our results are in accordance with many commercially available and previously reported alkyl and aryl-substituted BODIPYs that show low cytotoxicity, high photo-stability, effective plasma membrane penetration and intracellular distribution in multiple organelles.<sup>30</sup>

**Table 2.14:** Major Subcellular Sites of Localization for BODIPYs in Hep2 cells.

Compound	Major sites of localization
<b>8</b>	ER, Mito
<b>4a</b>	ER, Lyso, Golgi, Mito
<b>4b</b>	ER, Mito
<b>4c</b>	ER, Lyso, Mito
<b>4d</b>	ER, Lyso, Golgi, Mito
<b>4e</b>	ER, Lyso, Golgi

### 2.3: Conclusion

In this work, the synthesis, spectroscopic and computational investigations of a new series of conformationally restricted BODIPY dyes have been investigated by introducing benzene units fused to the  $\beta,\beta'$ -pyrrolic positions of the BODIPY core. Two different synthetic routes (i.e. Route **A** and Route **B**) were investigated to provide a practical and straightforward approach to benzo-appended BODIPYs **4a-e**. Route **A** involved the formation of boron complex followed by benzannulation performed using DDQ, whereas in Route **B**, the aromatization step was performed prior to  $\text{BF}_2$ -complexation. Higher reaction yields for db-BODIPYs **4a-e** (except **4c**) were obtained via Route **A**, which is attributed to the better stability of BODIPYs **3a-e** over dipyrromethenes **2'a-e** under oxidation conditions. However, due to slow reactivity of BODIPY **3c** (bearing a *meso*-pentafluorophenyl group) towards oxidative conditions, the corresponding db-BODIPY **4c** could only be obtained from Route **B** in 35% yield. X-ray crystallographic analysis and additional computational modeling of these compounds employing DFT, provided further insight into the electronic features of such sterically-crowded BODIPY fluorophores. X-ray-structural analysis displays the progressively extended planarity of the chromophore which is in line with the increased conformational restriction in the series **3a-e**, **4a-e** and **5a-e**, leading to larger red-shifts of the absorption and emission wavelengths. The  $\pi$ -extended db-BODIPYs displayed strong bathochromic shifts in their absorption and emission profiles in the order of 589-658 nm and 598-680 nm respectively, with ~ 50-60 nm shifts per attached benzene subunit. In the series, BODIPY **4c** bearing *meso*-pentafluorophenyl group, displayed the highest red-shifted spectra (~ 20 nm more red-shift) and lowest fluorescence quantum yields, when compared to those, that had a *meso*-phenyl group. In general, the BODIPYs in the series **3a-e** and **4a-e**, tend to have small Stokes' shifts due to their rigid ring-fused framework which prevents the non-radiative deactivation of the excited state of the molecule. Moreover, the



absorption and emission wavelengths of such rigidified BODIPYs can be easily tuned to obtain BODIPY dyes absorbing at  $> 700$  nm by further modification at the 3,5-positions of the BODIPY core. In vitro biological investigations using HEP2 cells revealed low cytotoxicities, high plasma-membrane permeability and intracellular localization mainly in the cell endoplasmic reticulum along with other cell organelles. This work indicates that the red-emissive and photostable benzo-appended BODIPYs (e.g. db-BODIPYs **4b-e**) can supplement the existing dyes, for instance, rhodamines in more lipophilic applications such as doping of polymer particles/beads and study of less polar environments.

## **2.4: Experimental**

### **2.4.1: General Information**

All air and moisture sensitive reactions were performed under argon atmosphere in oven-dried glassware. Common reagents were obtained from commercial source and used without further purification, unless otherwise stated. Dry solvents were collected from PS-400 Solvent Purification System from PS-400 Solvent Purification System from Innovative Technology, Inc. Melting points were determined in open capillary and are uncorrected. Column Chromatography was performed on silica gel (Sorbent Technologies, 60 Å, 40-63  $\mu\text{m}$ ) slurry packed into glass columns. Analytical thin-layer-chromatography (TLC) was carried out using polyester backed TLC plates 254 (precoated, 200  $\mu\text{m}$ , Sorbent Technologies).  $^1\text{H}$  NMR and  $^{13}\text{C}$  NMR spectra were recorded on Bruker DPX-400 (operating at 400MHz for  $^1\text{H}$  NMR and 100 MHz for  $^{13}\text{C}$  NMR) in  $\text{CDCl}_3$  (7.26 ppm,  $^1\text{H}$  and 77.0 ppm,  $^{13}\text{C}$ ) with tetramethylsilane as internal standard. All spectra were recorded at 25°C and coupling constants ( $J$  values) are given in Hz. Chemical shifts are given in parts per millions (ppm). High resolution mass spectra were obtained at the LSU Department of Chemistry Mass Spectrometry Facility using an ESI or MALDI-TOF method, and

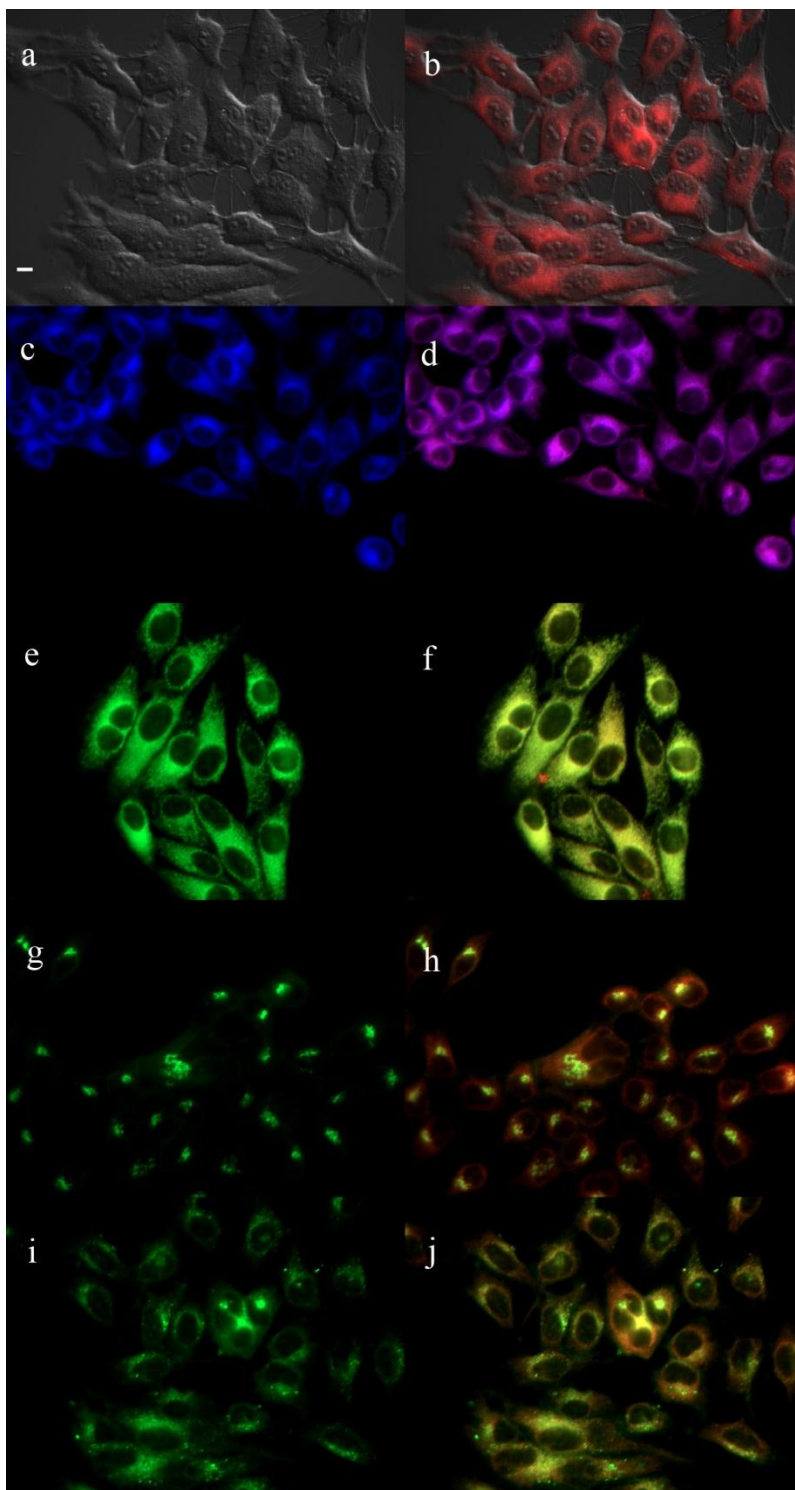


**Figure 2.19:** Subcellular localization of BODIPY **8** in HEp2 cells at 10  $\mu\text{M}$  for 6 h. (a) Phase contrast, (b) overlay of **8** fluorescence and phase contrast, (c) ER tracker Blue/White fluorescence, (e) MitoTracker Green fluorescence, (g) BODIPY Ceramide, (i) LysoSensor Green fluorescence, and (d, f, h, j) overlays of organelle tracers with **8** fluorescence. Scale bar: 10  $\mu\text{m}$ .

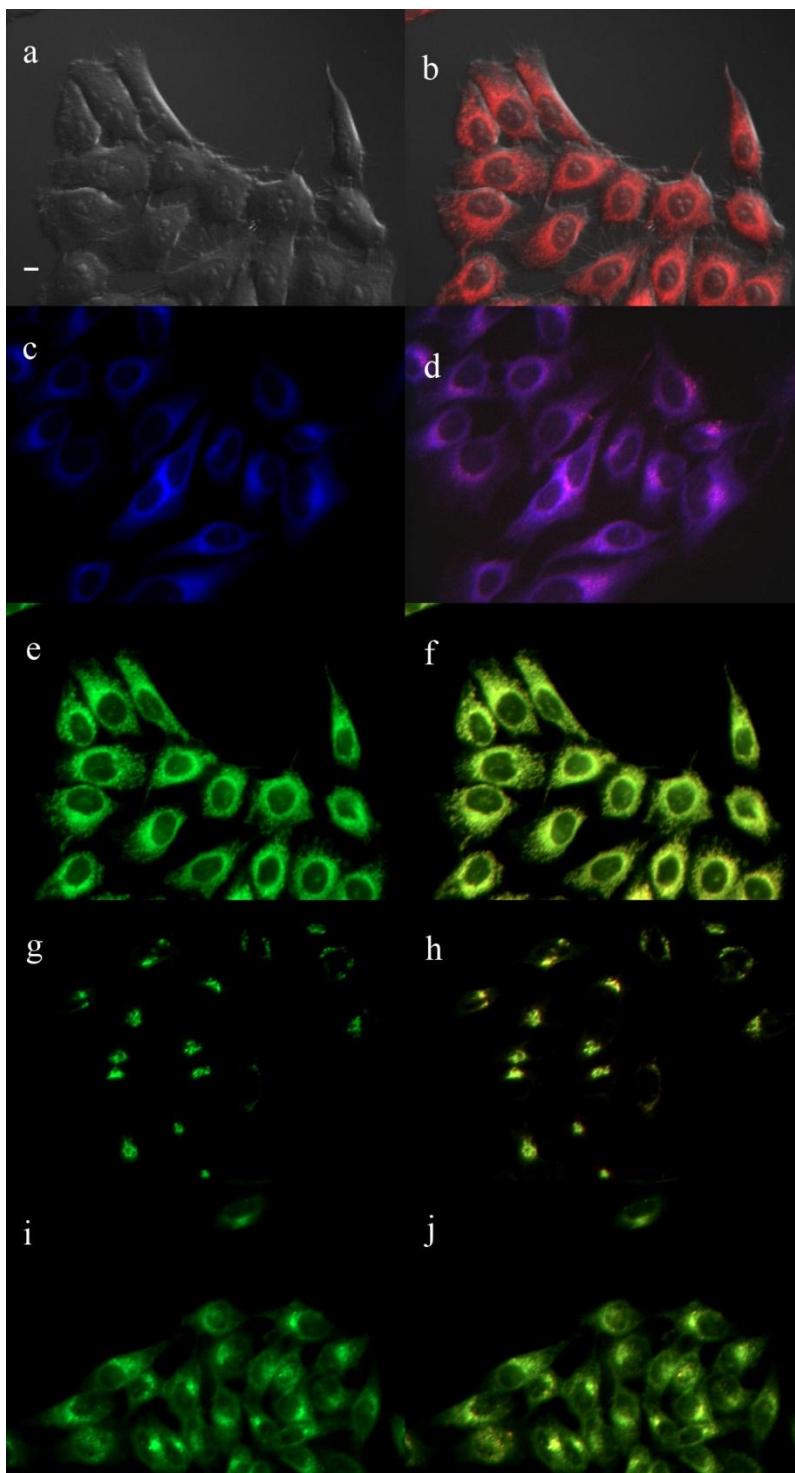


**Figure 2.20:** Subcellular localization of BODIPY **4a** in HEp2 cells at 10  $\mu$ M for 6 h. (a) Phase contrast, (b) overlay of **4a** fluorescence and phase contrast, (c) ER tracker Blue/White fluorescence, (e) MitoTracker Green fluorescence, (g) BODIPY Ceramide, (i) LysoSensor Green fluorescence, and (d, f, h, j) overlays of organelle tracers with **4a** fluorescence. Scale bar: 10  $\mu$ m.

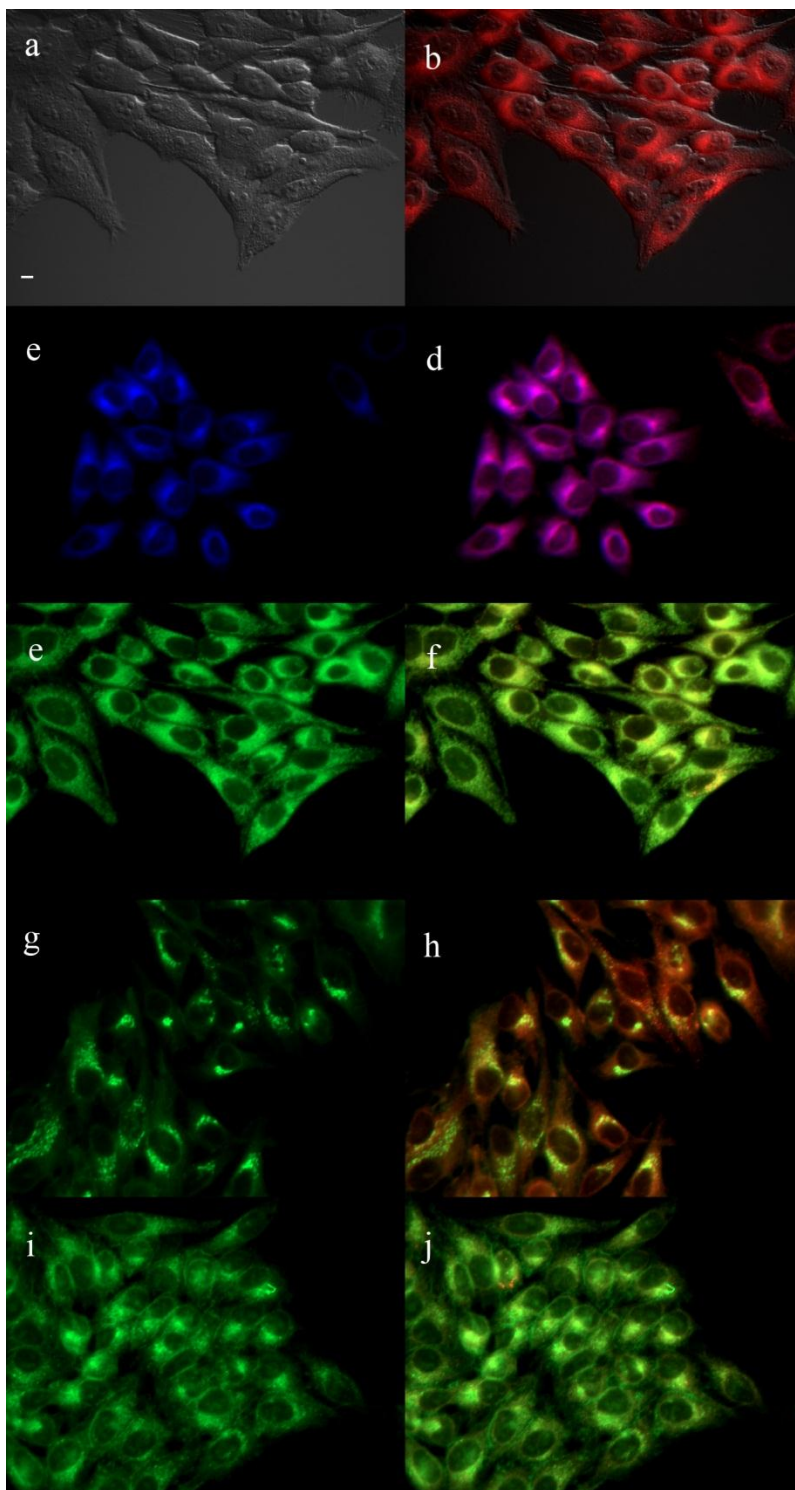


**Figure 2.21:** Subcellular localization of BODIPY **4b** in HEp2 cells at 10  $\mu$ M for 6 h. (a) Phase contrast, (b) overlay of **4b** fluorescence and phase contrast, (c) ER tracker Blue/White fluorescence, (e) MitoTracker Green fluorescence, (g) BODIPY Ceramide, (i) LysoSensor Green fluorescence, and (d, f, h, j) overlays of organelle tracers with **4b** fluorescence. Scale bar: 10  $\mu$ m.

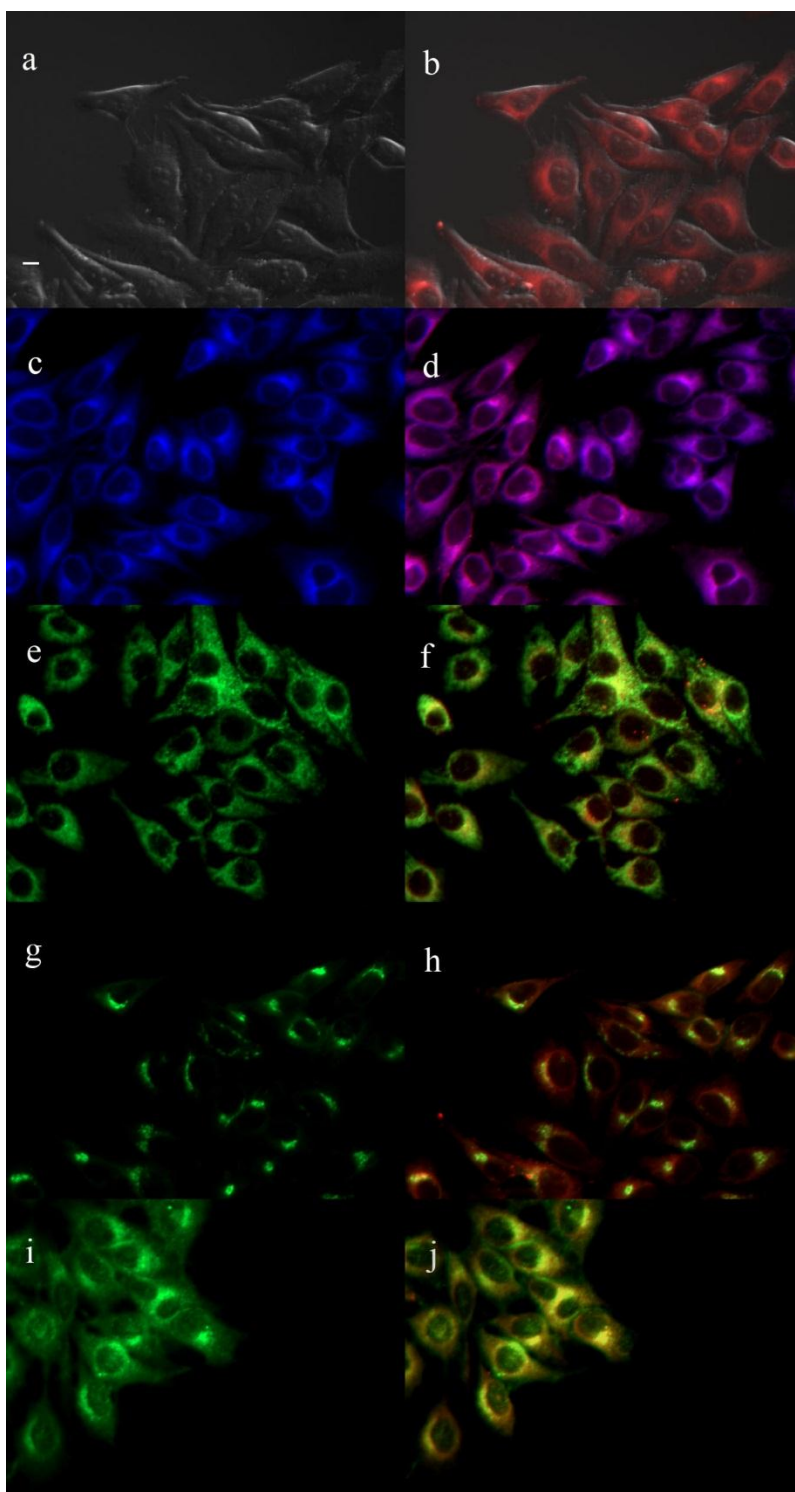


**Figure 2.22:** Subcellular localization of BODIPY **4c** in HEp2 cells at 10  $\mu$ M for 6 h. (a) Phase contrast, (b) overlay of **4c** fluorescence and phase contrast, (c) ER tracker Blue/White fluorescence, (e) MitoTracker Green fluorescence, (g) BODIPY Ceramide, (i) LysoSensor Green fluorescence, and (d, f, h, j) overlays of organelle tracers with **4c** fluorescence. Scale bar: 10  $\mu$ m.

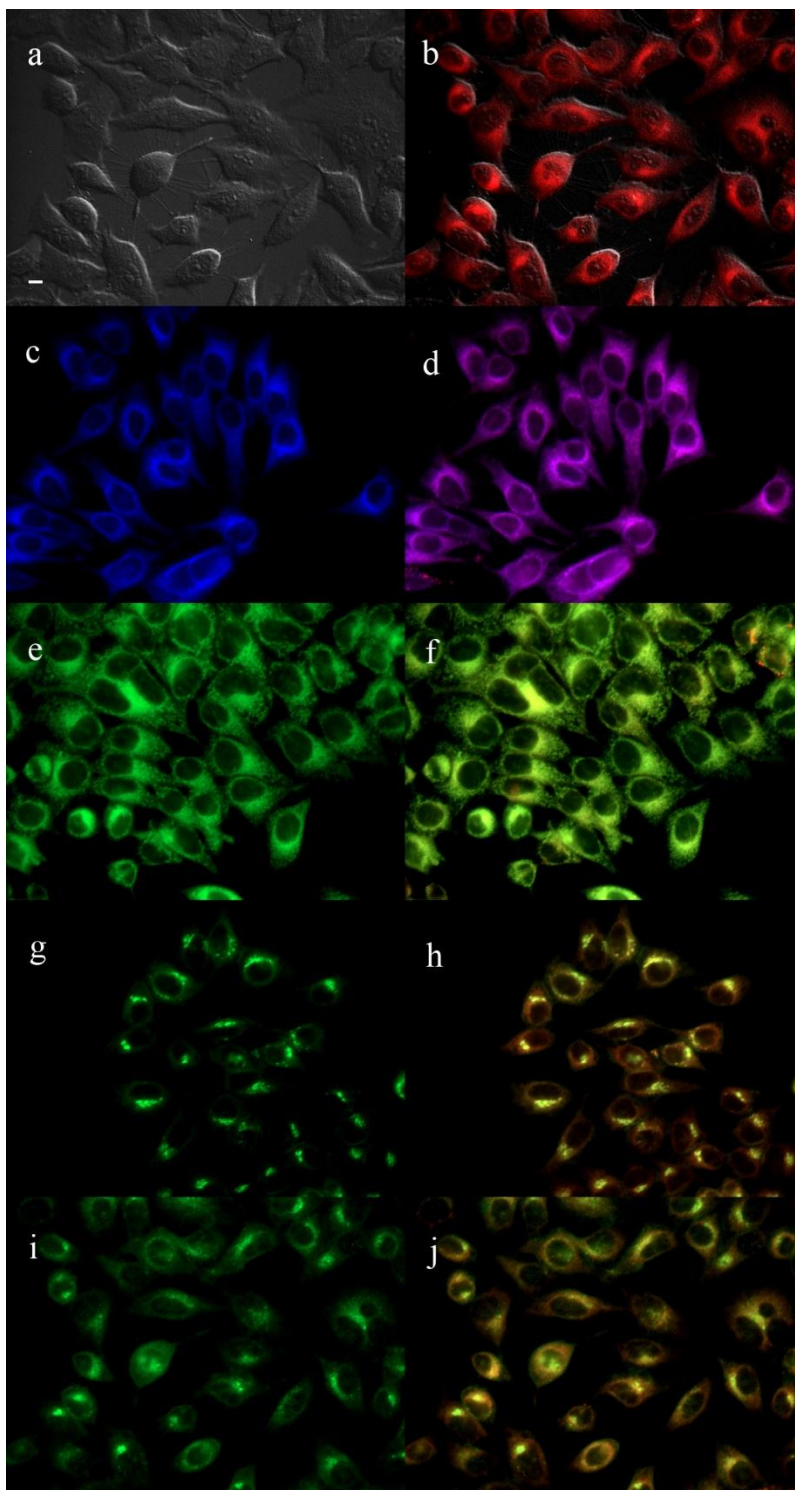


**Figure 2.23:** Subcellular localization of BODIPY **4d** in HEp2 cells at 10  $\mu$ M for 6 h. (a) Phase contrast, (b) overlay of 4d fluorescence and phase contrast, (c) ER tracker Blue/White fluorescence, (e) MitoTracker Green fluorescence, (g) BODIPY Ceramide, (i) LysoSensor Green fluorescence, and (d, f, h, j) overlays of organelle tracers with **4d** fluorescence. Scale bar: 10  $\mu$ m.

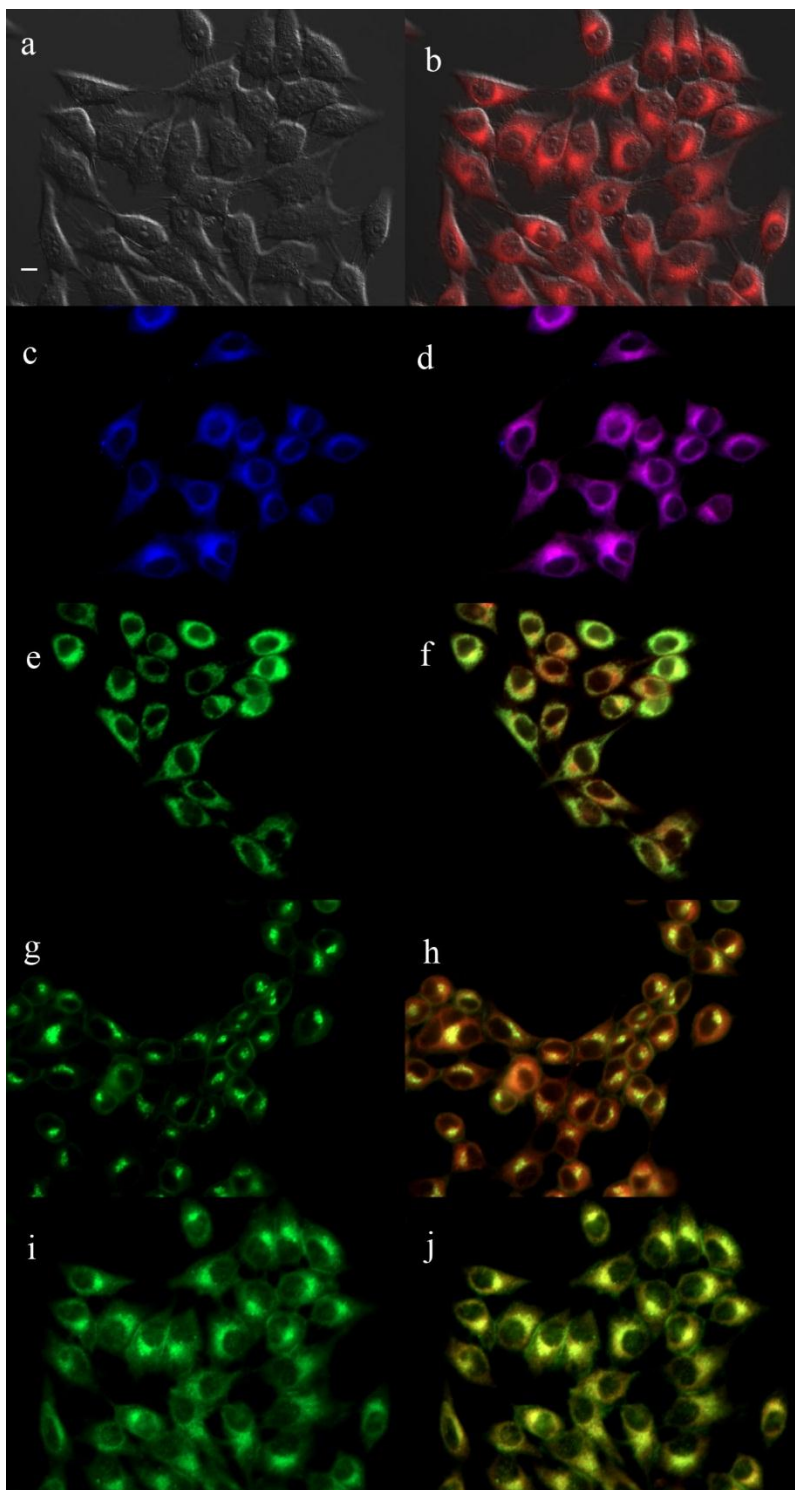


**Figure 2.24:** Subcellular localization of BODIPY **4e** in HEp2 cells at 10  $\mu$ M for 6 h. (a) Phase contrast, (b) overlay of **4e** fluorescence and phase contrast, (c) ER tracker Blue/White fluorescence, (e) MitoTracker Green fluorescence, (g) BODIPY Ceramide, (i) LysoSensor Green fluorescence, and (d, f, h, j) overlays of organelle tracers with **4e** fluorescence. Scale bar: 10  $\mu$ m.

a peak matching protocol to determine the mass error range of the molecular ion. Bis(3-ethoxycarbonyl-4,5,6,7-tetrahydro-2H-isoindolyl) methane (**2a**)<sup>14</sup> was synthesized as described previously.

## 2.4.2: Syntheses

### General procedure for synthesis of 8-aryl-bis(3-ethoxycarbonyl-4,5,6,7-tetrahydro-2H-isoindolyl)methanes (**2b-e**)

Pyrrole **1** (0.1007 g, 0.5 mmol) was treated with p-toluenesulfonic acid (0.0047 g, 0.025 mmol), n-tetrabutylammonium chloride (0.0036 g, 0.01 mmol) and corresponding aldehyde (0.3 mmol) in CH<sub>2</sub>Cl<sub>2</sub> (50 mL). The mixture was stirred overnight at room temperature under inert atmosphere, washed with saturated NaHCO<sub>3</sub> (2 x 30 mL), brine (1 x 30 mL) and dried over Na<sub>2</sub>SO<sub>4</sub>. The solvent was evaporated in vacuum and the residue was chromatographed on a silica column (hexane/ethyl acetate 5/1 for **2b**, **2d**, **2e** and hexane/ethyl acetate 7/3 for **2c**). The product was finally re-crystallized from CH<sub>2</sub>Cl<sub>2</sub>-hexane mixture.

**2b**: Yield 117 mg (95%), beige solid, mp (110-112°C) <sup>1</sup>H-NMR (CDCl<sub>3</sub>): δ 8.74 (br s, 2H), 7.32-7.08 (m, 5H), 5.42 (s, 1H), 4.22-4.15 (m, 4H), 2.78 (m, 4H), 2.21 (m, 4H), 1.68 (m, 8H), 1.28 (t, J = 7.12 Hz, 6H); <sup>13</sup>C NMR (CDCl<sub>3</sub>): δ 161.8, 139.1, 130.8, 129.2, 128.9, 128.2, 127.3, 119.7, 116.7, 59.7, 40.6, 23.3, 23.1, 21.2, 14.5; ESI-HRMS m/z 474.25; Calcd. for C<sub>29</sub>H<sub>34</sub>N<sub>2</sub>O<sub>4</sub> [M+H<sup>+</sup>] 475.2575

**2c**: Yield 123 mg (87%), beige solid, mp (106-108°C) <sup>1</sup>H-NMR (CDCl<sub>3</sub>): δ 8.71 (br s, 2H), 5.79 (s, 1H), 4.27 (q, J = 7.12 Hz, 4H), 2.27 (m, 4H), 2.26 (m, 2H), 2.12 (m, 2H), 1.70 (m, 8H), 1.33 (t, J = 7.12 Hz, 6H); <sup>13</sup>C NMR (CDCl<sub>3</sub>): δ 161.4, 146.0, 143.6, 141.9, 139.2, 139.1, 136.5, 128.9, 126.3, 120.2, 117.6, 113.4, 113.3, 113.1, 60.0, 29.8, 23.1, 23.0, 22.8, 21.0, 20.1, 14.4; ESI-HRMS m/z 564.20; Calcd. for C<sub>29</sub>H<sub>29</sub>F<sub>5</sub>N<sub>2</sub>O<sub>4</sub> [M+Na<sup>+</sup>] 587.1946.



**2d:** Yield 112 mg (89%), pale pink solid, mp (113-116°C) ; <sup>1</sup>H-NMR (CDCl<sub>3</sub>): δ 9.39 (br s, 2H), 7.91 (m, 2H), 7.15 (m, 2H), 5.50 (s, 1H), 4.18-4.06 (m, 4H), 3.91 (s, 3H), 2.74 (m, 4H), 2.26 (m, 4H), 1.69 (m, 8H), 1.24 (t, J = 7.12 Hz, 6H); <sup>13</sup>C NMR (CDCl<sub>3</sub>): δ 166.6, 161.9, 144.9, 130.2, 129.9, 129.2, 128.9, 128.1, 120.0, 117.2, 59.8, 52.1, 40.1, 23.3, 23.1, 23.1, 21.4, 14.4; ESI-HRMS m/z 504.26; Calcd. for C<sub>30</sub>H<sub>36</sub>N<sub>2</sub>O<sub>5</sub> [M+H<sup>+</sup>] 504.2576

**2e:** Yield 93 mg (70%), pale pink solid, mp (104-106°C) <sup>1</sup>H-NMR (CDCl<sub>3</sub>): δ 8.92 (br s, 2H), 7.94 (m, 2H), 7.16 (m, 2H), 5.47 (s, 1H), 4.17 (m, 4H), 3.91 (s, 3H), 2.76 (m, 4H), 2.21 (m, 4H), 1.68 (m, 8H), 1.27 (t, J = 7.12 Hz, 6H); <sup>13</sup>C NMR (CDCl<sub>3</sub>): δ, 166.3, 161.1, 146.2, 143.4, 142.0, 138.6, 132.3, 131.1, 129.8, 129.5, 127.6, 61.2, 52.5, 24.5, 23.2, 22.5, 21.7, 14.0; ESI-HRMS m/z 532.26; Calcd. for C<sub>31</sub>H<sub>36</sub>N<sub>2</sub>O<sub>6</sub> [M+H<sup>+</sup>] 533.2649.

**General procedure for synthesis of 8-aryl-bis(3-ethoxycarbonyl-4,5,6,7-tetrahydro-2H-isoindolyl)methenes (2'b-e)**

A solution of DDQ (0.36 mmoles, 1.2 equiv.) in dry dichloromethane (10mL) was added to a solution of **2'b-e** (0.3 mmoles, 1.0 equiv.) in dry dichloromethane (20 mL) at 0 °C. The solution was stirred under argon for 15-20 min until TLC indicated reaction completion. Further the reaction mixture was washed with saturated NaHCO<sub>3</sub> (2 x 30mL), brine (1 x 30mL) and dried over Na<sub>2</sub>SO<sub>4</sub>. The solvent was evaporated in vacuum and the residue was chromatographed on a silica column using dichloromethane/petroleum ether 5/1 as eluent. The product was finally recrystallized from CH<sub>2</sub>Cl<sub>2</sub>-hexane mixture to yield shiny deep green crystals.

**2'b:** Yield 106 mg (75%), mp (164-166°C) <sup>1</sup>H-NMR (CDCl<sub>3</sub>): δ 7.45 (m, 3H), 7.27 (m, 2H), 4.37 (q, J = 7.12 Hz, 4H), 2.69 (m, 4H), 1.57 (m, 4H), 1.51 (m, 4H), 1.42 (t, J = 7.12 Hz, 6H), 1.36 (m, 4H); <sup>13</sup>C NMR (CDCl<sub>3</sub>): δ 162.3, 143.8, 141.7, 139.7, 139.0, 137.0, 133.0, 129.1, 128.8, 128.7, 60.6, 24.2, 23.2, 23.1, 22.3, 14.4; ESI-HRMS m/z 472.2362; Calcd. for C<sub>29</sub>H<sub>32</sub>N<sub>2</sub>O<sub>4</sub> [M+H<sup>+</sup>] 473.2447.

**2c:** Yield 118 mg (70%), mp (158-160°C) <sup>1</sup>H-NMR (CDCl<sub>3</sub>): δ 4.37 (q, J = 7.12 Hz, 4H), 2.67 (m, 4H), 1.67 (m, 4H), 1.60 (m, 4H), 1.52 (m, 8H), 1.41 (t, J = 7.12 Hz, 6H); <sup>13</sup>C NMR (CDCl<sub>3</sub>): δ 161.8, 145.8, 143.2, 138.6, 137.8, 134.0, 132.4, 127.4, 60.9, 29.4, 23.3, 23.2, 23.0, 22.8, 22.4, 22.2, 22.0, 14.1 ; ESI-HRMS m/z 562.1891; Calcd. for C<sub>29</sub>H<sub>27</sub>F<sub>5</sub>N<sub>2</sub>O<sub>4</sub> [M+H<sup>+</sup>] 563.1978.

**2d:** Yield 123 mg (82%), mp (172-174°C) ;<sup>1</sup>H-NMR (CDCl<sub>3</sub>): δ 7.28 (m, 2H), 7.11 (m, 2H), 4.49 (q, J = 7.12 Hz, 4H), 4.07 (s, 3H), 3.05 (m, 4H), 1.96 (m, 4H), 1.53 (m, 8H), 1.22 (t, J = 7.12 Hz, 6H); <sup>13</sup>C NMR (CDCl<sub>3</sub>): δ 161.6, 160.3, 147.2, 142.7, 139.6, 133.0, 132.1, 129.2, 126.2, 114.2, 60.6, 55.3, 24.5, 23.2, 23.1, 22.4, 14.4; ESI-HRMS m/z 502.2467; Calcd. for C<sub>30</sub>H<sub>34</sub>N<sub>2</sub>O<sub>5</sub> [M+H<sup>+</sup>] 503.2560.

**2e:** Yield 108 mg (68%), , mp (155-157°C) <sup>1</sup>H-NMR (CDCl<sub>3</sub>): δ 8.18 (m, 2H), 8.01 (m, 2H), 4.49 (m, 4H), 3.95 (s, 3H), 2.67 (m, 4H), 1.65 (m, 4H), 1.53 (m, 4H), 1.42 (t, J = 7.12 Hz, 6H), 1.31 (m, 4H); <sup>13</sup>C NMR (CDCl<sub>3</sub>): δ, 166.3, 162.1, 146.2, 143.6, 142.2, 138.6, 133.0, 130.1, 129.8, 129.5, 128.0, 61.2, 52.5, 24.5, 23.2, 23.1, 22.4, 14.0; ESI-HRMS m/z 530.2417 Calcd. for C<sub>31</sub>H<sub>34</sub>N<sub>2</sub>O<sub>6</sub> [M+H<sup>+</sup>] 531.2480.

### General procedure to BODIPYs 3a-e

A solution of DDQ (0.6 mmoles, 1.2 equiv.) in dry THF (10mL) was added to a solution of **2a** (0.5 mmoles, 1.0 equiv.) in dry THF (10 mL) for **2a** or CH<sub>2</sub>Cl<sub>2</sub> for **2b-e**, at 0 °C. The solution was stirred under argon for 20 min. Et<sub>3</sub>N (3 mmol, 6 equiv.) and BF<sub>3</sub>.OEt<sub>2</sub> (5 mmol, 10 equiv.) were added dropwise and the solution was stirred for 20 min at 0 °C and then overnight at room temperature. Once TLC indicated reaction completion, the solvent was removed under reduced pressure and the residue was taken up in ethyl acetate and extracted with 0.1 M HCl (2 x 30mL) to remove excess DDQ, brine (1 x 30mL) and dried over anhydrous Na<sub>2</sub>SO<sub>4</sub>. The solvent was evaporated to dryness and residue purified by column chromatography (hexane/ethyl acetate, 3:2). The product was re-crystallized from CH<sub>2</sub>Cl<sub>2</sub>/hexane mixtures to yield the BODIPY.

**3a:** Yield 149 mg (67%), mp (169-171°C) <sup>1</sup>H-NMR (CDCl<sub>3</sub>): δ 5.30 (s, 1H), 4.42 (q, J=7.11 Hz, 4H), 2.65 (m, 8H), 1.76 (m, 8H), 1.42 (t, J = 7.11 Hz, 6H); <sup>13</sup>C NMR (CDCl<sub>3</sub>): δ 161.7, 144.1, 142.6, 134.4, 132.8, 129.6, 128.7, 128.6, 126.1, 121.2, 61.6, 60.7, 29.7, 23.1, 22.9, 22.8, 22.7, 22.4, 22.0, 21.5, 14.3, 14.1, 14.0; ESI-HRMS m/z 444.20; Calcd. for C<sub>23</sub>H<sub>27</sub>BF<sub>2</sub>N<sub>2</sub>O<sub>4</sub> [M+Na<sup>+</sup>] 467.1917.

**3b:** Yield 208 mg (80%), mp (209-211°C) <sup>1</sup>H-NMR (CDCl<sub>3</sub>): δ 7.52 (m, 3H), 7.23 (m, 2H), 4.44 (q, J = 7.12 Hz, 4H), 2.57 (m, 4H), 1.57 (m, 8H), 1.42 (t, J = 7.12 Hz, 6H), 1.39 (m, 4H); <sup>13</sup>C NMR (CDCl<sub>3</sub>): δ 161.6, 147.6, 143.8, 143.6, 134.6, 132.9, 132.5, 129.6, 129.5, 127.2, 61.7, 24.4, 22.6, 22.3, 22.0, 14.0; MALDI-TOF m/z 520.23; Calcd. for C<sub>29</sub>H<sub>31</sub>BF<sub>2</sub>N<sub>2</sub>O<sub>4</sub> [M+Na<sup>+</sup>] 543.237.

**3c:** Yield 229 mg (75%), mp (202-204°C) <sup>1</sup>H-NMR (CDCl<sub>3</sub>): δ 4.45 (q, J = 7.12 Hz, 4H), 2.60 (m, 4H), 1.81 (m, 4H), 1.65 (m, 4H), 1.59 (m, 4H), 1.45 (t, J = 7.12 Hz, 6H); <sup>13</sup>C NMR (CDCl<sub>3</sub>): δ 161.0, 145.6, 142.3, 137.8, 133.9, 133.5, 132.6, 128.3, 62.0, 29.6, 23.3, 23.2, 23.0, 22.8, 22.4, 22.1, 22.0, 14.0; MALDI-TOF m/z 610.19; Calcd. for C<sub>29</sub>H<sub>26</sub>BF<sub>7</sub>N<sub>2</sub>O<sub>4</sub> [M<sup>+</sup>] 610.1876.

**3d:** Yield 200 mg (73%), mp (181-183°C) <sup>1</sup>H-NMR (CDCl<sub>3</sub>): δ 7.12 (m, 2H), 7.03 (m, 2H), 4.43 (q, J = 7.1 Hz, 4H), 3.89 (s, 3H), 2.76 (m, 4H), 2.57 (m, 4H), 1.64 (m, 4H), 1.58 (m, 4H), 1.41 (t, J = 7.1 Hz, 6H), 1.40 (m, 4H); <sup>13</sup>C NMR (CDCl<sub>3</sub>): δ 161.5, 160.6, 147.9, 143.7, 143.4, 133.3, 132.4, 128.6, 126.5, 114.8, 61.6, 55.3, 24.7, 22.6, 22.3, 22.0, 14.0; ESI-HRMS m/z 550.25; Calcd. for C<sub>30</sub>H<sub>33</sub>BF<sub>2</sub>N<sub>2</sub>O<sub>5</sub> [M+Na<sup>+</sup>] 573.2361.

**3e:** Yield 174 mg (60%), mp (173-175°C) <sup>1</sup>H-NMR (CDCl<sub>3</sub>): δ 8.21 (m, 2H), 7.36 (m, 2H), 4.43 (q, J = 7.12 Hz, 4H), 3.99 (s, 3H), 2.57 (m, 4H), 1.56 (m, 8H), 1.44 (t, J = 7.12 Hz, 6H), 1.39 (m, 4H); <sup>13</sup>C NMR (CDCl<sub>3</sub>): δ 166.6, 161.4, 146.0, 144.1, 143.5, 139.2, 132.8, 132.4, 131.4, 130.7, 127.6, 61.8, 52.5, 24.6, 22.5, 22.3, 21.9, 14.0; ESI-HRMS m/z 578.24; Calcd. for C<sub>31</sub>H<sub>33</sub>BF<sub>2</sub>N<sub>2</sub>O<sub>6</sub> [M+H<sup>+</sup>] 577.2299.

### General procedure for the synthesis of BODIPYs 4 via Route A

BODIPYs **3a-e** (112 mg, 0.2665 mmol) were dissolved in toluene (30mL) and heated to about 110°C. A solution of DDQ (9 equiv.) in toluene (20mL) was then added and the mixture was refluxed under Ar. The reaction was monitored by UV-Vis. Upon the completion, the reaction mixture was cooled to room temperature and the solvent was removed under reduced pressure. The residue was taken up in CH<sub>2</sub>Cl<sub>2</sub> (30 mL) and extracted with 10% aq. NaHCO<sub>3</sub> (3 x 30 mL), brine (1 x 30 mL) and dried over Na<sub>2</sub>SO<sub>4</sub>. The solvent was removed under reduced pressure and the residue was purified by column chromatography (CH<sub>2</sub>Cl<sub>2</sub> to 0.1% MeOH in CH<sub>2</sub>Cl<sub>2</sub>). The product was re-crystallized from CH<sub>2</sub>Cl<sub>2</sub>/hexane mixtures to yield shiny copper-colored crystals.

**4a:** Yield 81 mg (69%), mp > 250°C <sup>1</sup>H-NMR (CDCl<sub>3</sub>): δ 8.45 (m, 2H), 8.15 (m, 2H), 7.55 (m, 2H), 7.41 (m, 2H), 4.60 (q, J=7.11 Hz, 4H), 1.55 (t, J = 7.3 Hz, 6H); <sup>13</sup>C NMR (CDCl<sub>3</sub>): δ 160.2, 140.2, 133.8, 130.9, 127.2, 124.5, 122.9, 62.4, 14.1; MALDI-TOF m/z 444.20; Calcd. for C<sub>23</sub>H<sub>27</sub>BF<sub>2</sub>N<sub>2</sub>O<sub>4</sub> [M+H<sup>+</sup>] 444.20

**4b:** Yield 91 mg (67%), mp > 250°C <sup>1</sup>H-NMR (CDCl<sub>3</sub>): δ 8.11 (m, 2H), 7.72 (m, 3H), 7.52 (m, 2H), 7.26 (m, 2H), 7.08 (m, 2H), 6.16 (m, 2H), 4.62 (q, J = 7.12 Hz, 4H), 1.55 (t, J = 7.12 Hz, 6H); <sup>13</sup>C NMR (CDCl<sub>3</sub>): δ 160.6, 141.2, 140.2, 134.7, 134.2, 131.2, 130.1, 129.8, 129.7, 129.1, 128.5, 126.5, 124.1, 121.7, 62.2, 14.1; ESI-HRMS m/z 512.17; Calcd. for C<sub>29</sub>H<sub>23</sub>BF<sub>2</sub>N<sub>2</sub>O<sub>4</sub> [M+Na<sup>+</sup>] 535.1633.

**4d:** Yield 132 mg (92%), mp > 250°C <sup>1</sup>H-NMR (CDCl<sub>3</sub>): δ 8.11 (m, 2H), 7.26 (m, 8H), 6.30 (m, 2H), 4.61 (q, J = 7.12 Hz, 4H), 4.02 (s, 3H), 1.55 (t, J = 7.12 Hz, 6H); <sup>13</sup>C NMR (CDCl<sub>3</sub>): δ 160.8, 160.6, 141.4, 139.9, 134.7, 131.1, 129.8, 129.6, 129.5, 126.4, 126.2, 124.0, 121.8, 115.1, 62.2, 55.5, 14.1; MALDI-TOF m/z 542.18; Calcd. for C<sub>30</sub>H<sub>25</sub> BF<sub>2</sub>N<sub>2</sub>O<sub>5</sub> [M<sup>+</sup>] 542.260.

**4e:** Yield 103 mg (68%), mp > 250°C <sup>1</sup>H-NMR (CDCl<sub>3</sub>): δ 8.39 (m, 2H), 8.12 (m, 2H), 7.65 (m, 2H), 7.27 (m, 2H), 7.09 (m, 2H), 6.12 (m, 2H), 4.62 (q, J = 7.12 Hz, 4H), 4.07 (s, 3H), 1.55 (t, J = 7.12 Hz, 6H); <sup>13</sup>C NMR (CDCl<sub>3</sub>): δ 166.3, 160.5, 140.6, 139.7, 138.8, 134.4, 131.8, 131.2, 131.0, 130.0, 128.9, 128.5, 126.7, 124.3, 121.4, 62.3, 52.6, 14.1; MALDI-TOF m/z 570.18; Calcd. for C<sub>31</sub>H<sub>25</sub>BF<sub>2</sub>N<sub>2</sub>O<sub>6</sub> [M+H<sup>+</sup>] 570.213

#### General procedure for the synthesis of dibenzo-fused dipyrins (**5a-e**)

Dipyrromethanes (**2a-e**) (112 mg, 0.2665 mmol) were dissolved in dry toluene (30mL) and heated to about 110°C. A solution of DDQ (9 equiv.) in dry toluene (20mL) was added and the mixture was refluxed under Ar. The reaction was monitored by UV-Vis and on completion the solvent was removed under reduced pressure. The purple residue was taken up in ethyl acetate and extracted with 0.1M HCl to remove any traces of DDQ (3 x 50 mL), brine (1 x 50 mL) and dried over Na<sub>2</sub>SO<sub>4</sub>. The solvent was removed under reduced pressure and the residue was purified by column chromatography (CH<sub>2</sub>Cl<sub>2</sub> for **5a**, **5b** and hexane/ethyl acetate, 2/1 for **5c**, **5d**, **5e**). The product was re-crystallized from CH<sub>2</sub>Cl<sub>2</sub>/MeOH mixtures to yield deep green crystals.

**5a:** Yield 57 mg (56%), mp 168-169°C, UV/vis (CH<sub>2</sub>Cl<sub>2</sub>) λ<sub>max</sub> (log ε) 568 (4.24), <sup>1</sup>H-NMR (CDCl<sub>3</sub>): δ 8.48 (m, 2H), 8.23 (m, 2H), 7.40 (m, 4H), 4.55 (q, J = 7.07 Hz, 4H), 1.55 (t, J = 7.3 Hz, 6H); <sup>13</sup>C NMR (CDCl<sub>3</sub>): δ 161.6, 137.1, 134.5, 133.3, 133.0, 131.3, 130.8, 128.7, 127.7, 127.0, 126.5, 126.4, 123.1, 123.0, 122.8, 118.9, 61.5, 61.2, 61.1, 29.6, 14.3, 14.5 ESI-HRMS m/z 388.14; Calcd. for C<sub>23</sub>H<sub>20</sub>N<sub>2</sub>O<sub>4</sub> [M+H<sup>+</sup>] 388.14.

**5b:** Yield 81 mg (66%), mp 146-147°C, UV/vis (CH<sub>2</sub>Cl<sub>2</sub>) λ<sub>max</sub> (log ε) 569 (4.48), <sup>1</sup>H-NMR (CDCl<sub>3</sub>): δ 8.19 (m, 2H), 7.66 (m, 5H), 7.24 (m, 2H), 6.97 (m, 2H), 6.12 (m, 2H), 5.30 (s, 1H), 4.58 (q, J = 7.12 Hz, 4H), 1.56 (t, J = 7.12 Hz, 6H); <sup>13</sup>C NMR (CDCl<sub>3</sub>): δ 161.8, 137.7, 136.4, 135.5, 135.0, 131.6, 129.5, 129.4, 129.1, 126.9, 126.0, 122.8, 122.0, 61.2, 14.4; ESI-HRMS m/z 464.17; Calcd. for C<sub>29</sub>H<sub>24</sub>N<sub>2</sub>O<sub>4</sub> [M+H<sup>+</sup>] 465.1788.

**5c:** Yield 91 mg (62%), mp 224-225°C UV/vis (CH<sub>2</sub>Cl<sub>2</sub>)  $\lambda_{\max}$  (log  $\epsilon$ ) 583 (4.63), <sup>1</sup>H-NMR (CDCl<sub>3</sub>):  $\delta$  8.25 (m, 2H), 7.33 (m, 2H), 7.18 (m, 2H), 6.34 (m, 2H), 4.56 (q, J = 7.12 Hz, 4H), 1.56 (t, J = 7.12 Hz, 6H); <sup>13</sup>C NMR (CDCl<sub>3</sub>):  $\delta$  161.4, 139.3, 134.6, 134.3, 131.8, 128.2, 126.8, 123.7, 119.8, 61.5, 14.4; ESI-HRMS m/z 554.13; Calcd. for C<sub>29</sub>H<sub>19</sub>F<sub>5</sub>N<sub>2</sub>O<sub>4</sub> [M+Na<sup>+</sup>] 555.1328.

**5d:** Yield 90 mg (69%), mp 197-199°C UV/vis (CH<sub>2</sub>Cl<sub>2</sub>)  $\lambda_{\max}$  (log  $\epsilon$ ) 569 (4.59), <sup>1</sup>H-NMR (CDCl<sub>3</sub>):  $\delta$  8.20 (m, 2H), 7.43 (m, 2H), 7.24 (m, 2H), 7.18 (m, 2H), 7.02 (m, 2H), 6.28 (m, 2H), 4.57 (q, J = 7.12 Hz, 4H), 4.01 (s, 3H), 1.56 (t, J = 7.12 Hz, 6H); <sup>13</sup>C NMR (CDCl<sub>3</sub>):  $\delta$  161.8, 135.7, 131.7, 130.6, 126.9, 126.0, 122.7, 122.1, 114.8, 61.2, 55.5, 14.4; MALDI-TOF m/z 494.18; Calcd. for C<sub>30</sub>H<sub>26</sub>N<sub>2</sub>O<sub>5</sub> [M+H<sup>+</sup>] 495.258.

**5e:** Yield 81 mg (58%), mp 208-209°C UV/vis (CH<sub>2</sub>Cl<sub>2</sub>)  $\lambda_{\max}$  (log  $\epsilon$ ) 572 (4.59), <sup>1</sup>H-NMR (CDCl<sub>3</sub>):  $\delta$  8.35 (m, 2H), 8.18 (m, 2H), 7.65 (m, 2H), 7.23 (m, 2H), 6.96 (m, 2H), 6.06 (m, 2H), 4.57 (q, J = 7.12 Hz, 4H), 4.06 (s, 3H), 1.56 (t, J = 7.12 Hz, 6H); <sup>13</sup>C NMR (CDCl<sub>3</sub>):  $\delta$  166.6, 161.7, 141.1, 138.1, 137.8, 135.3, 134.4, 131.7, 131.2, 130.7, 129.5, 128.8, 127.1, 126.2, 123.0, 121.7, 61.3, 52.5, 14.4; ESI-HRMS m/z 522.18; Calcd. for C<sub>31</sub>H<sub>26</sub>N<sub>2</sub>O<sub>6</sub> [M+H<sup>+</sup>] 522.1831

### General procedure for synthesis of BODIPYs 4 via Route B

A solution of db-dipyrins (**5a-e**) (0.1mmol) in toluene (20mL) was stirred at 0°C for 15 min under Argon atmosphere. Further, Et<sub>3</sub>N (0.089 mL, 0.64 mmol) and BF<sub>3</sub>.OEt<sub>2</sub> (0.13 mL, 1.024 mmol) were added and the mixture was stirred at room temperature for 30 min. The reaction was then refluxed at the boiling temperature of the solvent until the UV-Vis indicated reaction completion. The obtained fluorescent blue solution was washed with 10% aq. NaHCO<sub>3</sub> (3 x 20 mL), brine (1 x 20 mL) and dried over Na<sub>2</sub>SO<sub>4</sub>. The solvent was evaporated to dryness and the product was obtained as copper-colored crystals after re-crystallization from CH<sub>2</sub>Cl<sub>2</sub>/hexane mixtures. Yields obtained: **4a**, 24 mg (55%); **4b**, 40 mg (80%); **4c**, 34 mg (56%); **4d**, 49 mg (90%); **4e**, 43 mg (75%).

**4c:** mp > 250°C <sup>1</sup>H-NMR (CDCl<sub>3</sub>): δ 8.16 (m, 2H), 7.38-7.25 (m, 4H), 6.39 (m, 2H), 4.62 (q, J = 7.12 Hz, 4H), 1.54 (t, J = 7.12 Hz, 6H); <sup>13</sup>C NMR (CDCl<sub>3</sub>): δ 160.1, 142.0, 133.8, 131.3, 131.2, 128.5, 127.3, 125.1, 122.5, 119.5, 62.6, 14.1; MALDI-TOF m/z 602.12; Calcd. for C<sub>29</sub>H<sub>18</sub>BF<sub>7</sub>N<sub>2</sub>O<sub>4</sub> [M<sup>+</sup>] 602.179.

### **BODIPY 7**

Pyrrole **1** (150 mg, 0.7762 mmol) and **6** (162 mg, 0.7762 mmol) were dissolved in dry dichloromethane (20 mL) at 0°C and POCl<sub>3</sub> (0.14 mL, 0.9314 mmol) was added dropwise over 5 min. The reaction mixture was stirred at 0°C for 10 min and then left for overnight stirring at room temperature. After TLC indicated reaction completion, Et<sub>3</sub>N (0.5 mL, 3.9 mmol) was added dropwise at 0°C followed by BF<sub>3</sub>.OEt<sub>2</sub> (0.8 mL, 6.2 mmol) at 0°C. After the addition was over, the reaction was stirred for 16 h at room temperature. The solvent was removed under reduced pressure and residue was taken up in dichloromethane (20 mL) and washed with 10% aq. NaHCO<sub>3</sub> (2 x 20 mL), brine (2 x 20 mL) and dried over Na<sub>2</sub>SO<sub>4</sub>. The solvent was evaporated to dryness and residue was purified by column chromatography (hexane/ethyl acetate, 3/2). Fraction containing the product was collected, dried to vacuum and recrystallized from CH<sub>2</sub>Cl<sub>2</sub>/Hexane to obtain the pure BODIPY **7** (134 mg, 40%) as lustrous green solid. mp = 135-137°C; <sup>1</sup>H-NMR (CDCl<sub>3</sub>, 400 MHz): δ 7.04 (s, 1H), 4.37 (q, J = 7.12 Hz, 4H), 3.67 (s, 1H), 2.72 (m, 4H), 2.65 (overlapped m, 2H), 2.61 (s, 3H), 2.46 (m, 2H), 2.21 (s, 3H), 1.75 (m, 1H), 1.38 (t, J = 7.12 Hz, 3H); <sup>13</sup>C NMR (CDCl<sub>3</sub>, 100 MHz): δ 172.6, 165.5, 161.1, 141.7, 136.7, 136.5, 132.2, 131.9, 131.7, 120.8, 60.6, 51.8, 33.4, 23.3, 23.1, 22.4, 21.5, 19.4, 14.2, 13.7, 9.6; MALDI-TOF m/z 432.27; Calcd. for C<sub>22</sub>H<sub>27</sub>BF<sub>2</sub>N<sub>2</sub>O<sub>6</sub> [M+Na<sup>+</sup>] 455.251

### **BODIPY 8**

BODIPY **7** (100 mg, 0.2313 mmol) was dissolved in toluene (15 mL) and heated to about 110°C. A solution of DDQ (262 mg, 1.1566 mmol, 5 equiv.) in toluene (15 mL) was added and the

mixture was refluxed under Ar. Monitored the reaction using UV/Vis. Once the reaction was complete, cooled it to room temperature and the solvent was removed under the reduced pressure. The residue was taken in dichloromethane (20 mL) and extracted with saturated NaHCO<sub>3</sub> (20 mL), brine (20 mL) and dried over Na<sub>2</sub>SO<sub>4</sub>. The solution was evaporated to dryness and the residue was purified by column chromatography (Eluent: Hexane/EtOAc, 3/2). Fractions containing the compound were collected, dried to vacuum and recrystallized from CH<sub>2</sub>Cl<sub>2</sub>/Hexane to obtain the pure BODIPY **8** (59.4 mg, 60%) as lustrous green solid. mp = 162-164°C; <sup>1</sup>H-NMR (CDCl<sub>3</sub>, 400 MHz): δ 8.22 (m, 1H), 7.79 (m, 1H), 7.46 (s, 1H), 7.41 (m, 1H), 7.34 (m, 1H), 4.55 (q, J = 7.12 Hz, 2H), 3.69 (s, 1H), 2.75 (m, 2H), 2.64 (s, 3H), 2.49 (m, 2H), 2.28 (s, 3H), 1.51 (t, J = 7.12 Hz, 3H); <sup>13</sup>C NMR (CDCl<sub>3</sub>, 100 MHz): δ 172.6, 163.0, 160.4, 140.7, 135.8, 133.3, 131.3, 130.5, 128.5, 127.9, 126.3, 123.9, 118.7, 118.3, 61.4, 51.8, 33.6, 19.4, 14.3, 13.5, 9.6; MALDI-TOF m/z 428.24; Calcd. for C<sub>22</sub>H<sub>23</sub>BF<sub>2</sub>N<sub>2</sub>O<sub>4</sub> [M<sup>+</sup>] 428.224.

### 2.4.3: Crystal Data

Diffraction data were collected at low temperature on either a Nonius KappaCCD diffractometer equipped with MoK $\alpha$  radiation ( $\lambda=0.71073$  Å) or a Bruker Kappa Apex-II diffractometer equipped with CuK $\alpha$  radiation ( $\lambda=1.54178$  Å). Refinement was by full-matrix least squares using SHELXL, with H atoms in idealized positions, except for NH hydrogen atoms, which were located by difference maps and in most cases their positions refined. Disorder is present in several of the structures.

Crystal data: For **2a**: C<sub>23</sub>H<sub>30</sub>N<sub>2</sub>O<sub>4</sub>, monoclinic space group P2<sub>1</sub>/c, a=8.3020(6), b=18.1194(14), c=13.5258(10) Å,  $\beta=98.449(5)^\circ$ , V=2012.6(3) Å<sup>3</sup>, T=90.0(5) K, Z=4,  $\rho_{\text{calcd}}=1.315$  g cm<sup>-3</sup>,  $\mu(\text{CuK}\alpha)=0.73$  mm<sup>-1</sup>. A total of 13,289 data was collected at to  $\theta=69.0^\circ$ . R=0.062 for 2895 data with I>2 $\sigma$ (I) of 3597 unique data and 270 refined parameters.



For **2b EtOAc solvate**:  $C_{29}H_{34}N_2O_4 \cdot 1/2 C_4H_8O_2$ , triclinic space group P-1,  $a=8.698(3)$ ,  $b=14.961(5)$ ,  $c=21.472(9)$  Å,  $\alpha=86.86(3)$ ,  $\beta=88.15(2)$ ,  $\gamma=89.83(2)^\circ$ ,  $V=2788.5(18)\text{Å}^3$ ,  $T=90.0(5)$  K,  $Z=4$ ,  $\rho_{\text{calcd}}=1.235$  g cm<sup>-3</sup>,  $\mu(\text{CuK}\alpha)=0.67$  mm<sup>-1</sup>. 24,515 total data,  $\theta_{\text{max}}=58.8^\circ$ .  $R=0.087$  for 3895 data with  $I>2\sigma(I)$  of 7545 unique data and 692 refined parameters.

For **2c pentafluorobenzaldehyde cocrystal**:  $C_{29}H_{29}F_5N_2O_4 \cdot 1/2 C_7HF_5O$ , tetragonal space group  $I4_1/a$ ,  $a=24.931(2)$ ,  $c=40.838(4)$  Å,  $V=25,383(4)\text{Å}^3$ ,  $T=90.0(5)$  K,  $Z=32$ ,  $\rho_{\text{calcd}}=1.387$  g cm<sup>-3</sup>,  $\mu(\text{CuK}\alpha)=1.06$  mm<sup>-1</sup>. 95,523 total data,  $\theta_{\text{max}}=68.9^\circ$ .  $R=0.068$  for 8230 data with  $I>2\sigma(I)$  of 11630 unique data and 838 refined parameters.

For **2d**:  $C_{30}H_{36}N_2O_5$ , triclinic space group P-1,  $a=10.7765(10)$ ,  $b=11.1382(12)$ ,  $c=14.2929(13)$  Å,  $\alpha=100.304(5)$ ,  $\beta=103.378(4)$ ,  $\gamma=102.828(4)^\circ$ ,  $V=1578.7(3)\text{Å}^3$ ,  $T=90.0(5)$  K,  $Z=2$ ,  $\rho_{\text{calcd}}=1.189$  g cm<sup>-3</sup>,  $\mu(\text{CuK}\alpha)=0.58$  mm<sup>-1</sup>. 17,121 total data,  $\theta_{\text{max}}=68.4^\circ$ .  $R=0.060$  for 4767 data with  $I>2\sigma(I)$  of 5533 unique data and 354 refined parameters.

For **3b**:  $C_{29}H_{31}BF_2N_2O_4$ , monoclinic space group  $P2_1/c$ ,  $a=11.3252(15)$ ,  $b=24.088(5)$ ,  $c=9.778(2)$  Å,  $\beta=108.409(10)^\circ$ ,  $V=2530.9(8)$  Å<sup>3</sup>,  $T=150.0(5)$  K,  $Z=4$ ,  $\rho_{\text{calcd}}=1.366$  g cm<sup>-3</sup>,  $\mu(\text{MoK}\alpha)=0.10$  mm<sup>-1</sup>. 8398 total data,  $\theta_{\text{max}}=27.9^\circ$ .  $R=0.053$  for 3731 data with  $I>2\sigma(I)$  of 6018 unique data and 392 refined parameters.

For **3c**:  $C_{29}H_{26}BF_7N_2O_4$ , triclinic space group P-1,  $a=8.0664(4)$ ,  $b=14.5015(6)$ ,  $c=23.4495(12)$  Å,  $\alpha=92.042(4)$ ,  $\beta=97.547(4)$ ,  $\gamma=91.775(3)^\circ$ ,  $V=2715.8(2)\text{Å}^3$ ,  $T=90.0(5)$  K,  $Z=4$ ,  $\rho_{\text{calcd}}=1.493$  g cm<sup>-3</sup>,  $\mu(\text{CuK}\alpha)=1.14$  mm<sup>-1</sup>. 27,216 total data,  $\theta_{\text{max}}=60.3^\circ$ .  $R=0.063$  for 4428 data with  $I>2\sigma(I)$  of 8054 unique data and 780 refined parameters.

For **3d**:  $C_{30}H_{33}BF_2N_2O_5$ , monoclinic space group  $C2/c$ ,  $a=25.927(2)$ ,  $b=8.7936(10)$ ,  $c=25.782(2)$  Å,  $\beta=114.472(5)^\circ$ ,  $V=5350.0(8)$  Å<sup>3</sup>,  $T=90.0(5)$  K,  $Z=8$ ,  $\rho_{\text{calcd}}=1.367$  g cm<sup>-3</sup>,  $\mu(\text{CuK}\alpha)=0.84$  mm<sup>-1</sup>.

<sup>1</sup>. 13,921 total data,  $\theta_{\max}=68.3^\circ$ .  $R=0.039$  for 4024 data with  $I>2\sigma(I)$  of 4767 unique data and 364 refined parameters.

For **3e**:  $C_{31}H_{33}BF_2N_2O_6$ , monoclinic space group  $C2/c$ ,  $a=41.881(3)$ ,  $b=15.0780(15)$ ,  $c=27.105(2)$  Å,  $\beta=97.579(5)^\circ$ ,  $V=16,967(2)$  Å<sup>3</sup>,  $T=150.0(5)$  K,  $Z=24$ ,  $\rho_{\text{calcd}}=1.359$  g cm<sup>-3</sup>,  $\mu(\text{CuK}\alpha)=0.85$  mm<sup>-1</sup>. 64,554 total data,  $\theta_{\max}=68.4^\circ$ .  $R=0.043$  for 11,391 data with  $I>2\sigma(I)$  of 15,206 unique data and 1150 refined parameters.

For **4b**:  $C_{29}H_{23}BF_2N_2O_4$ , orthorhombic space group  $Pbca$ ,  $a=13.0867(9)$ ,  $b=23.649(2)$ ,  $c=15.7556(10)$  Å,  $V=4876.2(6)$  Å<sup>3</sup>,  $T=100.0(5)$  K,  $Z=8$ ,  $\rho_{\text{calcd}}=1.396$  g cm<sup>-3</sup>,  $\mu(\text{CuK}\alpha)=0.86$  mm<sup>-1</sup>. 43,842 total data,  $\theta_{\max}=68.3^\circ$ .  $R=0.036$  for 3670 data with  $I>2\sigma(I)$  of 4434 unique data and 345 refined parameters.

For **4d**:  $C_{30}H_{25}BF_2N_2O_5$ , orthorhombic space group  $Pbca$ ,  $a=16.208(3)$ ,  $b=12.384(2)$ ,  $c=24.802(4)$  Å,  $V=4978.3(15)$  Å<sup>3</sup>,  $T=90.0(5)$  K,  $Z=8$ ,  $\rho_{\text{calcd}}=1.447$  g cm<sup>-3</sup>,  $\mu(\text{CuK}\alpha)=0.90$  mm<sup>-1</sup>. 30,190 total data,  $\theta_{\max}=58.9^\circ$ .  $R=0.063$  for 2995 data with  $I>2\sigma(I)$  of 3557 unique data and 397 refined parameters.

For **4e**:  $C_{31}H_{25}BF_2N_2O_6$ , orthorhombic space group  $Pbca$ ,  $a=15.792(2)$ ,  $b=12.530(2)$ ,  $c=26.067(4)$  Å,  $V=5158.0(13)$  Å<sup>3</sup>,  $T=90.0(5)$  K,  $Z=8$ ,  $\rho_{\text{calcd}}=1.469$  g cm<sup>-3</sup>,  $\mu(\text{CuK}\alpha)=0.93$  mm<sup>-1</sup>. 34,135 total data,  $\theta_{\max}=60.3^\circ$ .  $R=0.078$  for 2405 data with  $I>2\sigma(I)$  of 3788 unique data and 382 refined parameters.

For **8**:  $C_{22}H_{23}BF_2N_2O_4$ , monoclinic space group  $P2_1/n$ ,  $a=11.4027(15)$ ,  $b=7.3503(10)$ ,  $c=24.381(3)$  Å,  $\beta=102.545(6)^\circ$ ,  $V=1994.7(5)$  Å<sup>3</sup>,  $T=100.0(5)$  K,  $Z=4$ ,  $\rho_{\text{calcd}}=1.426$  g cm<sup>-3</sup>,  $\mu(\text{MoK}\alpha)=0.11$  mm<sup>-1</sup>. 22,120 total data,  $\theta_{\max}=27.8^\circ$ .  $R=0.039$  for 3415 data with  $I>2\sigma(I)$  of 4679 unique data and 285 refined parameters.

For **5b hexane solvate**:  $C_{29}H_{24}N_2O_4 \cdot 0.2 C_6H_{14}$ , monoclinic space group  $C2/c$ ,  $a=18.5304(12)$ ,  $b=20.7226(14)$ ,  $c=6.8836(4) \text{ \AA}$ ,  $\beta=108.738(4)^\circ$ ,  $V=2503.2(3) \text{ \AA}^3$ ,  $T=90.0(5) \text{ K}$ ,  $Z=4$ ,  $\rho_{\text{calcd}}=1.285 \text{ g cm}^{-3}$ ,  $\mu(\text{MoK}\alpha)=0.09 \text{ mm}^{-1}$ . 10,372 total data,  $\theta_{\text{max}}=26.0^\circ$ .  $R=0.047$  for 1634 data with  $I>2\sigma(I)$  of 2478 unique data and 162 refined parameters.

For **5b precursor**:  $C_{29}H_{32}N_2O_4$ , triclinic space group  $P-1$ ,  $a=8.5674(5)$ ,  $b=11.1537(9)$ ,  $c=13.4356(10) \text{ \AA}$ ,  $\alpha=69.244(5)$ ,  $\beta=89.897(4)$ ,  $\gamma=81.625(4)^\circ$ ,  $V=1186.03(15) \text{ \AA}^3$ ,  $T=90.0(5) \text{ K}$ ,  $Z=2$ ,  $\rho_{\text{calcd}}=1.323 \text{ g cm}^{-3}$ ,  $\mu(\text{CuK}\alpha)=0.70 \text{ mm}^{-1}$ . 14,723 total data,  $\theta_{\text{max}}=69.3^\circ$ .  $R=0.038$  for 3608 data with  $I>2\sigma(I)$  of 4248 unique data and 349 refined parameters.

For **5c**:  $C_{29}H_{19}F_5N_2O_4$ , monoclinic space group  $P2_1/c$ ,  $a=15.3125(15)$ ,  $b=11.0509(10)$ ,  $c=15.6714(15) \text{ \AA}$ ,  $\beta=115.117(5)^\circ$ ,  $V=2401.1(4) \text{ \AA}^3$ ,  $T=90.0(5) \text{ K}$ ,  $Z=4$ ,  $\rho_{\text{calcd}}=1.534 \text{ g cm}^{-3}$ ,  $\mu(\text{CuK}\alpha)=1.11 \text{ mm}^{-1}$ . 17,798 total data,  $\theta_{\text{max}}=68.7^\circ$ .  $R=0.034$  for 3953 data with  $I>2\sigma(I)$  of 4323 unique data and 367 refined parameters.

For **5c precursor**:  $C_{29}H_{27}F_5N_2O_4$ , monoclinic space group  $P2_1/n$ ,  $a=8.9739(5)$ ,  $b=24.788(2)$ ,  $c=11.3754(10) \text{ \AA}$ ,  $\beta=100.947(5)^\circ$ ,  $V=22484.4(3) \text{ \AA}^3$ ,  $T=90.0(5) \text{ K}$ ,  $Z=4$ ,  $\rho_{\text{calcd}}=1.504 \text{ g cm}^{-3}$ ,  $\mu(\text{CuK}\alpha)=1.08 \text{ mm}^{-1}$ . 26,194 total data,  $\theta_{\text{max}}=68.6^\circ$ .  $R=0.034$  for 3823 data with  $I>2\sigma(I)$  of 4508 unique data and 367 refined parameters.

For **5d**:  $C_{30}H_{26}N_2O_5$ , monoclinic space group  $P2_1/n$ ,  $a=9.456(2)$ ,  $b=13.896(3)$ ,  $c=18.304(4) \text{ \AA}$ ,  $\beta=93.890(15)^\circ$ ,  $V=93.890(15) \text{ \AA}^3$ ,  $T=90.0(5) \text{ K}$ ,  $Z=4$ ,  $\rho_{\text{calcd}}=1.369 \text{ g cm}^{-3}$ ,  $\mu(\text{MoK}\alpha)=0.09 \text{ mm}^{-1}$ . 14,344 total data,  $\theta_{\text{max}}=26.0^\circ$ .  $R=0.051$  for 3109 data with  $I>2\sigma(I)$  of 4714 unique data and 339 refined parameters.

For **5d precursor**:  $C_{30}H_{34}N_2O_5$ , orthorhombic space group  $Pbca$ ,  $a=21.665(2)$ ,  $b=9.1272(10)$ ,  $c=26.015(2) \text{ \AA}$ ,  $V=5144.2(8) \text{ \AA}^3$ ,  $T=90.0(5) \text{ K}$ ,  $Z=8$ ,  $\rho_{\text{calcd}}=1.298 \text{ g cm}^{-3}$ ,  $\mu(\text{CuK}\alpha)=0.71 \text{ mm}^{-1}$ .

49,707 total data,  $\theta_{\max}=59.0^\circ$ .  $R=0.034$  for 3043 data with  $I>2\sigma(I)$  of 3696 unique data and 345 refined parameters.

#### **2.4.4: Computation Modeling**

The two reaction routes A and B were studied computationally in the framework of Density Function Theory. The hybrid density functional B3LYP was used at the 6-31G level. The geometry of compounds **2b-e**, **3b-e**, **4b-e**, and **5b-e** were optimized and the relative energies were evaluated. Potential energy surface minima were confirmed with frequency calculations. The solvent effects were accounted for using the Polarizable Continuum Model (PCM) All calculations were performed using Gaussian 09 program package.

#### **2.4.5: Steady-state Absorption and Fluorescence Spectroscopy**

The absorption measurements were carried out on a Varian Cary 50 UV/Vis spectrophotometer and the steady-state fluorescence spectroscopic studies were performed on a PTI Quantum Master4/2006SE spectrofluorimeter. For the fluorescence quantum yield measurements in solvents, dilute solutions with the absorbance between 0.04-0.06 at the excitation wavelength were used to minimize the reabsorption effects. The fluorescence quantum yields of BODIPYs **7** and **3a-e** were obtained by comparing the area under the corrected emission spectrum of the test sample with that of rhodamine 6G (0.80 in methanol). For BODIPYs **4a-e** and **8**, methylene blue (0.03 in methanol) and cresyl violet perchlorate (0.54 in ethanol) were used as external standards respectively.<sup>[28]</sup> All spectra were recorded at room temperature using non-degassed samples, spectroscopic grade solvents and a 10 mm quartz cuvette. In all the cases, correction for the refractive index was applied.

## 2.4.6: Cell Culture

All tissue culture media and reagents were obtained from Invitrogen. Human HEp2 cells were obtained from ATCC and maintained in a 50:50 mixture of DMEM:Advanced MEM containing 5% FBS. The Hep2 cells were sub-cultured biweekly to maintain sub-confluent stocks. The 4<sup>th</sup> to 15<sup>th</sup> passage cells were used for all the experiments.

*2.4.6.1: Time-Dependent Cellular Uptake.* The HEp2 cells were plated at 7500 per well in a Costar 96 well plate and allowed to grow for 36 h. BODIPY stocks were prepared in DMSO containing 1% Cremophor EL, at a concentration of 32 mM and then diluted into medium to final working concentrations. The cells were exposed to 10  $\mu$ M of each BODIPY compound for 0, 1, 2, 4, 8, and 24 h. At the end of the incubation time the loading medium was removed and the cells were washed with 200  $\mu$ L of PBS. The cells were solubilized upon addition of 100  $\mu$ L of 0.25% Triton X-100 (Calbiochem) in PBS. To determine the BODIPY concentration, fluorescence emission was read at 570/670 nm (excitation/emission) using a BMG FLUOstar plate reader. The cell numbers were quantified by the CyQuant cell proliferation assay (Invitrogen) as per manufactures instruction, and the uptake was expressed in terms of nM compound per cell.

*2.4.6.2: Cytotoxicity.* For the dark toxicity, the HEp2 cells were plated as described above and allowed 36-48 h to attach. The cells were exposed to increasing concentrations of BODIPY conjugate up to 400  $\mu$ M and incubated overnight. The loading medium was then removed and medium containing Cell Titer Blue (Promega) as per manufacturer's instructions was added to the cells. Cell viability was then measured by reading the fluorescence at 570/615nm using a BMG FLUOstar plate reader. The signal was normalized to 100% viable (untreated) cells and 0% viable (treated with 0.2% saponin) cells. For the phototoxicity, the HEp2 cells were prepared as described above for the dark cytotoxicity assay and treated with BODIOY conjugate

concentrations of 0, 6.25, 12.5, 25, 50 and 100  $\mu\text{M}$ . After compound loading overnight, the medium was removed and replaced with medium containing 50 mM HEPES pH 7.4. The cells were exposed to a Newport light system with 175 W halogen lamp for 20 min, filtered through a water filter to provide approximated  $1.5 \text{ Jcm}^{-2}$  light dose. The cells were kept cool by placing the culture on the  $5^\circ\text{C}$  Echotherm chilling/heating plate (Torrey Pines Scientific, Inc.). The cells were returned to the incubator overnight and assayed for viability as described above for the dark cytotoxicity experiment.

*2.4.6.3: Microscopy.* The cells were incubated in the glass bottom 6-well plate (MatTek) and allowed to grow for 48 h. The cells were then exposed to 10  $\mu\text{M}$  of each compound for 6 h. Organelle tracers were obtained from Invitrogen and used at the following concentrations: LysoSensor Green 50 nM, MitoTracker Green 250 nM, ER Tracker Blue/white 100 nM, and BODIPY FL C5 ceramide 1  $\mu\text{M}$ . The organelle tracers were diluted in medium and the cells were incubated concurrently with BODIPY and tracers for 30 minutes before washing 3 times with PBS and microscopy. Images were acquired using a Leica DMRXA microscope with 40 $\times$  NA 0.8dip objective lens and DAPI, GFP and Texas Red filter cubes (Chroma Technologies).

## 2.5: References

1. (a) Shen, Z.; Röhr, H.; Rurack, K.; Uno, H.; Spieles, M.; Schulz, B.; Reck, G.; Ono, N., Boron–Diindomethene (BDI) Dyes and Their Tetrahydrobicyclo Precursors—en Route to a New Class of Highly Emissive Fluorophores for the Red Spectral Range. *Chemistry – A European Journal* **2004**, *10* (19), 4853-4871; (b) Wang, Y. W.; Descalzo, A. B.; Shen, Z.; You, X. Z.; Rurack, K., Dihydronaphthalene-fused boron-dipyrromethene (BODIPY) dyes: insight into the electronic and conformational tuning modes of BODIPY fluorophores. *Chemistry* **2010**, *16* (9), 2887-903; (c) Descalzo, A. B.; Xu, H. J.; Xue, Z. L.; Hoffmann, K.; Shen, Z.; Weller, M. G.; You, X. Z.; Rurack, K., Phenanthrene-fused boron-dipyrromethenes as bright long-wavelength fluorophores. *Organic letters* **2008**, *10* (8), 1581-4; (d) Kowada, T.; Yamaguchi, S.; Ohe, K., Highly fluorescent BODIPY dyes modulated with spirofluorene moieties. *Organic letters* **2010**, *12* (2), 296-9.

2. Uppal, T.; Hu, X.; Fronczek, F. R.; Maschek, S.; Bobadova-Parvanova, P.; Vicente, M. G. H., Synthesis, Computational Modeling, and Properties of Benzo-Appended BODIPYs. *Chemistry – A European Journal* **2012**, *18* (13), 3893-3905.
3. Finikova, O. S.; Cheprakov, A. V.; Beletskaya, I. P.; Carroll, P. J.; Vinogradov, S. A., Novel versatile synthesis of substituted tetrabenzoporphyrins. *J Org Chem* **2004**, *69* (2), 522-35.
4. Jiao, L.; Yu, C.; Liu, M.; Wu, Y.; Cong, K.; Meng, T.; Wang, Y.; Hao, E., Synthesis and Functionalization of Asymmetrical Benzo-Fused BODIPY Dyes. *The Journal of Organic Chemistry* **2010**, *75* (17), 6035-6038.
5. (a) Nagai, A.; Chujo, Y., Aromatic Ring-Fused BODIPY-Based Conjugated Polymers Exhibiting Narrow Near-Infrared Emission Bands. *Macromolecules* **2009**, *43* (1), 193-200; (b) Goeb, S.; Ziessel, R., Convenient synthesis of green diisoindolodithienylpyrromethene-dialkynyl borane dyes. *Organic letters* **2007**, *9* (5), 737-40.
6. Kubo, Y.; Minowa, Y.; Shoda, T.; Takeshita, K., Synthesis of a new type of dibenzopyrromethene–boron complex with near-infrared absorption property. *Tetrahedron Letters* **2010**, *51* (12), 1600-1602.
7. Hayashi, Y.; Obata, N.; Tamaru, M.; Yamaguchi, S.; Matsuo, Y.; Saeki, A.; Seki, S.; Kureishi, Y.; Saito, S.; Yamaguchi, S.; Shinokubo, H., Facile Synthesis of Biphenyl-Fused BODIPY and Its Property. *Organic letters* **2012**, *14* (3), 866-869.
8. Haugland, R. P., *The Handbook A Guide to Fluorescent Probes and Labeling Technologies*. Tenth ed.; United States of America, 2005.
9. (a) Kang, H. C.; Haugland, R. P. 1995; (b) Ulrich, G.; Goeb, S.; De Nicola, A.; Retailleau, P.; Ziessel, R., Chemistry at boron: synthesis and properties of red to near-IR fluorescent dyes based on boron-substituted diisoindolomethene frameworks. *J Org Chem* **2011**, *76* (11), 4489-505.
10. Filatov, M. A.; Cheprakov, A. V.; Beletskaya, I. P., A Facile and Reliable Method for the Synthesis of Tetrabenzoporphyrin from 4,7-Dihydroisoindole. *European Journal of Organic Chemistry* **2007**, *2007* (21), 3468-3475.
11. Filatov, M. A.; Lebedev, A. Y.; Mukhin, S. N.; Vinogradov, S. A.; Cheprakov, A. V.,  $\pi$ -Extended Dipyrins Capable of Highly Fluorogenic Complexation with Metal Ions. *Journal of the American Chemical Society* **2010**, *132* (28), 9552-9554.
12. Zheng, Q.; Xu, G.; Prasad, P. N., Conformationally Restricted Dipyrromethene Boron Difluoride (BODIPY) Dyes: Highly Fluorescent, Multicolored Probes for Cellular Imaging. *Chemistry – A European Journal* **2008**, *14* (19), 5812-5819.
13. (a) H.R. Barton, D.; Kervagoret, J.; Zard, S. Z., A useful synthesis of pyrroles from nitroolefins. *Tetrahedron* **1990**, *46* (21), 7587-7598; (b) May, D. A.; Lash, T. D., Porphyrins with exocyclic rings. 2. Synthesis of geochemically significant tetrahydrobenzoporphyrins from 4,5,6,7-tetrahydro-2H-isoindoles. *The Journal of Organic Chemistry* **1992**, *57* (18), 4820-4828; (c) Bhattacharya, A.; Cherukuri, S.; Plata, R. E.; Patel, N.; Tamez Jr, V.; Grosso, J. A.;

Peddicord, M.; Palaniswamy, V. A., Remarkable solvent effect in Barton–Zard pyrrole synthesis: application in an efficient one-step synthesis of pyrrole derivatives. *Tetrahedron Letters* **2006**, *47* (31), 5481-5484.

14. Filatov, M. A.; Lebedev, A. Y.; Vinogradov, S. A.; Cheprakov, A. V., Synthesis of 5,15-diaryltetrabenzoporphyrins. *J Org Chem* **2008**, *73* (11), 4175-85.

15. Lindsey, J. S.; Schreiman, I. C.; Hsu, H. C.; Kearney, P. C.; Marguerettaz, A. M., Rothemund and Adler-Longo reactions revisited: synthesis of tetraphenylporphyrins under equilibrium conditions. *The Journal of Organic Chemistry* **1987**, *52* (5), 827-836.

16. Rumyantsev, E.; Marfin, Y.; Antina, E., Donor-acceptor complexes of dipyrrolylmethenes with boron trifluoride as intermediates in the synthesis of Bodipy. *Russian Chemical Bulletin* **2010**, *59* (10), 1890-1895.

17. Wood, T. E.; Thompson, A., Advances in the Chemistry of Dipyrrins and Their Complexes. *Chemical Reviews* **2007**, *107* (5), 1831-1861.

18. Burghart, A.; Kim, H.; Welch, M. B.; Thoresen, L. H.; Reibenspies, J.; Burgess, K.; Bergström, F.; Johansson, L. B. Å., 3,5-Diaryl-4,4-difluoro-4-bora-3a,4a-diaza-s-indacene (BODIPY) Dyes: Synthesis, Spectroscopic, Electrochemical, and Structural Properties. *The Journal of Organic Chemistry* **1999**, *64* (21), 7813-7819.

19. Sathyamoorthi, G.; Wolford, L. T.; Haag, A. M.; Boyer, J. H., Selective side-chain oxidation of peralkylated pyrromethene-BF<sub>2</sub> complexes. *Heteroatom Chemistry* **1994**, *5* (3), 245-249.

20. Tahtaoui, C.; Thomas, C.; Rohmer, F.; Klotz, P.; Duportail, G.; Mely, Y.; Bonnet, D.; Hibert, M., Convenient method to access new 4,4-dialkoxy- and 4,4-diaryloxy-diaza-s-indacene dyes: Synthesis and spectroscopic evaluation. *J Org Chem* **2007**, *72* (1), 269-72.

21. (a) Vives, G.; Giansante, C.; Bofinger, R.; Raffy, G.; Guerzo, A. D.; Kauffmann, B.; Batat, P.; Jonusauskas, G.; McClenaghan, N. D., Facile functionalization of a fully fluorescent perfluorophenyl BODIPY: photostable thiol and amine conjugates. *Chemical Communications* **2011**, *47* (37), 10425-10427; (b) Samaroo, D.; Vinodu, M.; Chen, X.; Drain, C. M., meso-Tetra(pentafluorophenyl)porphyrin as an Efficient Platform for Combinatorial Synthesis and the Selection of New Photodynamic Therapeutics using a Cancer Cell Line. *Journal of combinatorial chemistry* **2007**, *9* (6), 998-1011.

22. Chen, Y.; Wan, L.; Zhang, D.; Bian, Y.; Jiang, J., Modulation of the spectroscopic property of Bodipy derivatives through tuning the molecular configuration. *Photochemical & photobiological sciences : Official journal of the European Photochemistry Association and the European Society for Photobiology* **2011**, *10* (6), 1030-8.

23. Galangau, O.; Dumas-Verdes, C.; Meallet-Renault, R.; Clavier, G., Rational design of visible and NIR distyryl-BODIPY dyes from a novel fluorinated platform. *Organic & Biomolecular Chemistry* **2010**, *8* (20), 4546-4553.



24. Qin, W.; Baruah, M.; De Borggraeve, W. M.; Boens, N., Photophysical properties of an on/off fluorescent pH indicator excitable with visible light based on a borondipyrromethene-linked phenol. *Journal of Photochemistry and Photobiology A: Chemistry* **2006**, *183* (1–2), 190-197.
25. Loudet, A.; Burgess, K., BODIPY dyes and their derivatives: syntheses and spectroscopic properties. *Chem Rev* **2007**, *107* (11), 4891-932.
26. Ortiz, M. J.; Agarrabeitia, A. R.; Duran-Sampedro, G.; Bañuelos Prieto, J.; Lopez, T. A.; Massad, W. A.; Montejano, H. A.; García, N. A.; Lopez Arbeloa, I., Synthesis and functionalization of new polyhalogenated BODIPY dyes. Study of their photophysical properties and singlet oxygen generation. *Tetrahedron* **2012**, *68* (4), 1153-1162.
27. (a) Cui, A.; Peng, X.; Fan, J.; Chen, X.; Wu, Y.; Guo, B., Synthesis, spectral properties and photostability of novel boron–dipyrromethene dyes. *Journal of Photochemistry and Photobiology A: Chemistry* **2007**, *186* (1), 85-92; (b) Mula, S.; Ray, A. K.; Banerjee, M.; Chaudhuri, T.; Dasgupta, K.; Chattopadhyay, S., Design and Development of a New Pyrromethene Dye with Improved Photostability and Lasing Efficiency: Theoretical Rationalization of Photophysical and Photochemical Properties. *The Journal of Organic Chemistry* **2008**, *73* (6), 2146-2154.
28. Lim, S. H.; Thivierge, C.; Nowak-Sliwinska, P.; Han, J.; van den Bergh, H.; Wagnières, G.; Burgess, K.; Lee, H. B., In Vitro and In Vivo Photocytotoxicity of Boron Dipyrromethene Derivatives for Photodynamic Therapy. *Journal of Medicinal Chemistry* **2010**, *53* (7), 2865-2874.
29. Hinkeldey, B.; Schmitt, A.; Jung, G., Comparative photostability studies of BODIPY and fluorescein dyes by using fluorescence correlation spectroscopy. *Chemphyschem : a European journal of chemical physics and physical chemistry* **2008**, *9* (14), 2019-27.
30. Jiao, L.; Yu, C.; Uppal, T.; Liu, M.; Li, Y.; Zhou, Y.; Hao, E.; Hu, X.; Vicente, M. G. H., Long wavelength red fluorescent dyes from 3,5-diiodo-BODIPYs. *Organic & Biomolecular Chemistry* **2010**, *8* (11), 2517-2519.

## CHAPTER 3: SYNTHESIS AND CHARACTERIZATION OF NOVEL STYRYL- AND LYSYL-BODIPY CONJUGATES FOR BIOLABELING APPLICATIONS

### 3.1: Introduction

The technique of cell visualization and interrogation by labeling proteins or DNA with non-radioactive fluorescent labels is widely applicable for detection and elucidation of various cellular mechanisms.<sup>1</sup> In this context, BODIPY-based dyes have attracted considerable attention as very promising candidates for fluorescent labels and have emerged as a rising star in the fluorescent biomarker community.<sup>2</sup> As fluorescent markers, BODIPYs have many favorable characteristics, such as large molar absorption coefficients, high fluorescence quantum efficiencies, high photophysical stability and sharp yet tunable fluorescence frequencies.

An array of BODIPY fluorophores, reactive dyes and conjugates are commercially available and sold by Invitrogen. Fluorescent BODIPY conjugates of proteins, nucleotides, peptides, lipids and polysaccharides that span the entire visible spectrum are available for various biological labeling experiments including DNA sequencing, nucleic acid detection and protein analysis.<sup>3</sup> However, among the myriad of the commercially available BODIPY dyes, only few red-emitter BODIPYs, such as BODIPY-630/650, BODIPY-650/665, BODIPY FL-Ceramide-505/620 and BODIPY TR-Ceramide-592/618 are currently known, as shown in Figure 3.1. In addition, many Invitrogen BODIPY dyes and conjugates are emissive in the visible region of the spectrum, are exceedingly expensive and often unsuitable for typical bioconjugation protocols. Furthermore, most of these dyes have small Stokes shifts which require excitation and detection of these dyes at suboptimal wavelengths.

As a result, the most important challenges in current BODIPY chemistry include: (1) the development of dyes with longer-wavelength absorption and emission profiles, and (2) the

preparation of dyes with additional functional groups for covalent attachment to biomolecules. Both these aims are important to further stimulate the application of BODIPY dyes in biomolecular labeling.<sup>4</sup>

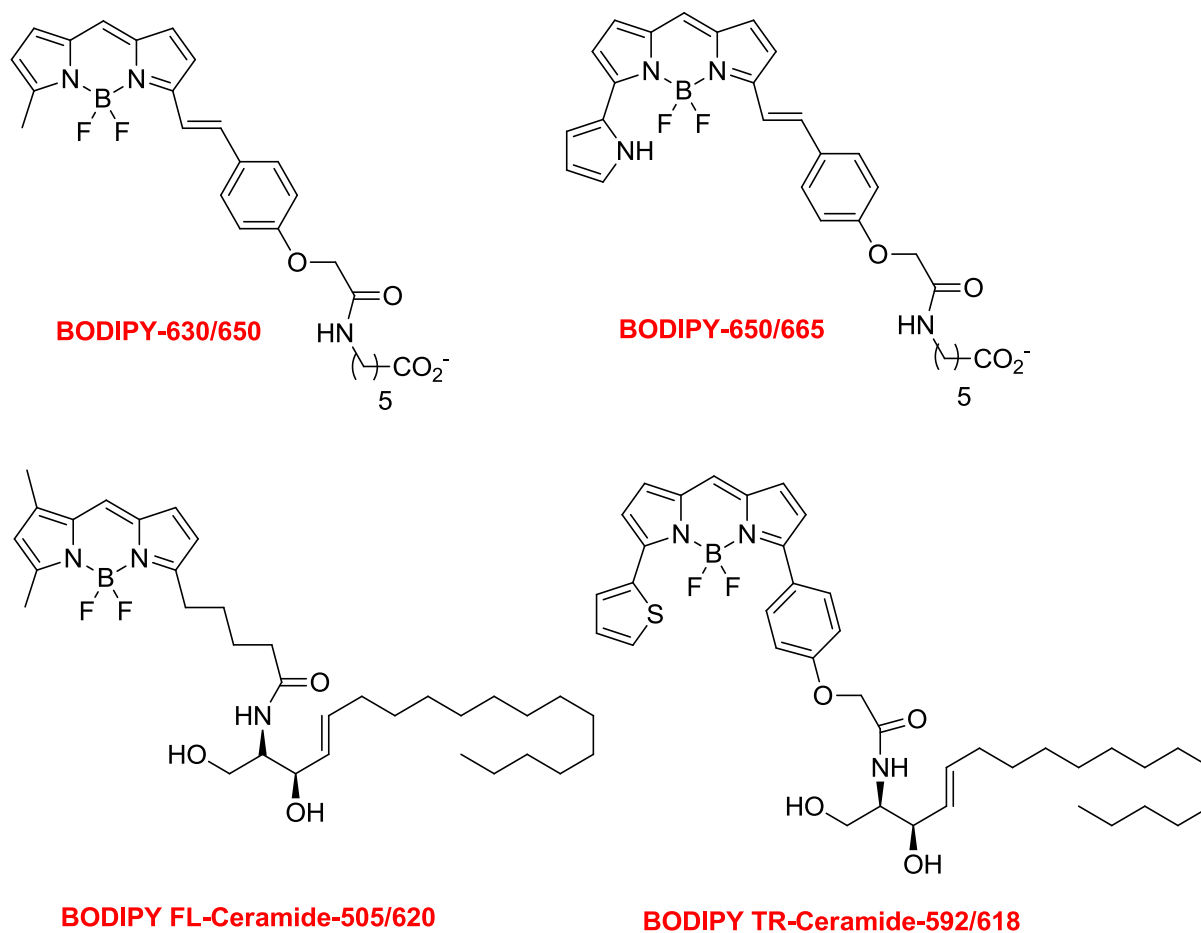


**Figure 3.1:** Chemical structures of long-wavelength amine-reactive BODIPYs from Invitrogen

BODIPY dyes absorb light in the green-yellow spectral region and emit fluorescence between 470-520 nm. On the contrary, red absorbing and emitting dyes often offer much better resolution and sensitivity in biological labeling applications. Therefore, the design and synthesis of far-red or NIR emitting dyes is of great interest and applicability. Several approaches have been developed for the synthesis of longer-wavelength emitting BODIPY fluorophores as all the

seven carbon atoms on the indacene core are readily accessible to the introduction of substituents.<sup>5</sup> Numerous functionalized BODIPY dyes have been engineered and realized by introducing substituents at the *meso*-, 2,6- and 3,5-positions, fusing aromatic rings to the BODIPY core and replacing pyrrole by isoindole. In general, long-wavelength absorbing and emitting BODIPY dyes are often realized by extending conjugation via post-functionalization of the BODIPY core rather than starting from appropriately substituted pyrrole.<sup>6</sup> In addition, substituents at the pyrrolic positions of the BODIPY dye allow coplanar geometries that maximize electronic coupling in comparison with the *meso*-positions which often lead to poor electronic conjugation due to their near-orthogonal geometry with respect to the aromatic BODIPY plane.<sup>7</sup>

Among these approaches, base-catalyzed Knoevenagel condensation of BODIPYs with aryl aldehydes to produce  $\pi$ -extended mono- and distyryl-BODIPY derivatives provides a facile and versatile route to fine-tune the optical properties of green emitting BODIPYs. Like other electron-deficient systems, the 3,5-methyls on BODIPYs are relatively nucleophilic and thus active in the Knoevenagel reaction, which allows the BODIPY fluorophore to be condensed with a variety of electron-donating aldehydes to form *trans* carbon-carbon double bonds.<sup>8</sup> The resulting 3-monostyryl and 3,5-distyryl BODIPY derivatives absorb at a longer wavelength in the red visible region, making them particularly useful for biomedical applications which require deeper light penetration into tissues for better illumination of deep seated lesions.

The biological application of a fluorescent dye is further dependent on its solubility in the aqueous media that surrounds the biomolecules and its efficient coupling to various water soluble biomolecule targets. It is advantageous to have amphiphilic fluorescent probes (biolabels) as hydrophobic interactions between a fluorescent dye and a target molecule often leads to self-aggregation and a decrease in photophysical properties of the fluorophore. In

addition, the bioactivity of a labeled biomolecule is affected by the nature and length of the linker unit that joins the label to its target molecule.<sup>9</sup> It has been demonstrated that a spacer helps to separate the fluorophore from its point of attachment, decreasing the interaction of the fluorophore with the conjugated biomolecule while making it more accessible to secondary target molecules.

With these considerations in mind, we describe herein, the synthesis and characterization of a series of novel BODIPY-based labeling agents prepared via Knoevenagel condensation of 1,3,5,7-tetramethyl-BODIPYs. These potential labeling reagents are functionalized appropriately to generate styryl-substituted far-red and NIR emitting BODIPY fluorophores. The fluorophores are further substituted with methylpropionyl linker arms that do not only increase the hydrophilicity of the BODIPYs, but also serve as a spacer between the fluorophore and the biomolecules. The performance of the new fluorescent labels is studied, with particular emphasis on the effect of various styryl substituents on the photophysical and *in vitro* photodynamic properties of the BODIPY dyes.

### **3.2: Results and Discussion**

The key step in the present study is the Knoevenagel condensation, a well-known organic reaction which was first discovered in 1894 by Emil Knoevenagel.<sup>10</sup> Typically, the Knoevenagel condensation is carried out by condensing a carbonyl compound (aldehyde or ketone) with an active methylene compound (for instance, malonates, acetoacetates, Meldrum's acid) in the presence of a base (Figure 3.2). The Knoevenagel condensation belongs to the general class of base-catalysed aldol-type condensation. As the methylene compounds are more acidic than the aldehydes or ketones used in the aldol condensation, the bases employed as catalysts are usually weaker than those used in aldol condensations. In general, primary, secondary or tertiary amines

or their corresponding ammonium salts are used as catalysts. The most widely used catalysts are pyridine with or without piperidine and ammonium salts, such as ammonium or piperidinium acetate. Various Lewis acids, such as magnesium perchlorate,  $\text{TiCl}_4$ ,  $\text{ZnCl}_2$ , high temperature conditions or microwave irradiations are used to promote the reaction independently from the employed catalytic systems.<sup>11</sup> Aromatic aldehydes treated with perchlorates of secondary amines form the corresponding dialkyliminium perchlorates in refluxing toluene, which are much more active electrophilic reactants than the parent aldehydes and form adducts with carbon-nucleophiles. Additionally, the condensation with aldehydes is generally much faster than ketones, hence reactions with ketones are more difficult to perform due to their decreased reactivity.<sup>10</sup>

Several mechanisms may be possible, however in general, the first step involves the reaction between the free aldehyde and an amine to give an imine/iminium salt, which then reacts with the carbanion derived from the active methylene compound. The final elimination step generates the styryl groups exclusively in a *trans* (E) configuration, along with water as by-product which is either removed azeotropically or by adding molecular sieves or  $\text{Na}_2\text{SO}_4$  (Figure 3.2).

The Knoevenagel condensation of BODIPYs with aryl aldehydes in general offers a great degree of versatility, as judged by the recent research interest.<sup>12</sup> This clearly stems from the following facts: (1) The Knoevenagel condensation is a straightforward and convenient way of BODIPY derivatization; (2) A wide variety of electron-donating aromatic aldehydes can be used to tether different styryl groups; (3) Styryl-BODIPYs tend to have extended  $\pi$ -conjugation with fluorescence maxima at  $\sim 620$ - $660$  nm; (4) the proper choice of appended styryl arms provide impressive opportunities to shift the optical properties of engineered dyes more towards the red and NIR absorbing window. The present work is therefore directed towards the synthesis,

spectral characterizations and cellular investigations of a series of 3-monostyryl and 3,5-distyryl-PMe BODIPY dyes (PMe = CH<sub>2</sub>CH<sub>2</sub>CO<sub>2</sub>Me) bearing “hidden” carboxylic acid tags for conjugation to amino acids, in order to explore their potential for effective cellular labeling. In the following section, we first describe the preparation of the PMe-BODIPY scaffolds, followed by their peripheral functionalization using the Knoevenagel condensation reaction, and subsequently, we discuss their conjugation to lysine, a basic amino acid.

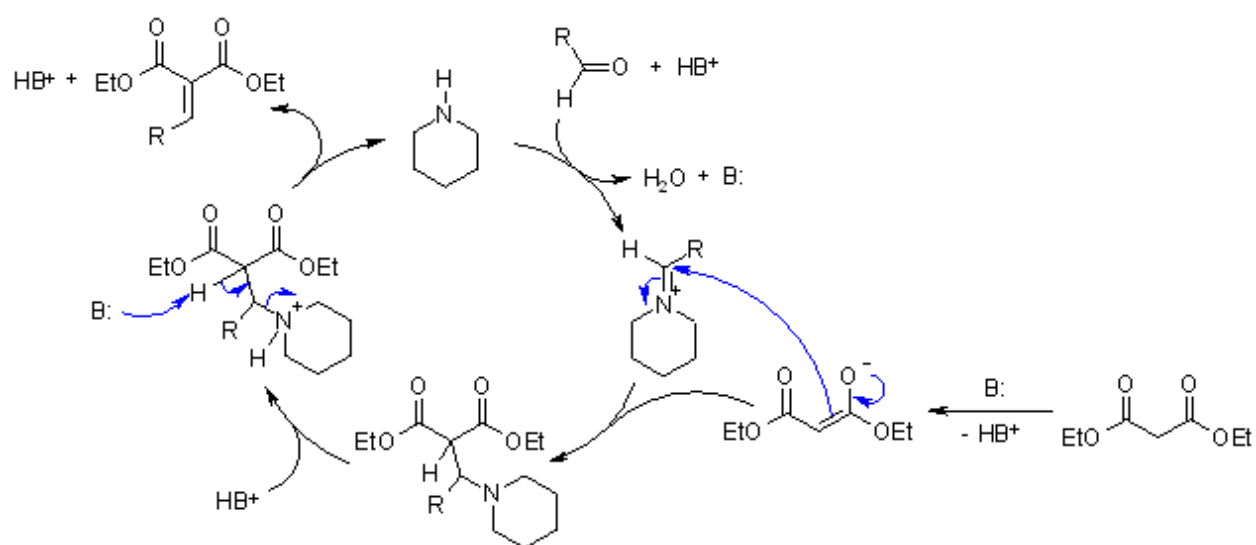
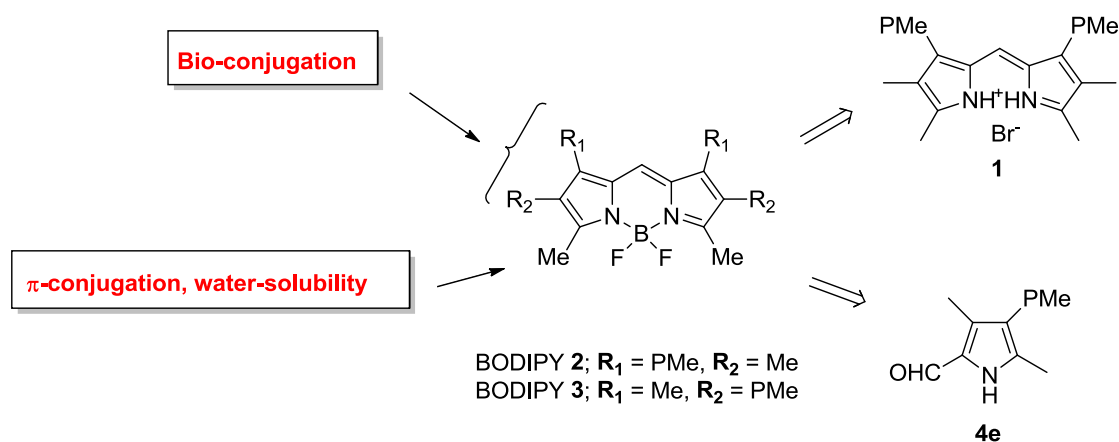


**Figure 3.2:** General mechanism of the Knoevenagel reaction using piperidine as organocatalyst<sup>13</sup>

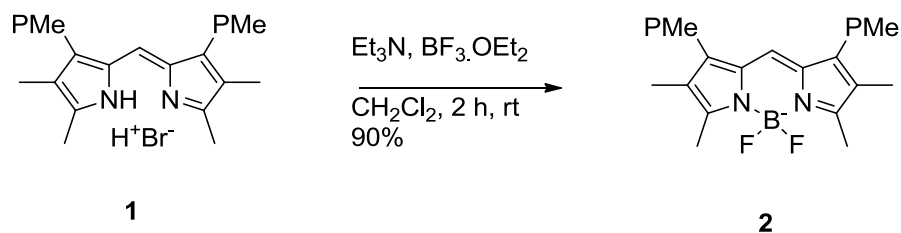
### 3.2.1: Syntheses

The model 1,3,5,7-tetramethyl PMe-BODIPY scaffold chosen to tether a set of different styryl-arms is depicted in Scheme 3.1, along with its retrosynthetic analysis. It is anticipated that the presence of electron-withdrawing 2,6-methylpropionyl moieties can further enhance the acidity of the methyl groups and initiate the Knoevenagel condensation of the methyls at the 3- and 5-positions.



**Scheme 3.1:** Structure and Retrosynthesis of tetramethyl PMe-BODIPY regioisomers

The synthetic route commenced with the synthesis of PMe-BODIPY regioisomers **2** and **3**. BODIPY **2** was synthesized from its dipyrromethene hydrobromide precursor **1**, as outlined in Scheme 3.2. The dipyrromethene hydrobromide derivatives were first described by Fischer et al. in synthesis of coporphyrins and mesoporphyrins.<sup>14</sup> Such symmetric/unsymmetric dipyrromethenes are normally synthesized by either self-condensation of a monopyrrole or by treatment of a pyrrole-2-carbaldehyde with an  $\alpha$ -free pyrrole in the presence of HBr and formic acid.<sup>15</sup>



**Scheme 3.2:** Synthetic route to PMe-BODIPY **2**

The dipyrromethene hydrobromide, **1** was dissolved in freshly distilled dichloromethane under argon. The solution was stirred at 0 °C for ten minutes and triethylamine was added dropwise. The resultant mixture was stirred for additional 20 minutes followed by dropwise



addition of  $\text{BF}_3 \cdot \text{OEt}_2$ . Formation of the boron complex was observed immediately after addition of  $\text{BF}_3 \cdot \text{OEt}_2$  from the green-yellow fluorescence of the reaction mixture. However, stirring was continued at room temperature and the reaction was monitored by TLC, until completion (~ 2 h). The reaction mixture was then diluted with dichloromethane, washed with basic water, dried over sodium sulfate and concentrated *in vacuo*. The crude product was purified over a pad of silica gel eluting with dichloromethane/petroleum ether (1/1, v/v) to get rid of polar oligomeric by-products. The fluorescent fraction was collected and the solvent was removed under reduced pressure to afford an orange-brown powder which was recrystallized using dichloromethane/hexane (5/1, v/v) to give shiny orange-green crystals of desired BODIPY **2** in 90% yield. The chemical structure of the BODIPY dye was confirmed by NMR spectra and high-resolution MS. MS-ESI gave a peak due to  $[\text{M}^+ + \text{Na}]$  at  $m/z$  443.18. An X-ray crystal structure of BODIPY **2** is shown in Figure 3.3. The  $^1\text{H-NMR}$  spectrum showed two singlet peaks at 1.96 and 2.47 ppm corresponding to two sets of methyl protons at the 2,6- and 3,5-positions, respectively, and one single peak at 7.07 ppm corresponding to the proton at the *meso*-position, as depicted in Figure 3.4.

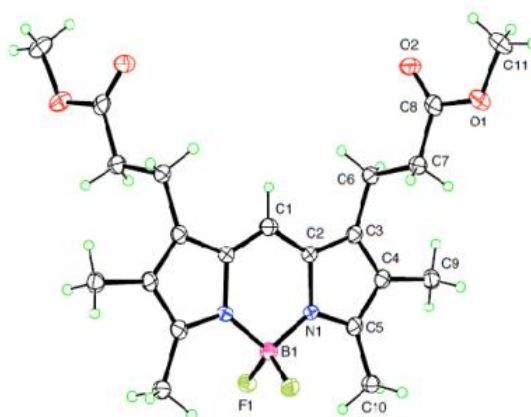


**Figure 3.3:** X-ray crystal structure of BODIPY **2**

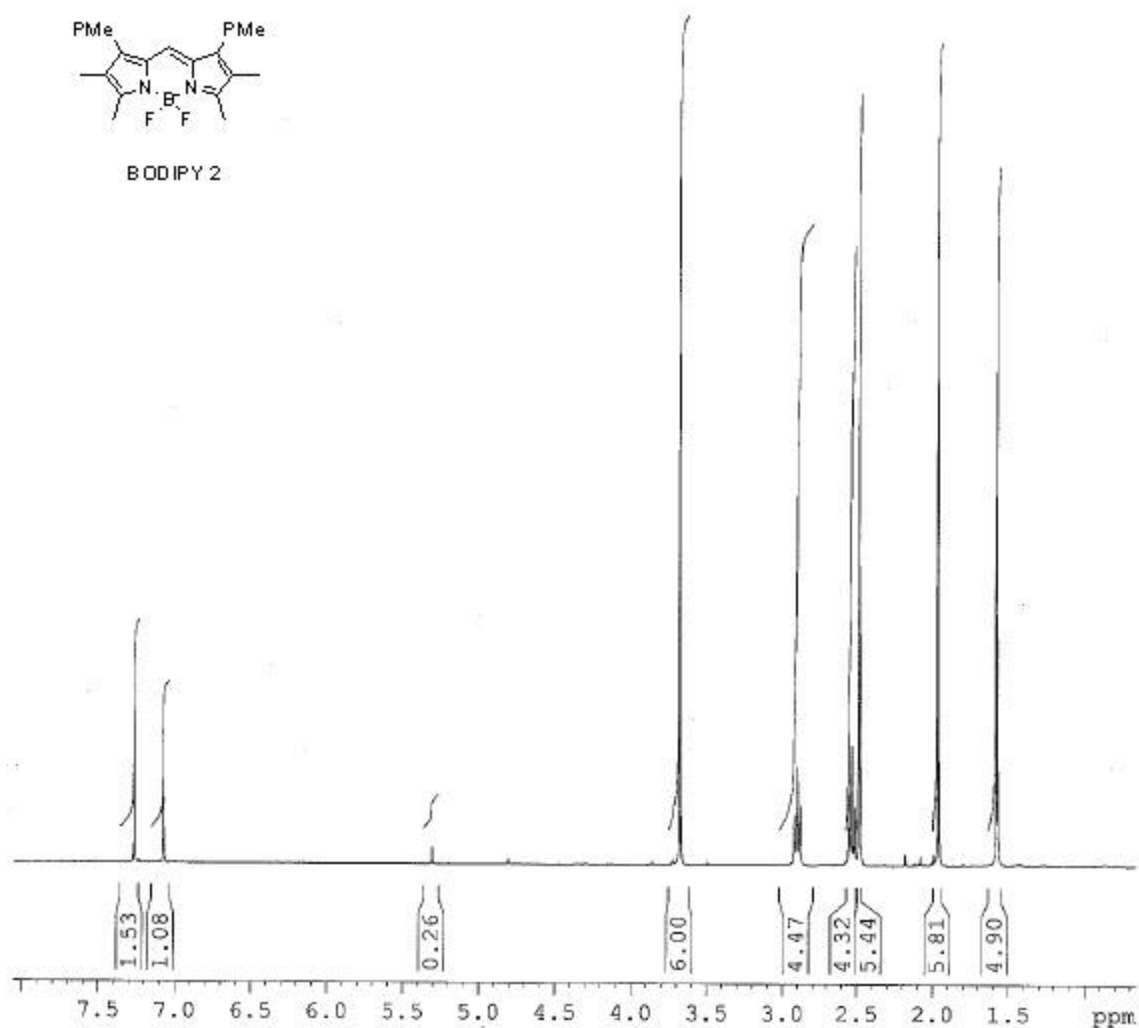
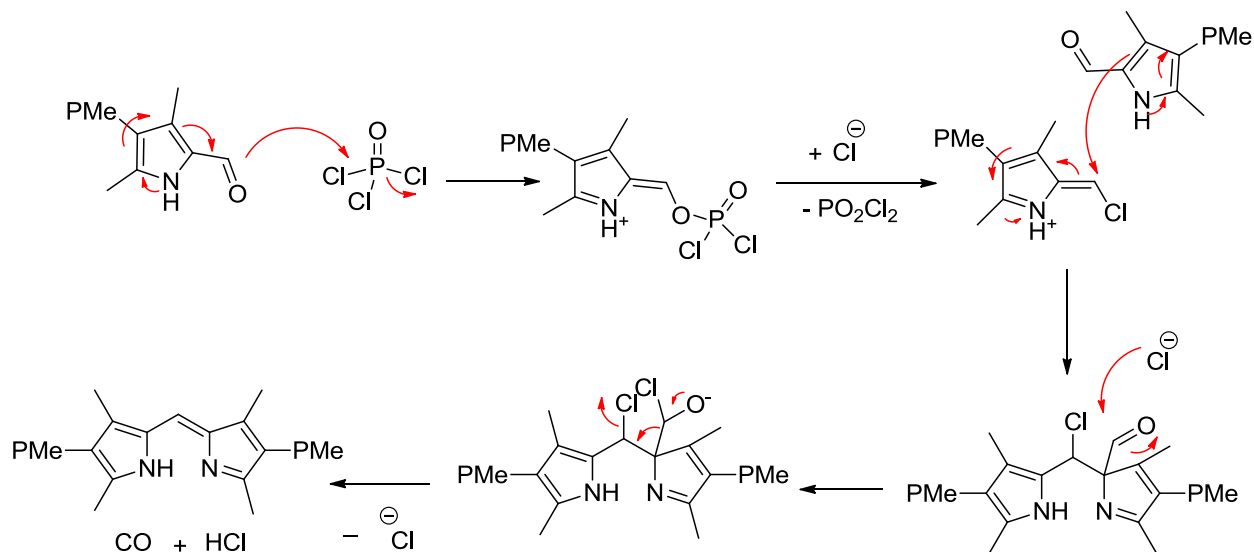


**Figure 3.4:** <sup>1</sup>H-NMR spectrum of BODIPY 2 in CDCl<sub>3</sub> at 400 MHz

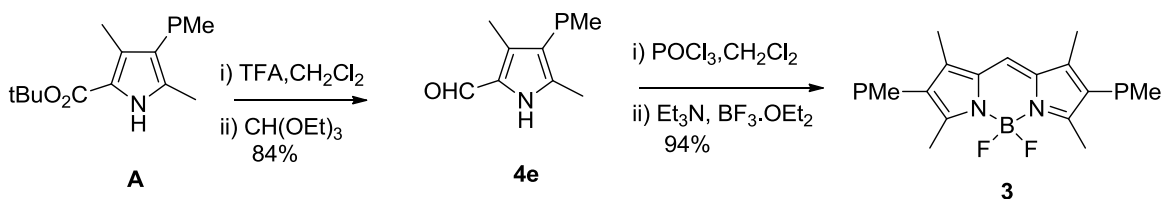
Recently, Wu and Burgess<sup>16</sup> described an interesting and highly efficient synthesis of symmetric BODIPY dyes by self-condensation of two equiv. of pyrrole-2-carbaldehyde (or 2-formyl pyrrole) in the presence of phosphorus oxychloride (POCl<sub>3</sub>). According to their serendipitous discovery, POCl<sub>3</sub> is capable of triggering the self-condensation of formyl-pyrroles, therefore, eliminating the use of an additional  $\alpha$ -free pyrrole. A possible mechanism involves the reaction of POCl<sub>3</sub> with one molecule of formyl pyrrole to generate a vinylogous Vilsmeier-

Haack reagent (a.k.a. chlorinated azafulvene, Scheme 3.3), which is then attacked by another pyrrole molecule. Formation of the product relies on subsequent attack by chloride ion, followed by decomposition of the unstable intermediate and *in situ* complexation with  $\text{BF}_3 \cdot \text{OEt}_2$  in the presence of a base.



**Scheme 3.3:** A possible mechanism for the formation of dipyrromethene from pyrrole-2-carbaldehyde **4e**<sup>17</sup>

BODIPY **3** with  $\beta$ -PMe functionality was synthesized from the corresponding pyrrole-2-carbaldehyde, **4e**, according to the above mentioned one-flask two-step approach, as shown in Scheme 3.4. Compound **4e** was synthesized from its *tert*-butyl protected pyrrole precursor (**A**) in two steps involving deprotection of ester with TFA, followed by formylation with triethyl orthoformate, as described in the previous Chapter (Compound **6**) and shown in Scheme 3.4.



**Scheme 3.4:** Synthetic route to PMe-BODIPY **3**

Pyrrole 2-carbaldehyde **4e** was dissolved in dry dichloromethane under argon and the solution stirred as the temperature was lowered to 0 °C. To this solution, POCl<sub>3</sub> was added dropwise over a period of one minute while stirring and maintaining the reaction temperature at 0 °C. The solution was then warmed to room temperature and stirred overnight (~ 12 h) until TLC indicated absence of any starting material. The mixture was cooled to 0 °C and triethylamine (5 equiv.) was added dropwise over 5 minutes, followed by addition of BF<sub>3</sub>.OEt<sub>2</sub> (8 equiv.). The reaction was stirred overnight and then passed through a short pad of silica gel eluting with pure dichloromethane to remove the polar impurities and any unreacted starting material. The solvent was then removed *in vacuo* and the crude product was re-dissolved in dichloromethane and washed with water, brine and dried over Na<sub>2</sub>SO<sub>4</sub>. The solvent was evaporated and the residue was purified by flash chromatography (dichloromethane/petroleum ether, 1/1) to give green fluorescent BODIPY **3** as a red solid in 94% yield. Crystals suitable for X-ray analysis were obtained by slow crystallization using dichloromethane/hexane (5/1) solvent mixture, as shown in Figure 3.5. The compound was further characterized by <sup>1</sup>H-NMR and MS. In the NMR spectrum, the two sets of methyl protons at 1,7- and 3,5-positions appeared as two distinct singlets at 2.18 and 2.45 ppm respectively. The 1,7-methyls experienced a shielding by approximately 0.27 ppm due to the ring-current shielding effect from the *meso*-phenyl ring. Another singlet was found at 6.98 ppm for the *meso*-proton. MS-ESI gave a peak due to [M<sup>+</sup>+Na] at m/z 443.35.

Post-modification of BODIPY **2** for the facile introduction of various functionalities to the chromophore was carried out by means of the Knoevenagel condensation reactions. BODIPY **2** was condensed with various commercially available aldehydes, **4a-d** using modified Knoevenagel condensation approach, as developed by Daub et al.<sup>18</sup> (Scheme 3.5, Table 3.1).

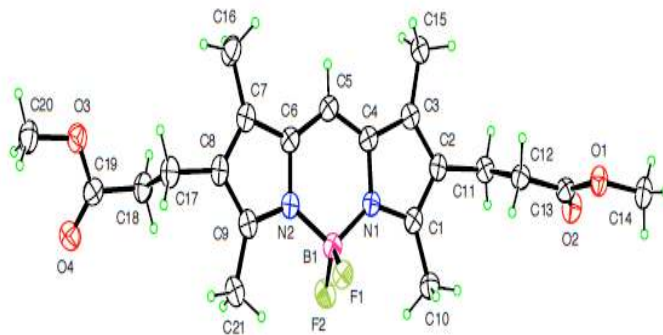
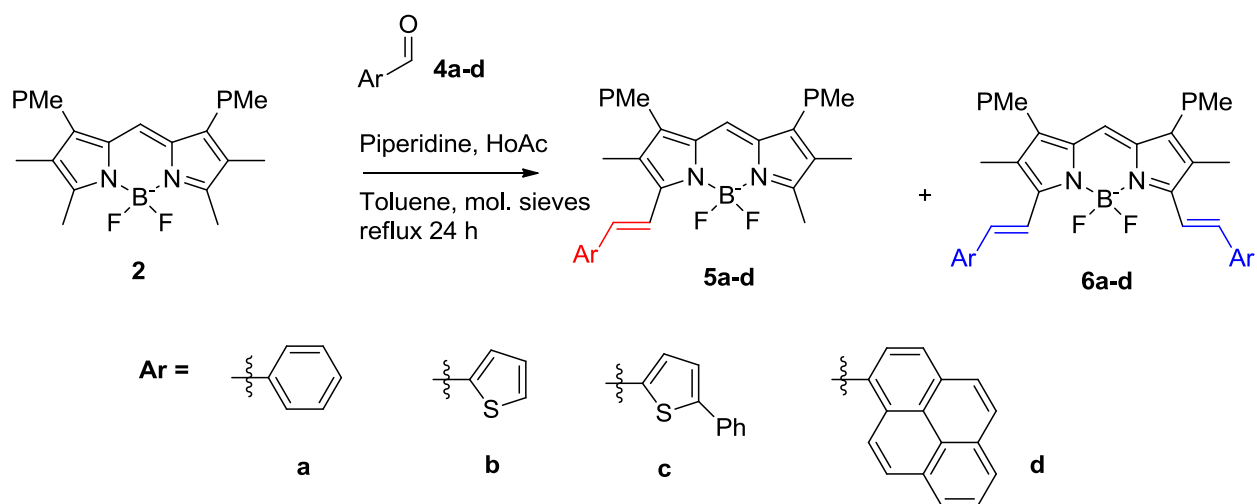


**Figure 3.5:** X-ray crystal structure of BODIPY **3**

1,3,5,7-tetramethyl BODIPY **2** and benzaldehyde **4a** (two equiv.) were refluxed at 110 °C in a mixture of dry toluene, piperidine, acetic acid, together with a small amount of activated molecular sieves (4Å, to adsorb the water produced during the reaction). The progress of the reaction was monitored by TLC, a pink-red spot corresponding to 3-monostyryl BODIPY **5a** appeared after 6 h and after overnight stir (~10 h), a slightly polar blue spot due to 3,5-distyryl BODIPY **6a** was observed. Though TLC indicated the presence of starting material, the reaction was stopped as molecular sieves could not withstand the high temperature and disintegrated during the reaction. After cooling to room temperature, the reaction mixture was passed through a filtration funnel to filter off the molecular sieves. The solvent was removed under reduced pressure and the crude mixture was loaded on top of a silica column and eluted with dichloromethane/hexane (20/1, v/v). The orange pink fraction containing the starting material and BODIPY **5a** was eluted first, followed by blue fraction which crystallized on standing giving shiny deep blue crystals of BODIPY **6a** in 35% yield. Mono-substituted BODIPY **5a** could not be properly purified due to contamination of the tetramethyl BODIPY **2**. The first distyryl BODIPY **6a** was fully characterized by NMR, MS-ESI and X-ray crystallography. <sup>1</sup>H-NMR spectrum of **6a** (Figure 3.6), clearly exhibits all the characteristic signals of the distyryl-BODIPY. The integration of fourteen protons between 7.13-7.77 ppm corresponds to the two

phenyl subunits and four vinyl protons on the distyryl arms. The singlet peak at 2.50 ppm due to 3,5-methyls disappeared with the formation of the vinyl bond. MS-ESI gave a molecular ion peak  $[M^+]$  at  $m/z$  595.25. The molecular structure of BODIPY **6a** confirming the *trans* configuration of the double bonds is shown in Figure 3.7.



**Scheme 3.5:** Styryl-derivatization of PMe BODIPY **2** with various aryl aldehydes **4a-d**

**Table 3.1:** Reaction conditions and percent yield for the derivatization of BODIPY **2** with **4a-d**

Entry	Aryl Aldehyde	Reaction time (h)	Yield % for 5a-d	Yield % for 6a-d
1	<b>4a</b>	12	28 (crude)	35
2	<b>4b</b>	48	< 2	-
3	<b>4c</b>	48	No reaction	No reaction
4	<b>4d</b>	48	< 2	-

A similar protocol was followed for condensation of BODIPY **2** with aldehydes **4b-d**. Interestingly, the reaction didn't give satisfactory results with any of these aldehydes. Varying the reaction conditions such as prolonged heating, excess of base, catalyst or aryl aldehyde failed

to generate the desired styryl-BODIPYs and the unreacted starting material was conveniently recovered during the purification process and recycled. This is not surprising, as the literature search via Scifinder Scholar® revealed a total of two publications mentioning about 3,5-thiophene or pyrene-derivatized BODIPYs and none of the publication reported the percent yield for the reaction. A plausible reason for the failure of these reactions could be the decrease in the electrophilicity of the carbonyl carbon due to neighbouring electron accepting thiophene or pyrene rings.

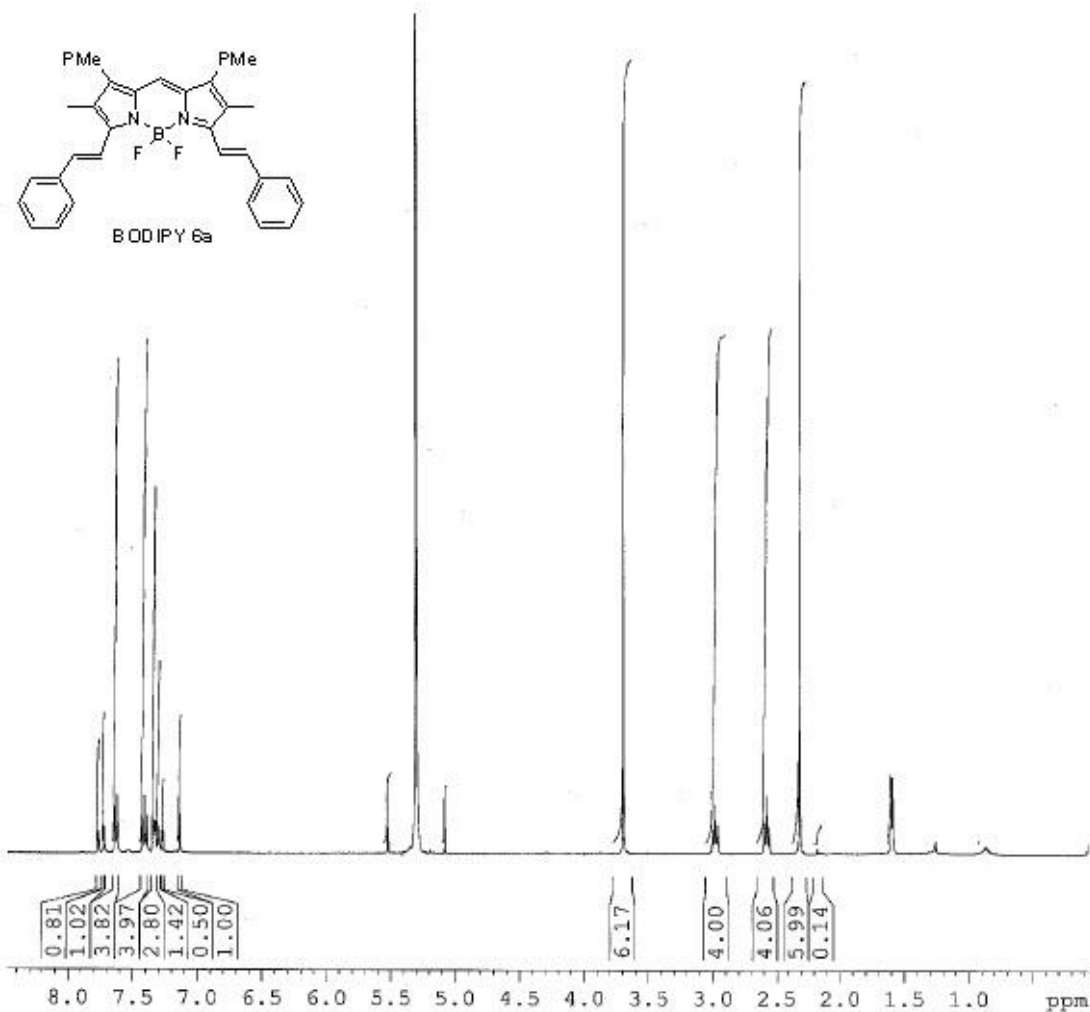


**Figure 3.6:** <sup>1</sup>H-NMR spectrum of BODIPY 6a in CDCl<sub>3</sub> at 400 MHz

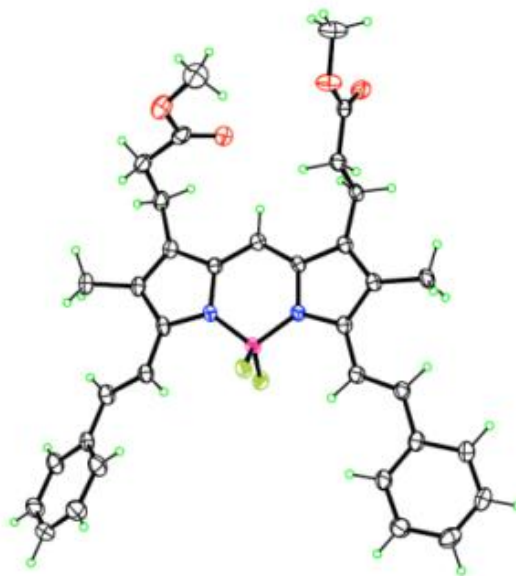
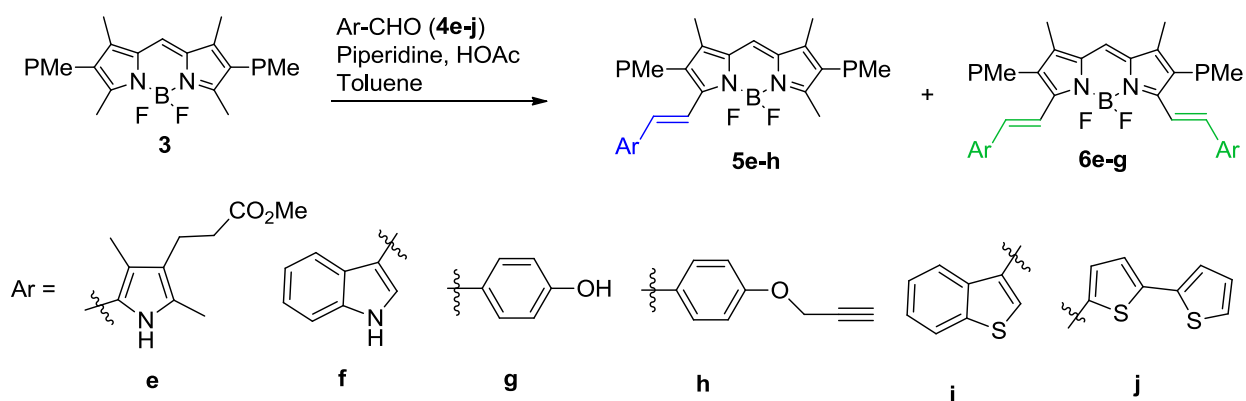


**Figure 3.7:** An X-ray crystal structure of BODIPY **6a**

The chemical robustness of heteroaromatic compounds for instance, indole, pyrrole and thiophene, and the easy tunability of their properties via facile structural modifications have added an array of functionalized materials in dye chemistry, drug design and biodiagnostics. A variety of pyrrole, indole and thiophene based materials have been utilized as optical indicators (fluorimetric or colorimetric) for recognition events involving proteins or DNA as well as optical sensors for ions of biological interest.<sup>19</sup> Especially appealing is the non-toxic and polar hydrophobic nature of these materials which assists their partition at the hydrophilic/hydrophobic interface in lipid bilayer via hydrogen bonding, thereby improving their cellular uptake and biological efficacy. In addition, several classes of indole-based inhibitors with valuable therapeutic effectiveness have been engineered due to their structural resemblance with tryptophan (Trp).<sup>20</sup> Also, many fluorescent pH-responsive BODIPY-based probes have been developed with *p*-phenolic subunit as the pH-sensitive group for selective sensing of alkaline and acidic pH. The presence of water-solubilising phenol group not only improves the amphiphilicity



of the BODIPY fluorophore, it enhances their passive cellular uptake as well. Further *O*-alkylation of hydroxyl-benzaldehydes with propargyl bromide helps to generate the alkylated benzaldehyde derivatives which could serve as important building blocks for functional BODIPY dyes bearing extra conjugation handles. Incorporation of ligation handles on the BODIPY core allows its covalent attachment to other bioactive molecules via alkyne/azide cycloaddition.<sup>21</sup> In order to study the relationship between the structure and optical properties in green emitter BODIPY **3**, it was condensed with aryl aldehydes **4e-j** in boiling toluene as depicted in Scheme 3.6.



**Scheme 3.6:** Synthetic route to mono- and distyryl-PMe BODIPYs

Initially we investigated the Knoevenagel condensation of BODIPY **3** with pyrrole **4e** via similar procedure as mentioned for BODIPY **6a**. The reaction successfully generated both single and double condensation products, however in relatively lower yields of 8 and 5.6 % respectively. The success of this reaction was encouraging enough and prompted us to find the optimized conditions for the condensation reaction. The reaction was then performed using forcing conditions (140 °C, highly concentrated reaction mixture) and Dean-Stark trap to avoid the use of molecular sieves. We were fortunate to observe that on refluxing BODIPY **3** with **4e**,

under modified conditions, both 3-monostyryl **5e**, and 3,5-distyryl BODIPYs **6e** could be generated with improved yields of 62% and 18% respectively (Table 3.2). Also, the yield percent of distyryl BODIPY **6e** increased from 18% to 31% when 4 equivalents of **4e** reagent is used instead of 2 equiv.

**Table 3.2:** Reaction conditions and yield % for functionalization of BODIPY **3**

Entry	Aldehyde	Reaction time (h)	Yield <b>5e-h</b> (%)	Yield <b>6e-g</b> (%)
1	<b>4e</b>	12	62	31
2	<b>4f</b>	12	55.6	41
3	<b>4g</b>	12	23.4	66.6
4	<b>4h</b>	72	3.5	-
5	<b>4i</b>	72	No reaction	No reaction
6	<b>4j</b>	72	No reaction	No reaction

Extending the reaction to aldehydes **4f** and **4g** smoothly generated the  $\pi$ -extended BODIPY dyes **5f**, **5g**, **6f** and **6g** in 55.6%, 23.4%, 41% and 66.6% yields respectively, after careful column chromatography. Interestingly, reaction with **4h** was successful in generating only trace amounts of monostyryl product **5h** due to instability of the ethynyl aryl groups at higher temperature.<sup>22</sup> As expected, no product could be formed in the case of substituted thiophene derivatives **4i** and **4h** due to their lower nucleophilicity. NMR and mass spectral data were in full agreement with the assigned molecular structures for the mono- and distyryl-BODIPY dyes **5e-h** and **6e-g**, respectively. <sup>1</sup>H-NMR spectra of monostyryl-BODIPYs **5e-g** (such as, Figure 3.8), when compared with the <sup>1</sup>H-NMR spectrum of BODIPY **3**, gave characteristic signals of vinylic protons in the 3-position as a pair of doublet at approximately 6.92 and 7.25 ppm. For **5e**, two single peaks appeared at 3.67 and 3.69 ppm, respectively, due to methyl ester protons along with additional peaks in between 2-3 ppm due to CH<sub>2</sub> and methyl protons of the

pyrrole substituent. For **5f**, **5g** and **5h**, signals corresponding to indolic NH (9.87 ppm) and *ortho* and *meta* protons appeared as doublets in the aromatic region with the most shielded one at 6.95 ppm. For **5h**, two equivalent protons of the propargylic methylene group showed up as a singlet at 4.73 ppm. In the  $^1\text{H-NMR}$  spectra of distyryl-BODIPYs **6e-g**, the single peak due to 3-methyl protons at 2.48 ppm was replaced by additional peaks of vinylic protons in the aromatic region (Figure 3.9).

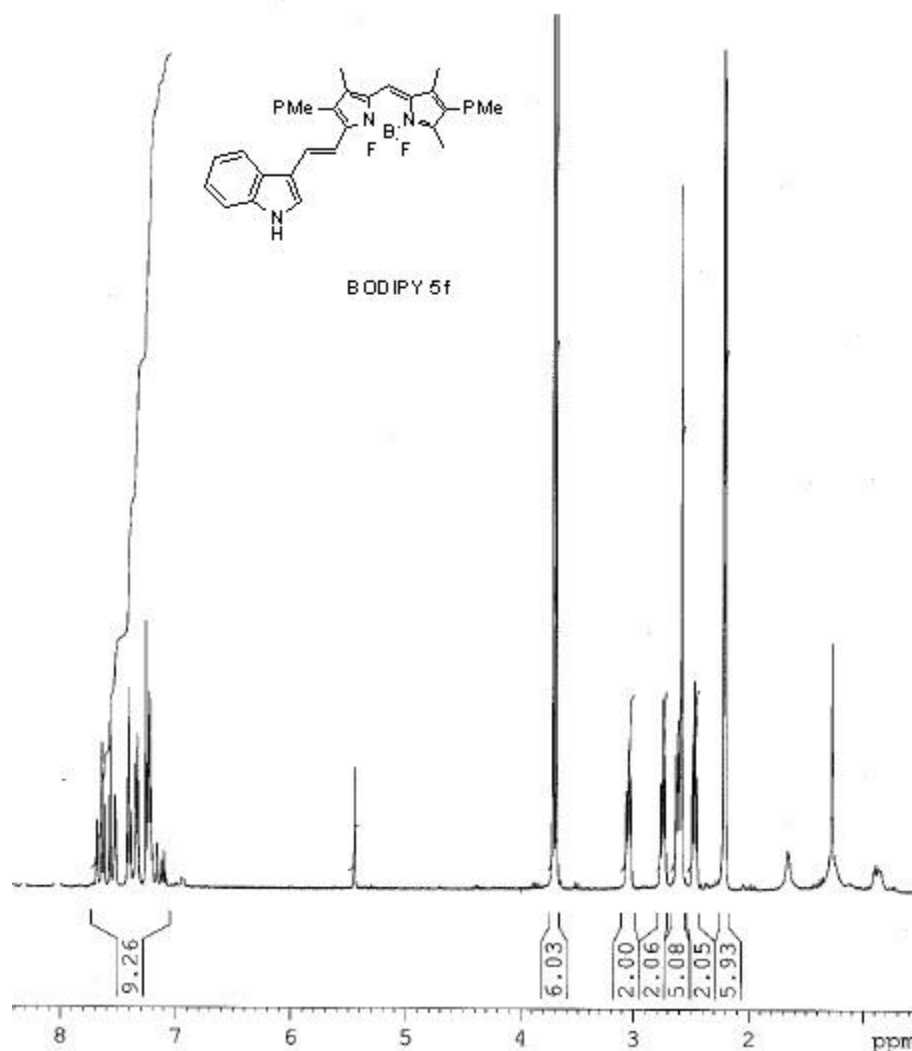


**Figure 3.8:**  $^1\text{H-NMR}$  spectrum of BODIPY **5f** in deuterated acetone at 400 MHz

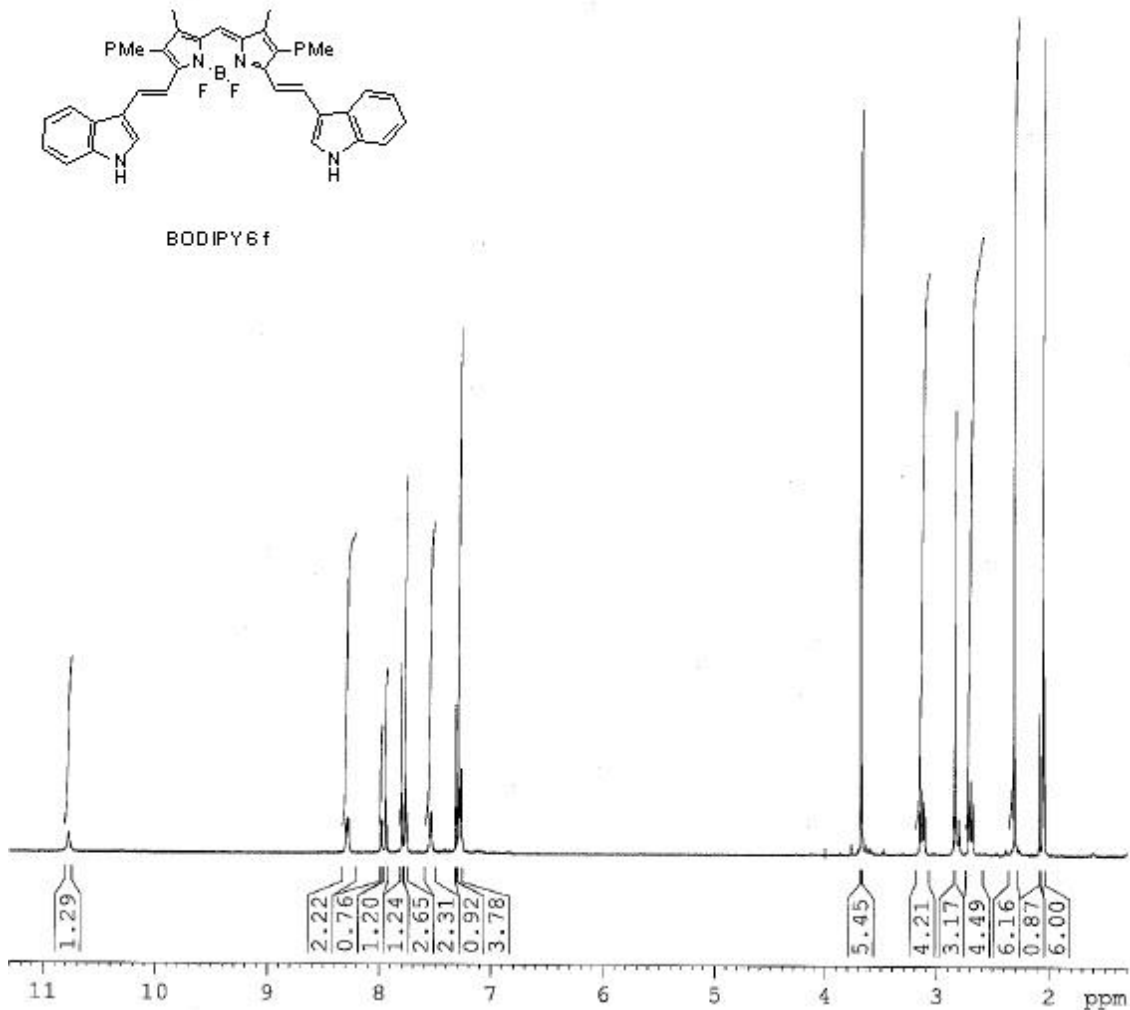


**Figure 3.9:** <sup>1</sup>H-NMR spectrum of BODIPY **6f** in deuterated acetone at 400 MHz

Single-crystal X-ray structures were obtained for compounds (**5e**, **6f** and **6g**) by slow diffusion of hexane into a solution of dichloromethane or acetone. The results of this study are presented in Figure 3.10 and cell parameters and refinement details are summarized in Table 3.3. Compound **5e** crystallizes in the monoclinic space group  $P2_1$  whereas crystals for **6f** and **6g** fall within the centrosymmetric triclinic space group. The average bond lengths for B-N and B-F [1.559(3), 1.394(3) Å for **6a** (Figure 3.7) and 1.551(3), 1.398(2) Å for **6f** respectively] and the

average bond angles for N-B-N and F-B-F [107.22(17)°, 109.02(18)° for **6a** and 107.48(15)°, 108.70(15)° for **6f** respectively] indicate a tetrahedral BF<sub>2</sub>N<sub>2</sub> configuration and are in good agreement with previously published data.<sup>23</sup> The average bond length of N1-C1, N2-C9 [1.370(3) Å for **6a** and 1.368(2) Å for **6f**] indicates double bond character, compared with the single bond character of N1-C4, N2-C6 [1.383(3) Å for **6a** and 1.394(2) Å for **6f**]. For all the compounds, there is a strong  $\pi$ -electron delocalization between the central six-membered ring and the two adjacent pyrrole rings.

The molecular structure of **6a** and **6f** confirms the presence of two vinyl arms with bond length C10-C11, C28-C29 [for **6a**] and C10-C11, C30-C31 [for **6f**] being 1.346(3) Å, 1.345(3) Å and 1.345(3) Å, 1.347(3) Å respectively, indicating the double bond is in a *trans*-conformation, giving the molecule a “V-shape”, as previously published.<sup>23b</sup> Single crystal X-ray crystallography of the mono-styryl BODIPY **5e** reveals nearly coplanar arrangement of the pyrrolyl-ethenyl moiety with one of the groups slightly off the molecular plane by 10°. The styryl group is also only slightly twisted by 5° out of the plane of the BODIPY core, suggesting efficient conjugation within the entire chromophore. It is interesting to note that both C10-H and C30-H are in optimal distances for hydrogen bonding of the fluorine atoms on the BF<sub>2</sub>-bridge.

**Table 3.3:** Selected crystallographic data and structure refinement for **5e**, **6a**, **6f** and **6g**<sup>[a]</sup>

Parameters	<b>5e</b>	<b>6a</b>	<b>6f</b>	<b>6g</b>
Formula	C <sub>32</sub> H <sub>40</sub> BF <sub>2</sub> N <sub>3</sub> O <sub>6</sub>	C <sub>35</sub> H <sub>35</sub> BF <sub>2</sub> N <sub>2</sub> O <sub>4</sub>	C <sub>39</sub> H <sub>37</sub> BF <sub>2</sub> N <sub>4</sub> O <sub>4</sub>	C <sub>38</sub> H <sub>41</sub> BF <sub>2</sub> N <sub>4</sub> O <sub>7</sub>
M <sub>r</sub>	611.48	596.46	674.54	686.54
Cell system	Monoclinic	Triclinic	Triclinic	Triclinic
Space group	P2 <sub>1</sub> /n	P $\bar{1}$	P $\bar{1}$	P $\bar{1}$
T [K]	90	100	90	90

**Table 3.3:** (continued)

Parameters	5e	6a	6f	6g
a [Å]	15.063(2)	13.6417(3)	10.1096(9)	7.9104(6)
b [Å]	6.6224(10)	15.1278(3)	12.4151(10)	11.7055(9)
c [Å]	31.049(5)	15.8439(3)	13.8619(14)	19.9798(15)
$\alpha$ [°]	nd	90.034(1)	77.952(5)	74.172(3)
$\beta$ [°]	96.512(8)	94.162(1)	85.239(4)	89.368(3)
$\gamma$ [°]	nd	111.875(1)	79.271(4)	76.456(3)
V [Å <sup>3</sup> ]	3077.3(8)	3024.92(11)	1670.0(3)	1727.6(2)
Z	4	4	2	2
$\rho_{\text{calcd}}$ [Mg m <sup>-3</sup> ]	1.320	1.310	1.341	1.320
F(000)	1296	1256	708	724
Crystal size [mm]	0.25 x 0.15 x 0.08	0.32 x 0.13 x 0.06	0.24 x 0.21 x 0.06	0.30 x 0.26 x 0.12
$\mu$ [mm <sup>-1</sup> ]	0.82	0.76	0.78	0.81
$\Theta_{\text{max}}$ [°]	67.2	68.5	68.2	67.6
Measured reflns	18925	33183	13932	17540
Independent reflns	5416	10666	5746	5891
Observed reflns	2357	7251	4618	5482
R [F <sup>2</sup> > 2 $\sigma$ (F <sup>2</sup> )]	0.152	0.044	0.043	0.044
wR(F <sup>2</sup> )	0.451	0.119	0.119	0.117
Max/min peaks	0.71/-0.40	0.26/-0.24	0.24/-0.21	0.34/-0.27

[a] Criterion for observed reflections:  $I > 2 \sigma(I)$ . Refinement on F<sup>2</sup>

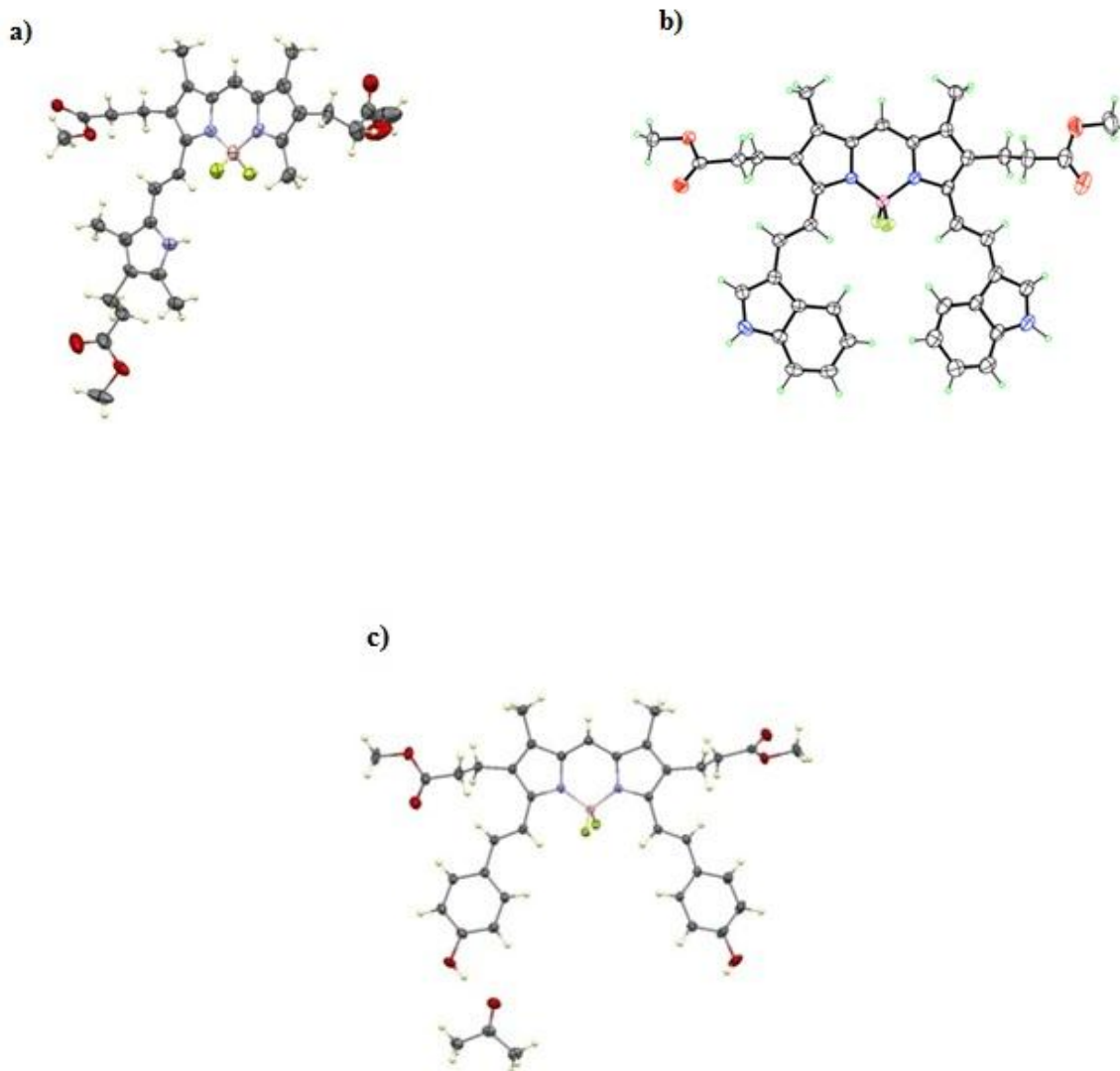
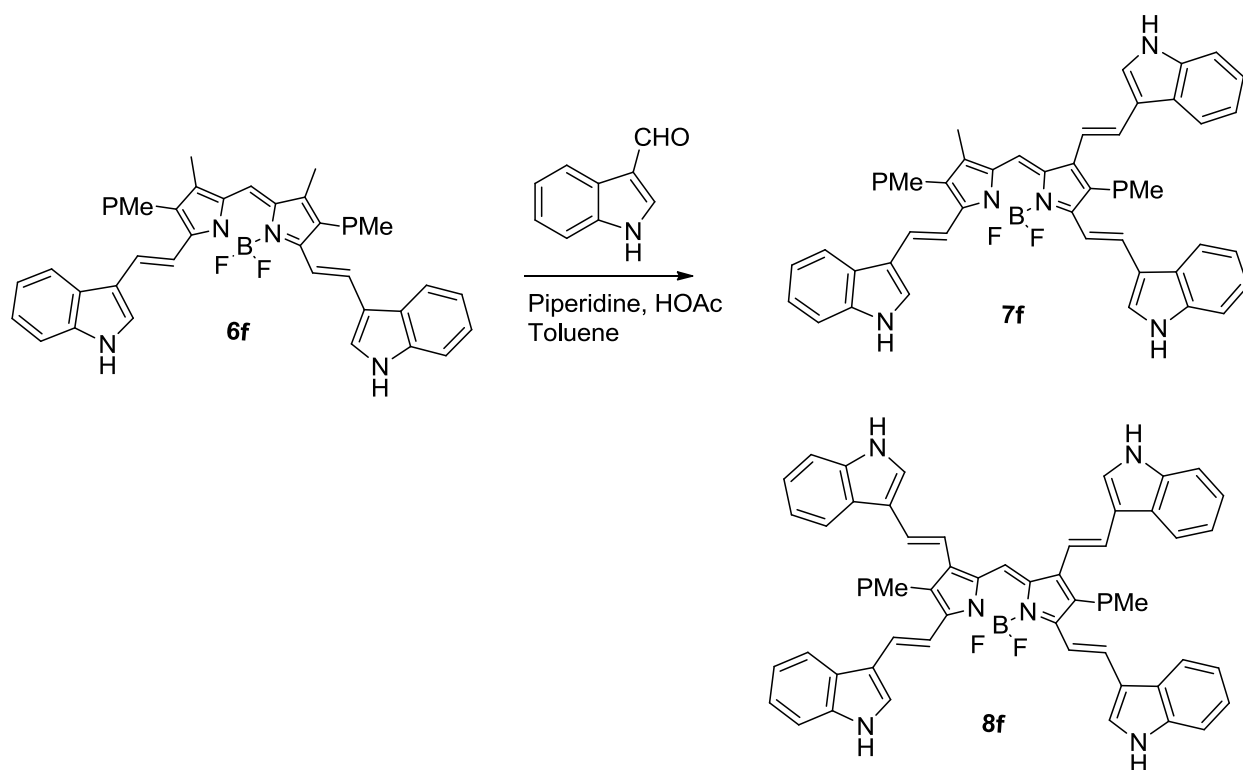


**Figure 3.10:** ORTEP plots of a) **5e**; b) **6f** and c) **6g** with co-crystallized acetone solvent molecule at the 50% probability level

Recently, Akkaya et al.<sup>24</sup> performed a Mulliken-charge calculation on the core carbon atoms of 1,3,5,7-tetramethyl BODIPY derivatives. The electron density of the carbon atoms was found to vary in the order  $2,6 \gg 1,7 > 3,5$ , indicating that 1,7-methyls are nearly as acidic as 3,5-methyls. This group also reported the synthesis of tristyryl and tetrastyryl-BODIPY dyes by activating methyls at the 1,7-positions using electron-accepting 2,6-phenylethynyl groups. Later

Ziessel's group<sup>12a</sup> successfully synthesized butterfly-shaped BODIPY dyes by introducing four different vinyl arms on a single tetramethyl-BODIPY core. Encouraged by these observations, we adopted a similar methodology to generate tristyryl- and tetrastyryl-BODIPY dyes with unique chemical structures. Thus considering the possibility of further functionalization of the BODIPY scaffold, BODIPY **6f** with indolylstyryl substituent was chosen for a quadruple Knoevenagel condensation reaction.

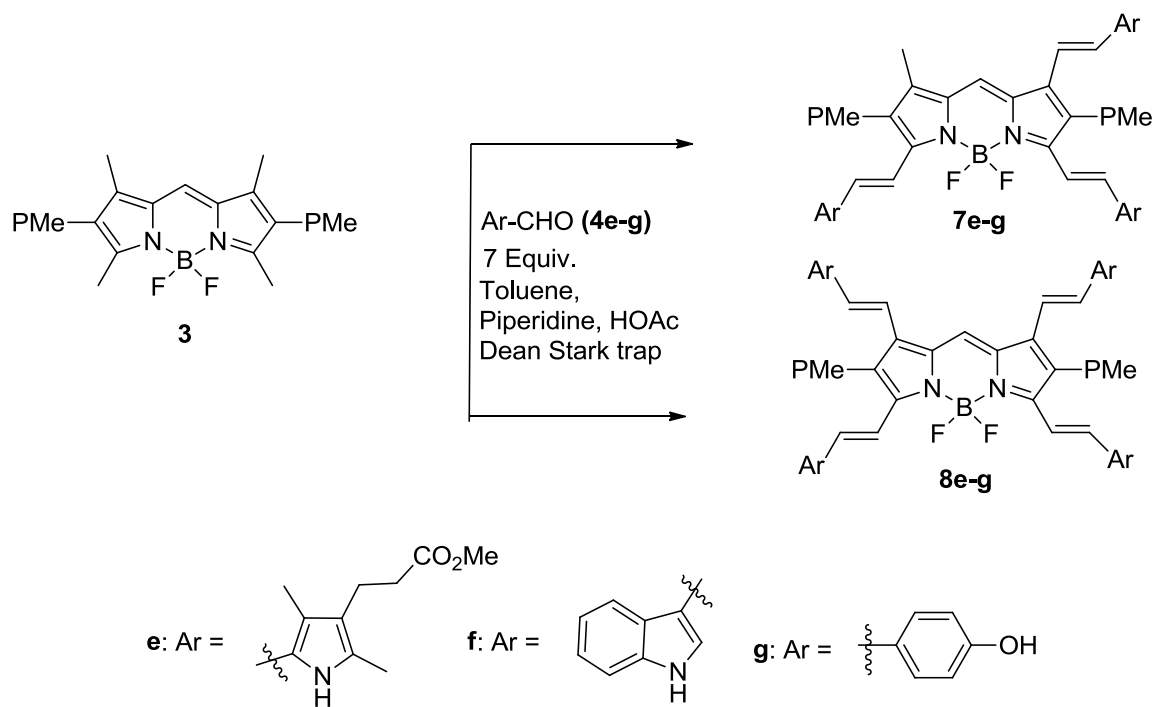


**Scheme 3.7:** Synthetic route to tristyryl and tetrastyryl-BODIPY dyes **7f** and **8f**

BODIPY **6f** and Indole-3-carbaldehyde **4f** (5 equiv.) were added to a refluxing mixture of dry toluene, piperidine and glacial acetic acid (Scheme **3.7**). However, due to poor solubility of the starting material in refluxing toluene, no product could be generated. Variations of solvent (DMSO, THF and DMF) to make the reaction viable were unsuccessful as we failed to identify



any triple or quadruple Knoevenagel condensation products and only a dark reaction mixture was obtained. We then modified our strategy and decided to prepare the desired BODIPYs **7f** and **8f** from tetramethyl BODIPY **3**, by using slight excess of indole-3-carbaldehyde (Scheme 3.8). It is worth noting, the major products obtained during the condensation were mono- and di-indolylstyryl-BODIPYs **5f** and **6f** respectively, indicating that the first methyls to react exclusively are 3,5-methyls. However, highly substituted BODIPYs **7f** and **8f** could be successfully generated (though in low yields, < 10% crude) under harsh reflux conditions by removal of most of the solvent. Despite the successful generation of BODIPYs **7f** and **8f**, the products could not be isolated from the reaction mixture as it required chromatographic purifications which were quite difficult to perform due to close R<sub>f</sub> values. The above reaction was then performed with BODIPY **3** and aldehydes **4e** and **4g** as shown in Scheme 3.8. All the four (mono, di, tri and tetra) condensation products could be identified by MALDI-TOF analysis.

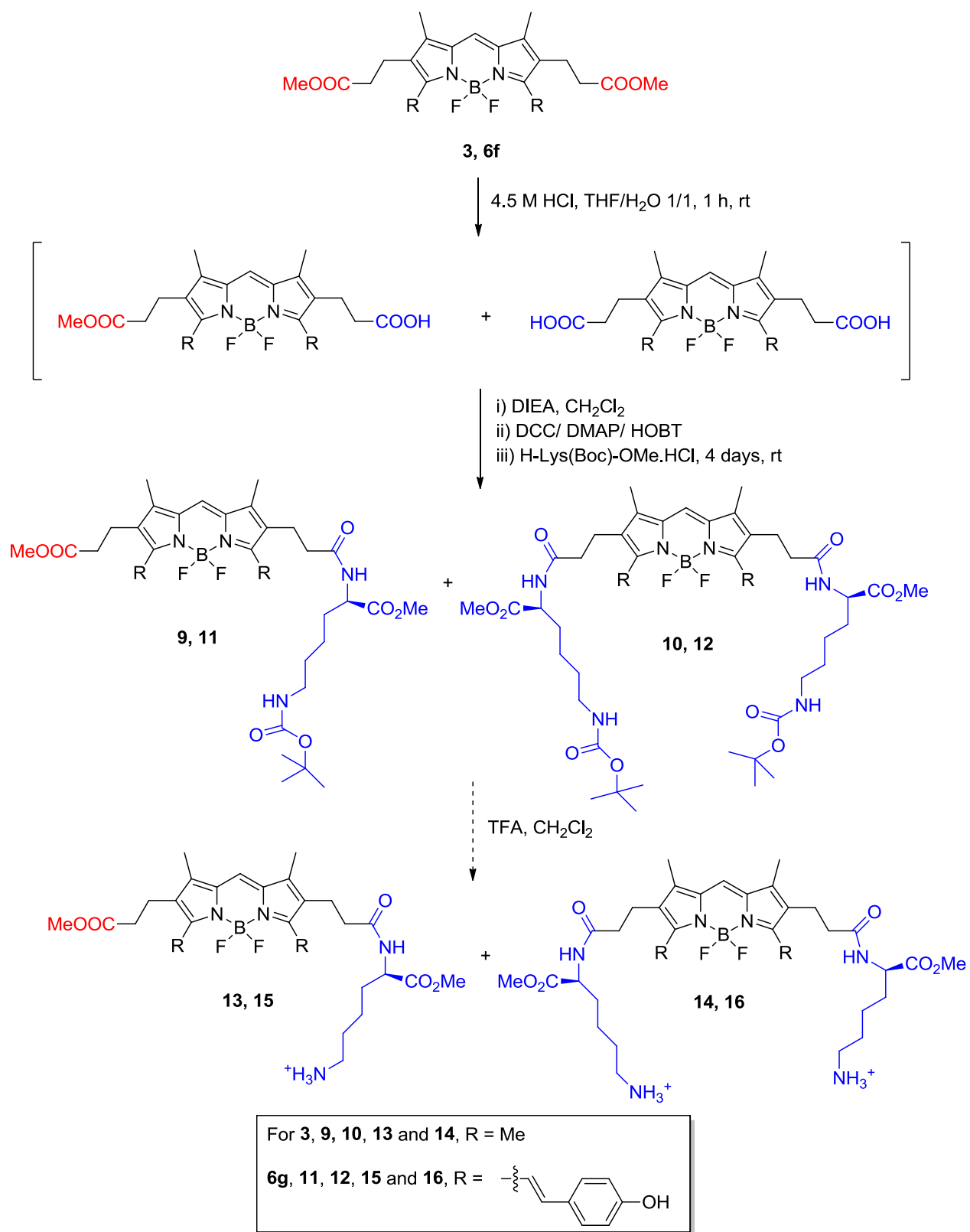


**Scheme 3.8:** Synthetic route to tristyril and tetrastyril-BODIPY dyes **7e-g** and **8e-g**

Though the attempts to isolate pure **7e** and **8e** from the reaction mixture failed due to purification difficulties, the first tristyryl- and tetrastyryl-BODIPYs **7g** and **8g** bearing polar phenol groups were successfully isolated in 8% and 6.2 % yield by careful silica gel column chromatography (dichloromethane/ethyl acetate, 10/1) followed by preparative TLC (ethyl acetate/acetone 1/1). MALDI-TOF indicated molecular ion peaks at  $m/z$  732.2 and 836.3 corresponding to BODIPYs **7g** and **8g** respectively. However, due to trace amounts of the product formed, well-resolved  $^1\text{H}$ -NMR spectra could not be obtained.

Mitochondria are membrane-enclosed energy producing organelles found in eukaryotic cells, making up to 10% of the cell volume. They are pleomorphic organelles with a pivotal role in a range of cellular processes (cell signaling, differentiation and cell death), hyper-proliferative diseases and cancer. However, there is only a partial understanding of mitochondrial morphology and functioning.<sup>25</sup> Therefore, mitochondrial specific probes will undoubtedly provide a more detailed understanding of organelle's activity, localization and abundance. Mitochondria possesses a net negative charge on the membrane, hence ideal biomarker for mitochondria should potentially be lipophilic with delocalized positive charge. Keeping this in mind, we hypothesized that the cationic lysyl-BODIPY conjugates bearing positive charge on the amine group might display enhanced affinity towards mitochondria.<sup>26</sup>

As the designed BODIPYs are functionalized with protected propionic acids at 2,6-positions, their ability for conjugation to amine group of lysine was investigated. BODIPY **3** was chosen as a model compound to study the hydrolysis of the methyl esters. Firstly, the basic hydrolysis of dimethyl esters on BODIPY **3** was carried out using standard conditions with LiOH and NaOH ( $\text{pH} < 10$ )<sup>12d, 27, 28, 29</sup>. Under these saponification conditions, BODIPY **3** didn't give any desired product, but resulted in destruction of the fluorophore (due to nucleophilic attack on boron) and generation of secondary fluorescent products. MALDI-TOF analysis of the reaction



**Scheme 3.9:** Synthetic route to ester hydrolysis and lysine conjugation of BODIPYs **3** and **6g**

mixture indicated a highly intense molecular ion peak at  $M^+-19$ , corresponding to molecular fragment without a fluoride ion (boremium cation). The hydrolysis of BODIPY **3** was ultimately accomplished under acidic conditions upon treatment with 4.5M HCl in THF/H<sub>2</sub>O mixture (3/5, v/v) at room temperature by modifying the procedure reported by Giebler and co-workers<sup>30</sup>, affording the mono- and dicarboxylic-acid BODIPY derivatives within 1 h (Scheme **3.9**). These intermediates were used as such without further purification in the conjugation step. *In situ* carbodiimide activation with DCC/DMAP (5:3 ratio) was chosen to activate the free carboxylic acid groups. Furthermore, coupling with H-lysine(OtBu)methyl ester.HCl (3 equiv.) generated the mono- and dilysine(OtBu) protected BODIPY-conjugates in 26.2% and 26.5% yields respectively. MALDI-TOF analysis showed two subsequent peaks at m/z 657.43 and 899.51, due to lysyl-BODIPY conjugates **9** and **10** respectively, and <sup>1</sup>H-NMR spectrum demonstrated the existence of new peaks due to the newly appended lysine residue. The optimized acid hydrolysis and conjugation conditions were then applied to distyryl-BODIPYs **6f** and **6g**. Due to limited solubility of BODIPYs in THF, an equimolar solvent mixture of THF/DMF was chosen to run the coupling reaction. Surprisingly, the conjugation of mono- and dicarboxylic-acid derivatives of BODIPY **6f** with lysine didn't give the desired conjugation product, presumably due to steric and/or electronic interactions within BODIPY **6f** which prevented the formation of lysyl-BODIPY conjugates. On the other hand, BODIPY **6g** effectively generate both mono- and dilysyl-BODIPY conjugates **11** and **12** in 11.4% and 34.8% yields respectively. <sup>1</sup>H-NMR spectra of **11** and **12** showed the disappearance of methyl ester protons with the formation of amide-bonds. Additionally, new peaks due to appended lysyl-group appeared between 2-3 ppm. MALDI-TOF analysis revealed the molecular ion peaks at m/z 856.44 and 1084.60 for lysyl-BODIPY conjugates **11** and **12** respectively. The deprotection of OtBu-group (Boc group) of lysyl-BODIPY conjugates with TFA can further generate the positively charged-BODIPY

derivatives that might have affinity towards mitochondria or other charged molecules such as phosphates or carboxylates.

### 3.2.2: Photophysical Studies

The UV/Vis absorption and fluorescence spectra of BODIPY dyes **5f**, **5g**, **6a**, **6e** and **6g** were studied in three solvents of different polarity, i.e. dichloromethane, THF and DMSO, along with those of unsubstituted BODIPYs **2** and **3**. The results obtained from these measurements are represented in Figures **3.11** to **3.13** and summarized in Table **3.4** to **3.6**. As is evident, all these BODIPYs exhibit the typical spectral characteristics of the BODIPY dyes with narrow absorption band due to  $S_0$ - $S_1$  transition, a weak and broad absorption band attributed to  $S_0$ - $S_2$  transition, high molar extinction coefficients ( $\log \epsilon = 4.27$ - $4.64$ ), an intense fluorescence emission band and small Stokes shifts in all the three solvents.<sup>31</sup> All fluorescence emission spectra are identical to absorption ones and are mirror image of the latter, indicating that the emitting species are similar to the absorbing ones. In comparison to non-styrylated BODIPYs, introduction of first styryl group induces a significant bathochromic shift in the absorption (50-80 nm) and emission maxima (56-105 nm), whereas grafting of second styryl moiety causes red-shifts of both absorption and emission maxima in the order of 125-176 nm and 132-200 nm respectively, depending on the attached styryl group. Hence by varying the aromatic aldehyde used to generate the styryl arm, one can synthetically modify the green emissive BODIPY scaffold to provide “any color you want”,<sup>32</sup> highlighting the usefulness of this facile transformation. The appended styryl substituents affect the spectral characteristics of BODIPYs by following the trend: **indole** > **hydroxy** > **phenyl** in all the solvents studied. BODIPY **6f** displayed the most red-shifted and much broader absorption and emission spectra at 693 nm and 711 nm respectively, along with relatively large Stokes shift in dichloromethane, which steadily

shifted to NIR region on moving to more polar solvent (absorption and emission spectra at 708 and 738 nm, respectively in DMSO). The solvatochromic fluorescence emission indicates that the dipole moment of the emissive state is significantly higher as compared to the ground state, a phenomenon that has been observed in similar compounds and explained in terms of intramolecular charge transfer (ICT) that occurs in the locally excited states, producing more polar and conformationally relaxed emissive excited states.<sup>33</sup>

**Table 3.4:** Spectral properties of BODIPYs **2**, **3**, **5f**, **5g**, **6a**, **6f** and **6g** in dichloromethane at room temperature

BODIPY	Absorbance $\lambda_{\max}/\text{nm}$	$\log \epsilon(\text{M}^{-1}.\text{cm}^{-1})$	Emission $\lambda_{\max}/\text{nm}$	$\Phi_f^{[a]}$	Stokes Shift (nm)
<b>2</b>	528	4.4242	531	0.81	3
<b>3</b>	534	4.3950	540	0.85	6
<b>5f</b>	605	4.6035	622	0.84	17
<b>5g</b>	588	4.2760	596	0.94	8
<b>6a</b>	649	4.5924	658	0.58	9
<b>6f</b>	693	4.6218	711	0.12	18
<b>6g</b>	659	4.6402	672	0.68	13

[a] Fluorescence quantum yields for BODIPYs **2**, **3** ( $\lambda_{\text{exc}} = 510$  nm), BODIPYs **5f-g** ( $\lambda_{\text{exc}} = 570$  nm), BODIPYs **6a** and **6g** ( $\lambda_{\text{exc}} = 620$  nm) and BODIPY **6f** ( $\lambda_{\text{exc}} = 650$  nm) were calculated using Rhodamine 6G (0.80 in methanol), cresyl violet perchlorate (0.54 in ethanol), methylene blue (0.03 in methanol) and ZnPc (0.28 in DMF) as the reference.<sup>[28]</sup>

All the observed spectral parameters are in good agreement with those reported previously for mono- and distyryl-BODIPYs in various organic solvents.<sup>18, 23b, 34</sup> Changing the solvent polarity causes only a slight red-shift in the absorption maxima of all the BODIPYs (3-15 nm) indicating a small difference between the dipole moment of the ground and the locally excited states.<sup>18</sup> On the other hand, the emission maxima for all BODIPYs studied, steadily

shifted to longer-wavelengths (10-27 nm) on moving from dichloromethane to DMSO, which once again can be attributed to the charge-transfer nature of the emitting state.<sup>35</sup>

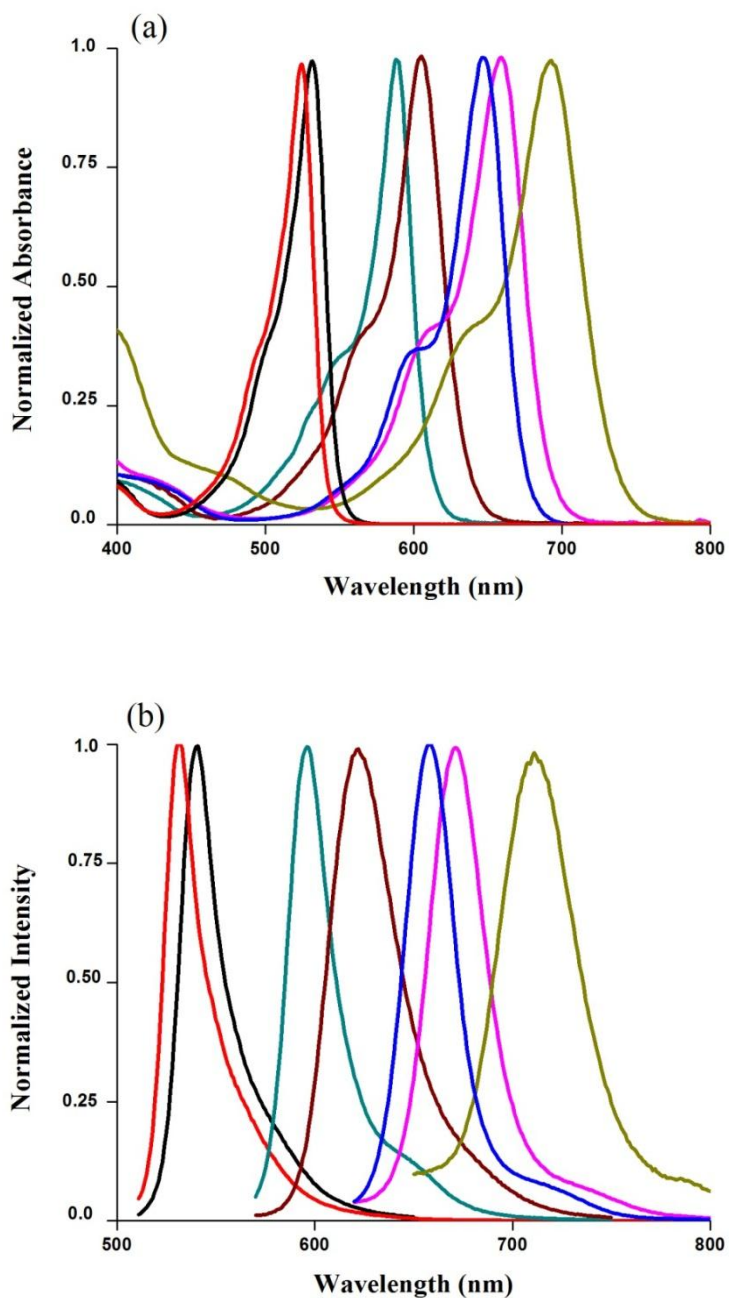


**Figure 3.11:** Normalized UV/Vis (a) and fluorescence spectra (b) of BODIPYs **2** (red), **3** (black), **5f** (brown), **5g** (cyan), **6a** (blue), **6f** (green) and **6g** (pink) in dichloromethane at 25 °C

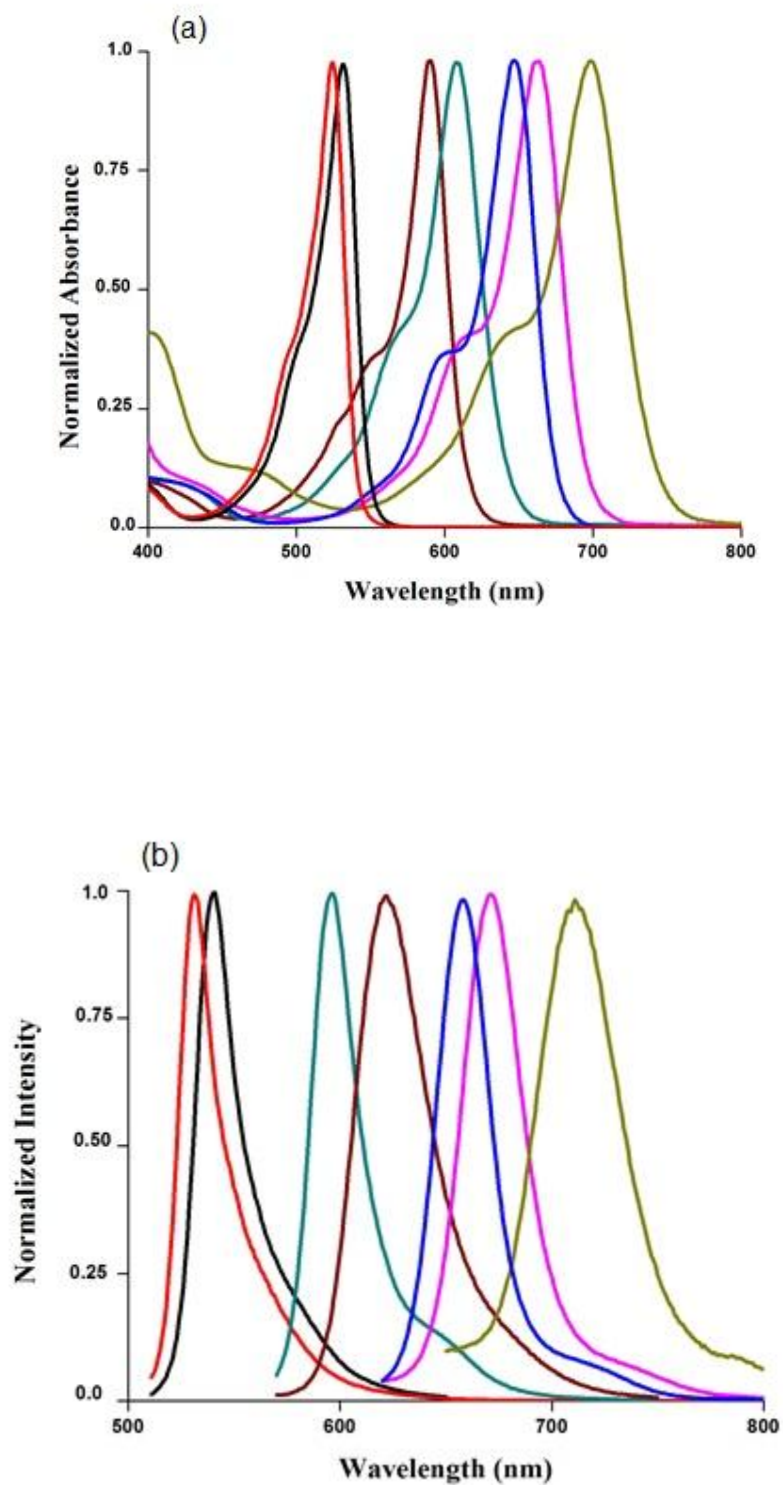


**Figure 3.12:** Normalized UV/Vis (a) and fluorescence spectra (b) of BODIPYs **2** (red), **3** (black), **5f** (brown), **5g** (cyan), **6a** (blue), **6f** (green) and **6g** (pink) in THF at 25 °C



**Table 3.5:** Spectral properties of BODIPYs **2**, **3**, **5f**, **5g**, **6a**, **6f** and **6g** in THF at room temperature

BODIPY	Absorbance $\lambda_{\max}/\text{nm}$	$\log \epsilon$ ( $\text{M}^{-1} \cdot \text{cm}^{-1}$ )	Emission $\lambda_{\max}/\text{nm}$	$\Phi_f^{[a]}$	Stokes shift (nm)
<b>2</b>	523	4.5125	527	0.57	4
<b>3</b>	529	4.4512	536	0.77	7
<b>5f</b>	608	4.5618	627	0.64	19
<b>5g</b>	591	4.1610	600	0.92	9
<b>6a</b>	648	4.2836	657	0.40	9
<b>6f</b>	699	4.5033	718	0.10	19
<b>6g</b>	663	4.6531	677	0.49	14

[a] Fluorescence quantum yields for BODIPYs **2**, **3** ( $\lambda_{\text{exc}} = 510$  nm), BODIPYs **5f-g** ( $\lambda_{\text{exc}} = 570$  nm), BODIPYs **6a** and **6g** ( $\lambda_{\text{exc}} = 620$  nm) and BODIPY **6f** ( $\lambda_{\text{exc}} = 650$  nm) were calculated using Rhodamine 6G (0.80 in methanol), cresyl violet perchlorate (0.54 in ethanol), methylene blue (0.03 in methanol) and ZnPc (0.28 in DMF) as the reference,<sup>[28]</sup> respectively using PTI Quantum Master4/2006SE spectrofluorimeter

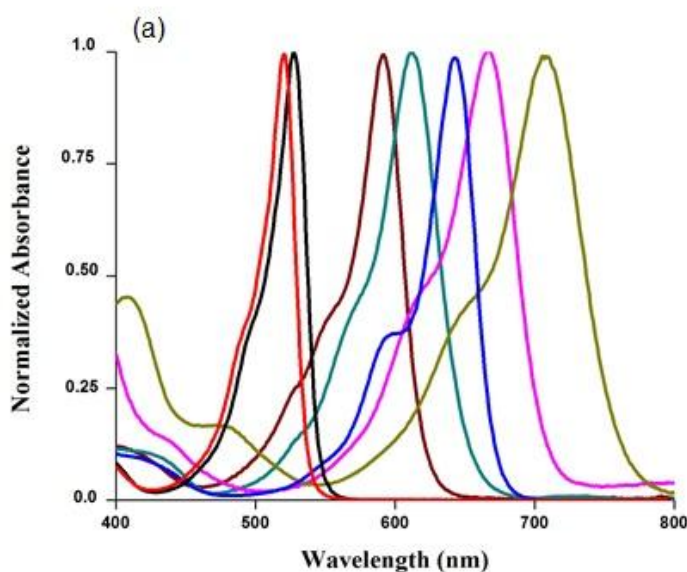


**Figure 3.13:** Normalized UV/Vis (a) and fluorescence spectra (b) of BODIPYs **2** (red), **3** (black), **5f** (brown), **5g** (cyan), **6a** (blue), **6f** (green) and **6g** (pink) in DMSO at 25 °C

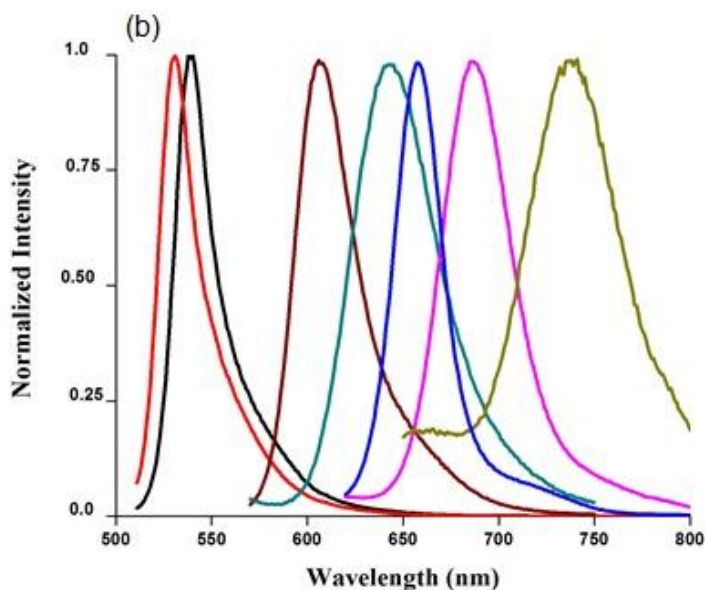


**Figure 3.13:** (continued)

**Table 3.6:** Spectral properties of BODIPYs **2**, **3**, **5f**, **5g**, **6a**, **6f** and **6g** in DMSO at rt

BODIPY	Absorbance $\lambda_{\max}/\text{nm}$	$\log \varepsilon (\text{M}^{-1} \cdot \text{cm}^{-1})$	Emission $\lambda_{\max}/\text{nm}$	$\Phi_f^{[a]}$	Stokes Shift (nm)
<b>2</b>	524	4.5035	530	0.78	7
<b>3</b>	532	4.2934	538	0.81	6
<b>5f</b>	612	4.4602	643	0.40	31
<b>5g</b>	591	4.0346	606	0.90	16
<b>6a</b>	646	4.3836	657	0.36	11
<b>6f</b>	708	4.3658	738	0.10	30
<b>6g</b>	667	4.6269	686	0.38	19

[a] Fluorescence quantum yields for BODIPYs **2**, **3** ( $\lambda_{\text{exc}} = 510$  nm), BODIPYs **5f-g** ( $\lambda_{\text{exc}} = 570$  nm), BODIPYs **6a** and **6g** ( $\lambda_{\text{exc}} = 620$  nm) and BODIPY **6f** ( $\lambda_{\text{exc}} = 650$  nm) were calculated using Rhodamine 6G (0.80 in methanol), cresyl violet perchlorate (0.54 in ethanol), methylene blue

(0.03 in methanol) and ZnPc (0.28 in DMF) as the reference,<sup>[28]</sup> respectively using PTI Quantum Master4/2006SE spectrofluorimeter

### 3.2.3: *In Vitro* Cellular Studies

In order to investigate the potential biological usefulness of the developed styryl- (**5e-g**, **6f**, **6g**, **7g**) and lysyl-BODIPY conjugates (**9-12**), the *in vitro* photodynamic activities, including cytotoxicity, cellular uptake and intracellular localization were assessed against human carcinoma HEP2 cell lines. Cremophor surfactant was added to increase the solubility of the dyes in the aqueous media. These studies were performed by Dr. Xiaoke Hu and N. V. S. Dinesh Bhupathiraju.

*3.2.3.1: Time-Dependent Cellular Uptake.* The results obtained for the time-dependent cellular uptake of styryl- and lysyl-BODIPY conjugates at a concentration of 10  $\mu$ M in HEP2 cells, over a period of 24 h are shown in Figure **3.14** and **3.15**, respectively. At this concentration, all the compounds were non-toxic to the cells, as evaluated using the Cell Titer Blue assay. First of all, it is interesting to note that the introduction of different aromatics at 3- and/or- 5-positions deeply influence the uptake of these BODIPY dyes by cells. The cellular uptake followed the order **5e** > **6f** > **5f** > **5g** > **6g** at all the time points studied. BODIPY **5e** bearing a mono pyrrolylstyryl side arm accumulated the most within the cells, followed by diindolyl styryl-BODIPY **6f**. BODIPYs **5f**, **5g** and **6g** showed similar uptake kinetics with a rapid accumulation at short time points (< 4 h), followed by a slower uptake at longer time points. The observed results are in good agreement with previous studies indicating that the neutral pyrrole and indole rings play an important role in facilitating the cellular uptake. Pyrroles and indoles are weak bases with pKa value of ~ 23.0 and 21.0 respectively. In other words, they are only partially ionized at cytosolic pH and can easily equilibrate between their ionized and unionized forms. This allows BODIPYs **5e** and **6f** to cross the cell membrane in their non-ionized forms via the

passive diffusion, while the presence of the ionized form renders them water-soluble, once inside the cell. BODIPYs **5g** and **6g** which contain strongly acidic phenol groups are fully ionized at intracellular pH and hence have difficulty crossing the lipophilic cell membrane, which affects their cellular uptake. Additionally, the movement of less polar pyrrole and indole through the hydrophobic core of the bilayer is more energetically favored in comparison to fully ionized phenolate group.<sup>36, 37</sup>

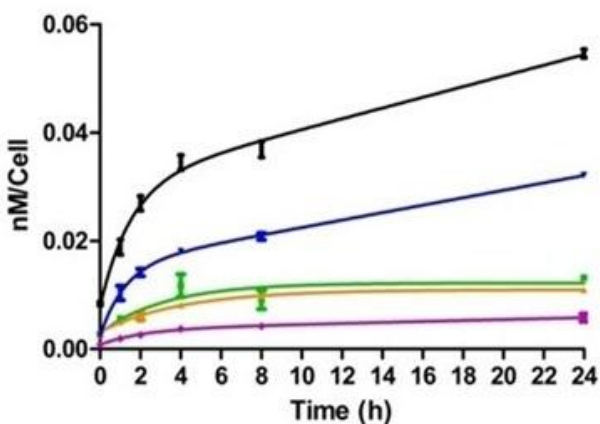


**Figure 3.14:** Time-dependent uptake of BODIPYs **5e** (black), **5f** (green), **5g** (orange), **6f** (blue) and **6g** (purple) at 10 μM by HEp2 cells

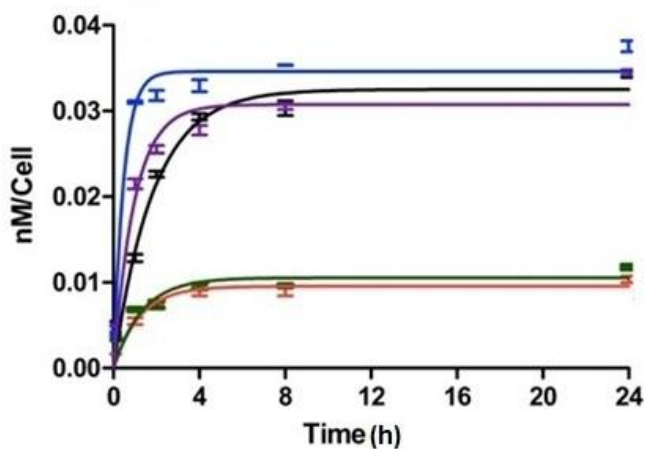


**Figure 3.15:** Time-dependent uptake of BODIPY conjugates **9** (orange), **10** (green), **11** (blue), **12** (black) and **7g** (purple) at 10 μM by HEp2 cells

Similarly, all lysyl-BODIPY conjugates **9-12**, were readily taken up by the cells, reaching a plateau after < 2 h exposure time to the cells (Figure **3.15**). The cellular uptake of the lysyl-BODIPY conjugates is dependent on the structure of the conjugate and their hydrophobic character. Lysyl-BODIPY conjugates **11** and **12** accumulated within the cells to a much higher extent (two-fold increase) than lysyl-BODIPY conjugates **9** and **10**, presumably due to the presence of two additional benzene rings which impart enhanced hydrophobicity and improved membrane permeability.<sup>25a, 26, 38</sup>

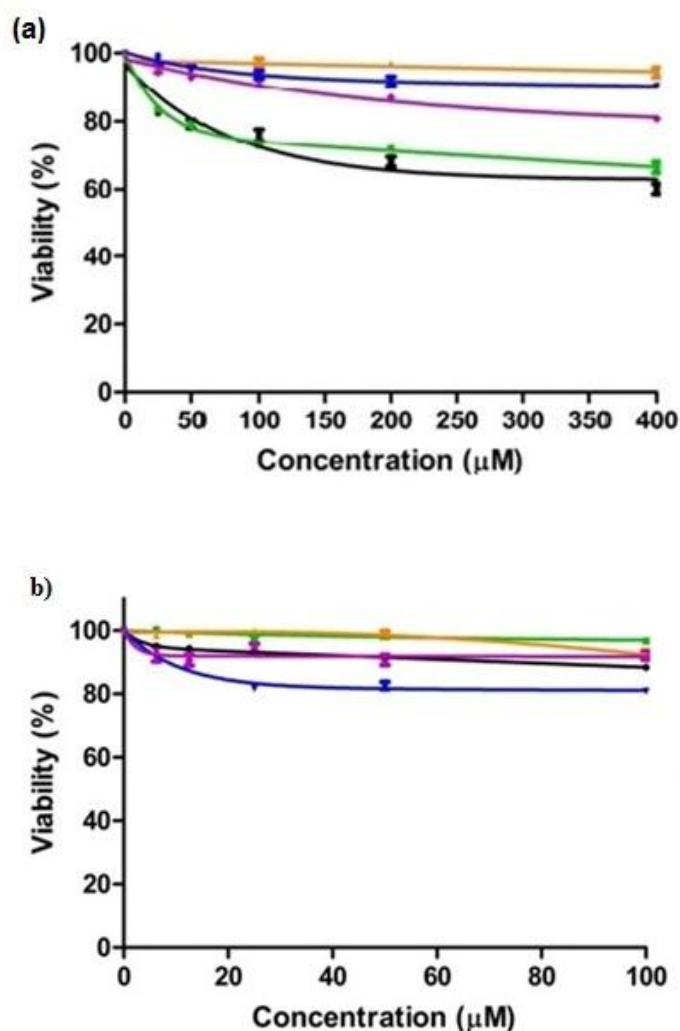


**Figure 3.16:** Dark toxicity and b) Phototoxicity of BODIPYs **5e** (black), **5f** (green), **5g** (orange), **6f** (blue) and **6g** (purple) toward HEp2 cells using 1 J/cm<sup>2</sup> light dose and CellTiter Blue assay.

3.2.3.2: *Cytotoxicity*. The dark toxicity and photo cytotoxicity of styryl- and lysyl-BODIPY conjugates was evaluated in HEP2 cells exposed to increasing concentration of each compound up to 400  $\mu\text{M}$ , using Promega's Cell Titer Blue viability assay. The results are shown in Figure 3.16 and 3.17, respectively. It can be seen that all the BODIPY-conjugates are essentially non-cytotoxic in the absence [ $\text{IC}_{50}$  (dark) > 300  $\mu\text{M}$ ] or presence of light [ $\text{IC}_{50}$  (1 J/cm<sup>2</sup>) > 100  $\mu\text{M}$ ] and the observed results are in consensus with the previously reported investigations.<sup>37a, b</sup>

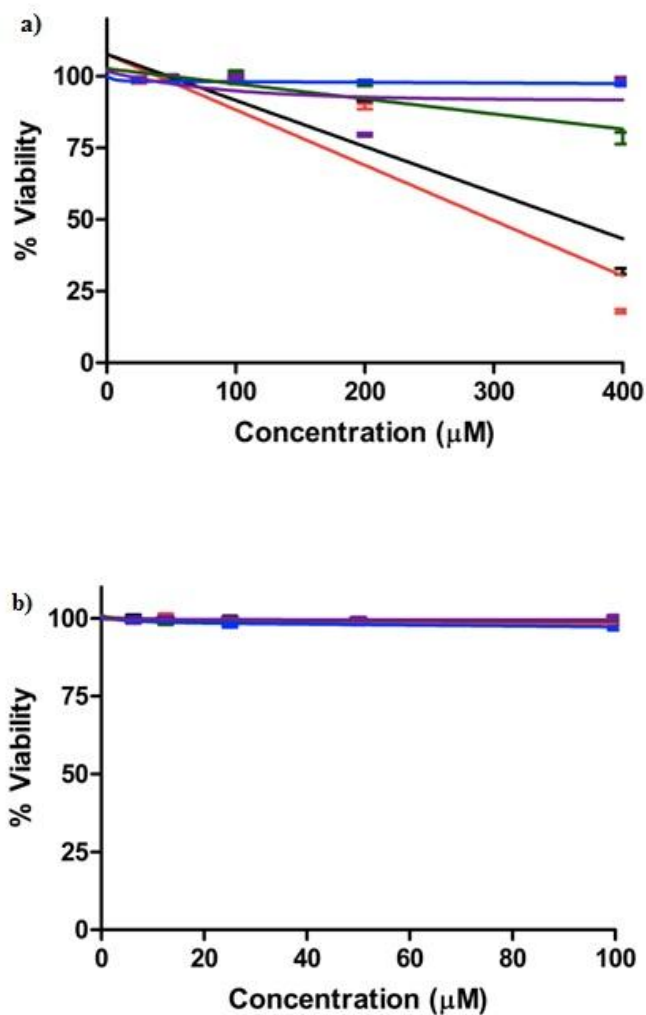


**Figure 3.17:** a) Dark toxicity and b) Phototoxicity of BODIPY-conjugates **9** (red), **10** (black), **11** (blue) (orange), **12** (green) and **7g** (purple) toward HEP2 cells using 1 J/cm<sup>2</sup> light dose and CellTiter Blue assay.

**Table 3.7:** Major (++) and Minor (+) Subcellular Localization sites for BODIPYs in HEp2 cells.

<b>BODIPY</b>	<b>ER</b>	<b>Mitochondria</b>	<b>Golgi</b>	<b>Lysosomes</b>
<b>2</b>	++	-	++	-
<b>3</b>	++	-	++	-
<b>5e</b>	++	-	++	+
<b>5f</b>	++	-	++	+
<b>5g</b>	+	++	+	++
<b>6a</b>	++	+	++	-
<b>6f</b>	++	-	++	+
<b>6g</b>	++	+	++	-

*3.2.3.3: Subcellular Localization.* The preferential sites of the subcellular localization of unsubstituted BODIPYs **2** and **3** along with styryl-BODIPY conjugates **5e-g**, **6a** and **6f-g** were investigated by fluorescence microscopy upon exposure of HEp2 cells to 10  $\mu$ M compound concentrations for 6 h, using the method described in Chapter 2 (Section 2.2.5.3). Colocalization experiments were performed for all compounds using ER-Tracker Blue/White, MitoTracker Green, BODIPY Ceramide and LysoSensor Green, which are specific fluorescent probes for endoplasmic reticulum, mitochondria, golgi apparatus and lysosomes respectively.<sup>26, 39</sup> Figure **3.18** to **3.25** display the fluorescence patterns observed for all compounds and Table **3.7** summarizes their main sites of subcellular distribution. All BODIPY derivatives showed substantial intracellular fluorescence and were found to preferentially accumulate in the endoplasmic reticulum and Golgi apparatus, and to a smaller extent in lysosomes, indicating similar mechanism of cellular uptake for all the BODIPYs studied. This is not surprising, as the commercially available green fluorescent BODIPY FL and red-orange fluorescent BODIPY-BSA conjugates are known cell-permeant ER- and Golgi-Tracker dyes.<sup>40</sup>

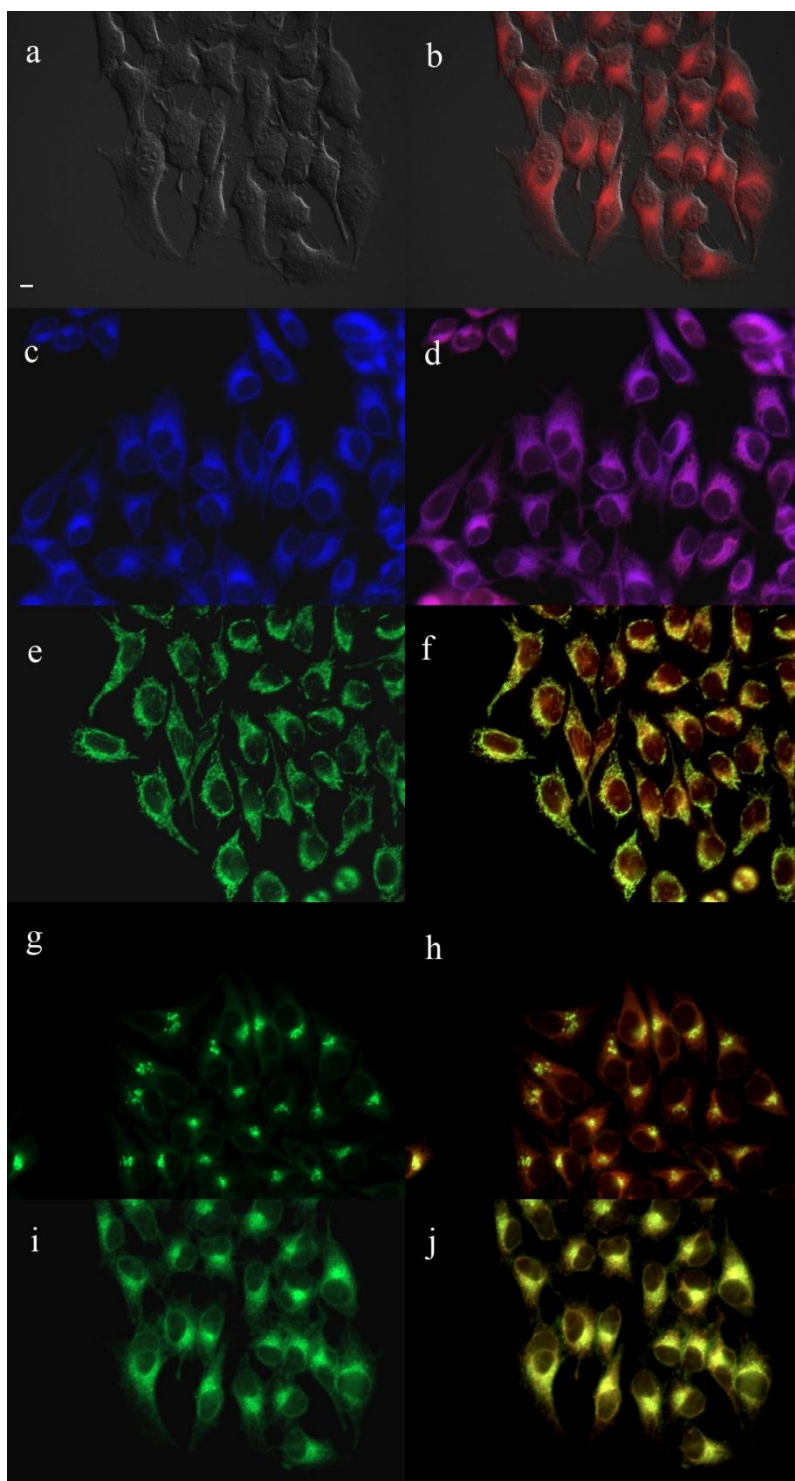


**Figure 3.18:** Subcellular localization of BODIPY **2** in HEp2 cells at 10  $\mu$ M for 6 h. (a) Phase contrast, (b) overlay of **2** fluorescence and phase contrast, (c) ER tracker Blue/White fluorescence, (e) MitoTracker Green fluorescence, (g) BODIPY Ceramide, (i) LysoSensor Green fluorescence, and (d, f, h, j) overlays of organelle tracers with **2** fluorescence. Scale bar: 10  $\mu$ m



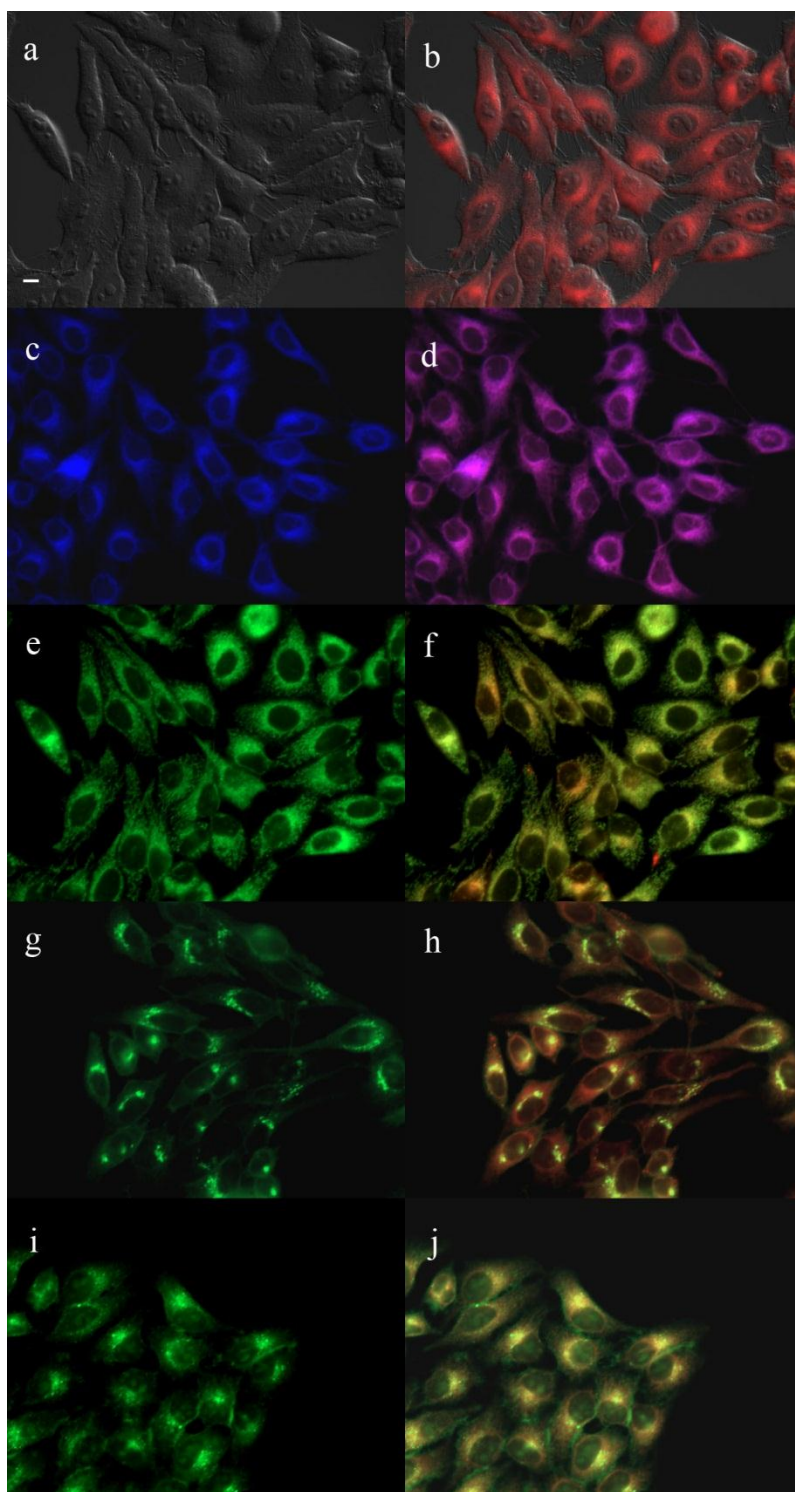


**Figure 3.19:** Subcellular localization of BODIPY **3** in HEp2 cells at 10  $\mu$ M for 6 h. (a) Phase contrast, (b) overlay of **3** fluorescence and phase contrast, (c) ER tracker Blue/White fluorescence, (e) MitoTracker Green fluorescence, (g) BODIPY Ceramide, (i) LysoSensor Green fluorescence, and (d, f, h, j) overlays of organelle tracers with **3** fluorescence. Scale bar: 10  $\mu$ m

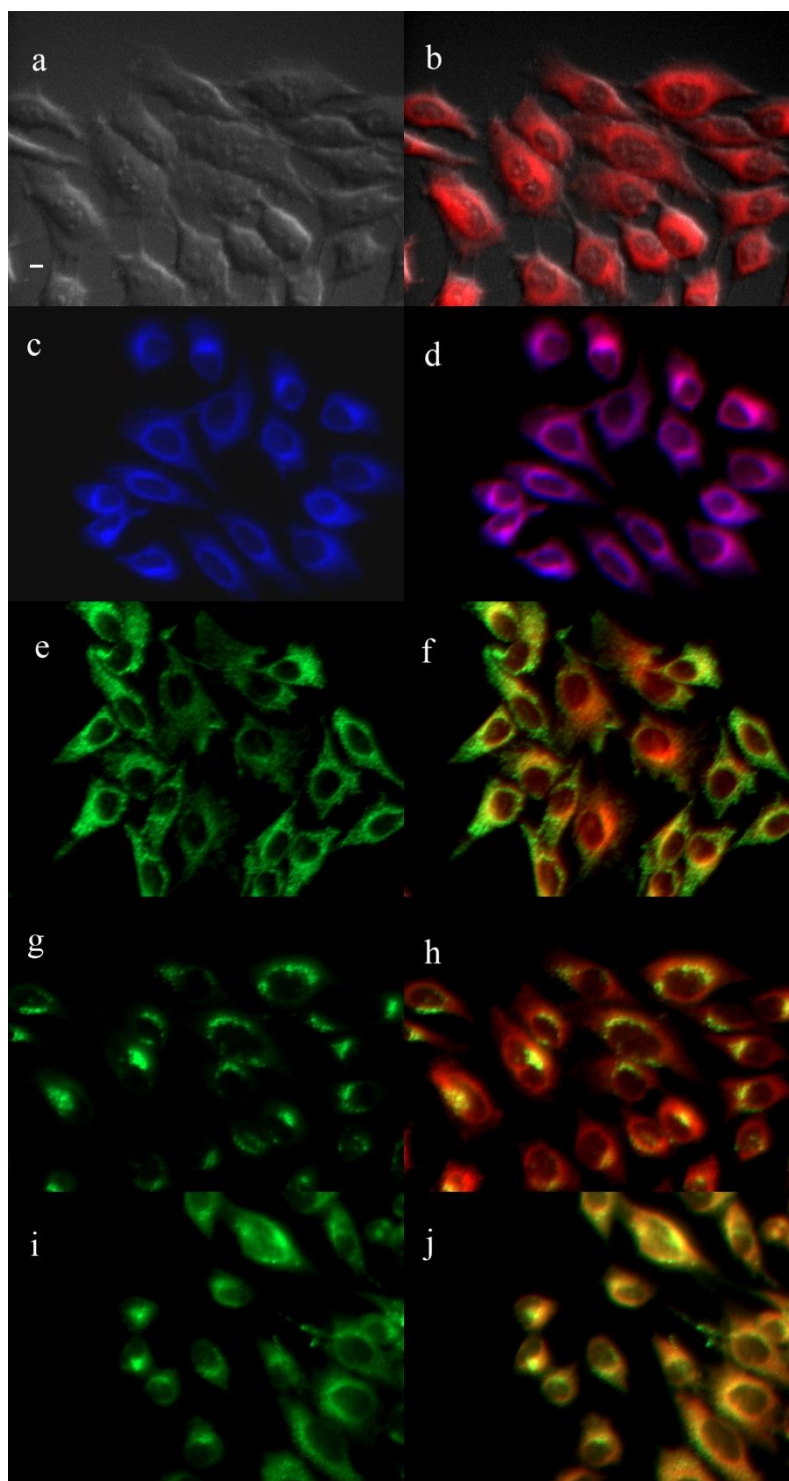


**Figure 3.20:** Subcellular localization of BODIPY **5e** in HEp2 cells at 10  $\mu$ M for 6 h. (a) Phase contrast, (b) overlay of **5e** fluorescence and phase contrast, (c) ER tracker Blue/White fluorescence, (e) MitoTracker Green fluorescence, (g) BODIPY Ceramide, (i) LysoSensor Green fluorescence, and (d, f, h, j) overlays of organelle tracers with **5e** fluorescence. Scale bar: 10  $\mu$ m

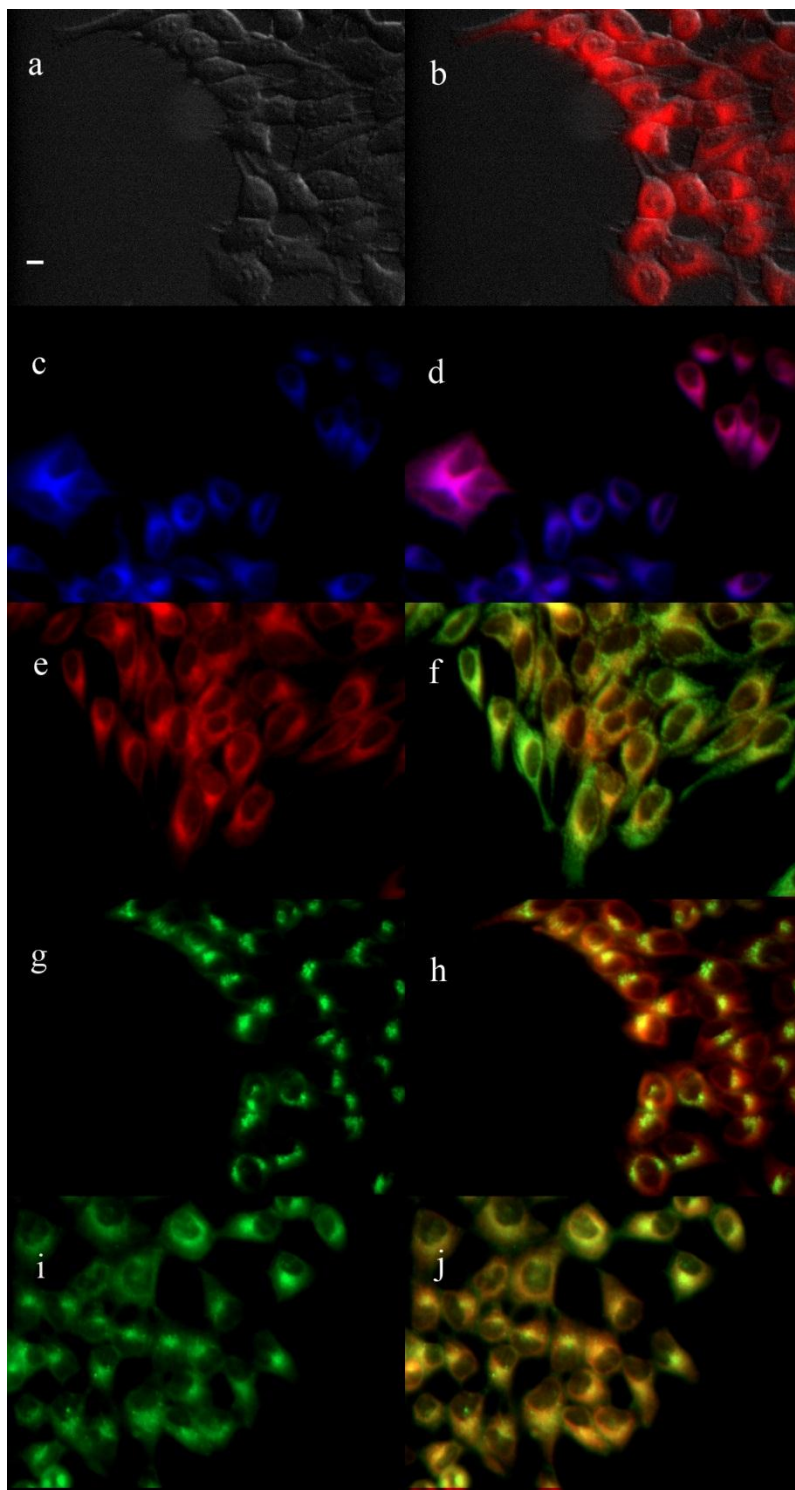


**Figure 3.21:** Subcellular localization of BODIPY **5f** in HEp2 cells at 10  $\mu$ M for 6 h. (a) Phase contrast, (b) overlay of **5f** fluorescence and phase contrast, (c) ER tracker Blue/White fluorescence, (e) MitoTracker Green fluorescence, (g) BODIPY Ceramide, (i) LysoSensor Green fluorescence, and (d, f, h, j) overlays of organelle tracers with **5f** fluorescence. Scale bar: 10  $\mu$ m

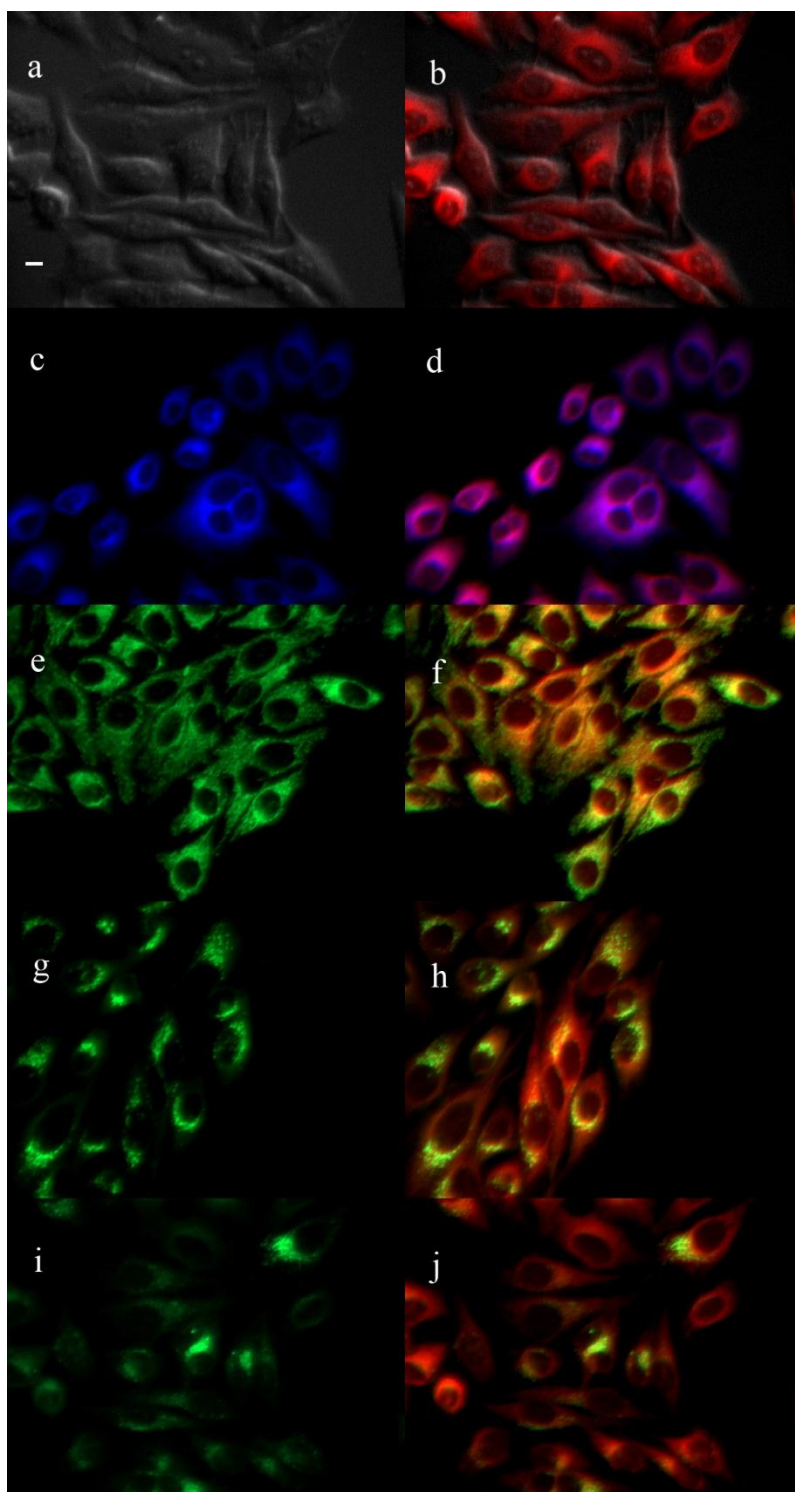


**Figure 3.22:** Subcellular localization of BODIPY **5g** in HEp2 cells at 10  $\mu$ M for 6 h. (a) Phase contrast, (b) overlay of **5g** fluorescence and phase contrast, (c) ER tracker Blue/White fluorescence, (e) MitoTracker Green fluorescence, (g) BODIPY Ceramide, (i) LysoSensor Green fluorescence, and (d, f, h, j) overlays of organelle tracers with **5g** fluorescence. Scale bar: 10  $\mu$ m

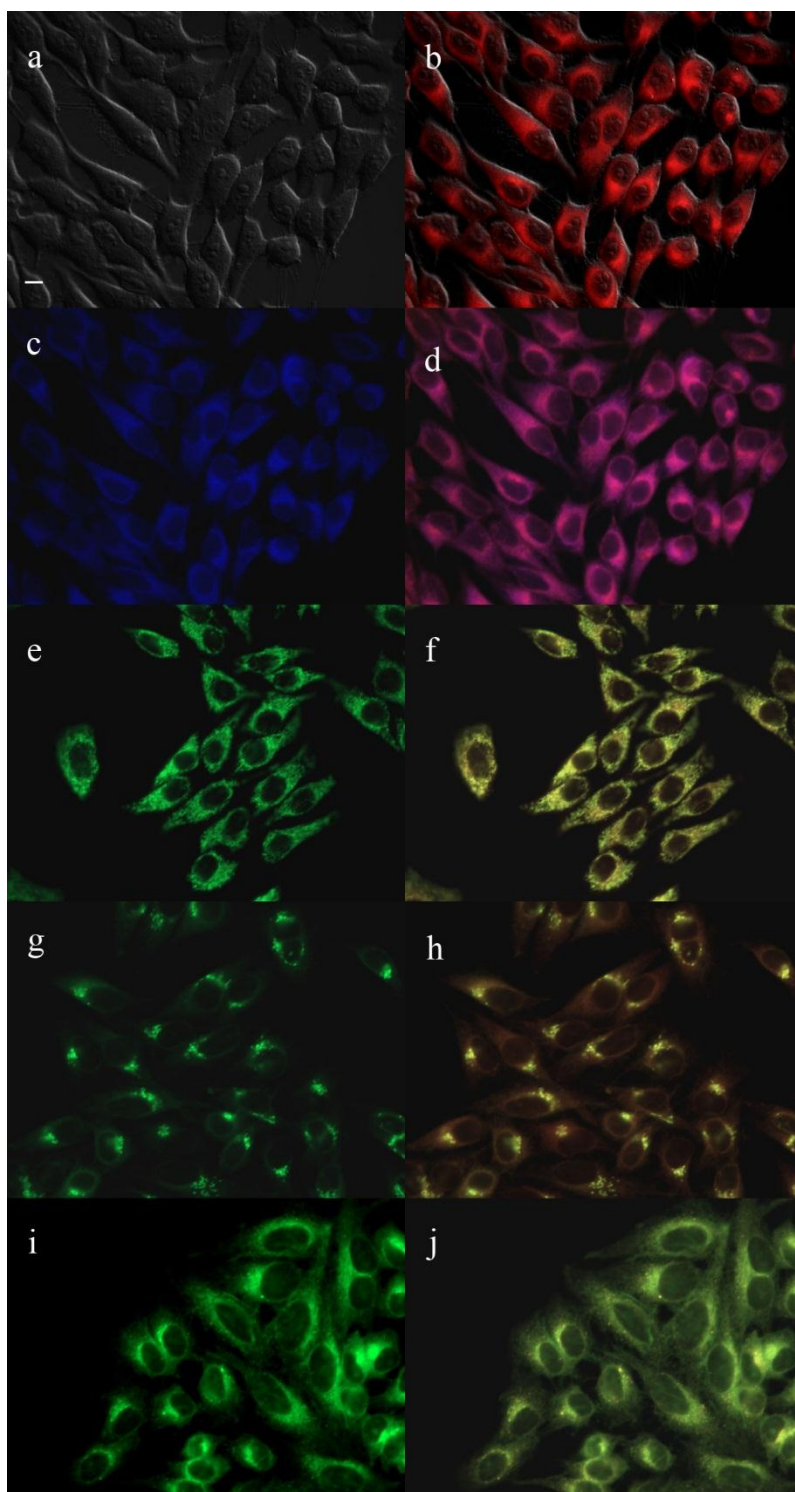


**Figure 3.23:** Subcellular localization of BODIPY **6a** in HEp2 cells at 10  $\mu$ M for 6 h. (a) Phase contrast, (b) overlay of **6a** fluorescence and phase contrast, (c) ER tracker Blue/White fluorescence, (e) MitoTracker Green fluorescence, (g) BODIPY Ceramide, (i) LysoSensor Green fluorescence, and (d, f, h, j) overlays of organelle tracers with **6a** fluorescence. Scale bar: 10  $\mu$ m

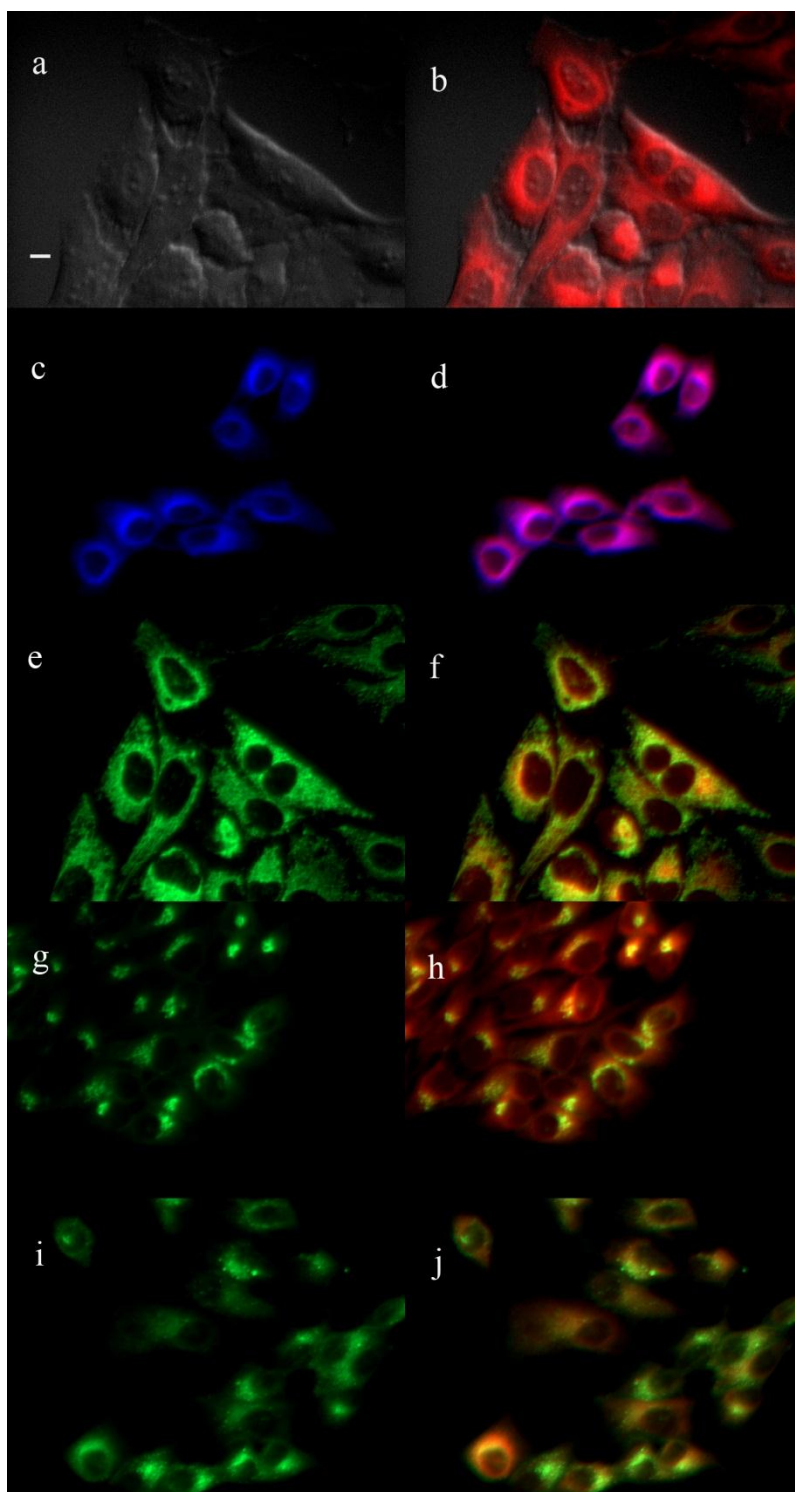


**Figure 3.24:** Subcellular localization of BODIPY **6f** in HEp2 cells at 10  $\mu$ M for 6 h. (a) Phase contrast, (b) overlay of **6f** fluorescence and phase contrast, (c) ER tracker Blue/White fluorescence, (e) MitoTracker Green fluorescence, (g) BODIPY Ceramide, (i) LysoSensor Green fluorescence, and (d, f, h, j) overlays of organelle tracers with **6f** fluorescence. Scale bar: 10  $\mu$ m

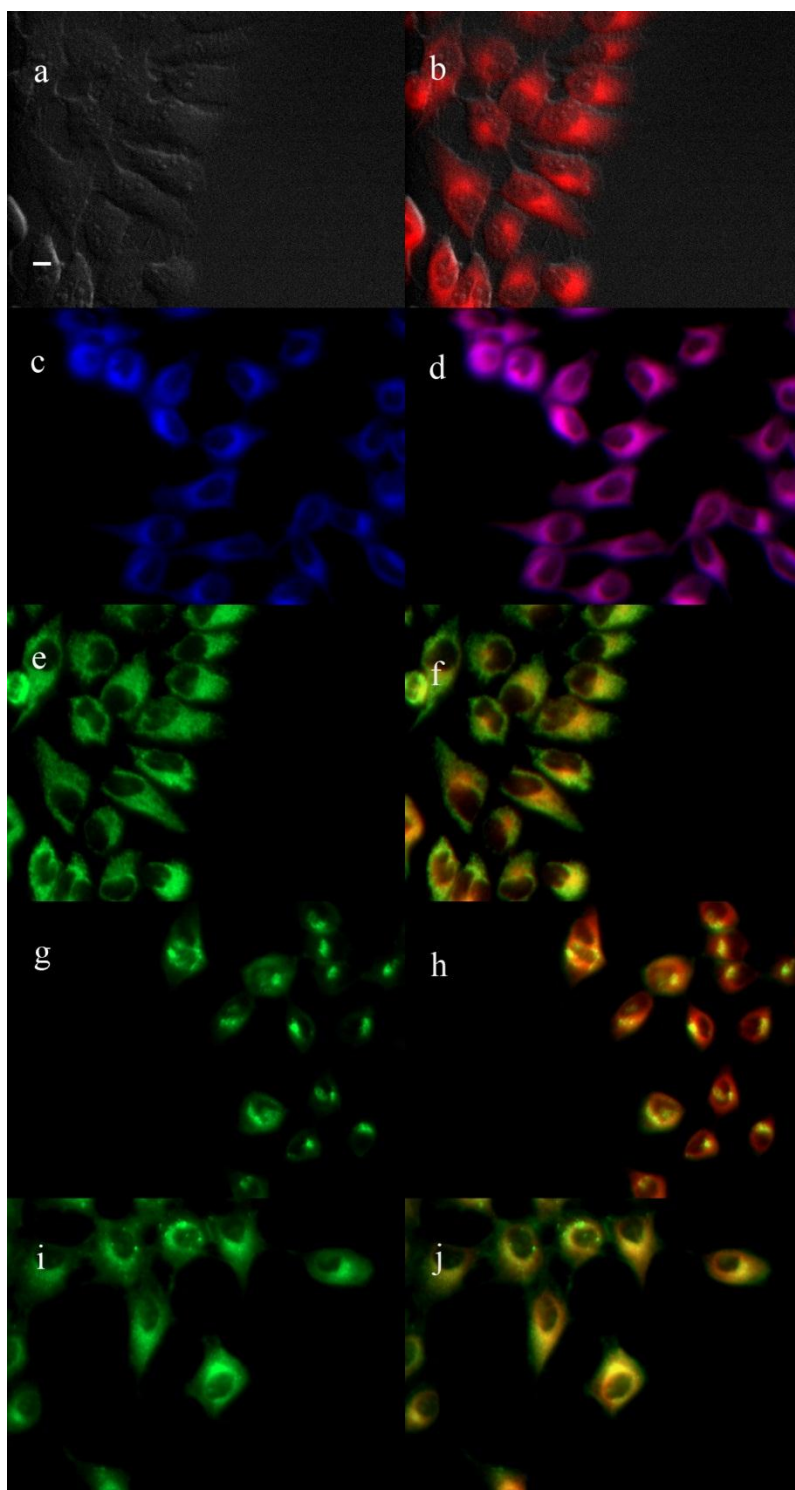


**Figure 3.25:** Subcellular localization of BODIPY **6g** in HEp2 cells at 10  $\mu$ M for 6 h. (a) Phase contrast, (b) overlay of **6g** fluorescence and phase contrast, (c) ER tracker Blue/White fluorescence, (e) MitoTracker Green fluorescence, (g) BODIPY Ceramide, (i) LysoSensor Green fluorescence, and (d, f, h, j) overlays of organelle tracers with **6g** fluorescence. Scale bar: 10  $\mu$ m

### 3.3: Conclusion

A series of new red and NIR emissive BODIPY dyes with different styryl substituents were prepared in moderate yields starting from green emissive 1,3,5,7-tetramethyl BODIPYs. All styryl-BODIPY derivatives are highly soluble in polar organic solvents and displayed fluorescence and quantum yields in the range of 591-738 nm and 0.12-0.90, respectively, in DMSO. BODIPY **6f** bearing two indolylstyryl arms displayed the most red-shifted absorption and fluorescence emission profiles in DMSO at 708 nm and 738 nm, respectively, reaching into the NIR region. *In vitro* biological studies using human carcinoma HEP2 cells revealed that the styryl-BODIPY conjugates (**2**, **3**, **5e-g**, **6a**, **6f**, **6g** and **7g**) and lysyl-BODIPY conjugates (**9-12**) are potential non-cytotoxic, photostable and cell-permeant optical probes with preferential localization in endoplasmic reticulum and Golgi apparatus and high cellular uptake, which depends significantly on the number and nature of the styryl group attached to the BODIPY core. This work presents a series of novel BODIPY derivatives that could be extensively used as non-toxic and non-photobleachable biolabels or fluorescent tracers for drug delivery or sensing applications. Currently, we are investigating; (1) different approaches to improve upon the synthesis and percent yield of tri- and tetrastyryl-BODIPY derivatives to obtain highly substituted NIR-emissive BODIPY dyes, and (2) TFA-mediated deprotection of Boc-protected lysyl-BODIPY conjugates **9-12**, to obtain positively-charged lysyl-BODIPY conjugates with increased affinity towards specific cell organelles.

### 3.4: Experimental

#### 3.4.1: General Information

All reagents were purchased from commercial sources and were used as received. All air and moisture sensitive reactions were performed under argon atmosphere in oven-dried glassware.



Dry solvents were collected from PS-400 Solvent Purification System from Innovative Technology Inc. Melting points were obtained without correction with a MEL-TEMP<sup>®</sup> capillary melting point apparatus. Analytical thin-layer-chromatography (TLC) was performed on polyester backed TLC plates 254 (pre-coated, 200  $\mu\text{m}$ , Sorbent Technologies). Column chromatography separations were performed using silica gel (Sorbent Technologies, 60  $\text{\AA}$ , 40-63  $\mu\text{m}$ , 230-400 mesh) slurry packed into glass columns. NMR spectra were recorded on Bruker DPX-400 (operating at 400MHz for  $^1\text{H}$  NMR and 100 MHz for  $^{13}\text{C}$  NMR) in  $\text{CDCl}_3$  (7.26 ppm,  $^1\text{H}$  and 77.0 ppm,  $^{13}\text{C}$ ) and acetone (2.05 ppm,  $^1\text{H}$  and 206.7 and 29.9 ppm,  $^{13}\text{C}$ ) with tetramethylsilane as internal standard. All spectra were recorded at 298K and coupling constants ( $J$  values) are given in Hz. Chemical shifts are given in parts per millions (ppm). High resolution mass spectra were obtained at the LSU Department of Chemistry Mass Spectrometry Facility using an ESI or MALDI-TOF method, and a peak matching protocol to determine the mass error range of the molecular ion.

### 3.4.2: Syntheses

#### **BODIPY 2**

To a solution of dipyrromethene hydrobromide **1** (540 mg, 1.20 mmol) in dry dichloromethane (80 mL) at 0  $^\circ\text{C}$ , added  $\text{Et}_3\text{N}$  (0.89 mL, 6.4 mmol) dropwise over a period of 10 min. After stirring for 20 min,  $\text{BF}_3\cdot\text{OEt}_2$  (1.30 mL, 10.24 mmol) was added dropwise to the solution over a period of 10 min. The reaction was then stirred at 25  $^\circ\text{C}$  until TLC indicated reaction completion. The solvent was removed under reduced pressure and residue was taken in dichloromethane and extracted with water, saturated  $\text{NaHCO}_3$ , brine and dried over  $\text{Na}_2\text{SO}_4$ . The solvent was removed under reduced pressure and the residue was purified over a pad of silica gel using dichloromethane/petroleum ether 1:1 as eluent. Recrystallization using DCM/Hexane (5:1 v/v)

gave BODIPY **2** (537 mg, 90%) as shiny orange-green crystals; m.p. (142°C); <sup>1</sup>H-NMR (CDCl<sub>3</sub>, 400 MHz): δ = 1.96 (s, 6H), 2.47(s, 6H), 2.52 (t, *J* = 7.6 Hz, 4H), 2.89 (t, *J* = 7.6 Hz, 4H), 3.67 (s,6H), 7.07 (s,1H); <sup>13</sup>C NMR (CDCl<sub>3</sub>, 100 MHz): δ = 7.99, 8.26, 11.98, 19.11, 34.27, 46.24, 51.06, 118.73, 124.53, 131.02, 138.92, 154.66, 172.16; ESI-HRMS: m/z calcd for C<sub>21</sub>H<sub>27</sub>BF<sub>2</sub>N<sub>2</sub>O<sub>4</sub> [M+Na<sup>+</sup>]: 443.188; found: 443.18.

### BODIPY **3**

To a solution of **4e** (123 mg, 0.5878 mmol) in dry dichloromethane (20 mL) at 0 °C, added POCl<sub>3</sub> (0.11 mL, 0.7054 mmol) dropwise over 5 min. The brown reaction mixture was kept for overnight stirring at 25 °C. When TLC indicated reaction completion, Et<sub>3</sub>N (0.89 mL, 2.9 mmol) was added dropwise over a period of 10 min at 0 °C. After stirring for 15 min, BF<sub>3</sub>·OEt<sub>2</sub> (1.30 mL, 4.7 mmol) was introduced dropwise over 10 min. The reaction was then stirred at 25 °C for 16 h. The solvent was removed under reduced pressure and residue was taken in dichloromethane and extracted with saturated NaHCO<sub>3</sub>, brine and dried over Na<sub>2</sub>SO<sub>4</sub>. The solvent was removed under reduced pressure and the residue was purified by column chromatography using dichloromethane/petroleum ether 1:1 as eluent and recrystallized using dichloromethane/Hexane (5:1 v/v) to afford BODIPY **3** (112 mg, 94%) as orange crystals with green lustre; m.p. (138°C); <sup>1</sup>H-NMR (CDCl<sub>3</sub>, 400 MHz): δ = 2.18 (s, 6H), 2.44 (t, *J* = 7.44 Hz, 4H), 2.50 (s, 6H), 2.71 (t, *J* = 7.44 Hz, 4H), 3.67 (s,6H), 6.98 (s,1H); <sup>13</sup>C NMR (CDCl<sub>3</sub>, 100 MHz): δ = 9.30, 12.39, 19.24, 33.87, 51.46, 118.98, 127.74, 132.23, 137.53, 154.81, 172.86; ESI-HRMS: m/z calcd for C<sub>21</sub>H<sub>27</sub>BF<sub>2</sub>N<sub>2</sub>O<sub>4</sub> [M+Na<sup>+</sup>]: 443.188; found: 443.35.

### Distyryl BODIPY **5a** and **6a**

BODIPY **2** (112mg, 0.2665 mmol) and benzaldehyde **4a** (0.055 mL, 0.533 mmol) were refluxed in dry toluene (50 mL) along with piperidine (0.4 mL), glacial acetic acid (0.4 mL) and a small

amount of activated molecular sieves. Once the reaction was complete, the mixture was cooled to room temperature, filtered off to remove the molecular sieves and the solvent was removed under the reduced pressure. The crude was purified by silica column and eluted with dichloromethane/hexane (20/1). The blue fraction was collected and recrystallized from dichloromethane to yield BODIPY **6a** as blue shiny needles (56 mg, 35%); m.p. (172°C); <sup>1</sup>H-NMR (CDCl<sub>3</sub>, 400 MHz): δ = 2.31(s, 6H), 2.58 (t, *J* = 7.6 Hz, 4H), 2.97 (t, *J* = 7.6 Hz, 4H), 3.69 (s,6H), 7.13 (s,1H), 7.77-7.13 (m, 10H); <sup>13</sup>C NMR (CDCl<sub>3</sub>, 100 MHz): δ = 12.22,14.21, 19.62, 22.78, 29.45, 29.78, 32.01, 35.18, 51.92, 117.73, 120.20, 126.78, 127.47, 128.87, 128.95, 131.03, 134.25, 137.18, 137.22, 140.22, 151.76, 172.93; ESI-HRMS: m/z calcd for C<sub>35</sub>H<sub>35</sub>BF<sub>2</sub>N<sub>2</sub>O<sub>4</sub> [M<sup>+</sup>]: 596.2785; found: 595.25.

#### **Mono and Distyryl BODIPY 5e and 6e**

A mixture of BODIPY **3** (100 mg, 0.2379 mmol), 5-formyl pyrrole **4e** (194.2 mg, 0.9516 mmol), piperidine (0.4 mL) and glacial acetic acid (0.4 mL) were refluxed overnight in dry toluene (50 mL) using Dean-Stark apparatus to remove any water formed azeotropically. Crude product was then concentrated under reduced pressure and purified by silica gel column chromatography (eluent: dichloromethane/ethyl acetate 20:1). The blue fraction was collected and the solvent removed under reduced pressure to obtain BODIPY **5e** in the form of blue needles (90.16 mg, 62%); m.p. (176°C); <sup>1</sup>H-NMR (CDCl<sub>3</sub>, 400 MHz): δ = 2.04 (s, 3H), 2.24 (s, 6H), 2.27 (s, 3H), 2.43 (m, 4H), 2.45 (s, 3H), 2.58 (t, *J* = 7.8 Hz, 2H), 2.70 (m, 4H), 3.01 (t, *J* = 7.8 Hz, 2H), 3.67 (s, 6H), 3.69 (s, 3H), 6.86 (s, 1H), 6.94 (d, *J* = 16.6 Hz, 1H), 7.25 (d, *J* = 16.7 Hz, 1H), 8.49 (s, 1H); <sup>13</sup>C NMR (CDCl<sub>3</sub>, 100 MHz): δ = 9.1, 9.5, 11.5, 12.5, 19.6, 19.7, 21.4, 33.3, 34.3, 34.9, 51.5, 51.6, 51.7, 109.6, 115.8, 120.3, 124.3, 124.4, 126.3, 127.2, 128.5, 130.6, 132.5, 134.4, 135.3, 138.4, 152.0, 152.5, 173.1, 173.2, 173.5; MALDI-TOF: m/z calcd for C<sub>32</sub>H<sub>40</sub>BF<sub>2</sub>N<sub>3</sub>O<sub>6</sub> [M<sup>+</sup>]: 611.30; found: 611.372.

The green fraction was collected and the solvent was removed under reduced pressure. Recrystallization with dichloromethane/ethyl acetate (1:1 v/v) afforded the desired BODIPY **6e** as lustrous green needles (59.2 mg, 31%); m.p. (< 250°C); <sup>1</sup>H-NMR (Acetone-d<sub>6</sub>, 400 MHz): δ = 2.04 (s, 6H), 2.14 (s, 6H), 2.43 (t, *J* = 7.8 Hz, 4H), 2.58 (t, *J* = 7.8 Hz, 4H), 2.67 (t, *J* = 7.8 Hz, 4H), 2.79 (s, 6H), 2.97 (t, *J* = 7.8 Hz, 4H), 3.60 (s, 6H), 3.65 (s, 6H), 7.11 (s, 1H); <sup>13</sup>C NMR (Acetone-d<sub>6</sub>, 100 MHz): δ = 9.1, 9.5, 11.5, 12.5, 19.6, 19.7, 21.4, 33.3, 34.3, 34.9, 51.5, 51.6, 51.7, 109.6, 115.8, 120.3, 124.3, 124.4, 126.3, 127.2, 128.5, 130.6, 132.5, 134.4, 135.3, 138.4, 152.0, 152.5, 173.1, 173.2, 173.5; MALDI-TOF: m/z calcd for C<sub>43</sub>H<sub>53</sub>BF<sub>2</sub>N<sub>4</sub>O<sub>8</sub> [M<sup>+</sup>]: 802.39; found: 802.457.

### **Mono and Distyryl BODIPY 5f and 6f**

BODIPY **3** (100 mg, 0.2379 mmol), indole-3-carboxaldehyde **4f** (103.6 mg, 0.7137 mmol), piperidine (0.4 mL) and glacial acetic acid (0.4 mL) were refluxed overnight in dry toluene (50 mL) using Dean-Stark apparatus. The crude was then concentrated under reduced pressure and purified by silica gel column chromatography (eluent: ethyl acetate/hexane 2:1). The deep blue fraction was collected and the solvent removed under reduced pressure to obtain BODIPY **5f** as blue solid (72.9 mg, 55.6%); m.p. (185°C); <sup>1</sup>H-NMR (CDCl<sub>3</sub>, 400 MHz): δ = 2.20 (s, 6H), 2.46 (t, *J* = 7.8 Hz, 2H), 2.57 (m, 5H), 2.74 (t, *J* = 7.8 Hz, 2H), 3.04 (t, *J* = 7.8 Hz, 2H), 3.69 (s, 6H), 3.71 (s, 3H), 7.10-8.03 (m, 9H), 8.64 (s, 1H); <sup>13</sup>C NMR (CDCl<sub>3</sub>, 100 MHz): δ = 11.8, 12.1, 17.3, 20.7, 22.1, 35.2, 36.5, 51.9, 101.0, 110.1, 111.1, 116.1, 118.7, 119.6, 119.8, 120.7, 121.7, 127.7, 128.9, 129.5, 131.4, 133.4, 137.1, 138.4, 146.6, 173.3, 184.4; MALDI-TOF: m/z calcd for C<sub>30</sub>H<sub>32</sub>BF<sub>2</sub>N<sub>3</sub>O<sub>4</sub> [M<sup>+</sup>]: 547.25; found: 547.302

The green fraction was collected and the solvent was removed under reduced pressure afforded the desired BODIPY **6f** as shiny green needles (65.7 mg, 41%); m.p. (195°C); <sup>1</sup>H-NMR (Acetone-d<sub>6</sub>, 400 MHz): δ = 2.30 (s, 6H), 2.69 (t, *J* = 7.8 Hz, 4H), 3.13 (t, *J* = 7.8 Hz, 4H), 3.67

(s, 6H), 7.13 (s,1H), 7.25-7.31 (m, 5H), 7.54 (m, 2H), 7.76 (m, 3H), 7.79 (s, 1H), 7.93 (s, 1H), 7.98 (s, 1H), 8.28 (m, 2H);  $^{13}\text{C}$  NMR (Acetone- $d_6$ , 100 MHz):  $\delta$  = 8.3, 20.9, 33.1, 50.9, 112.1, 115.2, 115.7, 116.0, 121.0, 122.6, 125.3, 128.4, 128.6, 130.4, 134.4, 137.9, 150.9, 172.6; MALDI-TOF: m/z calcd for  $\text{C}_{39}\text{H}_{37}\text{BF}_2\text{N}_4\text{O}_4$  [ $\text{M}^+$ ]: 674.29; found: 674.416.

### **Mono and Distyryl BODIPY 5g and 6g**

BODIPY **3** (100 mg, 0.2379 mmol), *p*-hydroxy benzaldehyde **4g** (87.2 mg, 0.7137 mmol), piperidine (0.4 mL) and glacial acetic acid (0.4 mL) were refluxed overnight in dry toluene (50 mL) using Dean-Stark apparatus. The crude was then concentrated under reduced pressure and purified by silica gel column chromatography (eluent: dichloromethane/ethyl acetate 20:1). The red fraction was collected and the solvent removed under reduced pressure to obtain BODIPY **5g** as red solid (29 mg, 23.4%); m.p. (172°C);  $^1\text{H}$ -NMR (Acetone- $d_6$ , 400 MHz):  $\delta$  = 2.04 (s, 6H), 2.21 (s, 3H), 2.09 (t,  $J$  = 7.6 Hz, 2H), 2.35 (t,  $J$  = 7.6 Hz, 2H), 2.50 (t,  $J$  = 7.6 Hz, 2H), 2.79 (t,  $J$  = 7.6 Hz, 2H), 3.68 (s,6H), 5.35 (s, 1H), 6.95 (d,  $J$  = 16.8 Hz, 1H), 6.99 (d,  $J$  = 16.8 Hz, 1H), 6.65 (d,  $J$  = 8.3 Hz, 2H), 7.26 (d,  $J$  = 8.3 Hz, 2H), 7.49 (s, 1H);  $^{13}\text{C}$  NMR (Acetone- $d_6$ , 100 MHz):  $\delta$  = 11.8, 12.1, 17.3, 20.7, 22.1, 35.2, 36.5, 51.9, 101.1, 115.8, 116.1, 119.6, 120.7, 123.5, 130.1, 130.6, 131.2, 131.4, 138.4, 146.6, 157.7, 164.6; MALDI-TOF: m/z calcd for  $\text{C}_{28}\text{H}_{31}\text{BF}_2\text{N}_2\text{O}_5$  [ $\text{M}^+$ ]: 524.23; found: 524.266

The blue fraction was collected and the solvent was removed under reduced pressure to afford the desired BODIPY **6g** as shiny green needles (99.5 mg, 66.6%); m.p. (183°C);  $^1\text{H}$ -NMR (Acetone- $d_6$ , 400 MHz):  $\delta$  = 2.14 (s, 6H), 2.62 (t,  $J$  = 7.8 Hz, 4H), 3.05 (t,  $J$  = 7.8 Hz, 4H), 3.65 (s, 6H), 6.94 (d,  $J$  = 8.3 Hz, 4H), 7.40 (d,  $J$  = 16.8 Hz, 2H), 7.53 (d,  $J$  = 8.3 Hz, 4H), 7.59 (d,  $J$  = 16.8 Hz, 2H);  $^{13}\text{C}$  NMR (Acetone- $d_6$ , 100 MHz):  $\delta$  = 8.39, 20.8, 33.0, 50.9, 115.9, 116.6, 117.4, 128.8, 129.0, 129.1, 134.7, 134.1, 136.1, 138.5, 150.8, 158.7, 172.5, 184.9; MALDI-TOF: m/z calcd for  $\text{C}_{35}\text{H}_{35}\text{BF}_2\text{N}_2\text{O}_6$  [ $\text{M}^+$ ]: 628.26; found: 628.295

### Monostyryl-BODIPY **5h**

BODIPY **3** (100 mg, 0.2379 mmol), 4-(prop-2-ynyloxy) benzaldehyde **5h** (115 mg, 0.7137 mmol), piperidine (0.4 mL) and glacial acetic acid (0.4 mL) were heated under reflux overnight in dry toluene (50 mL) using Dean-Stark apparatus. The crude was then concentrated under reduced pressure and purified by silica gel column chromatography (eluent: dichloromethane/ethyl acetate 20:1). The first red fraction was collected and the solvent removed under reduced pressure to obtain BODIPY **5h** as red solid (4.68 mg, 3.5%); <sup>1</sup>H-NMR (CDCl<sub>3</sub>, 400 MHz): δ = 2.17 (s, 6H), 2.22 (t, *J* = 7.6 Hz, 2H), 2.48 (s, 3H), 2.55 (t, *J* = 7.6 Hz, 2H), 2.71 (t, *J* = 7.6 Hz, 2H), 3.02 (t, *J* = 7.6 Hz, 2H), 3.68 (s, 3H), 3.71 (s, 3H), 4.73 (s, 2H), 6.98 (m, 3H), 7.54 (m, 3H), 7.26 (s, 1H); MALDI-TOF: *m/z* calcd for C<sub>31</sub>H<sub>33</sub>BF<sub>2</sub>N<sub>2</sub>O<sub>5</sub> [M<sup>+</sup>]: 562.28; found: 562.289.

### Tri- and Tetrastiry-BODIPY **7g** and **8g**

BODIPY **3** (100 mg, 0.2379 mmol) and *p*-hydroxy benzaldehyde **4g** (203.4 mg, 1.6653 mmol) were added to a round bottom flask containing dry toluene (50 mL) and to this solution was added piperidine (0.4 mL) and glacial acetic acid (0.4 mL). The mixture was refluxed overnight using Dean-Stark apparatus. The crude was then concentrated under reduced pressure and purified by preparative thin layer chromatography (eluent: ethyl acetate). The first blue-green fraction was collected, dissolved in acetone and filtered. The solvent was then removed under reduced pressure to obtain BODIPY **7g** as blue solid (13 mg, 8%); MALDI-TOF: *m/z* calcd for C<sub>42</sub>H<sub>39</sub>BF<sub>2</sub>N<sub>2</sub>O<sub>7</sub> [M<sup>+</sup>]: 732.28; found: 732.289.

The second blue-green fraction was collected, dissolved in acetone and filtered. The solvent was then removed under reduced pressure to obtain BODIPY **8g** as blue solid (12.3 mg, 6.2%); MALDI-TOF: *m/z* calcd for C<sub>49</sub>H<sub>43</sub>BF<sub>2</sub>N<sub>2</sub>O<sub>8</sub> [M<sup>+</sup>]: 836.31; found: 836.31.

### General procedure for synthesis of Lysyl-BODIPY conjugates 9-12

PMe-BODIPY (38 mg, 0.0904 mmole) was dissolved in a mixture of THF (4.9 mL), H<sub>2</sub>O (3.3 mL) and 4.5 M HCl (2.0 mL). After stirring at room temperature for 1 hour, dichloromethane was added (10 mL) and the two phases were separated. The aqueous phase was extracted with dichloromethane (2 x 10 mL) and the combined organic phase was washed with brine and concentrated in vacuo. The crude was dried in the oven overnight and then dissolved in dry dichloromethane (10 mL) containing N, N-Diisopropylethylamine (0.5434 mmole, 6 equiv.). After stirring the reaction mixture for 1 hour, HOBt (0.113 mmole, 1.25 equiv.), DCC (0.113 mmole, 1.25 equiv.) and DMAP (0.0678 mmole, 0.75 equiv.) were added and reaction was allowed to stir for an additional 1 hour. Finally, H-lysyl(Boc)OMe.HCl (0.1650 mmole) was added and the reaction was left for overnight stirring. It was then diluted with dichloromethane and washed with 5% aqueous citric acid, followed by a wash with brine and water. It was dried over anhydrous Na<sub>2</sub>SO<sub>4</sub> and then evaporated to dryness. The residue was dissolved in 12% acetone/dichloromethane and purified via preparative thin layer chromatography with the same mobile phase to afford mono- and dilysyl-BODIPY derivatives **9-12**.

**BODIPY 9:** Yield (15.4 mg, 26.2%); <sup>1</sup>H-NMR (acetone-d<sub>6</sub>, 400 MHz): δ 1.0-2.0 (m, 8H), 1.36 (s, 9H), 2.39 (s, 6H), 2.41 (m, 2H), 2.48 (s, 6H), 2.70 (m, 4H), 2.95 (m, 2H), 3.60 (s, 3H), 3.63 (s, 3H), 7.34 (s, 1H), 7.44 (s, 2H); MALDI-TOF: m/z calcd for C<sub>32</sub>H<sub>47</sub>BF<sub>2</sub>N<sub>4</sub>O<sub>7</sub> [M+Na<sup>+</sup>]: 634.35; found: 657.43 and 899.51.

**BODIPY 10:** Yield (20.8 mg, 26.5%); <sup>1</sup>H-NMR (acetone-d<sub>6</sub>, 400 MHz): δ 1.27 (m, 4H), 1.38 (s, 18H), 1.60 (m, 2H), 1.73 (m, 2H), 2.39 (s, 6H), 2.41 (m, 4H), 2.45 (s, 6H), 2.70 (m, 4H), 3.60 (s, 6H), 7.41 (s, 2H); MALDI-TOF: m/z calcd for C<sub>43</sub>H<sub>67</sub>BF<sub>2</sub>N<sub>6</sub>O<sub>10</sub> [M+Na<sup>+</sup>]: 876.50; found: 899.51.

**BODIPY 11:** Yield (3.5 mg, 11.4%);  $^1\text{H-NMR}$  (acetone- $d_6$ , 400 MHz):  $\delta$  1.19 (m, 3H), 1.34 (s, 8H), 2.40 (s, 6H), 2.48 (s, 6H), 2.60 (m, 4H), 2.65 (m, 2H), 2.70 (m, 4H), 2.95 (m, 2H), 3.66 (s, 3H), 6.94 (m, 4H), 7.42-7.58 (m, 5H), 8.45 (s, 1H); MALDI-TOF:  $m/z$  calcd for  $\text{C}_{32}\text{H}_{47}\text{BF}_2\text{N}_4\text{O}_7$  [ $\text{M}^+$ ]: 856.40; found: 856.44.

**BODIPY 12:** Yield (13.6 mg, 34.8 %);  $^1\text{H-NMR}$  (acetone- $d_6$ , 400 MHz):  $\delta$  1.37 (m, 3H), 1.36 (s, 21H), 1.47 (m, 4H), 1.68 (m, 4H), 2.39 (s, 6H), 2.41 (m, 4H), 2.48 (s, 6H), 2.60 (s, 6H), 2.95 (m, 8H), 3.65 (s, 6H), 6.92-7.58 (m, 10H), 7.96 (s, 2H); MALDI-TOF:  $m/z$  calcd for  $\text{C}_{32}\text{H}_{47}\text{BF}_2\text{N}_4\text{O}_7$  [ $\text{M}^+$ ]: 1084.55; found: 1084.60.

### **Crystal Data**

A single crystal of compound was selected under a microscope and mounted on a glass fiber. The unit-cell parameters and diffraction data were collected at low temperature on either a Nonius KappaCCD diffractometer equipped with  $\text{MoK}\alpha$  radiation ( $\lambda=0.71073 \text{ \AA}$ ) or a Bruker Kappa Apex-II diffractometer equipped with  $\text{CuK}\alpha$  radiation ( $\lambda=1.54178 \text{ \AA}$ ). The structures were determined by direct methods and refined by full-matrix least squares method with the SHELXL program, with H atoms in idealized positions, except for NH hydrogen atoms, which were located by difference maps and in most cases their positions refined. Disorder is present in several of the structures.

### **3.4.3: Steady-state Absorption and Fluorescence Spectroscopy**

UV/Vis absorption spectra of BODIPYs were recorded on a Varian Cary 50 UV/Vis spectrophotometer and the steady-state fluorescence spectroscopic studies were performed on a PTI Quantum Master4/2006SE spectrofluorimeter. All measurements were carried out at room temperature within 2 h of solution preparation, using non-degassed samples, HPLC grade



solvents and a 10 mm quartz cuvette. For the fluorescence experiments, only dilute solutions with the optical density between 0.04-0.06 at the excitation wavelength were used. Fluorescence quantum yields ( $\Phi_f$ ) were determined using a relative method by comparing the area under the corrected emission spectrum of BODIPYs **2** and **3** relative to rhodamine 6G (0.80 in methanol), BODIPYs **5c** and **5d** relative to cresyl violet perchlorate (0.54 in ethanol) and BODIPYs **5b** and **6a** and **6g** with respect to methylene blue (0.03 in methanol) and **6f** with respect to ZnPc (0.28 in DMF) as external standards respectively. In all the cases, correction for the refractive index was applied.

**3.4.4: Cellular Studies.** All tissues culture media and reagents were obtained from Invitrogen. Human carcinoma HEP2 cells were obtained from ATCC and maintained in a 50:50 mixture of D-MEM:Advanced MEM supplemented with 5% Fetal Bovine Serum (FBS), 1% Primocin antibiotic and 5% CO<sub>2</sub> at 37°C. The cells were sub-cultured twice per week to maintain sub-confluent stocks. The fourth to fifteenth passage cells were used for all the experiments.

*3.4.4.1: Time-Dependent Cellular Uptake.* The HEP2 cells were plated at 7500 cells per well in a Costar 96-well plate and allowed to grow for 48 h at 37°C under 5% CO<sub>2</sub>. The BODIPYs stock solutions were prepared at 32 mM in DMSO and Cremophor (1% of Cremophor EL in DMSO). For the uptake result, the compounds were diluted to 20  $\mu$ M (2 x stock solution) and added to the 96-well plate to give a final working concentration of 10  $\mu$ M at 0, 1, 2, 4, 8, 12 and 24 h interval. At the end of the incubation period, the loading medium was removed and the cells were rinsed with 200  $\mu$ L of Phosphate buffer saline (PBS). The cells were then solubilized using 100  $\mu$ L of 0.25% Triton X-100 (Calbiochem) in PBS. The fluorophore concentration was measured using a BMG FLUOstar plate reader. The cell numbers were quantified by the CyQuant cell proliferation assay (Invitrogen) as per manufactures instructions, as previously reported.<sup>ref</sup> The uptake is expressed in terms of nM compound per cell.

*3.4.4.2: Dark Cytotoxicity.* The HEp2 cells were plated as described above for the uptake experiment. The cells were treated with BODIPY conjugate concentrations of 25, 50, 100, 200 and 400  $\mu\text{M}$  and incubated overnight. After compound loading overnight, the loading medium was replaced by medium containing CellTiter Blue (Promega) as per manufacturer's instructions. Cell toxicity was then measured with untreated cells considered as 100% viable and cells treated with 0.2% saponin as 0% viable. The  $\text{IC}_{50}$  values were determined from dose-dependent survival curves obtained using GraphPad Prism software.

*3.4.4.3: Phototoxicity.* The cells were prepared as described above for the dark cytotoxicity assay with BODIPY conjugate concentrations of 0, 6.25, 12.5, 25, 50 and 100  $\mu\text{M}$ . After loading overnight, the medium was removed and replaced with medium containing 50 mM HEPES pH 7.4. The cells were exposed to a NewPort light system with 175 W halogen lamp for 20 min, filtered through a water filter to provide approximately  $1.5 \text{ Jcm}^{-2}$  light dose. The cells were kept cool by placing the culture on a  $5^{\circ}\text{C}$  EchoTherm chilling/heating plate (Torrey Pines Scientific, Inc.). After exposure to light for 20 min, the plate was incubated overnight in a  $37^{\circ}\text{C}$  incubator. Cells were assayed for viability using CellTiter Blue Viability Assay Kit, as described above for the dark cytotoxicity experiment.

*3.4.4.4: Microscopy.* The cells were incubated in the glass bottom 6-well plate (MatTek) and allowed to grow for 48 h. The cells were then exposed to 10  $\mu\text{M}$  of each compound for 6 h and stained with organelle tracers (Invitrogen) at the following concentrations: ER Tracker Blue/white (100 nM), MitoTracker Green (250 nM), BODIPY FL C5 ceramide (1  $\mu\text{M}$ ) and LysoSensor Green (50 nM), which are specific fluorescent dyes for Endoplasmic Reticulum, Mitochondria, Golgi Apparatus and Lysosomes respectively. After 30 min incubation, both the media and the organelle tracers were removed and the cells were rinsed with PBS (3 times, to remove any unincorporated fluorophore). Images were taken using a Leica DMRXA microscope

with 40× NA 0.8 dip objective lens and DAPI, GFP and Texas Red filter cubes (Chroma Technologies). The subcellular localization was revealed by comparing the intracellular fluorescence images caused by the organelle tracers and the BODIPY dyes.

### 3.5: References

1. Kowada, T.; Yamaguchi, S.; Ohe, K., Highly fluorescent BODIPY dyes modulated with spirofluorene moieties. *Organic letters* **2010**, *12* (2), 296-9.
2. Bozdemir, O. A.; Guliyev, R.; Buyukcakir, O.; Selcuk, S.; Kolemen, S.; Gulseren, G.; Nalbantoglu, T.; Boyaci, H.; Akkaya, E. U., Selective Manipulation of ICT and PET Processes in Styryl-Bodipy Derivatives: Applications in Molecular Logic and Fluorescence Sensing of Metal Ions. *Journal of the American Chemical Society* **2010**, *132* (23), 8029-8036.
3. Haugland, R. P., *The Handbook A Guide to Fluorescent Probes and Labeling Technologies*. Tenth ed.; United States of America, 2005.
4. Jacobsen, J. A.; Stork, J. R.; Magde, D.; Cohen, S. M., Hydrogen-bond rigidified BODIPY dyes. *Dalton Transactions* **2010**, *39* (3), 957-962.
5. Wang, Y. W.; Descalzo, A. B.; Shen, Z.; You, X. Z.; Rurack, K., Dihydronaphthalene-fused boron-dipyrromethene (BODIPY) dyes: insight into the electronic and conformational tuning modes of BODIPY fluorophores. *Chemistry* **2010**, *16* (9), 2887-903.
6. Jiao, L.; Yu, C.; Li, J.; Wang, Z.; Wu, M.; Hao, E.,  $\beta$ -Formyl-BODIPYs from the Vilsmeier–Haack Reaction. *The Journal of Organic Chemistry* **2009**, *74* (19), 7525-7528.
7. Boens, N.; Leen, V.; Dehaen, W., Fluorescent indicators based on BODIPY. *Chemical Society Reviews* **2012**, *41* (3), 1130-1172.
8. Ulrich, G.; Ziessele, R.; Harriman, A., The Chemistry of Fluorescent Bodipy Dyes: Versatility Unsurpassed. *Angewandte Chemie International Edition* **2008**, *47* (7), 1184-1201.
9. Meltola, N. J.; Wahlroos, R.; Soini, A. E., Hydrophilic labeling reagents of dipyrromethene-BF<sub>2</sub> dyes for two-photon excited fluorometry: syntheses and photophysical characterization. *Journal of fluorescence* **2004**, *14* (5), 635-47.
10. Jones, G., The Knoevenagel Condensation. In *Organic Reactions*, John Wiley & Sons, Inc.: 2004.
11. Xie, B.-H.; Guan, Z.; He, Y.-H., Biocatalytic Knoevenagel reaction using alkaline protease from *Bacillus licheniformis*. *Biocatalysis and Biotransformation* **2012**, *30* (2), 238-244.
12. (a) Bura, T.; Retailleau, P.; Ulrich, G.; Ziessele, R., Highly substituted Bodipy dyes with spectroscopic features sensitive to the environment. *J Org Chem* **2011**, *76* (4), 1109-17; (b)

Atilgan, S.; Kutuk, I.; Ozdemir, T., A near IR di-styryl BODIPY-based ratiometric fluorescent chemosensor for Hg(II). *Tetrahedron Lett* **2010**, *51* (6), 892-894; (c) Shiraishi, Y.; Maehara, H.; Sugii, T.; Wang, D.; Hirai, T., A BODIPY–indole conjugate as a colorimetric and fluorometric probe for selective fluoride anion detection. *Tetrahedron Letters* **2009**, *50* (29), 4293-4296; (d) Brellier, M.; Duportail, G.; Baati, R., Convenient synthesis of water-soluble nitrilotriacetic acid (NTA) BODIPY dyes. *Tetrahedron Letters* **2010**, *51* (9), 1269-1272.

13. [www.organic-chemistry.org](http://www.organic-chemistry.org).

14. Fischer, H.; Friedrich, H.; Lamatsch, W.; Morgenroth, K., Synthesen von Koproporphyrin I und II, sowie Mesoporphyrin II, V und XII. *Justus Liebigs Annalen der Chemie* **1928**, *466* (1), 147-178.

15. Dolphin, D., Porphyrinogens and porphodimethenes, intermediates in the synthesis of meso-tetraphenylporphins from pyrroles and benzaldehyde. *Journal of Heterocyclic Chemistry* **1970**, *7* (2), 275-283.

16. Wu, L.; Burgess, K., A new synthesis of symmetric boraindacene (BODIPY) dyes. *Chem Commun* **2008**, *28* (40), 4933-5.

17. Boens, N.; Leen, V.; Dehaen, W., Fluorescent indicators based on BODIPY. *Chem Soc Rev* **2012**, *41* (3), 1130-72.

18. Rurack, K.; Kollmannsberger, M.; Daub, J., Molecular Switching in the Near Infrared (NIR) with a Functionalized Boron–Dipyrromethene Dye. *Angewandte Chemie International Edition* **2001**, *40* (2), 385-387.

19. (a) Barbarella, G.; Melucci, M.; Sotgiu, G., The Versatile Thiophene: An Overview of Recent Research on Thiophene-Based Materials. *Advanced Materials* **2005**, *17* (13), 1581-1593; (b) Sessler, J. L.; Cho, D.-G.; Lynch, V., Diindolylquinoxalines: Effective Indole-Based Receptors for Phosphate Anion. *Journal of the American Chemical Society* **2006**, *128* (51), 16518-16519; (c) Reinke, A. A.; Gestwicki, J. E., Insight into Amyloid Structure Using Chemical Probes. *Chemical Biology & Drug Design* **2011**, *77* (6), 399-411; (d) Basu, A.; Das, G., Neutral Acyclic Anion Receptor with Thiadiazole Spacer: Halide Binding Study and Halide-Directed Self-Assembly in the Solid State. *Inorganic chemistry* **2011**, *51* (2), 882-889; (e) Yu, C.; Xu, Y.; Jiao, L.; Zhou, J.; Wang, Z.; Hao, E., Isoindole-BODIPY Dyes as Red to Near-Infrared Fluorophores. *Chemistry – A European Journal* **2012**, *18* (21), 6437-6442.

20. Gale, P. A., Synthetic indole, carbazole, biindole and indolocarbazole-based receptors: applications in anion complexation and sensing. *Chem Commun (Camb)* **2008**, (38), 4525-40.

21. Murtagh, J.; Frimannsson, D. O.; O'Shea, D. F., Azide conjugatable and pH responsive near-infrared fluorescent imaging probes. *Organic letters* **2009**, *11* (23), 5386-9.

22. Li, Z.; Bittman, R., Synthesis and Spectral Properties of Cholesterol- and FTY720-Containing Boron Dipyrromethene Dyes. *The Journal of Organic Chemistry* **2007**, *72* (22), 8376-8382.

23. (a) Shen, Z.; Röhr, H.; Rurack, K.; Uno, H.; Spieles, M.; Schulz, B.; Reck, G.; Ono, N., Boron–Diindomethene (BDI) Dyes and Their Tetrahydrobicyclo Precursors—en Route to a New Class of Highly Emissive Fluorophores for the Red Spectral Range. *Chemistry – A European Journal* **2004**, *10* (19), 4853-4871; (b) Yu, Y.-H.; Descalzo, A. B.; Shen, Z.; Röhr, H.; Liu, Q.; Wang, Y.-W.; Spieles, M.; Li, Y.-Z.; Rurack, K.; You, X.-Z., Mono- and Di(dimethylamino)styryl-Substituted Borondipyrromethene and Borondiindomethene Dyes with Intense Near-Infrared Fluorescence. *Chemistry – An Asian Journal* **2006**, *1* (1-2), 176-187.
24. Buyukcakir, O.; Bozdemir, O. A.; Kolemen, S.; Erbas, S.; Akkaya, E. U., Tetrastyril-Bodipy Dyes: Convenient Synthesis and Characterization of Elusive Near IR Fluorophores. *Organic letters* **2009**, *11* (20), 4644-4647.
25. (a) Blemings, K. P.; Crenshaw, T. D.; Benevenga, N. J., Mitochondrial Lysine Uptake Limits Hepatic Lysine Oxidation in Rats Fed Diets Containing 5, 20 or 60% Casein. *The Journal of Nutrition* **1998**, *128* (12), 2427-2434; (b) Guo, D.; Chen, T.; Ye, D.; Xu, J.; Jiang, H.; Chen, K.; Wang, H.; Liu, H., Cell-permeable iminocoumarine-based fluorescent dyes for mitochondria. *Organic letters* **2011**, *13* (11), 2884-7.
26. Jinadasa, R. G. W.; Hu, X.; Vicente, M. G. H.; Smith, K. M., Syntheses and Cellular Investigations of 173-, 152-, and 131-Amino Acid Derivatives of Chlorin e6. *Journal of Medicinal Chemistry* **2011**, *54* (21), 7464-7476.
27. Dodani, S. C.; He, Q.; Chang, C. J., A Turn-On Fluorescent Sensor for Detecting Nickel in Living Cells. *Journal of the American Chemical Society* **2009**, *131* (50), 18020-18021.
28. Urano, Y.; Asanuma, D.; Hama, Y.; Koyama, Y.; Barrett, T.; Kamiya, M.; Nagano, T.; Watanabe, T.; Hasegawa, A.; Choyke, P. L.; Kobayashi, H., Selective molecular imaging of viable cancer cells with pH-activatable fluorescence probes. *Nat Med* **2009**, *15* (1), 104-109.
29. Boiadjiev, S. E.; Lightner, D. A., Syntheses and properties of benzodipyrinones. *Journal of Heterocyclic Chemistry* **2003**, *40* (1), 181-185.
30. Gießler, K.; Griesser, H.; Göhringer, D.; Sabirov, T.; Richert, C., Synthesis of 3'-BODIPY-Labeled Active Esters of Nucleotides and a Chemical Primer Extension Assay on Beads. *European Journal of Organic Chemistry* **2010**, *2010* (19), 3611-3620.
31. (a) Zheng, Q.; Xu, G.; Prasad, P. N., Conformationally Restricted Dipyrromethene Boron Difluoride (BODIPY) Dyes: Highly Fluorescent, Multicolored Probes for Cellular Imaging. *Chemistry – A European Journal* **2008**, *14* (19), 5812-5819; (b) Galangau, O.; Dumas-Verdes, C.; Meallet-Renault, R.; Clavier, G., Rational design of visible and NIR distyryl-BODIPY dyes from a novel fluorinated platform. *Organic & Biomolecular Chemistry* **2010**, *8* (20), 4546-4553.
32. Gomez-Duran, C. F. A.; Garcia-Moreno, I.; Costela, A.; Martin, V.; Sastre, R.; Banuelos, J.; Lopez Arbeloa, F.; Lopez Arbeloa, I.; Pena-Cabrera, E., 8-PropargylaminoBODIPY: unprecedented blue-emitting pyrromethene dye. Synthesis, photophysics and laser properties. *Chemical Communications* **2010**, *46* (28), 5103-5105.

33. Singh, A. K.; Asefa, A., A fluorescence study of differently substituted 3-styrylindoles and their interaction with bovine serum albumin. *Luminescence : the journal of biological and chemical luminescence* **2009**, *24* (2), 123-30.
34. (a) Qin, W.; Baruah, M.; De Borggraeve, W. M.; Boens, N., Photophysical properties of an on/off fluorescent pH indicator excitable with visible light based on a borondipyrromethene-linked phenol. *Journal of Photochemistry and Photobiology A: Chemistry* **2006**, *183* (1–2), 190-197; (b) Chen, J.; Mizumura, M.; Shinokubo, H.; Osuka, A., Functionalization of Boron Dipyrin (BODIPY) Dyes through Iridium and Rhodium Catalysis: A Complementary Approach to  $\alpha$ - and  $\beta$ -Substituted BODIPYs. *Chemistry – A European Journal* **2009**, *15* (24), 5942-5949.
35. Baruah, M.; Qin, W.; Flors, C.; Hofkens, J.; Vallée, R. A. L.; Beljonne, D.; Van der Auweraer, M.; De Borggraeve, W. M.; Boens, N., Solvent and pH Dependent Fluorescent Properties of a Dimethylaminostyryl Borondipyrromethene Dye in Solution. *The Journal of Physical Chemistry A* **2006**, *110* (18), 5998-6009.
36. Cunningham, C. W.; Mukhopadhyay, A.; Lushington, G. H.; Blagg, B. S. J.; Prisinzano, T. E.; Krise, J. P., Uptake, Distribution and Diffusivity of Reactive Fluorophores in Cells: Implications toward Target Identification. *Molecular Pharmaceutics* **2010**, *7* (4), 1301-1310.
37. (a) Lim, S. H.; Thivierge, C.; Nowak-Sliwinska, P.; Han, J.; van den Bergh, H.; Wagnières, G.; Burgess, K.; Lee, H. B., In Vitro and In Vivo Photocytotoxicity of Boron Dipyrromethene Derivatives for Photodynamic Therapy. *Journal of Medicinal Chemistry* **2010**, *53* (7), 2865-2874; (b) Uppal, T.; Hu, X.; Fronczek, F. R.; Maschek, S.; Bobadova-Parvanova, P.; Vicente, M. G. H., Synthesis, Computational Modeling, and Properties of Benzo-Appended BODIPYs. *Chemistry – A European Journal* **2012**, *18* (13), 3893-3905; (c) Ziessel, R.; Bonardi, L.; Ulrich, G., Boron dipyrromethene dyes: a rational avenue for sensing and light emitting devices. *Dalton Trans* **2006**, *21* (23), 2913-8.
38. Sibrian-Vazquez, M.; Jensen, T. J.; Fronczek, F. R.; Hammer, R. P.; Vicente, M. G. H., Synthesis and Characterization of Positively Charged Porphyrin–Peptide Conjugates. *Bioconjugate Chemistry* **2005**, *16* (4), 852-863.
39. He, H.; Lo, P.-C.; Yeung, S.-L.; Fong, W.-P.; Ng, D. K. P., Preparation of unsymmetrical distyryl BODIPY derivatives and effects of the styryl substituents on their in vitro photodynamic properties. *Chemical Communications* **2011**, *47* (16), 4748-4750.
40. Cole, L.; Davies, D.; Hyde, G. J.; Ashford, A. E., ER-Tracker dye and BODIPY-brefeldin A differentiate the endoplasmic reticulum and golgi bodies from the tubular-vacuole system in living hyphae of *Pisolithus tinctorius*. *J Microsc* **2000**, *197* (Pt 3), 239-49.

## CHAPTER 4: SYNTHESIS AND APPLICATION OF NOVEL BODIPY-PEG AND BODIPY- CARBOHYDRATE CONJUGATES AS POWERFUL TOOLS FOR BIOIMAGING

### 4.1: Introduction

Molecular imaging is defined as the *in vivo* visualization and characterization of various cellular and molecular pathways occurring in living animals and human patients.<sup>1</sup> Progress in this field is becoming more advanced due to the multi-disciplinary collaborations among various chemists, physicists, imaging scientists, clinicians and molecular biologists. As a result, molecular imaging is often considered as the future for medical imaging.<sup>2</sup>

A number of diagnostic imaging modalities such as magnetic resonance imaging (MRI), positron emission tomography (PET), X-ray computed tomography (CT), nuclear imaging and ultrasound have been successfully utilized in clinical diagnosis for the past decades. However, most of these predominant modalities are either highly expensive or lack the specificity and sensitivity needed for early disease detection, coupled with the deleterious radioactive risks.<sup>3</sup> Moreover, several “contrast agents” (such as super-paramagnetic or paramagnetic metals for MRI, radioisotopes for PET and microbubbles for ultrasound) used to improve the visibility of internal bodily structures and to extract valuable information from these imaging modalities, often tend to be nonspecific, unstable and toxic, which limits their repeated use. In order to attain truly targeted imaging of specific molecules that exist in relatively low concentrations in the tissues, the imaging dyes and techniques must be highly effective and sensitive.<sup>1</sup>

Optical bioimaging, on the other hand, is emerging as a promising non-invasive, real-time and high resolution technique that uses sophisticated fluorescent probes to visualize normal and abnormal biological processes *in vivo*.<sup>4</sup> Among the various optical imaging technologies, NIR fluorescence imaging (within the wavelength range 700-900 nm) has attracted much

attention due to the improved deep tissue penetration and low auto-fluorescence characteristics associated with the NIR radiation. As a result, satisfactory cell targeting and imaging of living organisms relies greatly on the development of stable, highly sensitive and targeted NIR imaging probes.<sup>5</sup>

A general and simple approach to improving the target-specific accumulation of an imaging probe is to conjugate the far-red and NIR fluorophore with targeting ligands (such as amino acids, peptides, proteins, antibodies, aptamers, enzymes and other small molecules) which have been applied in molecular imaging.<sup>1</sup> Targets for the fluorescent imaging probes are usually over-expressed cell membrane receptors (such as human epidermal growth factor receptor (EGFR2), cell-specific membrane antigens, vascular endothelial growth factor receptor (VEGFR2) or molecules that are abundant in the extracellular matrix (such as integrins, matrix metalloproteinases).<sup>6</sup>

NIR dyes have rapidly emerged as fluorescent probes for the imaging of biological processes *in vitro* and *in vivo*. Along with the stringent spectral characteristics i.e. red visible or NIR absorption and emission, the fluorescent probes that are bright, small, amphiphilic and contain no net charge are useful candidates for *in vivo* bioimaging.<sup>3</sup> For most biological applications, good solubility in aqueous media and resistance to the formation of non-fluorescent aggregates is highly essential.<sup>7</sup> Low water solubility of a fluorescent probe often leads to self-aggregation and modification or loss of its absorption and fluorescence properties. Moreover, fluorescent probes that are electrically neutral have numerous advantages over their ionic analogues, as they avoid potential nonspecific binding through electrostatic interactions between the dye and the targeted molecule.<sup>8</sup>

Among the multitude of available synthetic fluorophores (such as Cyanines, Quantum dots, fluorescent nanoparticles) exhibiting high extinction coefficients, high quantum yields,



narrow emission bands, and good physicochemical stability, many have limited biological utility due to poor solubility and tendency for aggregation in aqueous media that surrounds a biomolecule. Furthermore, the lack of reactive functional groups limits modification of the fluorophoric core, which results in significantly reduced target-selective accumulation and the biological efficacy of the fluorophore.

Several strategies have been investigated to enhance aqueous solubility as well as tumor specificity of fluorescent probes including introduction of ionizable hydrophilic groups (such as carboxylic acid, phosphonic acid, sulfonic acid, and ammonium groups)<sup>9</sup> within the chromophoric core, or grafting the hydrophobic molecule onto hydrophilic and biodegradable macromolecules (such as oligonucleotides, polyethylene glycol and carbohydrates).<sup>7, 10</sup> Both these methodologies have been widely used with cyanine, fluorescein, rhodamine and oxazine dyes, resulting in a number of new amphipathic fluorescent labels. Surprisingly, little synthetic effort has been devoted towards the use of these strategies with hydrophobic, yet tunable BODIPY fluorophores, resulting in only a handful of BODIPY-based imaging probes currently known.<sup>11, 12</sup> Further, many of these derivatives have not been applied to imaging due to their poor uptake by the target molecules and short excitation/emission wavelength.<sup>12b</sup>

## **4.2: Our Approach**

Recently, interdisciplinary research at the interface of polymer chemistry, glycobiology and bioimaging sciences has led to an increasing use of hydrophilic polymers such as polyethylene glycol (PEG) chains and carbohydrates in the design of various targeted bioimaging probes for the diagnosis and treatment of diseases.<sup>13</sup> A combination of several imaging techniques and various biocompatible and hydrophilic polymers has generated more specific

bioimaging probes which could significantly differentiate the target areas from its background *in vivo*.

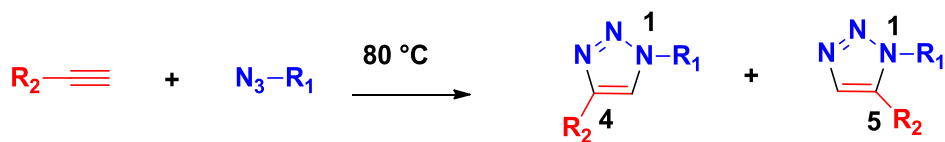
PEGylation was first described in the 1970s by Davis and Abuchowsky in context to albumin and catalase modifications.<sup>14</sup> Since then, the process of PEGylation has been extensively utilized in biomedical research for diagnosis and treatment of a disease. PEGylation is defined as a process by which one or more PEG chains are grafted on a biomolecule to improve its pharmacokinetic, pharmacodynamics and immunological properties. The PEG-based molecules (drugs or fluorescent probes) have numerous advantages over the non-PEGylated derivatives, such as improved serum half-lives, increased resistance to proteolysis, reduced toxicity and increased tumor accumulation along with reduced nonspecific binding.<sup>13, 15</sup> As a result, an array of covalently-linked PEG-conjugates of porphyrin,<sup>16</sup> phthalocyanines,<sup>17</sup> benzoporphyrins,<sup>18</sup> carbocyanines,<sup>19</sup> quantum dots,<sup>20</sup> nanoparticles<sup>21</sup> and radiometal chelators<sup>22</sup> have been developed either as therapeutic or bioimaging agents for cancer targeting and imaging.

Another important approach, widely utilized for the modification of a protein, peptide or a non-protein molecule to increase its pharmacokinetic profile is via glycosylation. Glycosylation refers to the process which attaches carbohydrate chains to target proteins, lipids or other organic molecules. Carbohydrates in the form of glycopeptides, glycolipids, proteoglycans or other glycoconjugates regulate a myriad of biological and pathological processes including protein folding, energy storage, signal transduction, inflammation, viral entry and as structural motifs for cell-cell communications.<sup>23</sup> As a result, carbohydrate conjugates have been investigated for targeting various cells including hepatocytes, macrophages, vascular endothelial cells and various cancer cells including lectins.<sup>24</sup> Intense research efforts have been focused on developing tumor-specific carbohydrate-based therapeutic and diagnostic agents by targeting cell membrane proteins. Carbohydrate-functionalized macromolecules have shown promise in photodynamic

therapy and *in vivo* optical imaging due to their enhanced interactions with tumor cell receptors via carbohydrate-mediated cell recognition processes, and increased cellular uptake and solubility, without significant alterations of the physicochemical and photophysical properties.<sup>25</sup>

The indispensable role of PEG- and carbohydrate-functionalized macromolecules in drug discovery and tumor imaging has initiated the work presented herein to design, synthesize and investigate a series of novel PEG- and carbohydrate-functionalized BODIPY conjugates as potential candidates for *in vivo* imaging. The key step in this synthesis is the 1,3-dipolar cycloaddition between a terminal alkyne and an azide, often referred to as the azide/alkyne-“Click”-reaction or “CuAAC reaction”.

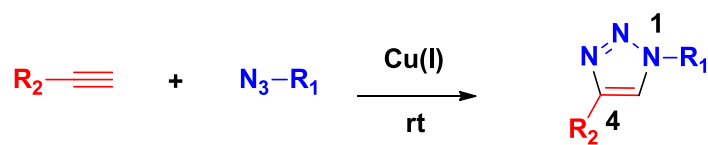
Since being first introduced by Nobel Laureate Dr. Barry Sharpless in 2001, Click chemistry has become a popular concept with wide utility in diverse fields. Click chemistry refers to a group of reactions that are fast, high-yielding, simple to use, easy to purify, versatile and regioselective.<sup>26</sup> This concept covers a wide range of reactions such as cycloadditions, nucleophilic ring opening, non-aldol carbonyl chemistry, addition to carbon-carbon multiple bonds etc. While there are a number of reactions that fulfill the criteria, the copper-catalyzed Huisgen 1,3-dipolar cycloaddition of azides and terminal alkynes, abbreviated as CuAAC (Copper-catalyzed azide alkyne cycloaddition) is the best known click reaction.<sup>27</sup>



**Scheme 4.1:** 1,3-Dipolar cycloaddition of azides and alkynes pioneered by Rolf Huisgen

The azide/alkyne cycloaddition reaction which combines an alkyne and an azide together by heating, to produce a mixture of 1,4- and 1,5-triazoles (Scheme 4.1), was first discovered by Rolf Huisgen. However, the harsh reaction conditions were considerably softened by the use of a

copper catalyst (as discovered independently by Sharpless and Meldal groups) which accelerates the rate of the reaction by 7 orders of magnitude.<sup>28</sup> In contrast to the uncatalyzed conditions, the use of copper (I) salts ensures the exclusive 1,2,3-triazole regioselective formation of the 1,4-regioisomer (Scheme 4.2). The reaction has several unique characteristics including simple reaction conditions (insensitive to oxygen and water), readily available starting materials, simple product isolation and purification. For these reasons, the reaction has been widely used in carbohydrate chemistry as it is especially suitable for fragile compounds, and more generally for the synthesis of biomolecules.<sup>27</sup>

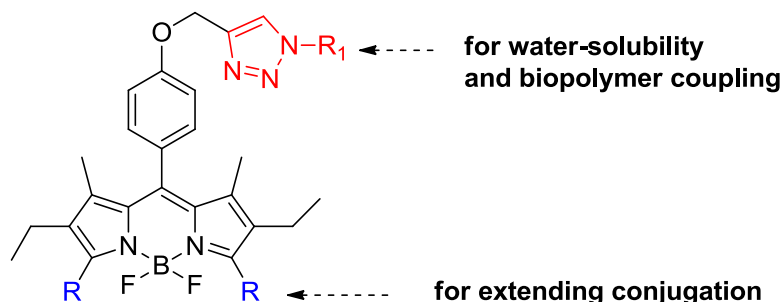


**Scheme 4.2:** Copper catalyzed 1,3-Dipolar cycloaddition by Sharpless/Meldal

The ever-increasing success of the CuAAC reaction is rooted in its selectivity, efficiency and versatility. The CuAAC reaction is a virtually quantitative, very robust, insensitive to the environment, and the orthogonal ligation reaction, suitable for even biomolecular ligation and *in vivo* tagging or as a polymerization reaction for synthesis of long linear polymers. The triazole formed is stable to acid and base hydrolysis, reductive and oxidative conditions, and is relatively resistant to metabolic degradation.<sup>29</sup> In this work, Click chemistry was chosen as the preferred facile synthetic methodology to conjugate BODIPYs to several azido-PEGs and azido-carbohydrates due to the: (1) great versatility of the reaction and various functional group tolerance (2) mild reaction conditions that could be well tolerated by the BODIPY scaffold, and (3) straightforward reaction work-up involving simple purification techniques.

### 4.3: Results and Discussion

The main aim of the present work was to design and synthesize a series of new fluorescent bioconjugates consisting of a BODIPY fluorophore bearing non-hydrolysable 1,2,3-triazole ring, linked either by an ethylene glycol spacer (for attachment to biomolecules) or carbohydrate moiety (for target-specific accumulation). Additionally, the major goal was to move the emission wavelength into the red and NIR region while making use of the unique BODIPY chemistry along with versatile Huisgen alkyne/azide cycloaddition methodology (Scheme 4.3). The facile and efficient strategy for the generation of BODIPY-PEG and BODIPY-carbohydrate conjugates discussed below, has been previously explored on porphyrins and related macrocycles, resulting in an array of porphyrin-carbohydrate<sup>30</sup> and pegylated-porphyrin<sup>15, 31</sup> conjugates for use as photosensitizers in photodynamic therapy.

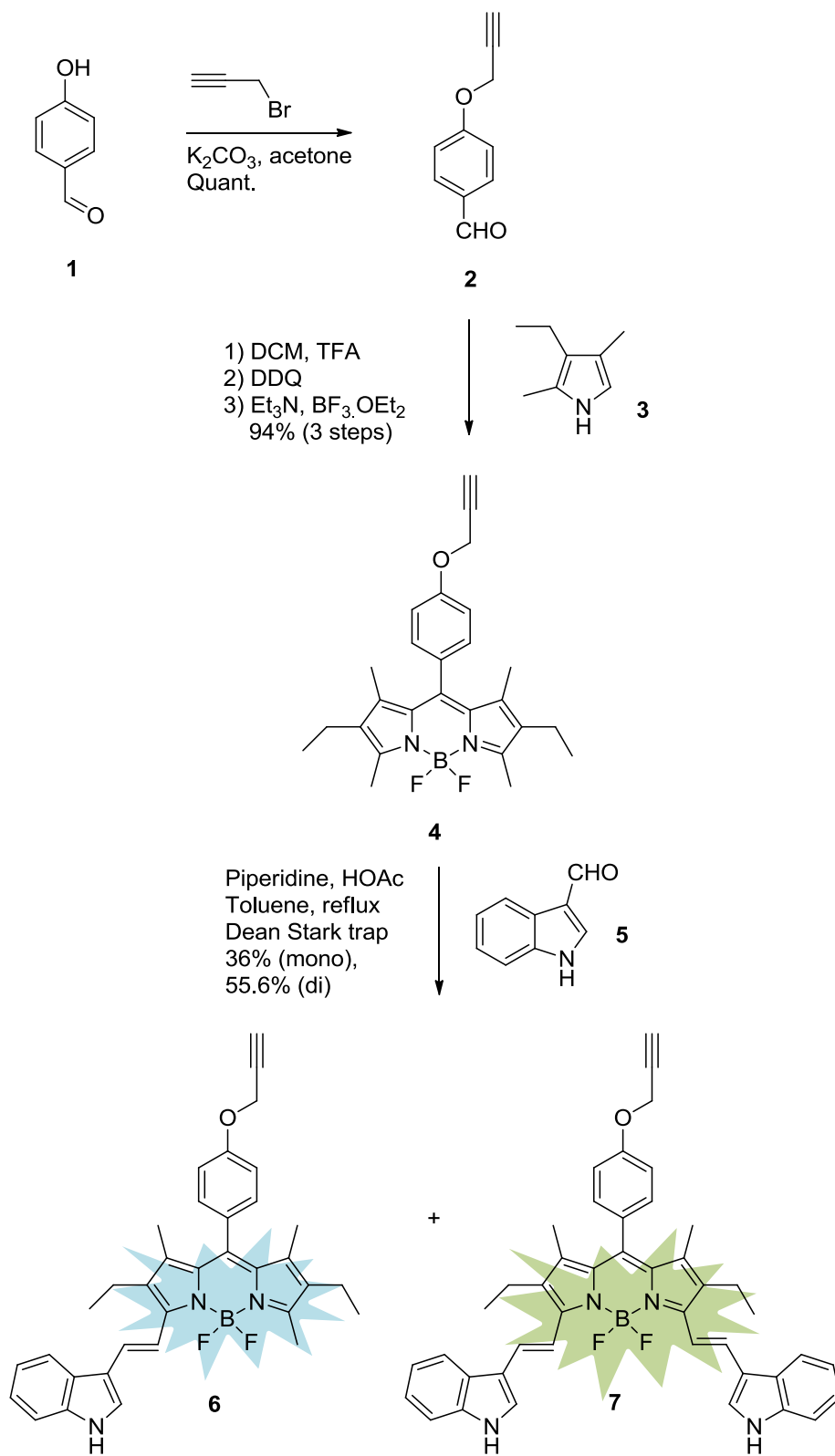


**Scheme 4.3:** The general structure of BODIPY derivatives prepared in this work

A careful investigation of porphyrin-conjugates generated via click chemistry indicated that the click labeling of biomolecules is generally completed on the functionalized macrocycle (except one case in which the click reaction was performed on the precursor of the porphyrin).<sup>27</sup> Hence, a similar methodology was adopted for the work described in this Chapter. The key step

in the synthesis is the placement of the terminal alkyne “handle” on the BODIPY fluorophore, to generate the so-called “clickable BODIPY fluorophores”.

*p*-Hydroxy benzaldehyde was O-alkylated by Williamson reaction, using propargyl bromide and potassium carbonate in acetone, according to the literature procedure,<sup>32</sup> to generate *p*-propargyloxy-benzaldehyde, **2** in quantitative yield. *Meso*-alkynylphenyl-BODIPY **4**, containing alkynyl functionality at the C-8 position was then synthesized according to the three-step one-pot classical approach, starting from *p*-propargyloxy-benzaldehyde **2** and two equiv. of 3-ethyl-2,4-dimethyl pyrrole **3**, in the presence of a catalytic amount of TFA and dry dichloromethane as solvent (Scheme 4.4). The final reaction mixture was stirred under argon and the reaction was monitored by TLC until completion (~16 h). The resulting mixture was cooled down to 0 °C and treated with 1.2 equiv. of DDQ oxidant. After stirring for 20 min., triethylamine was added dropwise over a period of 5 min. while stirring and maintaining the temperature at 0 °C. After 30 min. stirring, the reaction mixture was treated with BF<sub>3</sub>.OEt<sub>2</sub> and the resulting reaction mixture was stirred at room temperature under argon. The progress of the reaction was closely monitored by TLC and UV-Vis (for a band at 525 nm) until completion. The reaction mixture was then filtered through a pad of silica gel to separate the oxidized dipyrromethene derivative, higher molecular weight oligomers, unreacted DDQ and starting materials. The solvent was reduced *in vacuo* to afford the crude mixture which was then redissolved in a mixture of dichloromethane and water and stirred overnight to decompose any unreacted BF<sub>3</sub>.OEt<sub>2</sub>. The subsequent reaction mixture was extracted with dichloromethane and the combined organic layers were dried over sodium sulfate and the solvent removed under the



**Scheme 4.4:** Synthetic route to BODIPYs **4**, **6** and **7**

reduced pressure. The crude product was purified on a silica gel column eluting with a solvent mixture of dichloromethane/petroleum ether in a 1:1 ratio. The first orange-green fluorescent band containing the product was collected and after solvent evaporation, afforded the desired BODIPY **4** in 94% over three steps. This compound was characterized by NMR ( $^1\text{H}$ ,  $^{13}\text{C}$ ) in deuterated chloroform and MS (MALDI) giving a molecular ion peak  $[\text{M}^+]$  at  $m/z$  434.23. The  $^1\text{H}$ -NMR spectrum showed the *ortho* and *meta* protons as doublets in the aromatic region, and the resonance corresponding to the CH protons in the terminal position of the propargyl group was identified as a singlet at  $\delta$  2.52 ppm. The two equivalent protons of the propargylic methylene group were identified as a broad doublet centered at 4.72 ppm and the ethyl protons appeared as a triplet at 0.98 ppm and a quartet at 2.29 ppm. The two sets of methyl protons (3,5 and 1,7) appear as singlets at 2.53 and 1.33 ppm, respectively. 1,7-methyls are in the shielding zone of the phenyl substituent and experience a shielding by approximately 1.2 ppm. The  $^1\text{H}$ -NMR spectrum for BODIPY **4** is shown in Figure 4.1.

The reactivity of the acidic 3- and 5-methyls on the BODIPY core and the syntheses of both monostyryl- and distyryl-derivatives from symmetric tetramethyl-BODIPY is now firmly established.<sup>11c, 33</sup> Styryl-derivatized BODIPY compounds are known to display red-shifted fluorescence emissions due to the extended  $\pi$ -conjugation, and their emission wavelengths vary according to the styryl moieties.<sup>34</sup> The introduction of two styryl groups on BODIPY **4** was accomplished with electron-rich indole-3-carbaldehyde **5** via classical Knoevenagel condensation, using piperidine and acetic acid in refluxing toluene and a Dean-Stark apparatus. The use of a Dean-Stark apparatus seems to be critical for removing the water formed in the reaction and thus shifting the equilibrium to the double condensation product, which is the distyryl BODIPY dye **7**.<sup>35</sup> The use of indole-3-carbaldehyde **5** for styryl-derivatization was based on the results obtained in Chapter 3. Additionally, indole derivatives have been long known for



their biological resemblance with tryptophan, a naturally occurring amino acid and an important component of many enzymes, peptides and proteins.<sup>36</sup> It is anticipated that the anchoring of the indolylstyryl arms on the BODIPY platform will further increase the biological efficacy of the fluorophore.

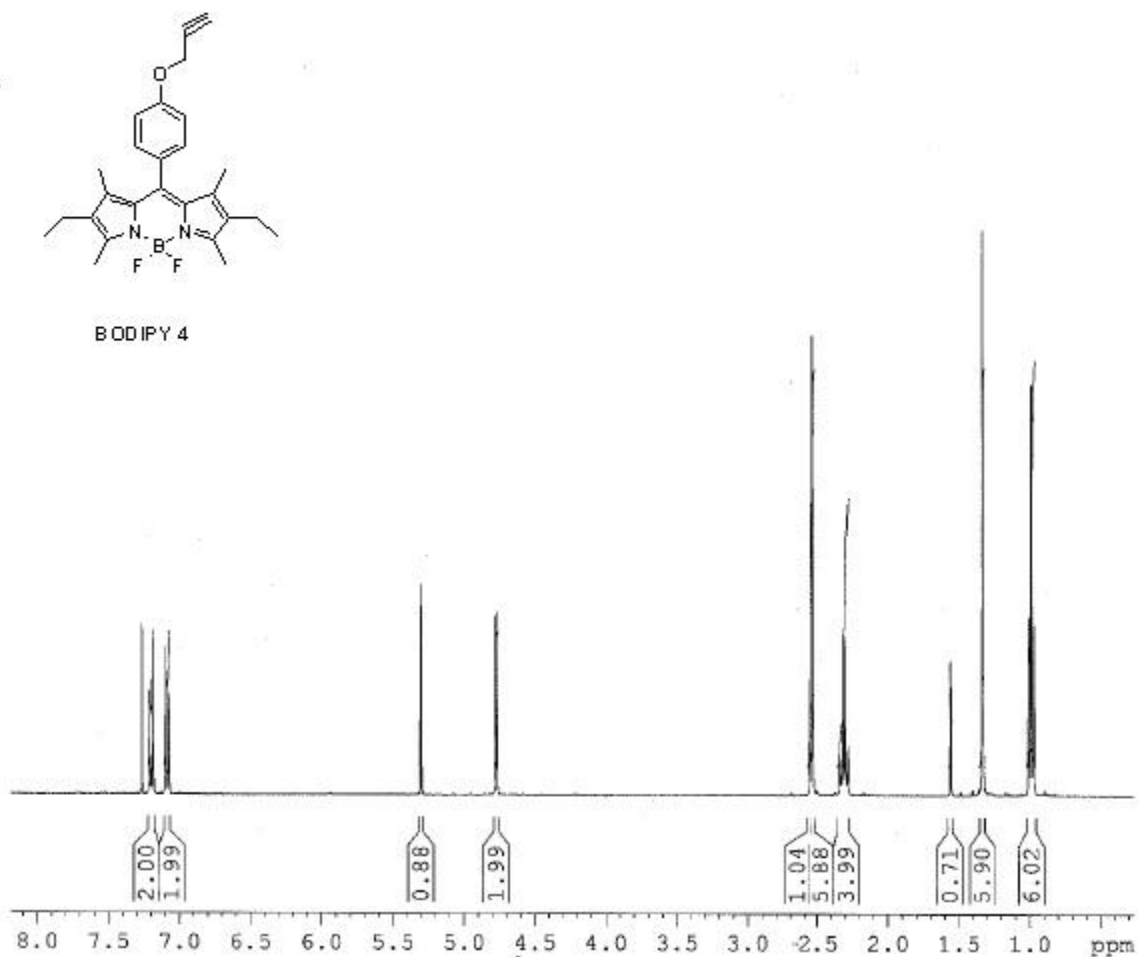


**Figure 4.1:** <sup>1</sup>H-NMR spectrum of BODIPY 4 in CDCl<sub>3</sub> at 400 MHz

BODIPY 4 and indole-3-carbaldehyde 5 in 1:3 ratio, were refluxed in a mixture of dry toluene, glacial acetic acid and piperidine. Any water formed during the reaction mixture was removed azeotropically by heating overnight in a Dean-Stark trap. The progress of the reaction

was followed by TLC analysis, a blue spot corresponding to the monostyryl-BODIPY derivative appeared after 2 h and after ~ 6 h, a slightly polar spot of the distyryl-BODIPY derivative appeared. However, as the TLC indicated the presence of starting material, the reaction was left to stir overnight. Once the reaction was complete (~14 h), the reaction mixture was cooled to room temperature and the solvent evaporated under reduced pressure. The crude product was purified by silica gel chromatography using dichloromethane/petroleum ether (in 2:1 ratio) as eluent and a mixture of three compounds was obtained, which could be further separated by column chromatography as three distinct bands due to the marked difference in their polarity. The orange-green fraction corresponding to the unreacted starting material was eluted first, followed by a reddish-blue fraction (monoindolyl styryl-BODIPY **6**) and a deep-green fraction (diindolyl styryl-BODIPY **7**). All the bands were collected separately and after solvent removal *in vacuo*, afforded BODIPY **4** (recycled), BODIPY **6** and BODIPY **7** in 2%, 36% and 55.6% yields, respectively. Mass spectrometry of the derivatized BODIPYs was performed using MALDI-TOF. MS analysis gave a peak at *m/z* 561.35 and 688.32, corresponding to BODIPY **6** and BODIPY **7** respectively. The <sup>1</sup>H-NMR spectra of BODIPYs **6** and **7**, as shown in Figures **4.3** and **4.4** respectively, showed some interesting features. For BODIPY **6**, bearing monoindolyl styryl- arm and in comparison with the <sup>1</sup>H-NMR spectrum of BODIPY **4**, characteristic signals of protons belonging to indolic NH (10.7 ppm), fused aryl (additional *ortho* and *meta* protons) and  $\alpha$ -pyrrolic (7.74 ppm) units of indole moiety were observed. In particular, in the NMR spectrum of BODIPY **6**, the vinylic protons in the 3-positions appeared as a single shielded doublet at 7.91 ppm and 7.65 ppm. In the case of symmetrically substituted distyryl-BODIPY **7**, the vinylic protons in the 3 and 5-positions appear as two pairs of *trans* coupled protons, the most shielded at 8.05 ppm.

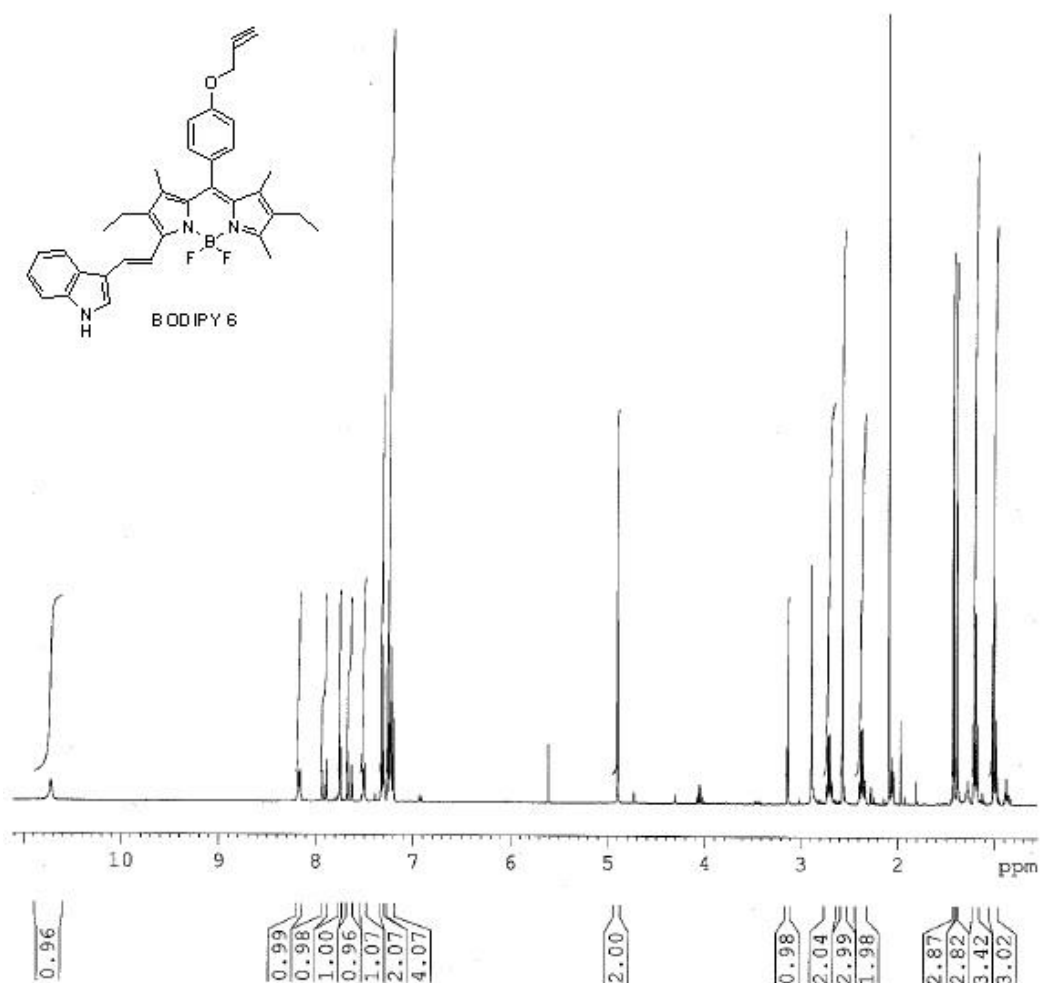


**Figure 4.2:**  $^1\text{H-NMR}$  spectrum of BODIPY **6** in deuterated acetone at 400 MHz

The use of PEG as carrier or covalently attached to a macromolecule is widely known.<sup>37</sup> In general, low molecular weight PEG spacers have shown to be effective linkers between a porphyrin-based fluorophore and target biological entity, as they: (1) minimize the steric hindrance between the two moieties, (2) favor extended conformation for the bioconjugates, (3) enhance the enthalpic interactions of the fluorophore with polar solvents including water, and (4) minimize fluorophore aggregation in biological media.<sup>16a</sup> Hence, in order to increase the amphiphilicity of BODIPYs and for effective conjugation with various biomolecules, the spacers

consisting of hydrophilic triethylene glycol and hexaethylene glycol chains were chosen for click chemistry with BODIPY **6**.

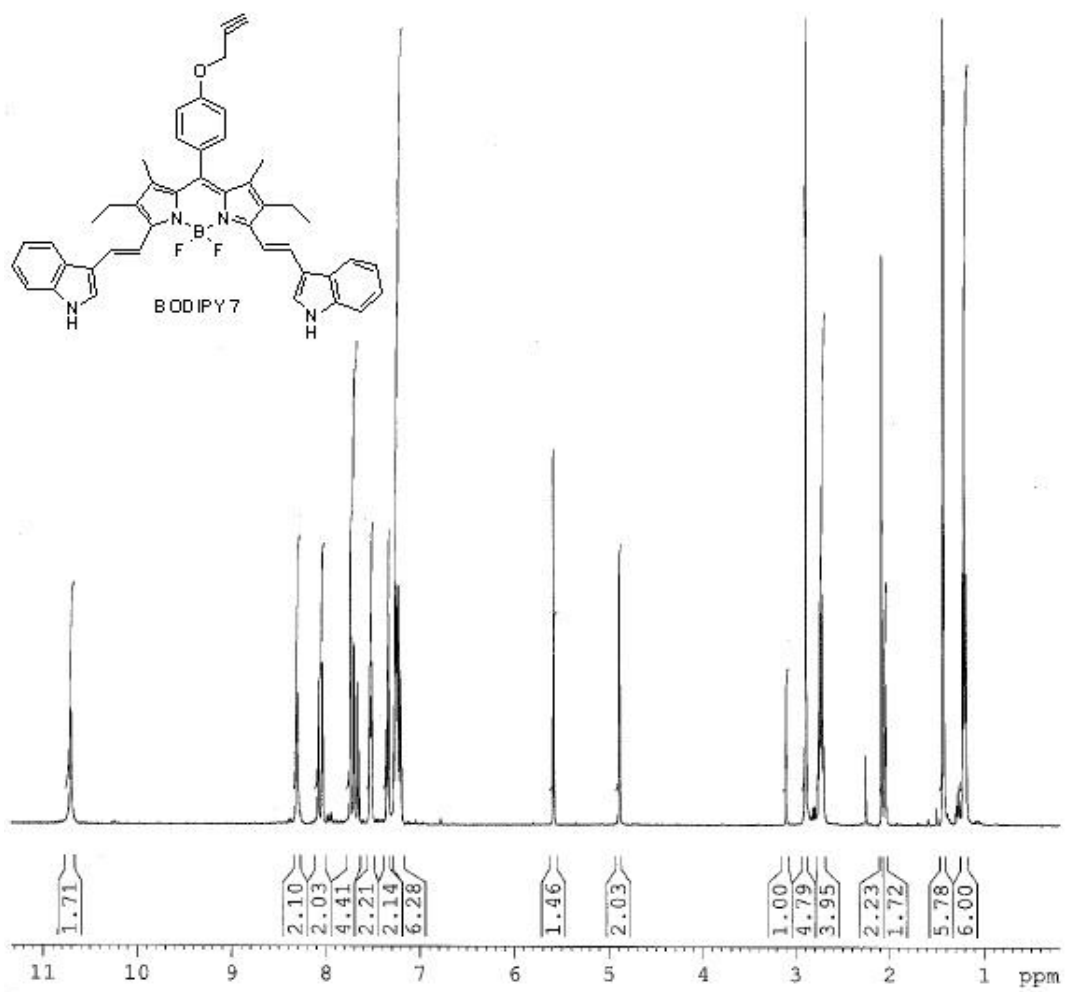
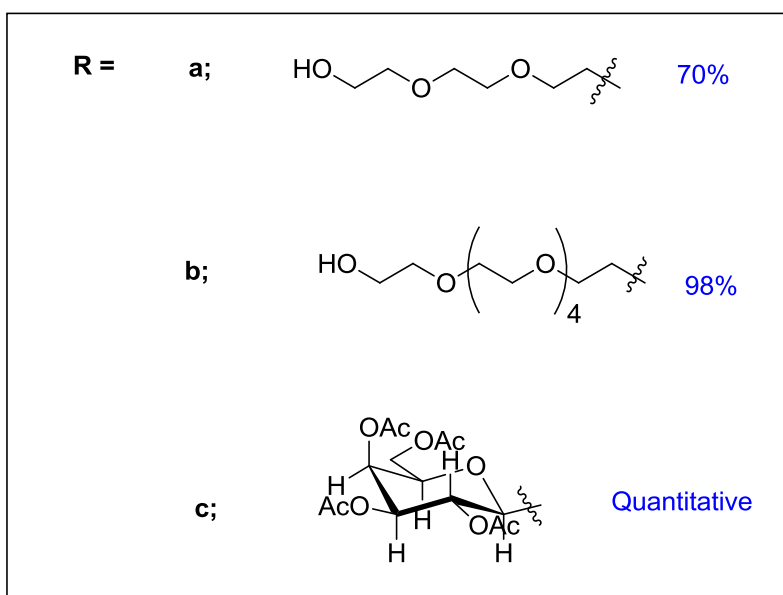
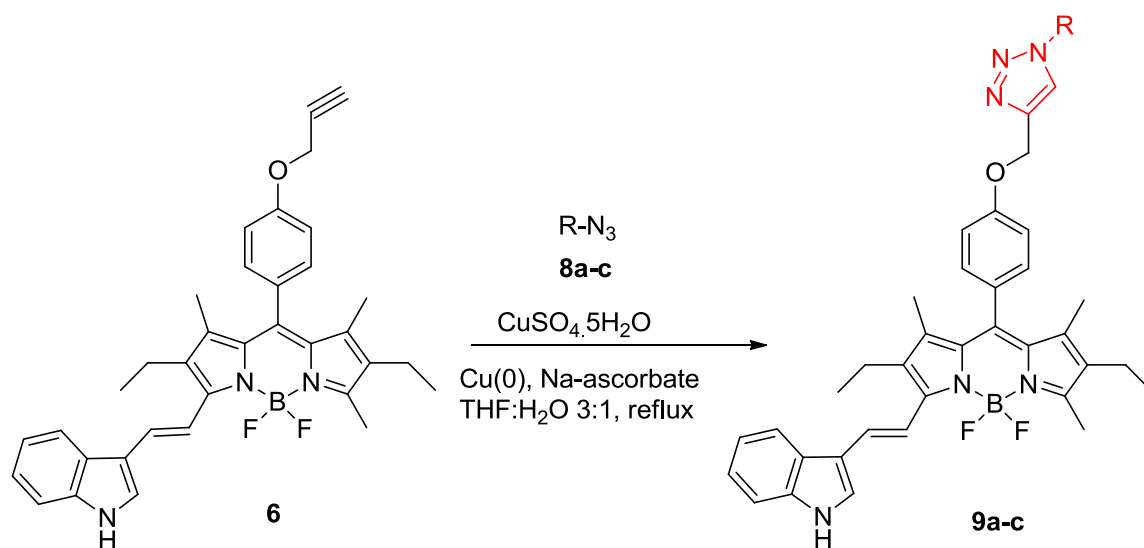


**Figure 4.3:** <sup>1</sup>H-NMR spectrum of BODIPY **7** in deuterated acetone at 400 MHz



**Scheme 4.5:** Synthetic route to BODIPY conjugates **9a-c**

The hetero-bifunctional PEG linkers **8a** and **8b** that possess terminal hydroxyl and azido groups were obtained from Dinesh Bhupathiraju, a fellow colleague in the Vicente group. Azido-PEGs **8a** and **8b** could be prepared from commercially available triethylene glycol and hexaethylene glycol by a two-step conversion involving selective mesylation in the presence of

excess mesyl chloride, followed by nucleophilic substitution by sodium azide at room temperature. Both the reactions are high-yielding and generally afford the products in moderate to high yields.<sup>38</sup>

Finally the conjugation of the PEG **8a** and **8b** to the BODIPY **6** was performed using click chemistry. The mild aqueous conditions required for azide/alkyne cycloadditions offer distinct advantages when utilized for bioconjugations. To demonstrate the utility of “click chemistry” on BODIPY dyes, conjugation of PEG-groups to the BODIPY scaffold was performed by solution phase “click reaction” in the presence of CuSO<sub>4</sub>/Cu/sodium ascorbate in THF/water (3:1), as shown in Scheme 4.5.<sup>38a</sup>

A solution of *meso*-alkynylphenyl-BODIPY **6**, azido-PEG **8a** (2.6 equiv) and Cu (0) (1.0 equiv) in a solvent mixture of THF:H<sub>2</sub>O (8 mL, 3:1) was treated with a solution of CuSO<sub>4</sub>·5H<sub>2</sub>O (0.20 equiv) and Na-ascorbate (0.5 equiv.) in THF:H<sub>2</sub>O (8 mL, 3:1). The elemental copper serves as a convenient reductant for Cu(II) in aqueous solution to generate Cu(I), which is a powerful catalyst for the formation of 1,2,3-triazoles from terminal alkynes and azides.<sup>39</sup> The reaction mixture was heated for 6 h at 70 °C, under inert gas atmosphere. Once the reaction was complete, the mixture was cooled to room temperature and partitioned between EtOAc and water. The aqueous layer was re-extracted with EtOAc (to remove copper salts) and the combined organic layers were dried over Na<sub>2</sub>SO<sub>4</sub>. The solvent was evaporated under reduced pressure and the crude product was purified by silica gel preparative TLC eluting with 10:1 dichloromethane/ethylacetate solution, to afford the first 1,2,3-triazole cycloadduct **9a** in 70% yield. The reaction was repeated with Azido-PEG **8b**, in order to study the effect of increased PEG chain length on the synthesis and *in vitro* biological investigations, affording cycloadduct **9b** in excellent yield (98%). MS (MALDI) analysis of cycloadducts **9a** and **9b** gave a molecular ion peak at m/z 736.40 and 868.48 respectively. <sup>1</sup>H-NMR spectral analysis of these cycloadducts

(Figures 4.4 and 4.5) gave the most characteristic signal of the proton on the triazole ring at 8.16 ppm as a broad singlet. The signals of protons belonging to spacer group showed up between 3.50-3.94 ppm.

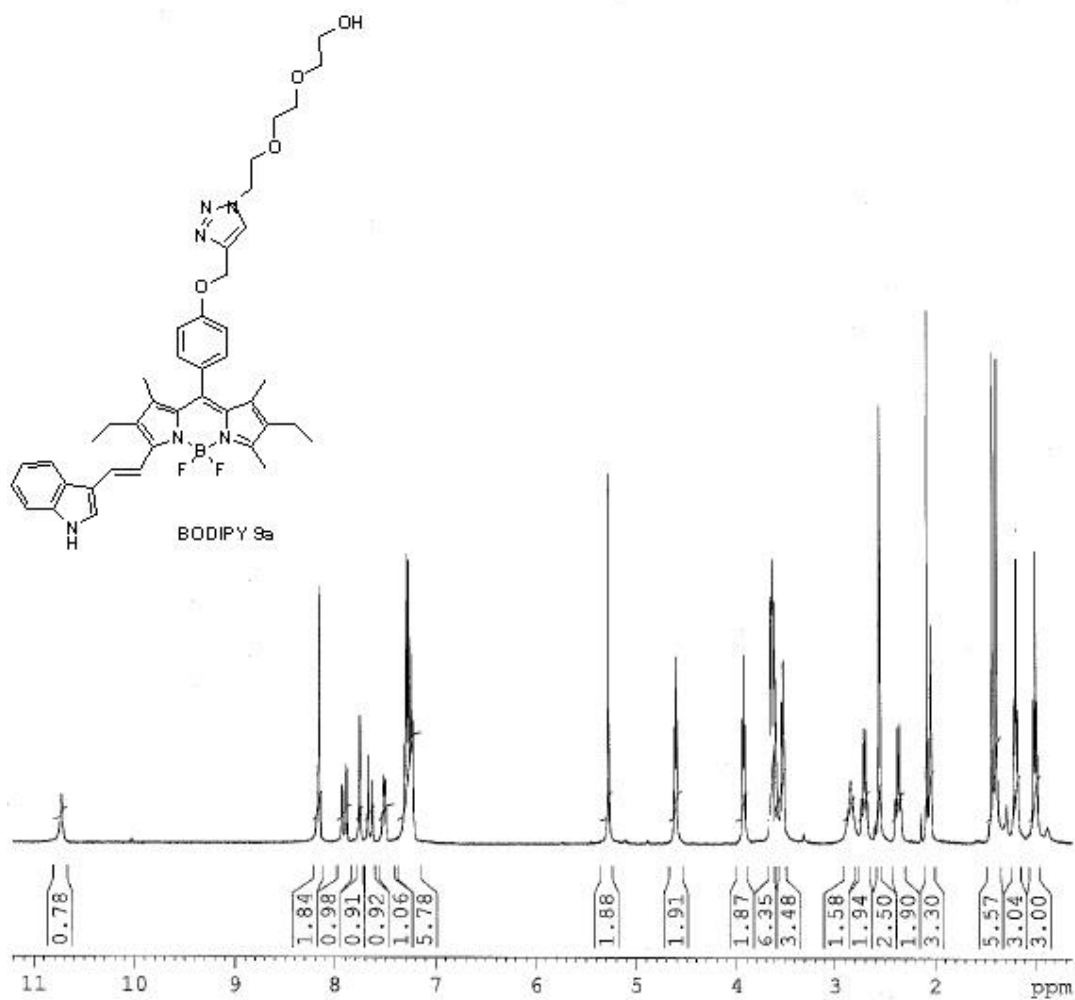


**Figure 4.4:** <sup>1</sup>H-NMR spectrum of BODIPY-PEG cycloadduct **9a** in deuterated acetone at 400 MHz

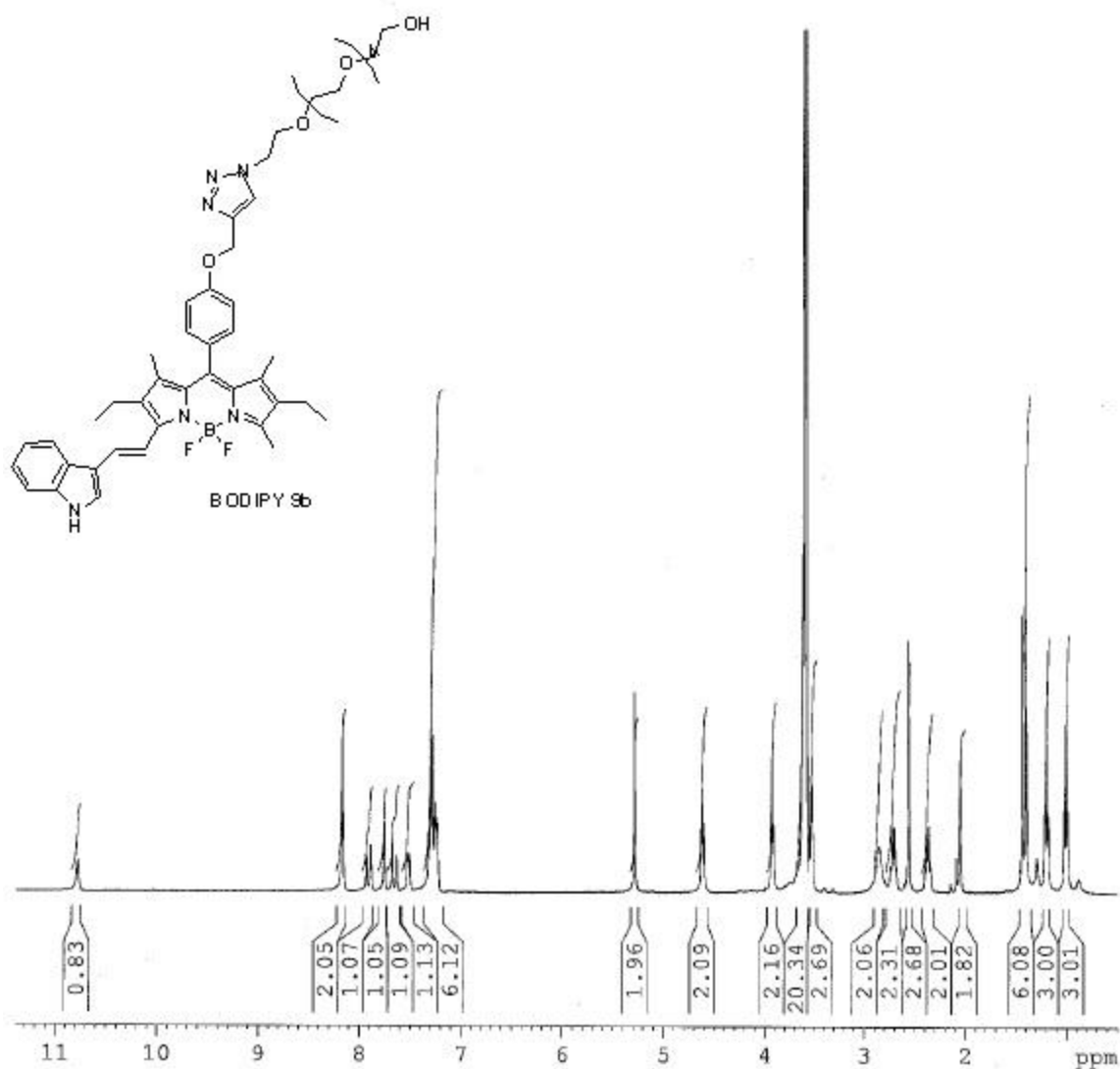


**Figure 4.5:**  $^1\text{H-NMR}$  spectrum of BODIPY-PEG cycloadduct **9b** in deuterated acetone at 400 MHz

To demonstrate the functional group tolerance of azides with BODIPY **6**, commercially available carbohydrate-azide (1-azido-1-deoxy- $\beta$ -D-galactopyranoside tetraacetate), **8c** was tested for “click” ligation. Azido-sugars have frequently been used for click labeling of surface glycoproteins.<sup>40</sup> The acetyl protecting group “masks” the otherwise reactive hydroxyl group while increasing the cell permeability of the carbohydrates and allowing the unnatural sugars to easily pass through the cell membrane. Once the monosaccharide is in the cell, the



carboxyesterases enzyme cleaves the acetyl groups, thereby unmasking the protected hydroxyl moiety. The BODIPY-carbohydrate cycloadduct **9c** was prepared in virtually quantitative amount, using the optimized reaction conditions as developed for cycloadduct **9a** and **9b**. For cycloadduct **9c**, <sup>1</sup>H-NMR spectrum displayed singlet peaks at 2.21, 2.05, 2.03 and 1.90 ppm due to four acetyl groups on sugar respectively, along with the broad singlet of the proton on the triazole ring at 8.17 ppm, as shown in Figure 4.6. MS (MALDI-TOF) further confirmed the successful synthesis of cycloadduct **9c** (molecular ion peak at m/z 934.42).

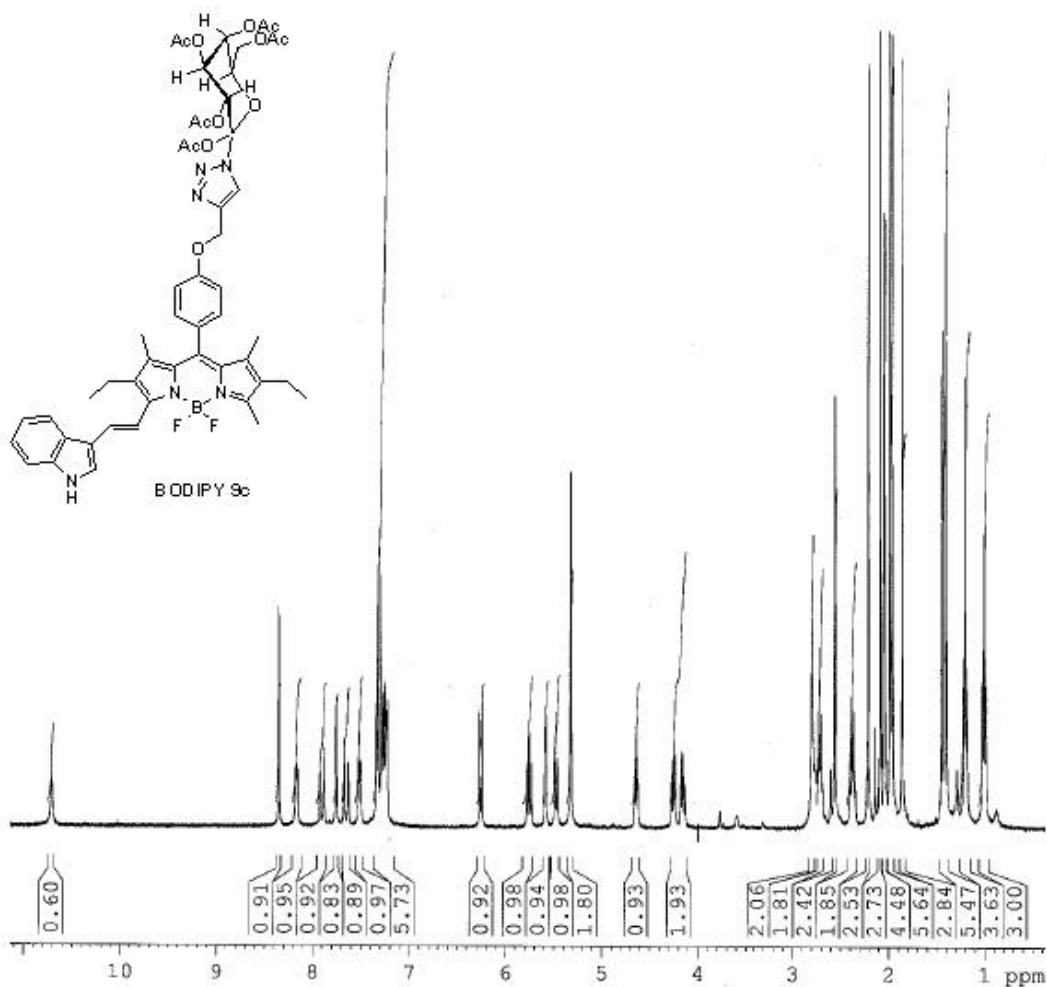


**Figure 4.6:** <sup>1</sup>H-NMR spectrum of BODIPY-carbohydrate cycloadduct **9c** in deuterated acetone at 400 MHz

**Table 4.1:** Isolated yields of ligation experiment performed on diindolyl styryl BODIPY **7**\*

Entry	Azido-derivative	Cycloadduct Yield (%)
1	<b>8a</b>	15
2	<b>8b</b>	20
3	<b>8c</b>	57.3
4	<b>8d</b>	18.2
5	<b>8e</b>	22.5

\* In each case TLC analysis indicated complete consumption of the starting materials.

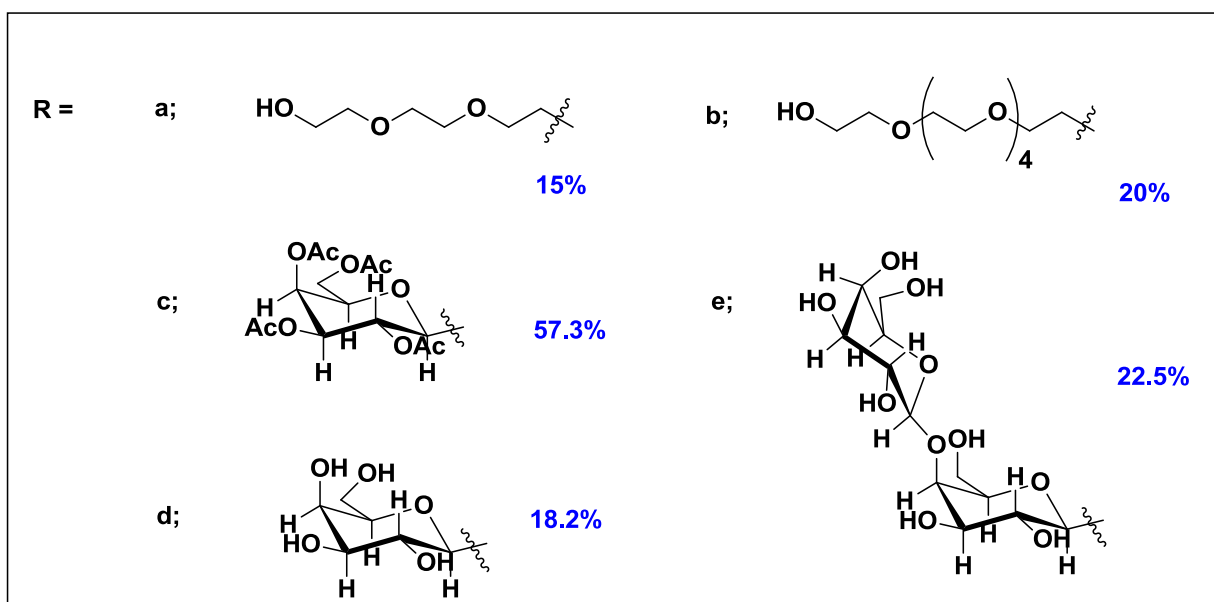
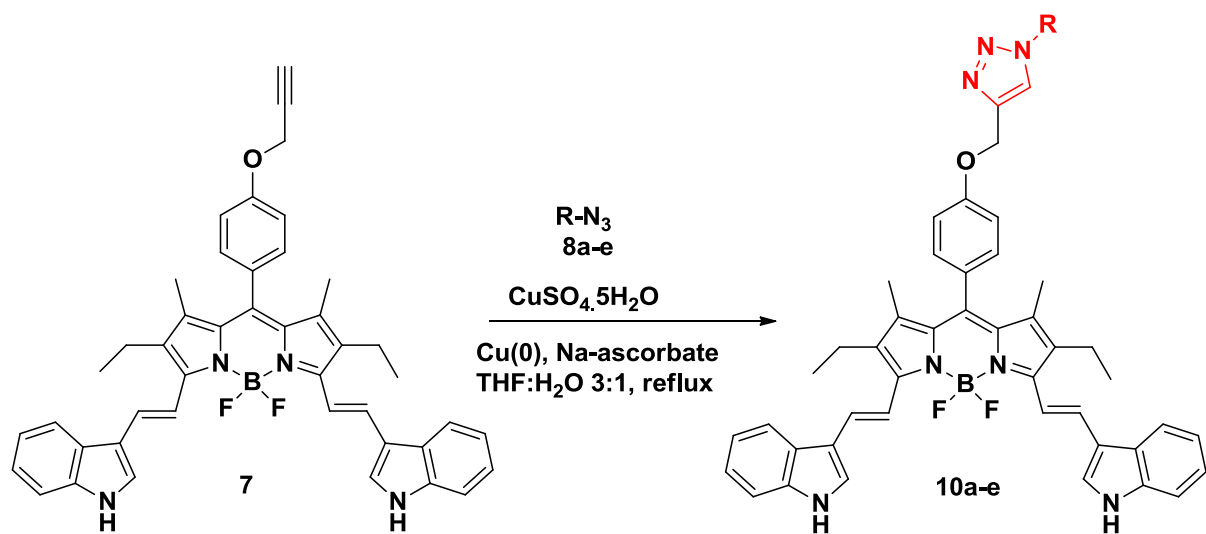
The click labeling strategy was extended to prepare another series of PEG- and carbohydrate-functionalized cycloadducts **10a-e**, as fluorescently labeled biological building blocks, starting from diindolyl styryl-BODIPY **7**, as shown in Table **4.1** and Scheme **4.6**. Along with azido-derivatives **8a-c**, two commercially available azido-sugars namely, 1-azido-1-deoxy- $\beta$ -D-glucopyranoside (**8d**) and 1-azido-1-deoxy- $\beta$ -D-lactopyranoside (**8e**) were used to generate glucose- and lactose-conjugated BODIPYs as potential chemical probes for galectin proteins, a lectin that is often over-expressed in tumor cells for tumor growth and development. The cycloadducts **10a-e** were obtained in moderate yields providing further proof for the efficiency of the CuAAC reaction in ligation process. All the BODIPY cycloadducts were fully characterized using NMR and MALDI-TOF analysis. Well-resolved  $^1\text{H-NMR}$  spectra of PEG- and carbohydrate-functionalized cycloadducts **10a-e** showed typical proton on the triazole ring at approximately 8.18 ppm. For **10a** and **10b**, the characteristic signals of protons belonging to the ethylene group appeared between 3.51-4.61 ppm. For **10c**, the four acetyl groups showed up as four singlets at 2.21, 2.05, 2.03 and 1.96 ppm, respectively. Glucose and lactose units in cycloadducts **10d** and **10e** were found to resonate in a very crowded region of the NMR

spectrum, between 3.31-4.26 ppm and 3.49-4.67 ppm, respectively. MALDI analysis gave a molecular ion peak at m/z **10a**: 863.42; **10b**: 995.50; **10c**: 1061.40; **10d**: 893.42 and **10e**: 1055.45.

Carbohydrates are known as ligands of various cell surface lectins.<sup>30a</sup> Intense research efforts have been focused to develop tumor-specific imaging probes by targeting cell membrane glycoproteins, such as galectins. The galectins are a family of small soluble proteins that play significant roles in numerous types of cancer.<sup>41</sup> Galectins are defined by a highly conserved carbohydrate recognition domain (CRD) and their affinity for glycoconjugates. Among the galectins, Galectin-1 (Gal-1) and Galectin-3 (Gal-3) have been the most widely studied as they are abundant in tumor cells to promote tumor growth and development, angiogenesis and metastasis. Because the mechanisms by which galectins play a role are generally poorly understood, novel carbohydrate-based fluorescent probes would be particularly useful for detection of galectins in tissues, in order to generate a better understanding of this protein.<sup>42</sup>

Clickable BODIPY **4** is highly versatile chromophore and can be conveniently derivatized with suitably substituted benzaldehyde (for instance, Compound **2**) to produce BODIPYs **11** and **12**, with two or more alkyne “handles” for further click tagging (Scheme **4.7**). The envisioned synthesis makes use of a convergent click reaction build up approach with strategically placed Huisgen alkyne click components. This approach not only allows the synthesis of long wavelength emissive BODIPYs, but also two or more biomolecules could be tagged to BODIPY fluorophore in a straightforward sequence of reactions.

BODIPY **4** was condensed with compound **2** (3 equiv.) using classical Knoevenagel condensation approach as described above for the synthesis of BODIPYs **6** and **7** (Scheme **4.7**). The reaction was monitored using TLC and after 2 days, the reaction mixture still had a substantial amount of unreacted starting material. Thus 4 equiv. of compound **2** were introduced

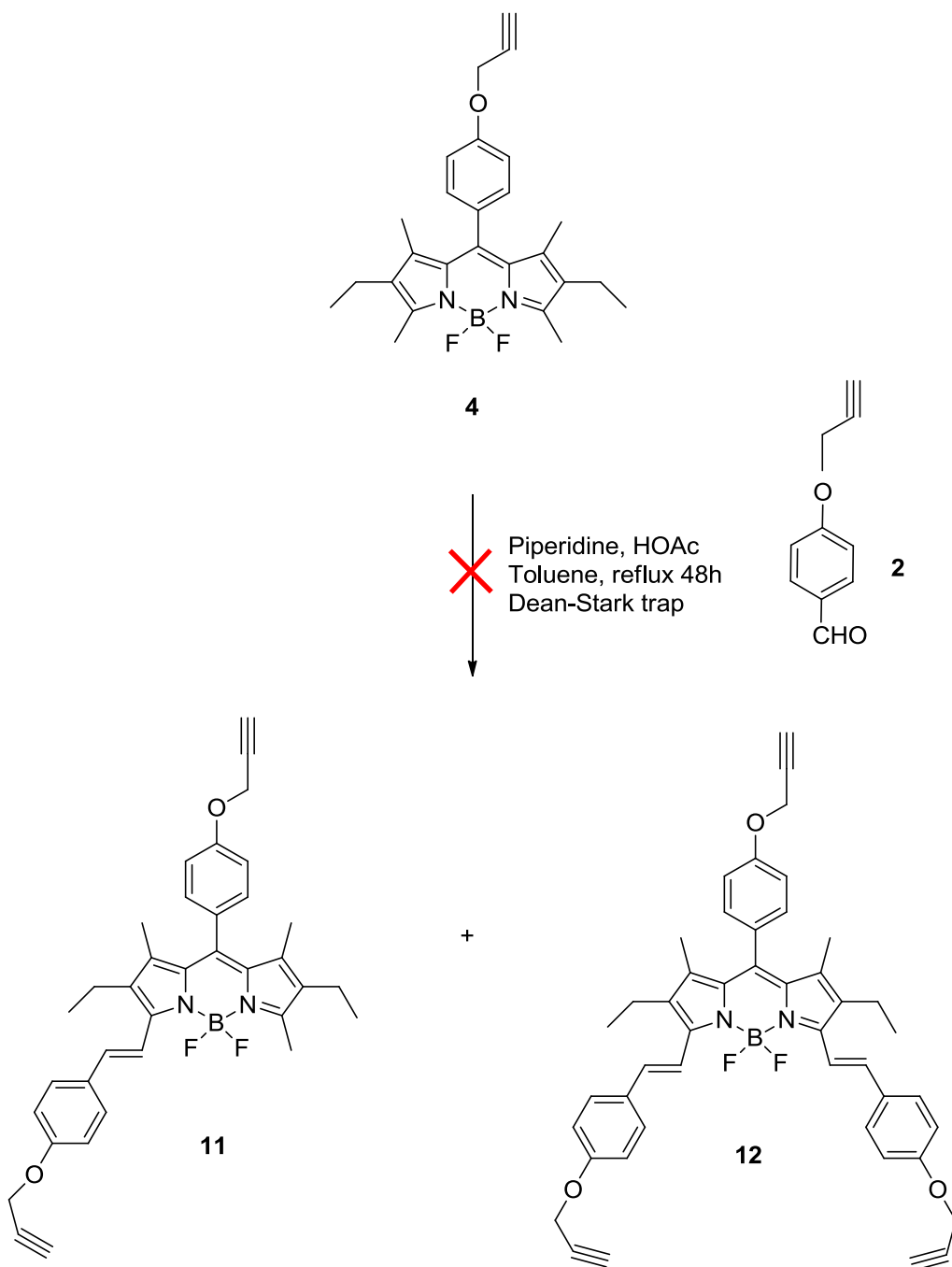


**Scheme 4.6:** Synthetic route to BODIPY conjugates **10a-e**

and the reaction was allowed to reflux for 24 h, but TLC barely indicated the formation of any product. It was then concluded that compound **2** was not nucleophilic enough for the electron-deficient BODIPY system. This was not surprising as several electron-poor aldehydes have been found unreactive when condensed with electron-deficient BODIPY dyes during Knoevenagel

condensation reaction.<sup>43</sup> An alternate route to BODIPY **11** and **12** was then developed as shown in Scheme **4.8**. It was anticipated that electron-donating *p*-hydroxy benzaldehyde (compound **1**) would be a better candidate for Knoevenagel condensation and that terminal alkyne units could be generated on the functionalized BODIPY instead, by O-alkylation using propargyl bromide. Knoevenagel condensation of BODIPY **4** was first attempted via the classical approach, similar to the one reported for the synthesis of BODIPY **6** and **7**, i.e. by treating the tetramethyl BODIPY **4** with *p*-hydroxy benzaldehyde **1**, piperidine and glacial acetic acid in boiling toluene. Unfortunately, in our hands, this reaction did not give any satisfactory results.

Recently, a modified version of the Knoevenagel condensation was described, which employs the addition of Lewis acids such as ZnCl<sub>2</sub>, TiCl<sub>4</sub> etc to promote the Knoevenagel condensation between poorly reactive BODIPYs and aromatic aldehydes.<sup>44</sup> A similar modified procedure as developed by Raymond et al.<sup>44b</sup> was followed using a catalytic amount of *p*-TsOH. Compound **1** and BODIPY **4** were refluxed in a mixture of dry toluene, piperidine and a crystal of *p*-TsOH. The solution was heated at reflux until the solvent evaporated to dryness. The resulting crude was washed with water and extracted with dichloromethane. The organic phase was dried over magnesium sulfate and the solvent evaporated under reduced pressure. The crude residue was subjected to several silica gel columns in order to get rid of the starting material and other side products which were difficult to separate. As a result, BODIPY **13** could only be isolated in < 2% yield and could not be characterized by <sup>1</sup>H-NMR. However, MALDI-TOF analysis indicated the product formation by a molecular ion peak at *m/z* 538.26.



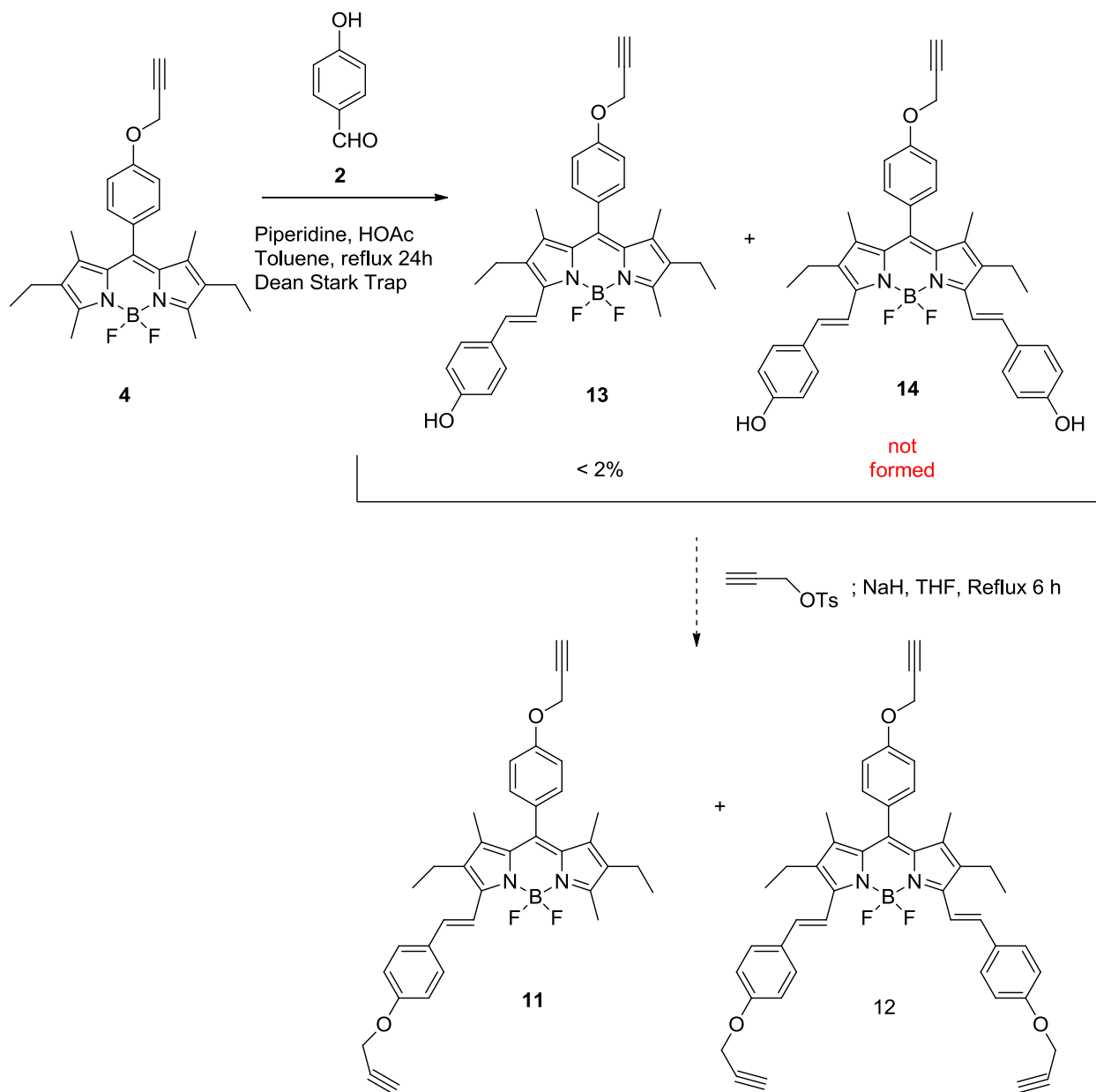
**Scheme 4.7:** Synthetic route to BODIPYs **11** and **12**

Enhancing the donor-acceptor balance between the vinyl arm and the BODIPY core further shifts its absorption and fluorescence emission towards the red. A careful investigation of the electron density change upon the excitation of the BODIPY dyes indicates that the C-8

experiences a marked increase in electron density in the excited state of the BODIPY. Hence, introduction of a strong electron-withdrawing group such as *p*-bromophenyl on the *meso*-position of BODIPY should bring a concomitant increase in the acidity of the 3- and 5- methyl groups, which should result in higher reactivity of the BODIPY dyes toward Knoevenagel condensation reaction.<sup>45</sup> Hence, another approach towards the synthesis of BODIPYs with two alkyne “handles” was adopted as displayed in Scheme 4.9.

*Meso*-(*p*-bromophenyl) BODIPY **15** was synthesized using the classical approach as mentioned for the synthesis of BODIPY **4**. *p*-Bromo-benzaldehyde and 3-ethyl-2,4-dimethyl pyrrole **3** were dissolved in dry dichloromethane under argon at room temperature. Three drops of TFA was added and the reaction was stirred overnight at room temperature. The reaction was followed via TLC and upon completion, a solution of DDQ in dichloromethane was added and the reaction was stirred for another 15 min. Subsequently, triethylamine and BF<sub>3</sub>.OEt<sub>2</sub> were added and the reaction was stirred overnight. Upon completion, the reaction mixture was passed through a short silica plug eluting with pure dichloromethane and the solvent was removed *in vacuo*. The crude product was re-dissolved in a mixture of dichloromethane and water and the product was extracted with dichloromethane. The organic layers were collected and dried over magnesium sulfate and the solvent evaporated under reduced pressure. The resulting crude mixture was purified by silica gel column chromatography using 1:1 dichloromethane/petroleum ether solvent mixture. The product containing fluorescent orange-green fraction was collected and the solvent was removed. The pure product was dissolved in minimum amount of dichloromethane and crystallized by gradually adding hexane to obtain shiny green crystals which were then dried *in vacuo*. The obtained BODIPY **15** was fully characterized using <sup>1</sup>H-NMR and MS (MALDI) giving a peak at *m/z* 458.13. This methodology follows the procedure

already developed by Noll et al.,<sup>46</sup> though minor variations of the procedure made it possible to synthesize the BODIPY in higher yields with minimal chromatography.



**Scheme 4.8:** Alternative route to BODIPYs **11** and **12**



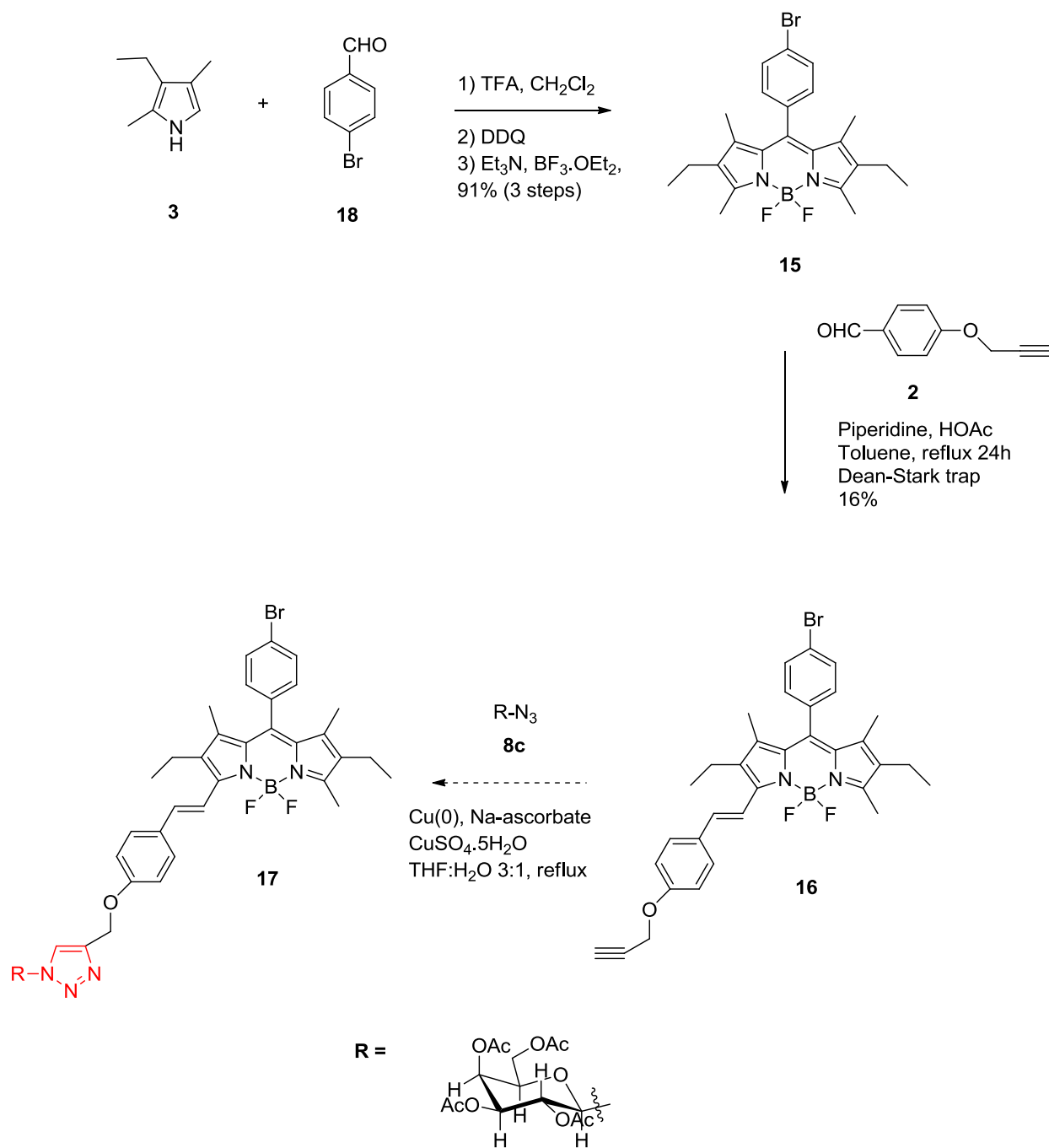
In order to introduce the alkyne “handles” on the BODIPY **15**, Knoevenagel condensation with compound **2** was performed using piperidium acetate and glacial acetic acid in boiling toluene using a Dean-Stark apparatus. The efficiency of styryl derivatization was evaluated using several reaction conditions as depicted in Table **4.2**. The reaction was repeated several times by varying the reaction conditions such as longer reaction time, excess catalyst/base/solvent. Longer reaction times and excess base/reactant increased the percent yield of the monostyryl-BODIPY **16** (from 2% to ~ 16%), along with generation of a complex mixture of products which could not be fully characterized by <sup>1</sup>H-NMR spectrum. Surprisingly, no distyryl-BODIPY derivative could be obtained under these conditions.

**Table 4.2:** Isolated yields of Knoevenagel condensation reaction performed on BODIPY **15**

Entry	Compound <b>2</b>	Piperidine-HOAc	Reflux time	Yield of product (BODIPY <b>16</b> )
1	1 equiv.	0.2 mL - 0.2 mL	24 h	1.8 %
2	2 equiv.	0.4 mL- 0.4 mL	24 h	1.5 %
3	4 equiv.	1 mL-1 mL	24 h	2.2 %
4	7 equiv.	2 mL- 2 mL	24 h	2.9 %
5	10 equiv.	4 mL- 4 mL	48 h	10 %
6	20 equiv.	8 mL- 8 mL	48 h	16 %

### 4.3.2: Photophysical Studies

UV/vis absorbance and fluorescence emission spectra of BODIPY-conjugates **9a-c** and **10a-e** were recorded in DMSO at room temperature along with their unconjugated precursor BODIPYs **4**, **6** and **7** (Figure **4.7**) and the key values are summarized in Table **4.3**. In the absorption spectra, a strong absorbance band centered at 525, 613 and 703 nm for BODIPY **4**,



**Scheme 4.9:** Synthetic route to BODIPYs **15** and **16**

monoindolyl styryl-BODIPY **6** and diindolyl styryl-BODIPY **7**, respectively is assigned to the  $S_0$ - $S_1$  transition. In the wavelength region below the absorption maximum, there exists a

“shoulder” due to 0-1 vibrational transition and a second higher energy absorption maximum peak due to  $S_0$ - $S_2$  transition. These three peaks constitute the main spectral characteristics of the absorption spectrum of the BODIPY system.<sup>47</sup> All BODIPYs showed absorptions with high molar extinction coefficients ( $\log \epsilon = 4.1$ - $4.5$ ) and narrow fluorescence emission bands. Upon excitation at 480, 575 and 660 nm, BODIPYs **4**, **6** and **7** showed a fluorescence emission centered at 534, 644 and 732 nm respectively. As expected, styryl-derivatization caused a large bathochromic shift in the absorption and emission spectra, of about

**Table 4.3:** Spectral properties of BODIPYs **4**, **6**, **7**, **9a-c** and **10a-e** in DMSO at room temperature

<b>BODIPY</b>	<b>Absorbance <math>\lambda_{\max}/\text{nm}</math></b>	<b><math>\log \epsilon (\text{M}^{-1} \cdot \text{cm}^{-1})</math></b>	<b>Emission <math>\lambda_{\max}/\text{nm}</math></b>	<b>Stokes shift (nm)</b>
<b>4</b>	525	4.4363	534	9
<b>6</b>	613	4.5286	643	30
<b>9a</b>	613	4.4938	642	29
<b>9b</b>	613	4.4482	644	31
<b>9c</b>	613	4.7723	644	31
<b>7</b>	702	4.3847	732	30
<b>10a</b>	704	4.1482	731	27
<b>10b</b>	702	4.1473	730	28
<b>10c</b>	703	4.5614	732	29
<b>10d</b>	703	4.5575	732	29
<b>10e</b>	703	4.5567	731	28

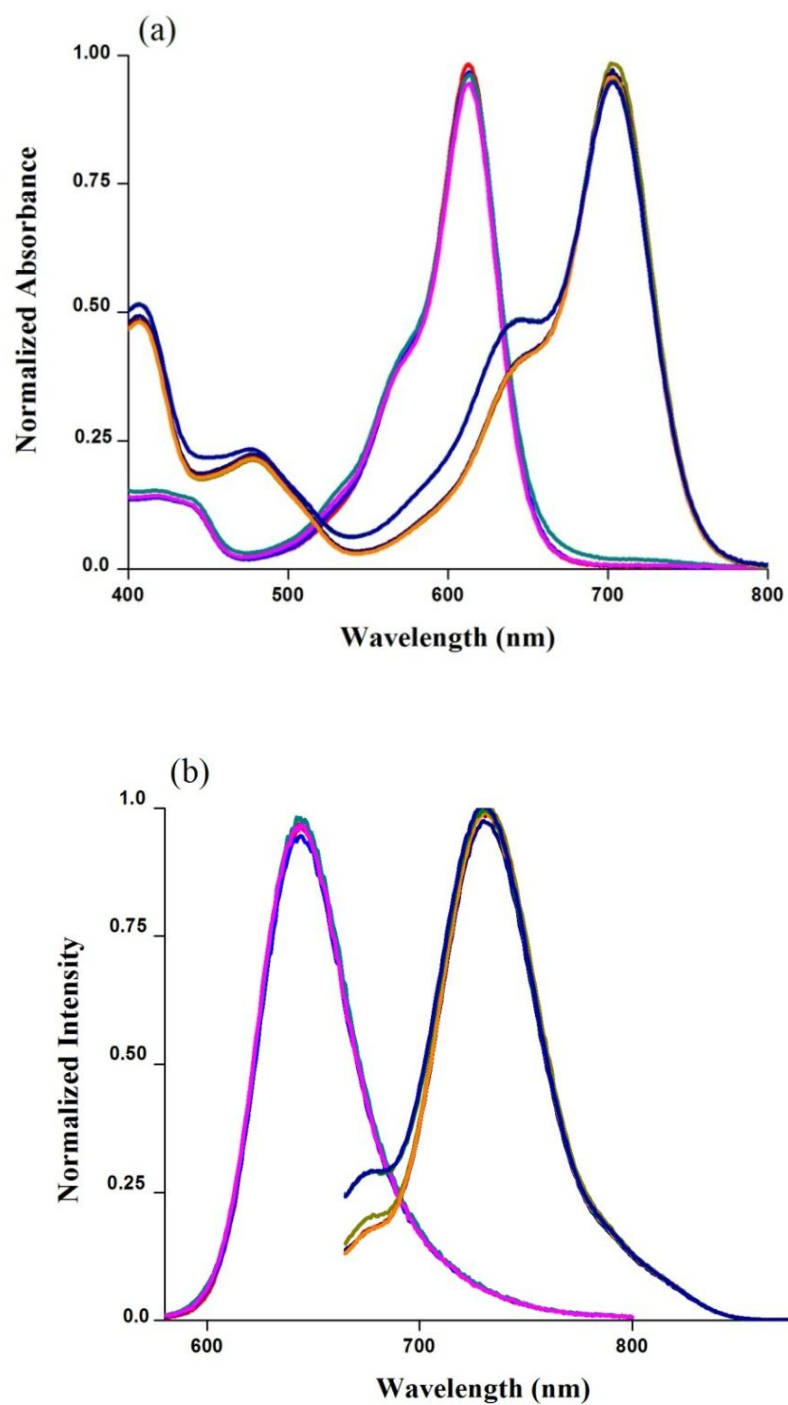


**Figure 4.7:** Normalized (a) absorption spectra ( $1.5 \times 10^{-5}$  M), and (b) fluorescence emission spectra ( $1.5 \times 10^{-6}$  M) of BODIPYs **6** (red), **7** (dark yellow), **9a** (dark cyan), **9b** (magenta), **9c** (blue), **10a** (olive), **10b** (royal), **10c** (navy), **10d** (wine) and **10e** (orange) in DMSO at room temperature

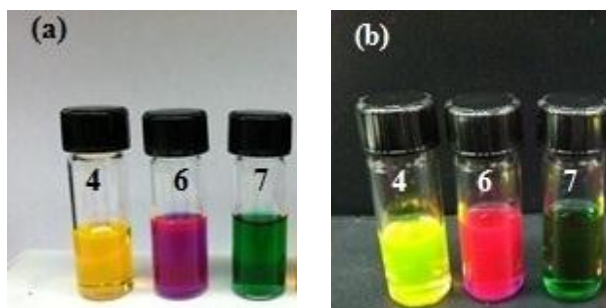


**Figure 4.8:** Solutions of BODIPYs **4**, **6** and **7** in dilute DMSO under (a) normal and (b) UV light

90-100 nm per each styryl arm. For instance, the single Knoevenagel condensation of BODIPY **4** to produce monoindolyl styryl-BODIPY **6** lead to nearly a 80 nm bathochromic shift in the absorption and emission bands, whereas double Knoevenagel condensation to generate diindolyl styryl-BODIPY **7** lead to an approximate 100 nm red-shift. The spectral properties of BODIPY-conjugates **9a-c** and **10a-e** in DMSO showed little difference from each other (1-3 ppm) or from the starting alkyne BODIPY derivatives **6** and **7** respectively, demonstrating that cycloaddition reaction does not alter the spectral properties of the BODIPYs. The Stokes shifts for all the BODIPYs (except **4**) were in the range of 27-30 nm. Measurement of the fluorescence quantum yields of the BODIPYs reported herein are underway in our laboratory. In photographs of solutions for BODIPYs **4**, **6** and **7** in DMSO (Figure 4.8), the solutions of the unsubstituted BODIPY **4** are clearly orange, whereas those of **6** and **7** are deep blue and green, respectively. Under UV light ( $\lambda_{\text{excitation}} = 365 \text{ nm}$ ), these solutions exhibit strong fluorescence.

#### 4.3.3: *In Vitro* Cellular Studies

Preliminary *in vitro* cellular investigation, including dark and photo cytotoxicity and cellular uptake were investigated against human carcinoma HEp2 cell lines in order to investigate the biological efficacy of the PEG- and carbohydrate-functionalized BODIPY-

conjugates. Cremophor surfactant was added to increase the solubility of the dyes in the aqueous media. These studies were performed by N. V. S. Dinesh Bhupathiraju, a fellow colleague in Vicente research group.

*4.3.3.1: Time-Dependent Cellular Uptake.* The time-dependent uptake of BODIPY-conjugates **9a-c** and **10a-e**, by human carcinoma HEP2 cells was investigated at a concentration of 10  $\mu$ M and the results are shown in Figure **4.9**. For comparison purposes, the uptake of unconjugated BODIPYs **6** and **7** was also determined. At this concentration, all conjugates were non-toxic to cells as evaluated using the Cell Titer Blue assay. All conjugates displayed similar uptake kinetics showing a rapid accumulation at short time points, within 2-4 h, after BODIPY exposure. Significant differences in the cellular uptake were observed indicating, the nature and structure of the conjugates along with the chain length of the PEG moiety affect the cellular uptake of the conjugates. In general, the monoindolyl styryl-BODIPY conjugates **9a-c** accumulated within the cells nearly 5 times more than the diindolyl styryl-BODIPY conjugates **10a-e**, at all the time points studied. This can be attributed to the low molecular weight, increased polar hydrophobic nature and enhanced solubility of the conjugates **9a-c** over conjugates **10a-e**. Additionally, the PEG-functionalized BODIPYs showed a much higher uptake by the cells than the carbohydrate-functionalized BODIPYs, for both the series, except conjugate **10d** with glucose functionality, which had the similar uptake as conjugate **10b**. These results are in good agreement with previous studies<sup>48, 16a, 47a</sup> indicating that the use of PEG groups enhance the hydrophobic/ hydrophilic interactions of the conjugates with the cell membrane and improve their cellular uptake. For the **9a-c** series, the uptake trend followed the order **9b** > **9a** > **9c**. While the uptake of **9a** and **9c** was similar in the first 2 h, however after 24 h, the amount of **9a** accumulated in the cells is about 25% higher than that of **9c**. For the **10a-e** series of conjugates, uptake trend followed the order, **10b** ~ **10d** > **10a** > **10c** ~ **10e**. Once again, the highest uptake in

the series was that of **10b**, i.e. hexaethylene glycol-functionalized BODIPY followed by **10a**, which was rapidly taken up by the cells within the first 1 h after BODIPY exposure. Interestingly, conjugates **10c** and **10e**, containing tetraacetate galactose and lactose, were the least accumulated within cells at all the time points studied. Although there was a slight difference in the uptake of **10e** compared with the corresponding **10c**, this difference was not significant and probably reflects, better ability of **10e** to bind to specific cell receptors.

*4.3.3.2: Cytotoxicity.* The dark toxicity and photo cytotoxicity of BODIPYs and BODIPY-conjugates was evaluated in HEp2 cells exposed to increasing concentration of each compound up to 100  $\mu\text{M}$ , using Cell Titer Blue viability assay (Promega). The results are shown in Figure 4.10. It can be seen that all the compounds are essentially non-cytotoxic in the absence [ $\text{IC}_{50}$  (dark) > 100  $\mu\text{M}$ ] or presence of light [ $\text{IC}_{50}$  (1  $\text{J}/\text{cm}^2$ ) > 100  $\mu\text{M}$ ] and the observed results are in consensus with the previously reported investigations.

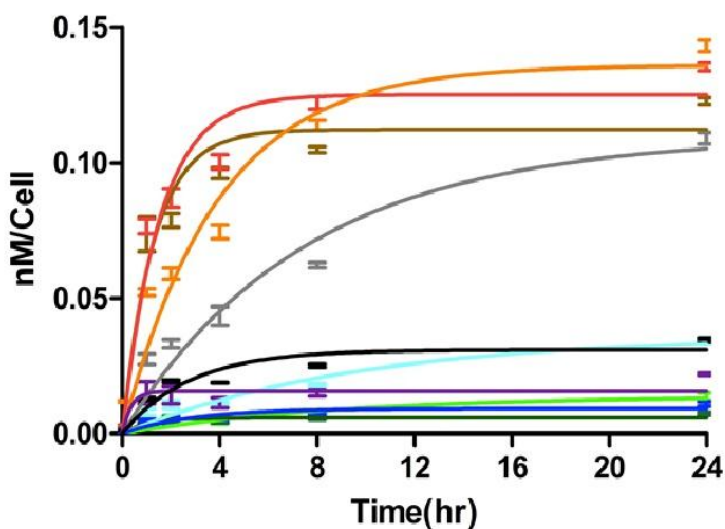


**Figure 4.9:** Time Dependent Cellular Uptake of BODIPYs **6** (Grey), **9a** (Red), **9b** (Orange), **9c** (Brown), **7** (Light Green), **10a** (Purple), **10b** (Black), **10c** (Dark Green), **10d** (Light Blue) and **10e** (Blue) at 10  $\mu\text{M}$  by HEp2 cells.

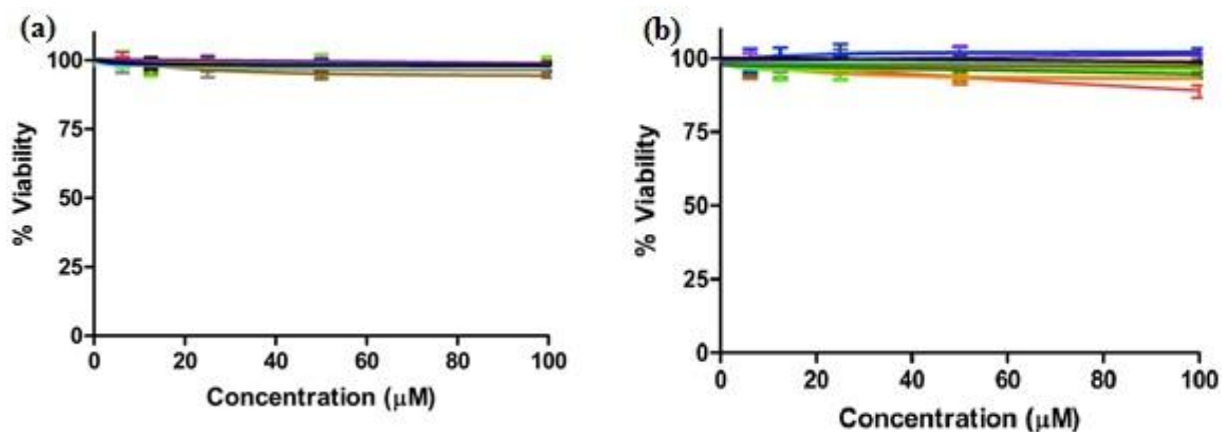


**Figure 4.10:** (a) Dark Cytotoxicity and (b) Photocytotoxicity of BODIPYs **6** (Grey), **9a** (Red), **9b** (Orange), **9c** (Brown), **7** (Light Green), **10a** (Purple), **10b** (Black), **10c** (Dark Green), **10d** (Light Blue) and **10e** (Blue) toward HEp2 cells using a Cell Titer Blue assay and  $1 \text{ J/cm}^2$  light dose.

#### 4.4: Conclusion

In conclusion, a series of ten novel red and NIR-emissive BODIPY-PEG and BODIPY-carbohydrate conjugates containing either one or two diindolyl styryl- arms at 3- and/or 5-positions were successfully synthesized in moderate to excellent yields using a very convenient, rapid and efficient Cu(I)-catalyzed azide-alkyne Huisgen cycloaddition (so called “click chemistry”). All these new conjugates were fully characterized using  $^1\text{H-NMR}$ ,  $^{13}\text{C-NMR}$ , Mass spectrometry (MALDI-TOF) and UV-Vis/fluorescence spectroscopy. BODIPY-PEG and BODIPY-Carbohydrate conjugates displayed good photophysical properties, i.e. strong absorbance and emission in the range of 525-704 and 534-732 nm, respectively and high molar extinction coefficient (4.1-4.5). Furthermore, the attractive cycloaddition strategy had negligible effects on the spectral characteristics of BODIPY-PEG and BODIPY-Carbohydrate conjugates. Preliminary in vitro studies using human carcinoma HEp2 cells indicated all the BODIPY-conjugates were cell permeable, non-cytotoxic with high cellular uptake. The monoindolyl styryl-BODIPY conjugates (**9a-c**) were the most efficiently taken up by the HEp2 cells,



accumulating nearly 5 times more than the di-indolyl styryl BODIPY (**10a-e**) conjugates. Since a plethora of azido-PEGs and carbohydrate azides are readily available, this flexible modular synthesis is expected to provide a versatile platform for vast arrays of functionalized BODIPYs possessing potential utility in *in vivo* imaging.

## 4.5: Experimental

### 4.5.1: General Information

Commercially available reagents were purchased from Sigma-Aldrich Co. Canada, Alfa Aesar Co. or TCI America Co. and were used without further purification. All solvents were purchased from Fisher Scientific (HPLC grade) and either used directly or dried and distilled according to the literature procedures. All air and moisture sensitive reactions were performed under argon atmosphere in oven-dried glassware. Melting points were measured on an Electrothermal MEL-TEMP instrument. Analytical thin-layer-chromatography (TLC) was performed on polyester backed TLC plates 254 (pre-coated, 200  $\mu\text{m}$ , Sorbent Technologies). Column chromatography was performed on silica gel (Sorbent Technologies, 60  $\text{\AA}$ , 40-63  $\mu\text{m}$ ) slurry packed into glass columns.  $^1\text{H}$  NMR and  $^{13}\text{C}$  NMR spectra were recorded using a Bruker DPX-400 spectrometer (operating at 400MHz for  $^1\text{H}$  NMR and 100 MHz for  $^{13}\text{C}$  NMR) in  $\text{CDCl}_3$  (7.26 ppm,  $^1\text{H}$  and 77.0 ppm,  $^{13}\text{C}$ ),  $(\text{CD}_3)_2\text{CO}$  (2.05 ppm,  $^1\text{H}$  and 29.84 ppm and 206.26 ppm,  $^{13}\text{C}$ ) and  $(\text{CD}_3)_2\text{SO}$  (2.50 ppm,  $^1\text{H}$  and 39.52 ppm,  $^{13}\text{C}$ ). Chemical shifts are given in parts per millions (ppm) relative to tetramethylsilane (TMS, 0 ppm); multiplicities are indicated as br (broad), s (singlet), d (doublet), t (triplet), q (quartet) and m (multiplet). All spectra were recorded at 298 K and coupling constants ( $J$  values) are given in Hz. High resolution mass spectra were obtained at the LSU Department of Chemistry Mass Spectrometry Facility using Bruker Omiflex MALDI Time-of-Flight Mass Spectrometer. The absorption measurements were carried out on a Varian

Cary 50 UV/Vis spectrophotometer and the steady-state fluorescence spectroscopic studies were performed on a PTI Quantum Master4/2006SE spectrofluorometer. All spectras were recorded at 298 K using non-degassed samples, spectroscopic grade solvents and a 10 mm quartz cuvette.

#### 4.5.2: Syntheses

##### 4-(prop-2-ynyloxy)-benzaldehyde (**2**)

4-hydroxybenzaldehyde, **1**, (3.00 g, 24.6 mmol) and propargyl bromide (11.70 g, 98.3 mmol, 4 equiv.) were added to a solution of potassium carbonate (13.58 g, 98.3 mmol) in 150 mL acetone. The reaction mixture was heated to reflux overnight and then cooled to room temperature. The heterogeneous solution was filtered off to remove solid potassium carbonate and the solvent was removed under reduced pressure. The crude product was dissolved in dichloromethane (30 mL) and washed successively with water (2 x 30 mL), 5% NaHCO<sub>3</sub> (1 x 30 mL) and brine (1 x 30 mL). The organic extracts were combined, dried over Na<sub>2</sub>SO<sub>4</sub> and concentrated under vacuum. The resulting crude product was purified by column chromatography using pure dichloromethane as the eluent to afford 3.70 g of the compound **2** as pale yellow solid (quantitative). m.p. 77-78°C; <sup>1</sup>H NMR (400 MHz, CDCl<sub>3</sub>) δ; 9.90 (s, 1H), 7.84 (d, *J* = 8.4 Hz, 2H), 7.09 (d, *J* = 8.4 Hz, 2H), 4.78 (d, *J* = 2.4 Hz, 2H), 2.57 (t, *J* = 2.4 Hz, 1H); MALDI-TOF *m/z* 161.059; calcd. for C<sub>10</sub>H<sub>9</sub>O<sub>2</sub>: 161.16.

##### BODIPY **4**

Kryptopyrrole, **3** (1.0 g, 8.1168 mmole, 2 equiv.) and compound **2** (0.6490 g, 4.0584 mmol, 1 equiv.) were dissolved in dry dichloromethane (80 mL) under the inert gas atmosphere. Three drops of trifluoroacetic acid were added and the reaction mixture was stirred overnight at room temperature. When the aldehyde was consumed (monitored by TLC), a solution of DDQ (0.9212 g, 4.0584 mmole, 1.2 equiv.) in dry dichloromethane (10 mL) was added via syringe at 0°C.

After stirring for 20 min at room temperature, triethylamine (4 mL, 7 equiv.) was added dropwise over a period of 5 min and reaction mixture was stirred for another 30 min at room temperature. Further, BF<sub>3</sub> Et<sub>2</sub>O (5.6 mL, 11 equiv.) was added dropwise at 0 °C over a period of 10 min and the mixture was stirred for 10h at room temperature. Once TLC indicated reaction completion, the reaction mixture was passed through a short pad of silica gel to get rid of the oxidized dipyrromethene derivatives and starting materials. The solvent was removed under reduced pressure and the residue was taken up in dichloromethane (30 mL) and kept for overnight stirring at room temperature to decompose any unreacted BF<sub>3</sub> Et<sub>2</sub>O. The subsequent reaction mixture was extracted with 0.1M HCl (2 x 30mL) to remove excess DDQ, brine (1 x 30 mL) and dried over Na<sub>2</sub>SO<sub>4</sub>. The organic extracts were collected, dried over Na<sub>2</sub>SO<sub>4</sub> and the solvent was evaporated. The crude product was purified by column chromatography using petroleum ether/dichloromethane (1/1, v/v) as eluent. The orange-green fluorescent fraction containing the desired BODIPY **4** was collected and recrystallized from dichloromethane/hexane mixtures to yield the title compound as lustrous orange-red solid. Yield: 1.656 g, 94%. <sup>1</sup>H NMR (400 MHz, CDCl<sub>3</sub>) δ; 7.19 (d, *J* = 8.8 Hz, 2H), 7.08 (d, *J* = 8.8 Hz, 2H), 4.76 (d, *J* = 2.0 Hz, 2H), 2.56 (d, *J* = 2.0 Hz, 1H), 2.53 (s, 6H), 2.29 (q, *J* = 7.6Hz, 4H), 1.33(s, 6H), 0.98 (t, *J* = 7.6 Hz, 6H); <sup>13</sup>C NMR (100 MHz, CDCl<sub>3</sub>) δ; 157.9, 153.6, 139.9, 138.4, 132.7, 129.5, 128.8, 115.5, 78.1, 75.8, 56.0, 17.0, 14.6, 12.4, 11.8; MALDI-TOF *m/z* 434.33; calcd. for C<sub>26</sub>H<sub>29</sub>BF<sub>2</sub>N<sub>2</sub>O: 434.23.

### **BODIPYs 6 and 7**

BODIPY **4** (0.3123 g, 0.7190 mmol) and indole-3-carbaldehyde, **5** (0.3131 g, 2.157 mmol, 3 equiv.) were added to a 150 mL single necked round bottom flask containing a mixture of dry toluene (50 ml), piperidine (0.4 ml) and glacial acetic acid (0.4 ml). The mixture was refluxed and any water formed during the reaction was removed azeotropically by using a Dean-Stark

trap. After completion of the reaction (monitored via thin-layer chromatography), the mixture was cooled to room temperature and the solvent was removed under reduced pressure. The residue was purified by silica gel column chromatography using dichloromethane/petroleum ether (2/1, v/v) as eluent.

**(BODIPY 6):** The first fraction with red fluorescence was dried in vacuo, affording BODIPY 6 as a red-blue solid (145 mg, yield 36%).  $^1\text{H}$  NMR (400 MHz,  $(\text{CD}_3)_2\text{CO}$ ):  $\delta$ ; 10.72 (s, NH), 8.16 (m, 1H), 7.91 (d,  $J = 8.1$  Hz, 1H), 7.74 (d, 1H), 7.65 (d,  $J = 8.1$  Hz, 1H), 7.49–7.51 (m, 2H), 7.20–7.32 (m, 6H), 4.89 (d,  $J = 2.0$  Hz, 2H), 3.13 (t,  $J = 2.0$  Hz, 1H), 2.69 (q,  $J = 7.6$  Hz, 2H), 2.56 (s, 3H), 2.36 (q,  $J = 7.6$  Hz, 2H), 1.41 (s, 3H), 1.38 (s, 3H), 1.19 (t,  $J = 7.6$  Hz, 3H), 0.99 (t,  $J = 7.6$  Hz, 3H);  $^{13}\text{C}$  NMR (100MHz,  $(\text{CD}_3)_2\text{CO}$ ):  $\delta$ ; 158.3, 152.1, 151.4, 129.8, 128.7, 128.2, 125.3, 122.5, 120.9, 120.7, 120.2, 115.8, 115.7, 115.6, 112.0, 78.5, 76.4 55.7, 18.0, 16.6, 14.1, 13.5, 11.8, 11.1, 10.9; MALDI-TOF  $m/z$  561.28; calc. for  $\text{C}_{35}\text{H}_{34}\text{BF}_2\text{N}_3\text{O}$ : 561.35.

**(BODIPY 7):** The second fraction with green fluorescence was dried in vacuo, affording BODIPY 7 as a green solid (0.275 g, yield 55.6%).  $^1\text{H}$  NMR (400 MHz,  $(\text{CD}_3)_2\text{CO}$ ):  $\delta$ ; 10.70 (br, 2H), 8.30 (d,  $J = 8.1$  Hz, 2H), 8.05 (d,  $J = 8.1$  Hz, 2H), 7.69 (m, 4H), 7.51 (d,  $J = 2.0$  Hz, 2H), 7.20–7.35 (m, 8H), 4.88 (d,  $J = 2.0$  Hz, 2H), 3.09 (s, 1H), 2.73 (q,  $J = 7.6$  Hz, 4H), 1.42 (s, 6H), 1.22 (t,  $J = 7.6$  Hz, 6H);  $^{13}\text{C}$  NMR (100 MHz,  $(\text{CD}_3)_2\text{CO}$ )  $\delta$ ; 184.3, 137.7, 137.0, 132.7, 130.2, 129.9, 128.4, 125.3, 124.6, 123.5, 122.5, 122.1, 121.3, 121.0, 120.5, 116.3, 116.0, 115.5, 112.0, 76.3, 55.7, 18.1, 13.5, 10.9; MALDI-TOF  $m/z$  688.36; calcd. for  $\text{C}_{44}\text{H}_{39}\text{BF}_2\text{N}_4\text{O}$ : 688.32.

### General procedure for click chemistry

Meso-alkynylphenyl-BODIPY (40 mg), azido-compound (2.6 equiv) and Cu (0) (1.0 equiv) were dissolved in a mixture of THF:H<sub>2</sub>O (8 mL, 3:1), under inert gas atmosphere. Next, a solution of CuSO<sub>4</sub>·5H<sub>2</sub>O (0.20 equiv) and Na-ascorbate (0.5 equiv.) in THF:H<sub>2</sub>O (8 mL, 3:1) was added (after sonication for 10 min) and the reaction mixture was heated for 6 h at 70°C. Once the

reaction was complete, the mixture was cooled to room temperature and partitioned between EtOAc (30 mL) and water (30 mL). The aqueous layer was re-extracted with EtOAc (2 x 30 mL) and the combined organic layers were dried over Na<sub>2</sub>SO<sub>4</sub> and the solvent was evaporated under reduced pressure. The crude product was then purified by preparative thin layer chromatography to obtain the desired product.

**(9a):** Eluent: Dichloromethane/EtOAc (10/1, v/v); Yield: 36.7 mg, 70%. <sup>1</sup>H NMR (400 MHz, (CD<sub>3</sub>)<sub>2</sub>CO): δ; 10.72 (s, NH), 8.16 (m, 2H), 7.92 (d, J = 8.1 Hz, 1H), 7.75 (s, 1H), 7.65 (d, J = 8.1 Hz, 1H), 7.50–7.52 (m, 2H), 7.22–7.33 (m, 6H), 4.60 (d, J = 2.0 Hz, 2H), 3.50–3.94 (m, 13H), 2.69 (q, J = 7.6 Hz, 2H), 2.55 (s, 3H), 2.36 (q, J = 7.6 Hz, 2H), 2.05 (s, 3H), 1.43 (s, 3H), 1.39 (s, 3H), 1.20 (t, J = 7.6 Hz, 3H), 1.00 (t, J = 7.6 Hz, 3H); <sup>13</sup>C NMR (100 MHz, (CD<sub>3</sub>)<sub>2</sub>CO): δ 159.3, 152.1, 151.4, 142.9, 139.0, 138.7, 137.8, 137.1, 132.7, 132.4, 132.2, 131.4, 130.3, 129.8, 128.2, 128.1, 125.3, 124.6, 122.5, 120.6, 120.2, 115.8, 115.7, 115.5, 112.0, 72.6, 70.1, 69.1, 61.7, 61.1, 49.8, 18.0, 16.6, 14.1, 13.5, 11.8, 11.1, 11.0; MALDI-TOF m/z 736.47; calcd. for C<sub>41</sub>H<sub>47</sub>BF<sub>2</sub>N<sub>6</sub>O<sub>4</sub>: 736.40.

**(9b):** Eluent: 12% acetone in EtOAc; Yield: 60.5 mg, 98%. <sup>1</sup>H NMR (400 MHz, (CD<sub>3</sub>)<sub>2</sub>CO): δ; 10.72 (s, NH), 8.16 (m, 2H), 7.88 (d, J = 8.1 Hz, 1H), 7.75 (s, 1H), 7.67 (d, J = 8.1 Hz, 1H), 7.50–7.52 (m, 2H), 7.22–7.31 (m, 6H), 4.61 (d, J = 2.0 Hz, 2H), 3.50–3.94 (m, 25H), 2.69 (q, J = 7.6 Hz, 2H), 2.55 (s, 3H), 2.35 (q, J = 7.6 Hz, 2H), 2.05 (s, 3H), 1.43 (s, 3H), 1.39 (s, 3H), 1.19 (t, J = 7.6 Hz, 3H), 1.00 (t, J = 7.6 Hz, 3H); <sup>13</sup>C NMR (100 MHz, (CD<sub>3</sub>)<sub>2</sub>CO): δ 159.3, 152.1, 151.4, 142.8, 139.0, 138.7, 137.8, 137.1, 132.7, 132.4, 132.3, 130.4, 129.8, 128.2, 125.3, 124.6, 122.5, 120.6, 120.2, 115.8, 115.6, 115.5, 112.1, 72.5, 70.2, 70.1, 69.2, 61.8, 61.0, 49.9, 18.0, 16.6, 14.1, 13.5, 11.8, 11.1, 11.0; MALDI-TOF m/z 868.61; calcd. for C<sub>47</sub>H<sub>59</sub>BF<sub>2</sub>N<sub>6</sub>O<sub>7</sub>: 868.48.

**(9c):** Eluent: 12% acetone in EtOAc; Yield: 65.0 mg, quantitative. <sup>1</sup>H NMR (400 MHz, (CD<sub>3</sub>)<sub>2</sub>CO): δ; 10.72 (s, NH), 8.34 (s, 1H), 8.17 (m, 1H), 7.90 (d, J = 8.1 Hz, 1H), 7.75 (s, 1H),

7.65 (d, J = 8.1 Hz, 1H), 7.50–7.52 (m, 2H), 7.22–7.33 (m, 6H), 6.25 (d, J = 9.2 Hz, 1H), 5.75 (t, J = 9.2 Hz, 1H), 5.57 (m, 1H), 5.46 (m, 2H), 5.32 (s, 2H), 4.63 (m, 1H), 4.12–4.27 (m, 2H), 2.72 (q, J = 7.6 Hz, 2H), 2.36 (q, J = 7.6 Hz, 2H), 2.21 (s, 3H), 2.05 (s, 3H), 2.03 (s, 3H), 1.90 (s, 3H), 1.80 (s, 3H), 1.44 (s, 3H), 1.40 (s, 3H), 1.19 (t, J = 7.6 Hz, 3H), 1.00 (t, J = 7.6 Hz, 3H); <sup>13</sup>C NMR (100 MHz, (CD<sub>3</sub>)<sub>2</sub>CO): δ 169.8, 169.6, 169.2, 168.4, 159.1, 151.4, 143.9, 137.8, 137.0, 132.6, 130.3, 129.9, 128.4, 128.1, 125.3, 122.8, 122.5, 120.6, 120.2, 115.8, 115.7, 115.4, 112.0, 85.5, 73.7, 70.9, 68.1, 67.3, 61.6, 61.4, 19.6, 19.5, 19.3, 18.0, 16.6, 14.1, 13.5, 11.8, 11.1, 11.0; MALDI-TOF m/z 934.58; calcd. for C<sub>49</sub>H<sub>53</sub>BF<sub>2</sub>N<sub>6</sub>O<sub>10</sub>: 934.42.

**(10a):** Eluent: Acetone/EtOAc (1/1, v/v); Yield: 8.6 mg, 15%. <sup>1</sup>H NMR (400 MHz, (CD<sub>3</sub>)<sub>2</sub>CO): δ 10.7 (br, 2H), 8.30 (m, 2H), 8.18 (s, 1H), 8.04 (d, J = 8.1 Hz, 2H), 7.76 (d, J = 8.1 Hz, 2H), 7.69 (m, 2H), 7.53 (m, 2H), 7.23–7.36 (m, 8H), 5.30 (s, 2H), 4.62–3.65 (m, 12H), 2.75 (q, J=7.6 Hz, 4H), 1.45 (s, 6H), 1.21 (t, J = 7.6 Hz, 6H); <sup>13</sup>C NMR (100 MHz, (CD<sub>3</sub>)<sub>2</sub>CO): δ 138.0, 137.8, 132.7, 130.2, 129.9, 128.6, 128.4, 125.3, 124.4, 122.4, 121.0, 120.5, 116.3, 116.0, 115.4, 112.0, 72.6, 70.1, 69.2, 61.7, 61.1, 49.8, 18.1, 13.5, 10.9; MALDI-TOF m/z 863.51; calcd. for C<sub>50</sub>H<sub>52</sub>BF<sub>2</sub>N<sub>7</sub>O<sub>4</sub>: 863.42.

**(10b):** Eluent: Acetone/EtOAc (1/1, v/v); Yield: 13.2 mg, 20%. <sup>1</sup>H NMR (400 MHz, (CD<sub>3</sub>)<sub>2</sub>CO): δ 10.7 (br, 2H), 8.30 (m, 2H), 8.18 (s, 1H), 8.03 (m, 2H), 7.23–7.54 (m, 14H), 5.30 (s, 2H), 3.51–4.61 (m, 24H), 2.73 (q, J=7.6 Hz, 4H), 1.38 (s, 6H), 1.15 (t, J = 7.6 Hz, 6H); <sup>13</sup>C NMR (100 MHz, (CD<sub>3</sub>)<sub>2</sub>CO): δ 150.3, 138.0, 137.7, 132.7, 130.2, 129.9, 128.4, 125.3, 124.4, 122.4, 121.0, 120.5, 116.3, 116.0, 115.4, 112.0, 72.5, 70.1, 69.2, 61.8, 61.0, 49.9, 18.1, 13.5, 10.9; MALDI-TOF m/z 995.65; calcd. for C<sub>56</sub>H<sub>64</sub>BF<sub>2</sub>N<sub>7</sub>O<sub>7</sub>: 995.50.

**(10c):** Eluent: Dichloromethane/EtOAc (1/1, v/v); Yield: 40.8 mg, 57.3%. <sup>1</sup>H NMR (400 MHz, (CD<sub>3</sub>)<sub>2</sub>CO): δ 10.70 (brs, 2H), 8.32 (m, 2H), 8.17 (m, 1H), 8.05 (d, J = 8.1 Hz, 2H), 7.67–7.77 (m, 4H), 7.54 (m, 2H), 7.23–7.36 (m, 8H), 6.25 (d, J = 9.1 Hz, 1H), 5.77 (t, J = 9.2 Hz, 1H), 5.57

(m, 1H), 5.46 (m, 1H), 5.31 (s, 2H), 4.63 (m, 1H), 4.13-4.28 (m, 2H), 2.73 (q, J=7.6 Hz, 4H), 2.21 (s, 3H), 2.05 (s, 3H), 2.03 (s, 3H), 1.96 (s, 3H), 1.44 (s, 6H), 1.20 (t, J = 7.6 Hz, 6H); <sup>13</sup>C NMR (100 MHz, (CD<sub>3</sub>)<sub>2</sub>CO): δ 184.4, 169.8, 169.7, 169.2, 168.4, 159.1, 150.3, 143.9, 138.0, 137.8, 137.1, 136.1, 132.7, 130.3, 129.8, 128.8, 128.5, 128.3, 125.3, 123.6, 122.9, 122.5, 122.1, 121.3, 121.07, 120.5, 116.3, 116.07, 116.02, 115.4, 112.1, 85.5, 73.7, 70.9, 68.1, 67.4, 61.6, 61.4, 19.69, 19.61, 19.3, 18.1, 13.5, 10.9; MALDI-TOF m/z 1061.65; calcd. for C<sub>58</sub>H<sub>58</sub>BF<sub>2</sub>N<sub>7</sub>O<sub>10</sub>: 1061.40.

**(10d):** Eluent: Acetone/EtOAc (1/1, v/v); Yield: 10.8 mg, 18.2%. <sup>1</sup>H NMR (400 MHz, (CD<sub>3</sub>)<sub>2</sub>SO): δ 10.7 (br, 2H), 8.48 (s, 1H), 8.08 (m, 2H), 7.80 (m, 4H), 7.54 (m, 4H), 7.13-7.32 (m, 8H), 5.56 (m, 2H), 5.23 (s, 2H), 5.01 (m, 2H), 4.45 (m, 1H), 4.13-4.28 (m, 2H), 3.31 (m, 2H), 2.66 (m, 2H), 1.38 (s, 6H), 1.15 (t, J = 7.6 Hz, 6H); MALDI-TOF m/z 893.39; calcd. for C<sub>50</sub>H<sub>50</sub>BF<sub>2</sub>N<sub>7</sub>O<sub>6</sub>: 893.42.

**(10e):** Eluent: Acetone/EtOAc (3/2, v/v); Yield: 15.8 mg, 22.5%. <sup>1</sup>H NMR (400 MHz, (CD<sub>3</sub>)<sub>2</sub>SO): 11.7 (br, 2H), 8.49 (s, 1H), 8.08 (m, 2H), 7.80 (m, 4H), 7.54 (m, 4H), 7.23 (m, 8H), 5.62 (m, 2H), 5.23 (s, 2H), 4.94 (m, 2H), 3.49-4.67 (m, 17H), 2.66 (m, 4H), 1.22 (s, 6H), 1.15 (t, J = 7.6 Hz, 6H); MALDI-TOF m/z 1055.62; calcd. for C<sub>56</sub>H<sub>60</sub>BF<sub>2</sub>N<sub>7</sub>O<sub>11</sub>: 1055.45.

## **BODIPY 15**

Kryptopyrrole (1.0 g, 8.1168 mmole, 2 equiv.) and *p*-Bromobenzaldehyde (0.7508 g, 4.0584 mmol, 1 equiv.) were dissolved in dry dichloromethane (80 mL) under the inert gas atmosphere. Three drops of trifluoroacetic acid were added and the reaction mixture was stirred overnight at room temperature. When the aldehyde was consumed (monitored by TLC), a solution of DDQ (0.9212 g, 4.0584 mmole, 1 equiv.) in dry dichloromethane (10mL) was added via syringe at 0°C. After stirring for 20 min at room temperature, triethylamine (4 mL, 7 equiv.) was added dropwise over a period of 5 min and reaction mixture was stirred for another 30 min at room

temperature. Further,  $\text{BF}_3 \cdot \text{Et}_2\text{O}$  (5.6 mL, 11 equiv.) was added dropwise at  $0^\circ\text{C}$  over a period of 10 min and the mixture was stirred for 3h at room temperature. Once TLC indicated reaction completion, the solvent was removed under reduced pressure and the residue was taken up in dichloromethane (30 mL) and extracted with 0.1M HCl (2 x 30mL) to remove excess DDQ, brine (1 x 30 mL) and dried over  $\text{Na}_2\text{SO}_4$ . The organic extracts were collected, dried over  $\text{Na}_2\text{SO}_4$  and the solvent was evaporated. The crude product was purified by column chromatography using petroleum ether/dichloromethane (1/1, v/v) as eluent. The red-orange fluorescent fraction containing the desired BODIPY **15** was collected and recrystallized from dichloromethane/hexane mixtures to yield title compound as lustrous green solid. Yield: 1.690 g, 91%.  $^1\text{H}$  NMR (400 MHz,  $\text{CDCl}_3$ ):  $\delta$  7.63 (m, 2H), 7.19 (m, 2H), 2.53 (s, 6H), 2.31(q,  $J = 7.6\text{Hz}$ , 4H), 1.32 (s, 6H), 0.98 (t,  $J = 7.6\text{ Hz}$ , 6H);  $^{13}\text{C}$  NMR (100 MHz,  $\text{CDCl}_3$ ):  $\delta$  154.1, 138.4, 138.1, 134.8, 133.0, 132.3, 130.5, 130.1, 123.0, 17.0, 14.5, 12.5, 11.9; MALDI-TOF  $m/z$  458.13; calcd. for  $\text{C}_{23}\text{H}_{26}\text{BBrF}_2\text{N}_2$ : 458.136.

### **BODIPY 16**

BODIPY **15** (1g, 2.48 mmol ) and compound **2** (8.0 g, 49.6 mmol, 20 equiv.) were added to a 150 mL single necked round bottom flask containing a mixture of dry toluene (50 mL), piperidine (2 mL) and glacial acetic acid (2 mL). The mixture was refluxed and any water formed during the reaction was removed azeotropically by using a Dean-Stark trap. After completion of the reaction (monitored via thin-layer chromatography), the mixture was cooled to room temperature and the solvent was removed under reduced pressure. The residue was purified by silica gel column chromatography using petroleum ether/dichloromethane (1/2, v/v) as eluent. The pink fluorescent fraction was collected, evaporated to dryness and recrystallized from dichloromethane/hexane mixtures to yield BODIPY **16** as lustrous solid. Yield: 238mg, 16%.  $^1\text{H}$  NMR (400 MHz,  $\text{CDCl}_3$ ):  $\delta$  7.64 (d,  $J = 8.0\text{ Hz}$ , 2H), 7.54-7.59 (m, 3H, 2H for ArH, 1H for



vinyllic), 7.19-7.21 (m, 3H, 2H for Ar H, 1H for vinyllic), 6.98 (d, J = 8.0 Hz, 2H), 4.72 (d, J = 2.3 Hz, 2H), 2.57 (m, 6H), 2.32 (q, J = 7.6Hz, 2H), 1.35 (s, 3H), 1.33 (s, 3H), 1.14 (t, J = 7.6 Hz, 3H), 0.99 (t, J = 7.6 Hz, 3H); <sup>13</sup>C NMR(100 MHz, CDCl<sub>3</sub>): δ 157.9, 155.5, 149.7, 142.2, 142.1, 138.4, 137.5, 134.9, 133.8, 132.3, 131.5, 130.2, 130.1, 128.9, 123.2, 121.3, 117.7, 117.5, 115.3, 78.2, 75.7, 55.9, 14.8, 14.6, 14.5, 12.5, 11.7, 10.9; MALDI-TOF m/z 600.18; calcd. for C<sub>33</sub>H<sub>32</sub>BBrF<sub>2</sub>N<sub>2</sub>O: 600.20.

#### **4.5.3: Steady-state Absorption and Fluorescence Spectroscopy**

All absorption spectra were recorded on a Varian Cary 50 UV/Vis spectrophotometer. All solvents used were HPLC grade and all studies were performed using non-degassed samples. Steady-state emission spectra were obtained on a PTI Quantum Master4/2006SE spectrofluorimeter. For the fluorescence experiments, only dilute solutions with the optical density between 0.04-0.06 at the excitation wavelength were used. All measurements were carried out at room temperature within 2 h of solution preparation, using a 10 mm path length spectrophotometric cell.

**4.5.4: Cellular Studies.** Human carcinoma HEp2 cells were maintained in a 50:50 mixture of DMEM:Advanced MEM (Invitrogen) supplemented with 5% FBS (Invitrogen), 1% Primocin antibiotic (Invitrogen) in a humidified, 5% CO<sub>2</sub> incubator at 37°C. The cells were sub-cultured biweekly to maintain sub-confluent stocks. The fourth to fifteenth passage cells were used for all the experiments.

*4.5.4.1: Time-Dependent Cellular Uptake.* The HEp2 cells were plated at 7500 cells per well in a Costar 96-well plate and allowed to grow for 48 h. Compound stock solutions were prepared at 32 mM in DMSO and Cremophor (1% of Cremophor EL in DMSO). Further dilution into the

cells of the 96-well plate gave a final concentration of 10  $\mu\text{M}$  with maximum DMSO concentration of 1% and Cremophor concentration of 0.1%. For the uptake test, the compounds were diluted to 20  $\mu\text{M}$  (2 x stock solution) and added to the 96-well plate to give a final concentration of 10  $\mu\text{M}$  at 0, 1, 2, 4, 8, 12 and 24h interval. The uptake was terminated by removing the loading medium and washing the wells with PBS (Phosphate buffer saline). The cells were then solubilized using 100  $\mu\text{L}$  of 0.25% Triton X-100 (Calbiochem) in PBS. The concentration of the compounds was measured using intrinsic fluorescence as measured with a BMG FLUOstar plate reader equipped with a 355 nm excitation and a 650 nm emission filter. The cells were measured using a CyQuant cell proliferation assay (Invitrogen) as per manufactures' instructions, and the uptake was expressed in terms of nM compound per cell.

*4.5.4.2: Dark Cytotoxicity.* The HEP2 cells were plated as described above for the uptake experiment and allowed 36-48 h to attach. The cells were exposed to increasing concentrations of BODIPYs up to 100  $\mu\text{M}$  and incubated overnight. After compound loading overnight, the loading medium was removed, and the cells were fed medium containing CellTiter Blue (Promega) as per manufacturer's instructions. Cytotoxicity was then measured with untreated cells considered as 100% viable and cells treated with 0.2% saponin as 0% viable. The  $\text{IC}_{50}$  values were determined from dose-response curves obtained using GraphPad Prism software.

*4.5.4.3: Phototoxicity.* The cells were prepared as described above for the dark cytotoxicity assay with compounds concentration range from 6.25 to 100  $\mu\text{M}$ . After loading overnight, the medium was removed and replaced with medium containing 50 mM HEPES pH 7.4. The cells were exposed to a 175 W halogen lamp filters through a 610 nm long pass filter to provide approximately 1.5  $\text{Jcm}^{-2}$  light dose. The cells were kept cool by placing the culture on a 5°C Echotherm chilling/heating plate (Torrey Pines Scientific, Inc.). After exposure to light for 20

min, the plate was incubated overnight in a 37°C incubator. Cells were assayed for viability using CellTitre Blue Viability Assay Kit, as described above for the dark cytotoxicity experiment.

#### 4.6: References

1. Joshi, B. P.; Wang, T. D., Exogenous Molecular Probes for Targeted Imaging in Cancer: Focus on Multi-modal Imaging. *Cancers* **2010**, 2 (2), 1251-1287.
2. Rudin, M.; Weissleder, R., Molecular imaging in drug discovery and development. *Nature reviews. Drug discovery* **2003**, 2 (2), 123-31.
3. Kobayashi, H.; Ogawa, M.; Alford, R.; Choyke, P. L.; Urano, Y., New strategies for fluorescent probe design in medical diagnostic imaging. *Chem Rev* **2010**, 110 (5), 2620-40.
4. He, X.; Wang, K.; Cheng, Z., In vivo near-infrared fluorescence imaging of cancer with nanoparticle-based probes. *Wiley interdisciplinary reviews. Nanomedicine and nanobiotechnology* **2010**, 2 (4), 349-66.
5. Rao, J.; Dragulescu-Andrasi, A.; Yao, H., Fluorescence imaging in vivo: recent advances. *Current opinion in biotechnology* **2007**, 18 (1), 17-25.
6. Alexis, F.; Pridgen, E.; Molnar, L. K.; Farokhzad, O. C., Factors affecting the clearance and biodistribution of polymeric nanoparticles. *Mol Pharm* **2008**, 5 (4), 505-15.
7. Niu, S. L.; Ulrich, G.; Ziessel, R.; Kiss, A.; Renard, P. Y.; Romieu, A., Water-soluble BODIPY derivatives. *Organic letters* **2009**, 11 (10), 2049-52.
8. Zhu, S.; Zhang, J.; Vegesna, G.; Luo, F.-T.; Green, S. A.; Liu, H., Highly Water-Soluble Neutral BODIPY Dyes with Controllable Fluorescence Quantum Yields. *Organic letters* **2010**, 13 (3), 438-441.
9. (a) Peneva, K.; Mihov, G.; Nolde, F.; Rocha, S.; Hotta, J.; Braeckmans, K.; Hofkens, J.; Uji-i, H.; Herrmann, A.; Mullen, K., Water-soluble monofunctional perylene and terrylene dyes: powerful labels for single-enzyme tracking. *Angew Chem Int Ed Engl* **2008**, 47 (18), 3372-5; (b) Reddington, M. V., Synthesis and properties of phosphonic acid containing cyanine and squaraine dyes for use as fluorescent labels. *Bioconjug Chem* **2007**, 18 (6), 2178-90; (c) Wang, H.; Lu, Z.; Lord, S. J.; Moerner, W. E.; Twieg, R. J., Modifications of DCDHF single molecule fluorophores to impart water solubility. *Tetrahedron Lett* **2007**, 48 (19), 3471-3474.
10. (a) Goussu, C.; Vasseur, J. J.; Bazin, H.; Trinquet, E.; Maurin, F.; Morvan, F., Optimized synthesis of functionalized fluorescent oligodeoxynucleotides for protein labeling. *Bioconjug Chem* **2005**, 16 (2), 465-70; (b) Katritzky, A. R.; Cusido, J.; Narindoshvili, T., Monosaccharide-based water-soluble fluorescent tags. *Bioconjug Chem* **2008**, 19 (7), 1471-5.

11. (a) Luo, Y.; Prestwich, G. D., Synthesis and selective cytotoxicity of a hyaluronic acid-antitumor bioconjugate. *Bioconjug Chem* **1999**, *10* (5), 755-63; (b) He, H.; Lo, P.-C.; Yeung, S.-L.; Fong, W.-P.; Ng, D. K. P., Synthesis and in Vitro Photodynamic Activities of Pegylated Distyryl Boron Dipyrromethene Derivatives. *Journal of Medicinal Chemistry* **2011**, *54* (8), 3097-3102; (c) He, H.; Lo, P.-C.; Yeung, S.-L.; Fong, W.-P.; Ng, D. K. P., Preparation of unsymmetrical distyryl BODIPY derivatives and effects of the styryl substituents on their in vitro photodynamic properties. *Chemical Communications* **2011**, *47* (16), 4748-4750; (d) Urano, Y.; Asanuma, D.; Hama, Y.; Koyama, Y.; Barrett, T.; Kamiya, M.; Nagano, T.; Watanabe, T.; Hasegawa, A.; Choyke, P. L.; Kobayashi, H., Selective molecular imaging of viable cancer cells with pH-activatable fluorescence probes. *Nat Med* **2009**, *15* (1), 104-109.
12. (a) Ojida, A.; Sakamoto, T.; Inoue, M.-a.; Fujishima, S.-h.; Lippens, G.; Hamachi, I., Fluorescent BODIPY-Based Zn(II) Complex as a Molecular Probe for Selective Detection of Neurofibrillary Tangles in the Brains of Alzheimer's Disease Patients. *Journal of the American Chemical Society* **2009**, *131* (18), 6543-6548; (b) Ono, M.; Watanabe, H.; Kimura, H.; Saji, H., BODIPY-Based Molecular Probe for Imaging of Cerebral  $\beta$ -Amyloid Plaques. *ACS Chemical Neuroscience* **2012**, *3* (4), 319-324.
13. Kim, J.-H.; Park, K.; Nam, H. Y.; Lee, S.; Kim, K.; Kwon, I. C., Polymers for bioimaging. *Progress in Polymer Science* **2007**, *32* (8-9), 1031-1053.
14. Veronese, F. M.; Pasut, G., PEGylation, successful approach to drug delivery. *Drug discovery today* **2005**, *10* (21), 1451-8.
15. Sibrian-Vazquez, M.; Jensen, T. J.; Vicente, M. G., Synthesis and cellular studies of PEG-functionalized meso-tetraphenylporphyrins. *Journal of photochemistry and photobiology. B, Biology* **2007**, *86* (1), 9-21.
16. (a) Sibrian-Vazquez, M.; Jensen, T. J.; Vicente, M. G. H., Synthesis and cellular studies of PEG-functionalized meso-tetraphenylporphyrins. *Journal of Photochemistry and Photobiology B: Biology* **2007**, *86* (1), 9-21; (b) Batinic-Haberle, I.; Spasojevic, I.; Stevens, R. D.; Bondurant, B.; Okado-Matsumoto, A.; Fridovich, I.; Vujaskovic, Z.; Dewhirst, M. W., New PEG-ylated Mn(III) porphyrins approaching catalytic activity of SOD enzyme. *Dalton Transactions* **2006**, (4), 617-624; (c) Zhang, J. X.; Hansen, C. B.; Allen, T. M.; Boey, A.; Boch, R., Lipid-derivatized poly(ethylene glycol) micellar formulations of benzoporphyrin derivatives. *Journal of Controlled Release* **2003**, *86* (2-3), 323-338.
17. (a) Durmuş, M.; Ayhan, M. M.; Gürek, A. G.; Ahsen, V., Peripherally alpha( $\alpha$ )-substituted novel phthalocyanines. *Dyes and Pigments* **2008**, *77* (3), 570-577; (b) Li, H.; Fronczek, F. R.; Vicente, M. G., Pegylated Phthalocyanines: Synthesis and Spectroscopic Properties. *Tetrahedron Lett* **2011**, *52* (50), 6675-6678; (c) Bai, M.; Lo, P. C.; Ye, J.; Wu, C.; Fong, W. P.; Ng, D. K., Facile synthesis of pegylated zinc(II) phthalocyanines via transesterification and their in vitro photodynamic activities. *Org Biomol Chem* **2011**, *9* (20), 7028-32.
18. Zhang, J. X.; Hansen, C. B.; Allen, T. M.; Boey, A.; Boch, R., Lipid-derivatized poly(ethylene glycol) micellar formulations of benzoporphyrin derivatives. *J Control Release* **2003**, *86* (2-3), 323-38.

19. (a) Xiao, L.; Zhang, Y.; Liu, Z.; Yang, M.; Pu, L.; Pan, D., Synthesis of the Cyanine 7 labeled neutrophil-specific agents for noninvasive near infrared fluorescence imaging. *Bioorganic & Medicinal Chemistry Letters* **2010**, *20* (12), 3515-3517; (b) Jiang, L.-L.; Dou, L.-F.; Li, B.-L., An efficient approach to the synthesis of water-soluble cyanine dyes using poly(ethylene glycol) as a soluble support. *Tetrahedron Letters* **2007**, *48* (33), 5825-5829.
20. (a) Gopee, N. V.; Roberts, D. W.; Webb, P.; Cozart, C. R.; Siitonen, P. H.; Latendresse, J. R.; Warbitton, A. R.; Yu, W. W.; Colvin, V. L.; Walker, N. J.; Howard, P. C., Quantitative Determination of Skin Penetration of PEG-Coated CdSe Quantum Dots in Dermabraded but not Intact SKH-1 Hairless Mouse Skin. *Toxicological Sciences* **2009**, *111* (1), 37-48; (b) Ballou, B.; Lagerholm, B. C.; Ernst, L. A.; Bruchez, M. P.; Waggoner, A. S., Noninvasive Imaging of Quantum Dots in Mice. *Bioconjugate Chemistry* **2003**, *15* (1), 79-86; (c) Gao, J.; Chen, K.; Xie, R.; Xie, J.; Yan, Y.; Cheng, Z.; Peng, X.; Chen, X., In vivo tumor-targeted fluorescence imaging using near-infrared non-cadmium quantum dots. *Bioconjug Chem* **2010**, *21* (4), 604-9.
21. (a) Cheng, J.; Teply, B. A.; Sherifi, I.; Sung, J.; Luther, G.; Gu, F. X.; Levy-Nissenbaum, E.; Radovic-Moreno, A. F.; Langer, R.; Farokhzad, O. C., Formulation of functionalized PLGA-PEG nanoparticles for in vivo targeted drug delivery. *Biomaterials* **2007**, *28* (5), 869-76; (b) Aktaş, Y.; Yemisci, M.; Andrieux, K.; Gürsoy, R. N.; Alonso, M. J.; Fernandez-Megia, E.; Novoa-Carballal, R.; Quiñoá, E.; Riguera, R.; Sargon, M. F.; Çelik, H. H.; Demir, A. S.; Hincal, A. A.; Dalkara, T.; Çapan, Y.; Couvreur, P., Development and Brain Delivery of Chitosan-PEG Nanoparticles Functionalized with the Monoclonal Antibody OX26. *Bioconjugate Chemistry* **2005**, *16* (6), 1503-1511; (c) Lee, H.; Yu, M. K.; Park, S.; Moon, S.; Min, J. J.; Jeong, Y. Y.; Kang, H. W.; Jon, S., Thermally cross-linked superparamagnetic iron oxide nanoparticles: synthesis and application as a dual imaging probe for cancer in vivo. *Journal of the American Chemical Society* **2007**, *129* (42), 12739-45.
22. (a) Wen, X.; Wu, Q. P.; Lu, Y.; Fan, Z.; Charnsangavej, C.; Wallace, S.; Chow, D.; Li, C., Poly(ethylene glycol)-conjugated anti-EGF receptor antibody C225 with radiometal chelator attached to the termini of polymer chains. *Bioconjug Chem* **2001**, *12* (4), 545-53; (b) Wen, X.; Wu, Q.-P.; Lu, Y.; Fan, Z.; Charnsangavej, C.; Wallace, S.; Chow, D.; Li, C., Poly(ethylene glycol)-Conjugated Anti-EGF Receptor Antibody C225 with Radiometal Chelator Attached to the Termini of Polymer Chains. *Bioconjugate Chemistry* **2001**, *12* (4), 545-553.
23. Davis, B. G.; Robinson, M. A., Drug delivery systems based on sugar-macromolecule conjugates. *Curr Opin Drug Discov Devel* **2002**, *5* (2), 279-88.
24. McCann, T. E.; Kosaka, N.; Mitsunaga, M.; Choyke, P. L.; Gildersleeve, J. C.; Kobayashi, H., Biodistribution and Excretion of Monosaccharide-Albumin Conjugates Measured with in Vivo Near-Infrared Fluorescence Imaging. *Bioconjugate Chemistry* **2010**, *21* (10), 1925-1932.
25. (a) Zheng, X.; Pandey, R. K., Porphyrin-carbohydrate conjugates: impact of carbohydrate moieties in photodynamic therapy (PDT). *Anticancer Agents Med Chem* **2008**, *8* (3), 241-68; (b) hao, E.; Jensen, T. J.; Vicente, M. G., Synthesis of porphyrin-carbohydrate conjugates using "click" chemistry and their preliminary evaluation in human HEP2 cells. *Journal of Porphyrins and Phthalocyanines* **2009**, *13* (1), 51-59.

26. Hein, C.; Liu, X.-M.; Wang, D., Click Chemistry, A Powerful Tool for Pharmaceutical Sciences. *Pharmaceutical Research* **2008**, *25* (10), 2216-2230.
27. Dumoulin, F.; Ahsen, V., ChemInform Abstract: Click Chemistry: The Emerging Role of the Azide—Alkyne Huisgen Dipolar Addition in the Preparation of Substituted Tetrapyrrolic Derivatives. *ChemInform* **2012**, *43* (6), no-no.
28. Meldal, M.; Tornøe, C. W., Cu-Catalyzed Azide—Alkyne Cycloaddition. *Chemical Reviews* **2008**, *108* (8), 2952-3015.
29. Tron, G. C.; Pirali, T.; Billington, R. A.; Canonico, P. L.; Sorba, G.; Genazzani, A. A., Click chemistry reactions in medicinal chemistry: applications of the 1,3-dipolar cycloaddition between azides and alkynes. *Medicinal research reviews* **2008**, *28* (2), 278-308.
30. (a) Asayama, S.; Mizushima, K.; Nagaoka, S.; Kawakami, H., Design of metalloporphyrin-carbohydrate conjugates for a new superoxide dismutase mimic with cellular recognition. *Bioconjug Chem* **2004**, *15* (6), 1360-3; (b) Li, G.; Pandey, S. K.; Graham, A.; Dobhal, M. P.; Mehta, R.; Chen, Y.; Gryshuk, A.; Rittenhouse-Olson, K.; Oseroff, A.; Pandey, R. K., Functionalization of OEP-based benzochlorins to develop carbohydrate-conjugated photosensitizers. Attempt to target beta-galactoside-recognized proteins. *J Org Chem* **2004**, *69* (1), 158-72; (c) Chen, X.; Hui, L.; Foster, D. A.; Drain, C. M., Efficient synthesis and photodynamic activity of porphyrin-saccharide conjugates: targeting and incapacitating cancer cells. *Biochemistry* **2004**, *43* (34), 10918-29; (d) Samaroo, D.; Vinodu, M.; Chen, X.; Drain, C. M., meso-Tetra(pentafluorophenyl)porphyrin as an efficient platform for combinatorial synthesis and the selection of new photodynamic therapeutics using a cancer cell line. *Journal of combinatorial chemistry* **2007**, *9* (6), 998-1011.
31. (a) Sibrian-Vazquez, M.; Jensen, T. J.; Fronczek, F. R.; Hammer, R. P.; Vicente, M. G., Synthesis and characterization of positively charged porphyrin-peptide conjugates. *Bioconjug Chem* **2005**, *16* (4), 852-63; (b) Sibrian-Vazquez, M.; Jensen, T. J.; Hammer, R. P.; Vicente, M. G., Peptide-mediated cell transport of water soluble porphyrin conjugates. *J Med Chem* **2006**, *49* (4), 1364-72.
32. Giguère, J.-B.; Thibeault, D.; Cronier, F.; Marois, J.-S.; Auger, M.; Morin, J.-F., Synthesis of [2]- and [3]rotaxanes through Sonogashira coupling. *Tetrahedron Letters* **2009**, *50* (39), 5497-5500.
33. (a) Kolemen, S.; Bozdemir, O. A.; Cakmak, Y.; Barin, G.; Erten-Ela, S.; Marszalek, M.; Yum, J.-H.; Zakeeruddin, S. M.; Nazeeruddin, M. K.; Gratzel, M.; Akkaya, E. U., Optimization of distyryl-Bodipy chromophores for efficient panchromatic sensitization in dye sensitized solar cells. *Chemical Science* **2011**, *2* (5), 949-954; (b) Atilgan, S.; Kutuk, I.; Ozdemir, T., A near IR di-styryl BODIPY-based ratiometric fluorescent chemosensor for Hg(II). *Tetrahedron Lett* **2010**, *51* (6), 892-894.
34. Lee, J. S.; Kang, N. Y.; Kim, Y. K.; Samanta, A.; Feng, S.; Kim, H. K.; Vendrell, M.; Park, J. H.; Chang, Y. T., Synthesis of a BODIPY library and its application to the development of live cell glucagon imaging probe. *Journal of the American Chemical Society* **2009**, *131* (29), 10077-82.

35. Deniz, E.; Isbasar, G. C.; Bozdemir, O. A.; Yildirim, L. T.; Siemiarczuk, A.; Akkaya, E. U., Bidirectional Switching of Near IR Emitting Boradiazaindacene Fluorophores. *Organic letters* **2008**, *10* (16), 3401-3403.
36. (a) Stefanescu, P. N., [Indole compounds and their biological importance]. *Stud Cercet Fiziol* **1968**, *13* (1), 63-78; (b) Sharma, V.; Kumar, P.; Pathak, D., Biological importance of the indole nucleus in recent years: A comprehensive review. *Journal of Heterocyclic Chemistry* **2010**, *47* (3), 491-502.
37. Li, H.; Jensen, T. J.; Fronczek, F. R.; Vicente, M. G., Syntheses and properties of a series of cationic water-soluble phthalocyanines. *J Med Chem* **2008**, *51* (3), 502-11.
38. (a) Murtagh, J.; Frimannsson, D. O.; O'Shea, D. F., Azide conjugatable and pH responsive near-infrared fluorescent imaging probes. *Organic letters* **2009**, *11* (23), 5386-9; (b) Bakleh, M. E.; Sol, V.; Estieu-Gionnet, K.; Granet, R.; Délérís, G.; Krausz, P., An efficient route to VEGF-like peptide porphyrin conjugates via microwave-assisted 'click-chemistry'. *Tetrahedron* **2009**, *65* (36), 7385-7392.
39. Wang, Q.; Chan, T. R.; Hilgraf, R.; Fokin, V. V.; Sharpless, K. B.; Finn, M. G., Bioconjugation by copper(I)-catalyzed azide-alkyne [3 + 2] cycloaddition. *Journal of the American Chemical Society* **2003**, *125* (11), 3192-3.
40. Shao, F.; Weissleder, R.; Hilderbrand, S. A., Monofunctional Carbocyanine Dyes for Bio- and Bioorthogonal Conjugation. *Bioconjug Chem* **2008**, *19* (12), 2487-2491.
41. Leffler, H.; Carlsson, S.; Hedlund, M.; Qian, Y.; Poirier, F., Introduction to galectins. *Glycoconj J* **2004**, *19* (7-9), 433-40.
42. van Scherpenzeel, M.; Moret, E. E.; Ballell, L.; Liskamp, R. M. J.; Nilsson, U. J.; Leffler, H.; Pieters, R. J., Synthesis and Evaluation of New Thiodigalactoside-Based Chemical Probes to Label Galectin-3. *ChemBioChem* **2009**, *10* (10), 1724-1733.
43. Boens, N.; Leen, V.; Dehaen, W., Fluorescent indicators based on BODIPY. *Chemical Society Reviews* **2012**, *41* (3), 1130-1172.
44. (a) Bartoli, G.; Bosco, M.; Carlone, A.; Dalpozzo, R.; Galzerano, P.; Melchiorre, P.; Sambri, L., ChemInform Abstract: Magnesium Perchlorate as Efficient Lewis Acid for the Knoevenagel Condensation Between  $\beta$ -Diketones and Aldehydes. *ChemInform* **2008**, *39* (30), no-no; (b) Bura, T.; Retailliau, P.; Ulrich, G.; Ziessel, R., Highly substituted Bodipy dyes with spectroscopic features sensitive to the environment. *J Org Chem* **2011**, *76* (4), 1109-17.
45. Buyukcakir, O.; Bozdemir, O. A.; Kolemen, S.; Erbas, S.; Akkaya, E. U., Tetrastaryl-Bodipy Dyes: Convenient Synthesis and Characterization of Elusive Near IR Fluorophores. *Organic letters* **2009**, *11* (20), 4644-4647.
46. Nöll, G.; Daub, J. r.; Lutz, M.; Rurack, K., Synthesis, Spectroscopic Properties, and Electropolymerization of Azulene Dyads. *The Journal of Organic Chemistry* **2011**, *76* (12), 4859-4873.

47. (a) Uppal, T.; Hu, X.; Fronczek, F. R.; Maschek, S.; Bobadova-Parvanova, P.; Vicente, M. G. H., Synthesis, Computational Modeling, and Properties of Benzo-Appended BODIPYs. *Chemistry – A European Journal* **2012**, *18* (13), 3893-3905; (b) Kim, K.; Jo, C.; Easwaramoorthi, S.; Sung, J.; Kim, D. H.; Churchill, D. G., Crystallographic, photophysical, NMR spectroscopic and reactivity manifestations of the "8-heteroaryl effect" in 4,4-difluoro-8-(C(4)H(3)X)-4-bora-3a,4a-diaza-s-indacene (X = O, S, Se) (BODIPY) systems. *Inorganic chemistry* **2010**, *49* (11), 4881-94.
48. Lim, S. H.; Thivierge, C.; Nowak-Sliwinska, P.; Han, J.; van den Bergh, H.; Wagnières, G.; Burgess, K.; Lee, H. B., In Vitro and In Vivo Photocytotoxicity of Boron Dipyrromethene Derivatives for Photodynamic Therapy. *Journal of Medicinal Chemistry* **2010**, *53* (7), 2865-2874.



## APPENDIX A: CHARACTERIZATION DATA FOR COMPOUNDS IN CHAPTER 2

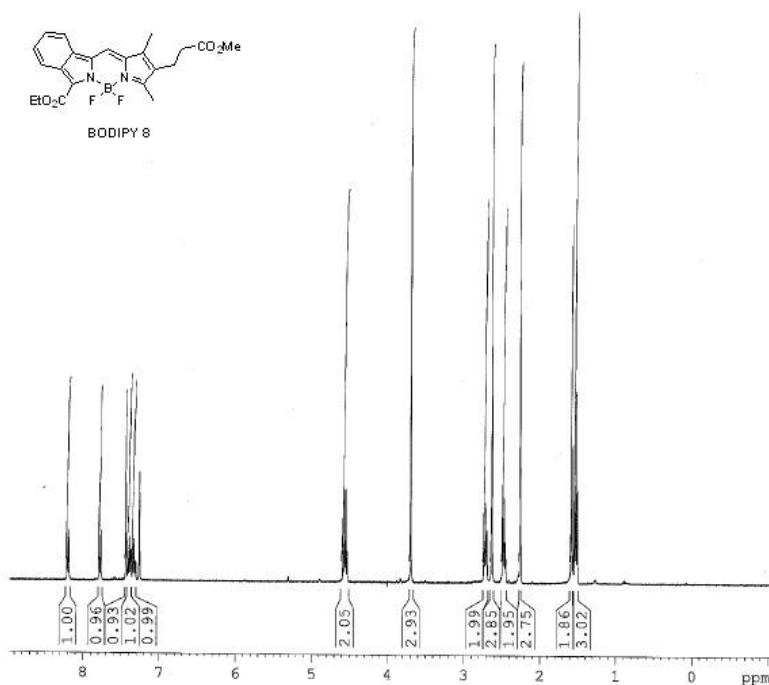


**Figure A.1:**  $^1\text{H-NMR}$  Spectrum of BODIPY **8** in  $\text{CDCl}_3$  at 400 MHz

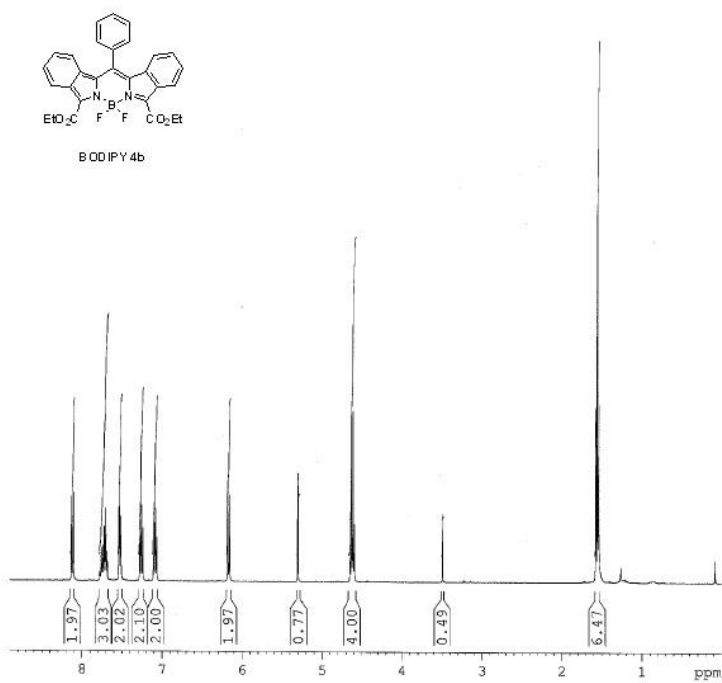


**Figure A.2:**  $^1\text{H-NMR}$  Spectrum of BODIPY **4b** in  $\text{CDCl}_3$  at 400 MHz

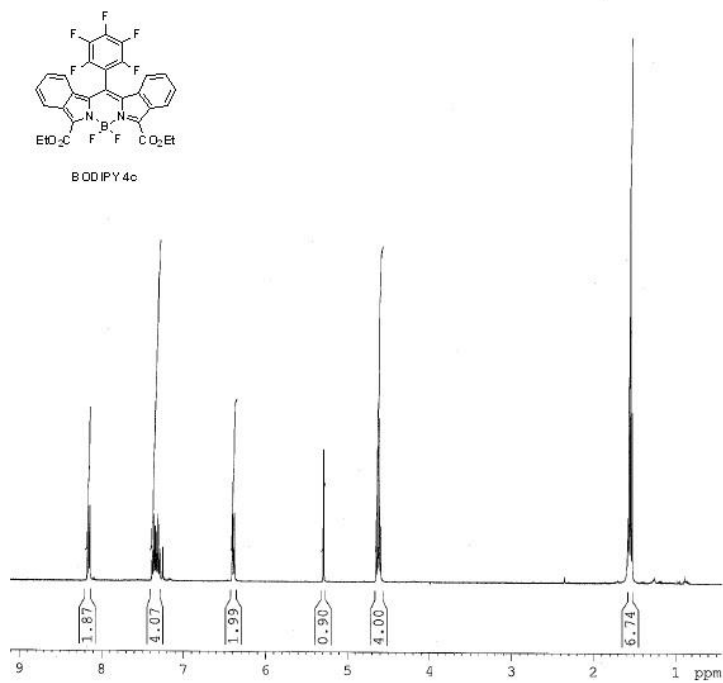


**Figure A.3:** <sup>1</sup>H-NMR Spectrum of BODIPY 4c in CDCl<sub>3</sub> at 400 MHz

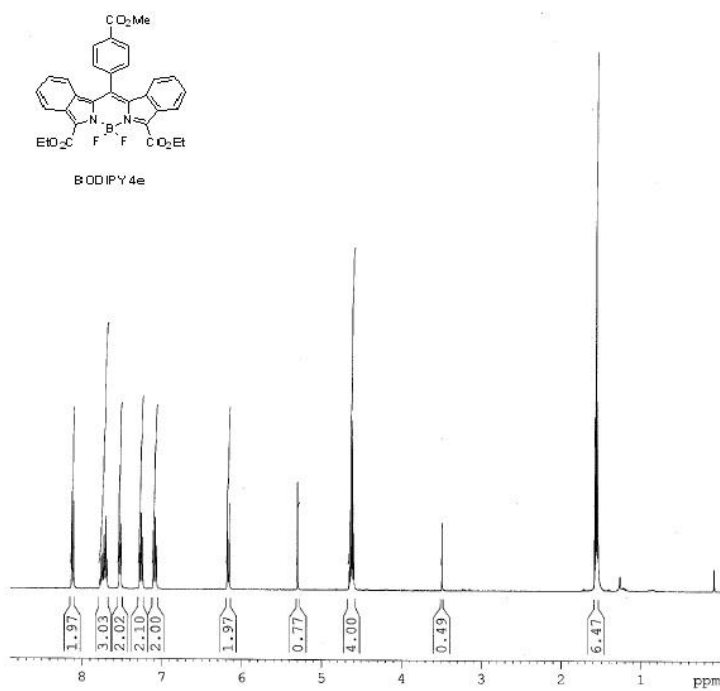


**Figure A.4:** <sup>1</sup>H-NMR Spectrum of BODIPY 4e in CDCl<sub>3</sub> at 400 MHz

## APPENDIX B: CHARACTERIZATION DATA FOR COMPOUNDS IN CHAPTER 3

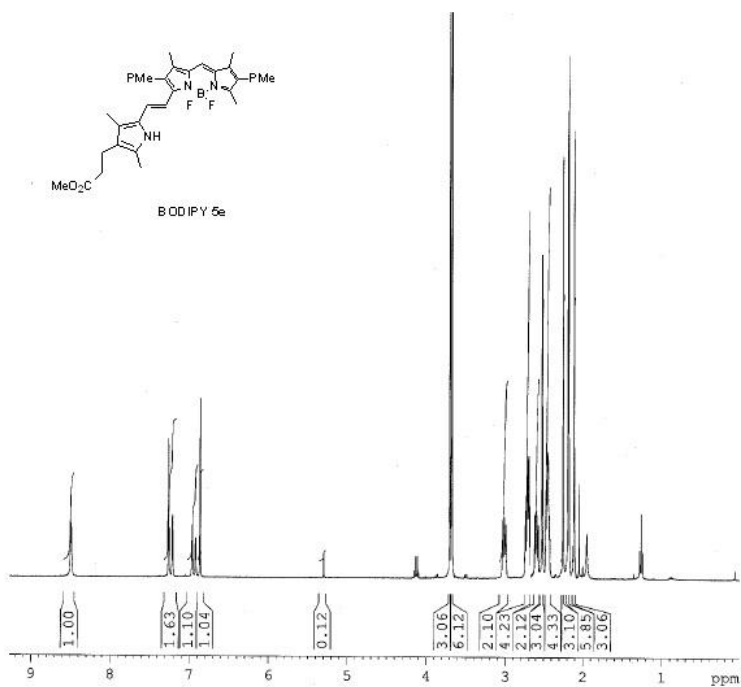


Figure B.1: <sup>1</sup>H-NMR Spectrum of BODIPY 5e in CDCl<sub>3</sub> at 400 MHz

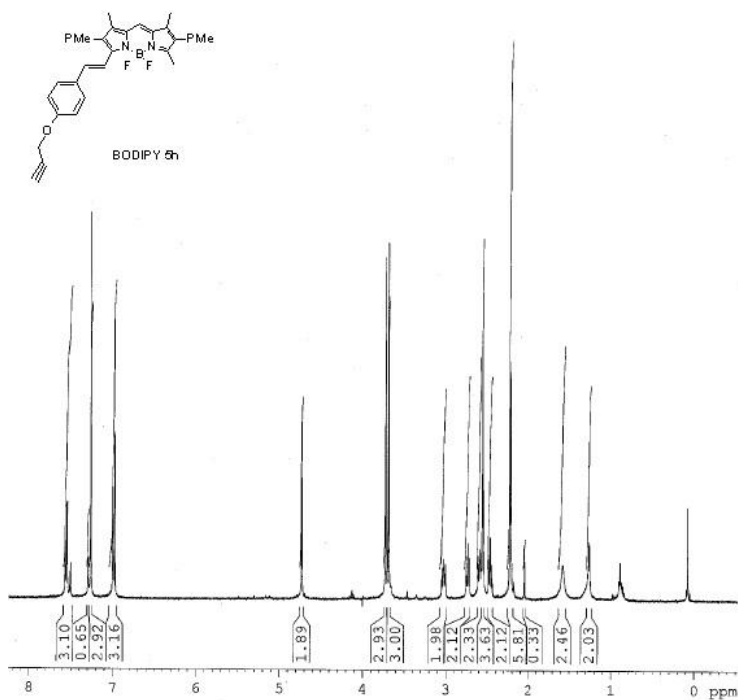
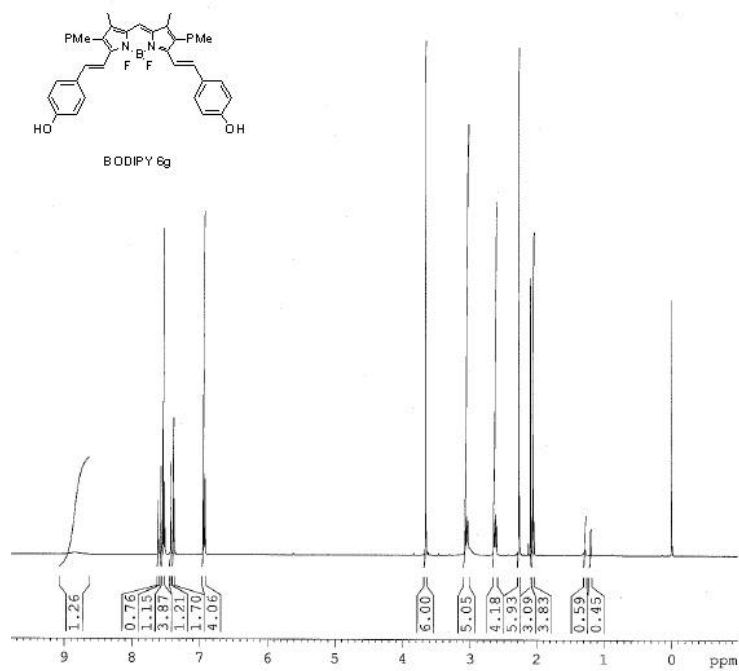
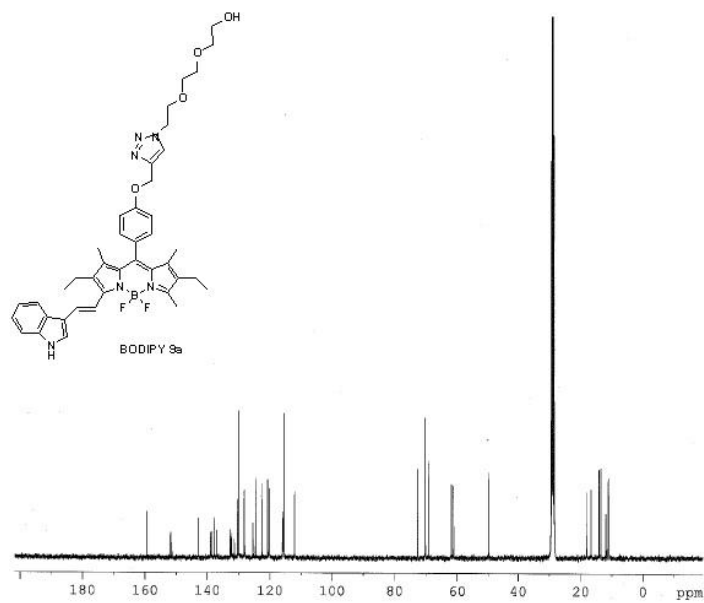


Figure B.2: <sup>1</sup>H-NMR Spectrum of BODIPY 5h in CDCl<sub>3</sub> at 400 MHz



**Figure B.3:** <sup>1</sup>H-NMR Spectrum of BODIPY 6g in deuterated acetone at 400 MHz

## APPENDIX C: CHARACTERIZATION DATA FOR COMPOUNDS IN CHAPTER 4



**Figure C.1:** <sup>13</sup>C-NMR spectrum of BODIPY **9a** in deuterated acetone at 400 MHz

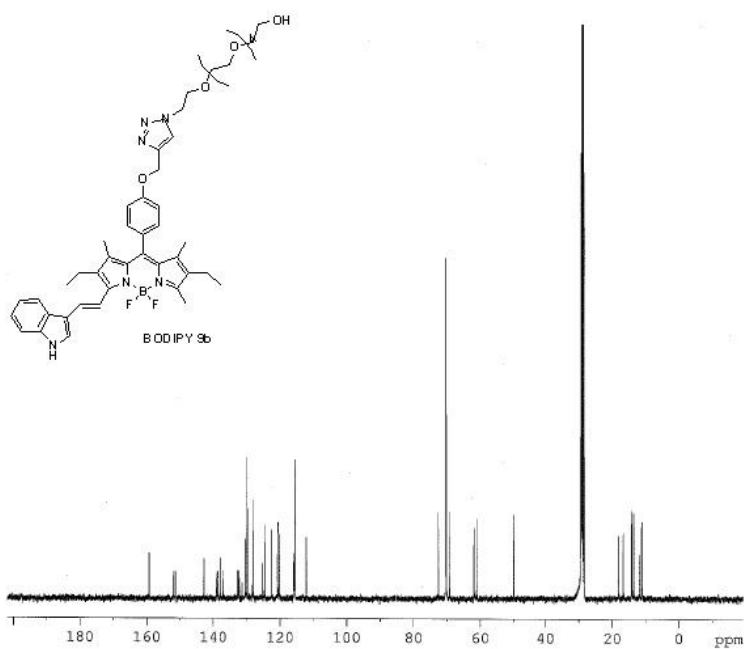


**Figure C.2:** <sup>13</sup>C-NMR spectrum of BODIPY **9b** in deuterated acetone at 400 MHz

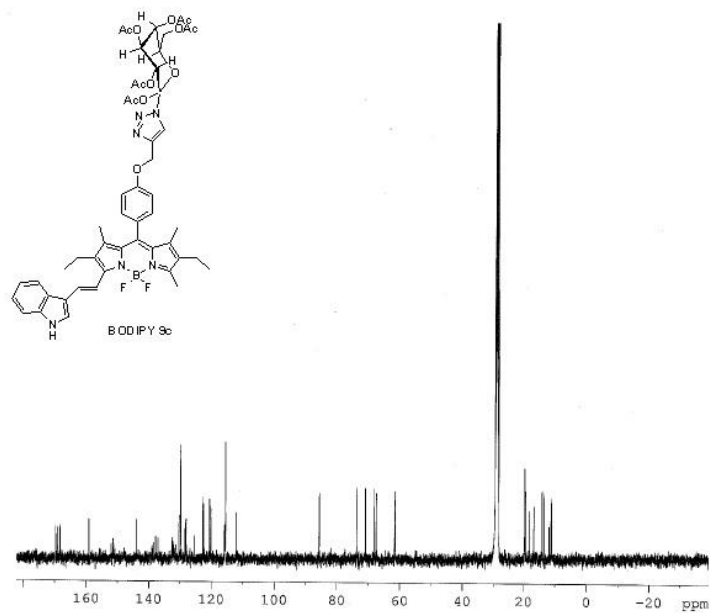


**Figure C.3:**  $^{13}\text{C}$ -NMR spectrum of BODIPY **9c** in deuterated acetone at 400 MHz

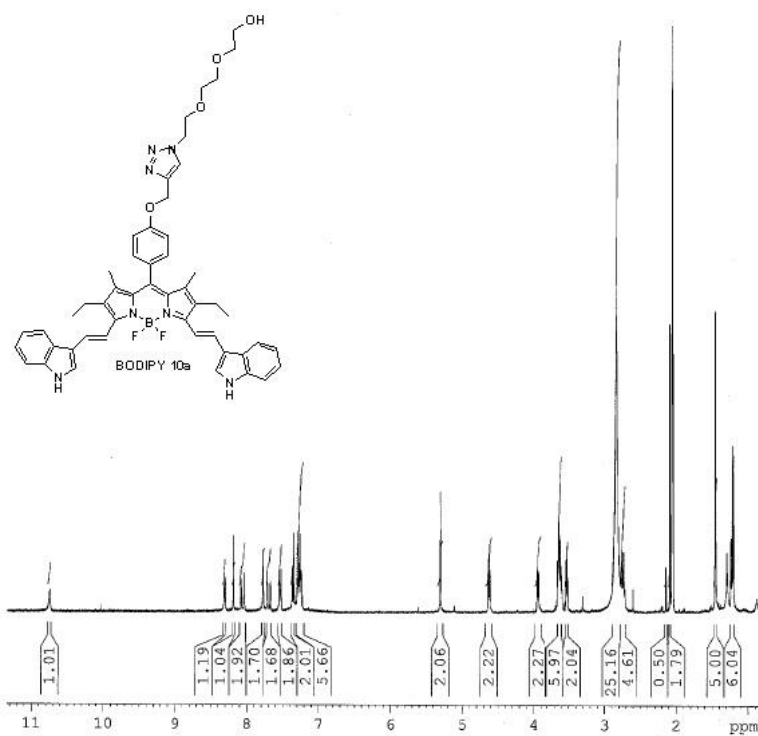


**Figure C.4:**  $^1\text{H}$ -NMR spectrum of BODIPY **10a** in deuterated acetone at 400 MHz

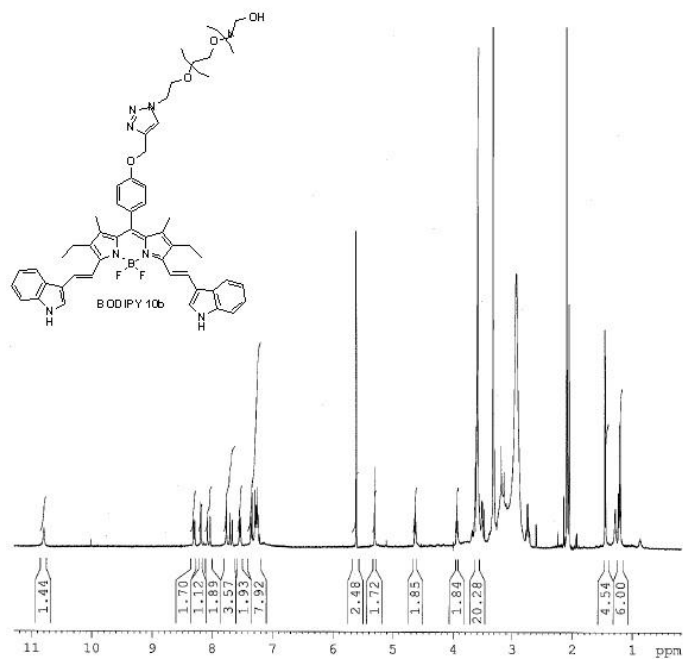


**Figure C.5:**  $^1\text{H}$ -NMR spectrum of BODIPY **10b** in deuterated acetone at 400 MHz

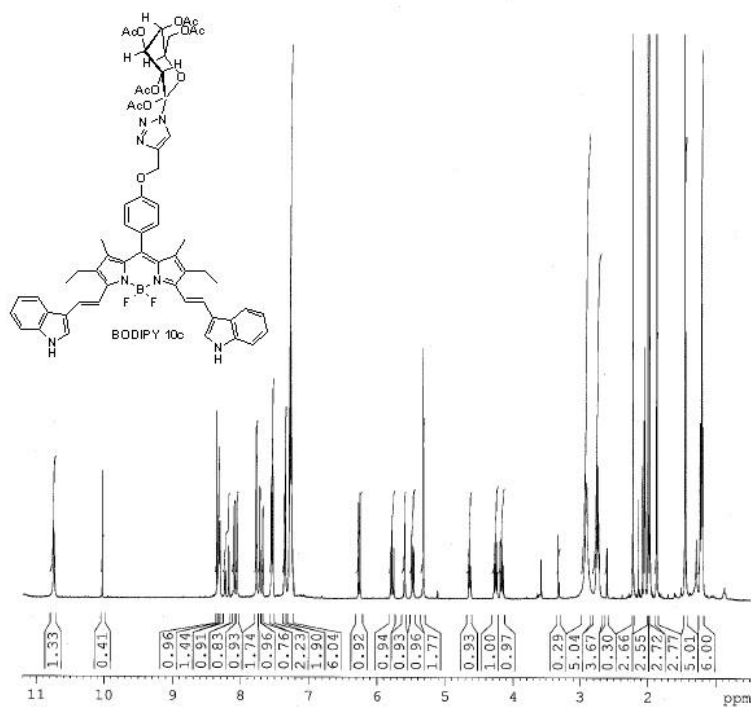


**Figure C.6:**  $^1\text{H}$ -NMR spectrum of BODIPY **10c** in deuterated acetone at 400 MHz

## APPENDIX D: LETTERS OF PERMISSION

Rightslink Printable License

Page 1 of 5

### JOHN WILEY AND SONS LICENSE TERMS AND CONDITIONS

Jun 09, 2012

This is a License Agreement between Timsy K Uppal ("You") and John Wiley and Sons ("John Wiley and Sons") provided by Copyright Clearance Center ("CCC"). The license consists of your order details, the terms and conditions provided by John Wiley and Sons, and the payment terms and conditions.

**All payments must be made in full to CCC. For payment instructions, please see information listed at the bottom of this form.**

License Number	2924040594212
License date	Jun 08, 2012
Licensed content publisher	John Wiley and Sons
Licensed content publication	Chemistry - A European Journal
Licensed content title	Synthesis, Computational Modeling, and Properties of Benzo-Appended BODIPYs
Licensed content author	Timsy Uppal,Xiaoke Hu, Frank R. Fronczek, Stephanie Maschek, Petia Bobadova-Parvanova, M. Graça H. Vicente
Licensed content date	Feb 24, 2012
Start page	3893
End page	3905
Type of use	Dissertation/Thesis
Requestor type	Author of this Wiley article
Format	Print and electronic
Portion	Full article
Will you be translating?	No
Order reference number	
Total	0.00 USD

Terms and Conditions

#### TERMS AND CONDITIONS

This copyrighted material is owned by or exclusively licensed to John Wiley & Sons, Inc. or one of its group companies (each a "Wiley Company") or a society for whom a Wiley Company has exclusive publishing rights in relation to a particular journal (collectively WILEY\*). By clicking "accept" in connection with completing this licensing transaction, you agree that the following terms and conditions apply to this transaction (along with the billing and payment terms and conditions established by the Copyright Clearance Center Inc., ("CCC's Billing and Payment terms and conditions"), at the time that you opened your Rightslink account (these are available at any time at <http://myaccount.copyright.com>)

Terms and Conditions

I. The materials you have requested permission to reproduce (the "Materials") are protected by copyright.





RightsLink®

[Home](#)[Account Info](#)[Help](#)ACS Publications  
high quality. high impact.

**Title:** Bright Ideas for Chemical Biology  
**Author:** Luke D. Lavis et al.  
**Publication:** ACS Chemical Biology  
**Publisher:** American Chemical Society  
**Date:** Mar 1, 2008

Logged in as:  
Tmsy Uppal  
Account #:  
3000541389

[Logout](#)

Copyright © 2008, American Chemical Society

**PERMISSION/LICENSE IS GRANTED FOR YOUR ORDER AT NO CHARGE**

This type of permission/license, instead of the standard Terms & Conditions, is sent to you because no fee is being charged for your order. Please note the following:

- Permission is granted for your request in both print and electronic formats, and translations.
- If figures and/or tables were requested, they may be adapted or used in part.
- Please print this page for your records and send a copy of it to your publisher/graduate school.
- Appropriate credit for the requested material should be given as follows: "Reprinted (adapted) with permission from (COMPLETE REFERENCE CITATION). Copyright (YEAR) American Chemical Society." Insert appropriate information in place of the capitalized words.
- One-time permission is granted only for the use specified in your request. No additional uses are granted (such as derivative works or other editions). For any other uses, please submit a new request.

[BACK](#)[CLOSE WINDOW](#)

Copyright © 2012 Copyright Clearance Center, Inc. All Rights Reserved. [Privacy statement](#).  
Comments? We would like to hear from you. E-mail us at [customerservice@copyright.com](mailto:customerservice@copyright.com)

ELSEVIER LICENSE  
TERMS AND CONDITIONS

Jun 12, 2012

This is a License Agreement between Timsy K Uppal ("You") and Elsevier ("Elsevier") provided by Copyright Clearance Center ("CCC"). The license consists of your order details, the terms and conditions provided by Elsevier, and the payment terms and conditions.

**All payments must be made in full to CCC. For payment instructions, please see information listed at the bottom of this form.**

Supplier	Elsevier Limited The Boulevard, Langford Lane Kidlington, Oxford, OX5 1GB, UK
Registered Company Number	1982084
Customer name	Timsy K Uppal
Customer address	232 Choppin Hall Department of Chemistry Baton Rouge, LA 70803
License number	2926610304415
License date	Jun 12, 2012
Licensed content publisher	Elsevier
Licensed content publication	Current Opinion in Chemical Biology
Licensed content title	<i>In vivo</i> near-infrared fluorescence imaging
Licensed content author	John V Frangioni
Licensed content date	October 2003
Licensed content volume number	7
Licensed content issue number	5
Number of pages	9
Start Page	626
End Page	634
Type of Use	reuse in a thesis/dissertation
Portion	figures/tables/illustrations
Number of figures/tables/illustrations	1
Format	both print and electronic
Are you the author of this Elsevier article?	No
Will you be translating?	No

## VITA

Timsy K. Uppal was born in New Delhi, India, to Dr. Balbir S. Uppal and Kulwant Kaur Uppal. She attended Rukmini Devi Public School from 1988-2000. Soon after completing her schooling, she enrolled at Miranda House, a premier women's institution of Delhi University, offering degrees in the Sciences and Liberal Arts, and earned her Bachelors of Science in chemistry in June of 2003. She later enrolled at University of Delhi for a Masters of Science in organic chemistry and successfully graduated in June 2005. In Fall 2007, she was accepted to Graduate School Doctoral program at Louisiana State University (LSU) in the Department of Chemistry. She joined Prof. M. Graça H. Vicente research group at Louisiana State University in the Spring of 2008. Timsy is currently a candidate for the Doctor of Philosophy in organic chemistry, which will be awarded to her at the August 2012 Commencement at LSU, Baton Rouge.